



Universitat de Lleida

Studies on the cuticle and cell walls of olive fruits: composition, ripening-related changes, and the influence of agronomic factors

Clara Diarte Cabezudo

<http://hdl.handle.net/10803/673769>

ADVERTIMENT. L'accés als continguts d'aquesta tesi doctoral i la seva utilització ha de respectar els drets de la persona autora. Pot ser utilitzada per a consulta o estudi personal, així com en activitats o materials d'investigació i docència en els termes establerts a l'art. 32 del Text Refós de la Llei de Propietat Intel·lectual (RDL 1/1996). Per altres utilitzacions es requereix l'autorització prèvia i expressa de la persona autora. En qualsevol cas, en la utilització dels seus continguts caldrà indicar de forma clara el nom i cognoms de la persona autora i el títol de la tesi doctoral. No s'autoritza la seva reproducció o altres formes d'explotació efectuades amb finalitats de lucre ni la seva comunicació pública des d'un lloc aliè al servei TDX. Tampoc s'autoritza la presentació del seu contingut en una finestra o marc aliè a TDX (framing). Aquesta reserva de drets afecta tant als continguts de la tesi com als seus resums i índexs.

ADVERTENCIA. El acceso a los contenidos de esta tesis doctoral y su utilización debe respetar los derechos de la persona autora. Puede ser utilizada para consulta o estudio personal, así como en actividades o materiales de investigación y docencia en los términos establecidos en el art. 32 del Texto Refundido de la Ley de Propiedad Intelectual (RDL 1/1996). Para otros usos se requiere la autorización previa y expresa de la persona autora. En cualquier caso, en la utilización de sus contenidos se deberá indicar de forma clara el nombre y apellidos de la persona autora y el título de la tesis doctoral. No se autoriza su reproducción u otras formas de explotación efectuadas con fines lucrativos ni su comunicación pública desde un sitio ajeno al servicio TDR. Tampoco se autoriza la presentación de su contenido en una ventana o marco ajeno a TDR (framing). Esta reserva de derechos afecta tanto al contenido de la tesis como a sus resúmenes e índices.

WARNING. Access to the contents of this doctoral thesis and its use must respect the rights of the author. It can be used for reference or private study, as well as research and learning activities or materials in the terms established by the 32nd article of the Spanish Consolidated Copyright Act (RDL 1/1996). Express and previous authorization of the author is required for any other uses. In any case, when using its content, full name of the author and title of the thesis must be clearly indicated. Reproduction or other forms of for profit use or public communication from outside TDX service is not allowed. Presentation of its content in a window or frame external to TDX (framing) is not authorized either. These rights affect both the content of the thesis and its abstracts and indexes.



**Universitat
de Lleida**

TESI DOCTORAL

(MENCIÓ INTERNACIONAL)

Studies on the cuticle and cell walls of olive fruits: composition, ripening-related changes, and the influence of agronomic factors

Clara Diarte Cabezudo

Memòria presentada per optar al grau de Doctor per la Universitat de Lleida

Programa de Doctorat en Ciència i Tecnologia Agrària i Alimentària

Directors:

Prof. Dr. Isabel Lara Ayala

Prof. Dr. Jordi Graell Sarlé

Tutora:

Prof. Dr. Isabel Lara Ayala

2021

The current research was performed at the Department of Chemistry of the University of Lleida, under the supervision of Prof. Dr. Isabel Lara Ayala and the co-direction of Prof. Dr. Jordi Graell Sarlé. The present Doctoral Thesis was funded by grant **AGL2015-64235-R** from the Plan Nacional de I+D, Ministry of Education and Science, Spain.

The PhD candidate was granted a fellowship from the University of Lleida to pursue the PhD degree.

Chapter VI, “Compositional, structural and functional cuticle analysis of *Prunus laurocerasus* L. sheds light on cuticular barrier plasticity”, was carried out at Julius-von-Sachs-Institute for Biosciences at the University of Würzburg (Würzburg, Germany), under the supervision of Dr. Jana Leide.

“If you are always trying to be normal, you will never know how amazing you can be.”

Maya Angelou.

A mis padres, Begoña y Jesús.

AGRAÏMENTS/ AGRADECIMIENTOS/ ACKNOWLEDGMENTS

En primer lloc, m'agradaria agrair als meus directors de tesi, Dra. Isabel Lara Ayala i Dr. Jordi Graell Sarlé. Donar les gràcies per tota la confiança i el suport rebut durant aquests anys. Per ensenyar-me i guiar-me en aquest infinit món de la investigació. Especialment a tu Isabel, per la teva paciència, la gran implicació que has tingut en tot moment amb la feina realitzada i, sobretot, per fer-me creure que era possible quan les meves inseguretats no m'ho permetien.

Dr. Agustí Romero, gràcies per la teva ajuda donada des de la distància, i també agrair als companys de IRTA Mas Bové.

Família *Sin espuma*: Anna, Ariadna, María, Júlia i Sara, per ser les que heu estat dia a dia, i segurament per ser un dels millor regals que un llarg camí et pot donar, la amistat. Per tots els dinars, sopar, viatges compartits... i per tots els que ens queden!!! Carles, per tots els cafés matutins on el món quedava més que arreglat amb el teu toc àcid sobre la vida. Winnie, Ana, Gloria, M^a Carmen y Magda, quienes habéis hecho mucho más sencilla y divertida esta aventura, y todas las sonrisas que me llevo de ella. I com no, a tu Mariona, per ser la motivació per a començar aquest camí.

Anna Iglesias, per ser la meva companya de batalles al nostre petit laboratori durant el meu primer any. Pels bons moments viscuts :)

Companys del Departament de Química, que tot i passar una bona temporada sola al laboratori, sempre heu estat acompanyant-me i donant-me un cop de mà en tot allò que he necessitat. Especial agraïment a tu Enrique i Pepita, amb qui segurament més temps i converses he compartit. Gràcies! També al servei científicotècnic, i a tu Montse, per tots els teus coneixements.

Thank you, Prof. Riederer, for giving me the opportunity to carry out a research stay at the Julius-von-Sachs-Institute for Biosciences at the University of Würzburg. Many thanks, especially, to Dr. Jana Leide, who during all three months, every day, she supervised me, and always received me with a big smile. Emilie, Aline and Amauri thank you for your positivity and for all shared moments. Gracias también al maravilloso grupo de “Españoles en Würzburg”, y sobre todo a Cristina, Marc, Dani, y a mi pareja favorita de alemanes/ salobreñeros, Birggit y Carsten, con quienes compartí esta bonita experiencia y me enseñaron los que para mí son los lugares más encantadores de aquellas tierras. Danke schön!!!

Buscant destí i Ungabulungas, per animar-me, treure'm un somriure quan més ho necessitava, celebrar junts les petites “victòries” aconseguides, i per aconseguir fer-me desconnectar del món. *Clan Colacao*, Andrea y Maria sobretodo, por ser los que siempre estáis, pese al tiempo que tardamos a veces en juntarnos, y la distancia con algunos de vosotros.

Y, por último, y seguramente el apoyo más importante que he tenido en esta etapa que llega a su fin para emprender nuevos caminos, mi familia. Mama y papa, por apoyarme en todas y cada una de las decisiones, y estar en cada una de las etapas de mi vida. Miguel y Marian, por confiar en que siempre llegaría a puerto y estar preparados para todo y más. A nuestra pequeña Laia, por ser luz en los días grises y la alegría de la familia en estos tiempos extraños. ¡Muchas gracias! I Josan, a tu, per estar i fer-me sentir que puc amb tot i més, però sobretot per la teva infinita paciència en aquesta etapa final de la meva tesis. Os quiero mucho family.

RESUM

El cultiu de l'olivera (*Olea europaea* L.) és un dels cultius tradicionals als països mediterranis, i la seva producció a Espanya té una gran importància econòmica, sent el major productor i exportador mundial d'oli d'oliva. Tenint en compte la complexitat del mercat, els coneixements sobre certes característiques bioquímiques, com ara la composició cuticular i de les parets cel·lulars, podrien millorar la competitivitat de les empreses en aquest mercat.

La composició i propietats de la cutícula i de les parets cel·lulars dels fruits poden influir en diferents aspectes de la producció, com els danys mecànics o la sensibilitat a plagues, o a d'altres aspectes com ara la resposta a les inclemències climàtiques. Tots aquests factors, tant abiòtics com biòtics, juguen un paper fonamental en les característiques del fruit, que tindran importància tant per a la preparació d'olives de taula com per a la producció d'oli d'oliva.

Per a les olives produïdes a la Denominació d'Origen Protegida (DOP) 'Les Garrigues', es van trobar diferències composicionals en la cutícula i les parets cel·lulars entre fruits cultivats amb reg i els que es trobaven en condicions de secà. Pel contrari, es van detectar poques diferències entre ambdós règims de reg per als fruits cultivats en la DOP 'Siurana'. Tenint en compte que les condicions climàtiques a la DOP 'Les Garrigues' són més extremes que a la DOP 'Siurana', aquestes observacions suggereixen un possible paper de la cutícula en la adaptació de la planta a les condicions adverses.

Els canvis a la cutícula del fruit al llarg de la maduració van ser diferents segons les varietats d'oliva analitzades. Els àcids maslínic i oleanòlic van ser els dos compostos més abundants en les ceres cuticulars (arribant en alguns casos a percentatges del 52 i 43 % sobre el total, respectivament). També es van analitzar les ceres dels olis monovarietals produïts a partir de les nou varietats objecte d'estudi, conclouent-se que no semblava existir una relació directa amb les ceres cuticulars del fruit de l'oliva. Quant a la matriu de cutina, els compostos més abundants van ser els àcids 18-hidroxi-octadecanoic i 16-hidroxi-hexadecanoic. La microtopografia de la superfície del fruit també va mostrar diferències entre totes nou varietats, i suggereix també una possible relació amb la resposta a alguns factors d'estrès abiòtic i biòtic, com ara la infestació per la mosca de l'oliva.

Per altra banda, les modificacions de la paret cel·lular van reflectir la progressiva solubilització dels polisacàrids que la integren. Un estudi més complet realitzat a la varietat 'Arbequina' va mostrar una disminució important de la fermesa del fruit en estadis primerencs de maduració en paral·lel amb la pèrdua dels sucres neutres. Per a totes nou varietats d'oliva estudiades, es van observar alts nivells d'activitat pectinmetilesterasa i un alt contingut en calci en etapes primerenques de maduració, possiblement relacionats amb els baixos nivells de pèrdua d'àcids urònics com a conseqüència del reforçament de les estructures de caixa d'ous entre poligalacturonans.

Els resultats obtinguts en aquesta Tesi Doctoral proporcionen informació útil sobre els canvis que pateixen la cutícula i les parets cel·lulars del fruit de l'oliva durant la seva maduració en resposta a diferents factors agronòmics, així com també una comparativa de les propietats cuticulars amb fruits i fulles de llorer cirerer (*Prunus laurocerasus* L.), i amb fruits de kiwi (*Actinidia spp.*).

RESUMEN

El cultivo del olivo (*Olea europaea* L.) es uno de los cultivos tradicionales en los países mediterráneos, y su producción en España tiene una gran importancia económica, tratándose del mayor productor y exportador mundial de aceite de oliva. Teniendo en cuenta la complejidad del mercado, los conocimientos sobre ciertas características bioquímicas, como la composición cuticular y de las paredes celulares, podría mejorar la competitividad de las empresas de este mercado.

La composición y propiedades de la cutícula y de las paredes celulares de los frutos pueden influir en diferentes aspectos de la producción, como los daños mecánicos o la sensibilidad a plagas, o a otros aspectos como por ejemplo las inclemencias climáticas. Todos estos factores, tanto abióticos como bióticos, juegan un papel fundamental en las características del fruto, que tendrán gran importancia tanto para la preparación de aceitunas de mesa como para la producción de aceite de oliva.

Para las olivas producidas en la Denominación de Origen Protegida (DOP) ‘Les Garrigues’, se encontraron diferencias composicionales en la cutícula y las paredes celulares entre los frutos cultivados con riego y los que se encontraban en condiciones de secano. Por el contrario, se detectaron pocas diferencias entre los dos regímenes de riego en los frutos cultivados en la DOP ‘Siurana’. Teniendo en cuenta que las condiciones climáticas en la DOP ‘Les Garrigues’ son más extremas que en la DOP ‘Siurana’, estas observaciones sugieren un posible papel de la cutícula en la adaptación de la planta a las condiciones adversas.

Los cambios en la cutícula del fruto de la oliva a lo largo de la maduración fueron distintos según la variedad de oliva analizada. Los ácidos maslínico y oleanólico fueron los compuestos más abundantes en las ceras cuticulares (alcanzando en algunos casos porcentajes del 52 y 43 % sobre el total, respectivamente). También se analizaron las ceras de los aceites monovarietales producidos a partir de las nueve variedades objeto de estudio, concluyendo que no parece existir una relación directa con las ceras cuticulares del fruto de la oliva. En cuanto a la matriz de cutina, los compuestos más abundantes fueron los ácidos 18-hidroxi-octadecanoico y 16-hidroxi-hexadecanoico. La microtopografía de la superficie del fruto también mostró diferencias entre las nueve variedades, y sugiere también una posible relación en respuesta a algunos factores de estrés abióticos y bióticos, como por ejemplo por la infestación de la mosca de la oliva.

Por otro lado, las modificaciones en la pared celular reflejaron la progresiva solubilización de los polisacáridos que la integran. Un estudio más completo realizado en la variedad ‘Arbequina’, mostró una disminución importante de la firmeza del fruto en etapas tempranas de maduración, en paralelo con la pérdida de los azúcares neutros. En todas las variedades estudiadas, se observó altos niveles de actividad pectinmetilesterasa y un alto contenido en calcio en etapas tempranas de maduración, posiblemente relacionadas con la baja pérdida de ácidos urónicos como consecuencia del refuerzo de las estructuras de la caja de huevos entre poligalacturonanos.

Los resultados obtenidos en esta Tesis Doctoral proporcionan información útil sobre los cambios que sufren la cutícula y las paredes celulares del fruto de la oliva durante su maduración en relación a distintos factores agronómicos, así como también una comparativa de las propiedades cuticulares con frutos y hojas de laurel cerezo (*Prunus laurocerasus* L.), y con frutos de kiwi (*Actidinia spp.*).

ABSTRACT

Olive (*Olea europaea* L.) is one of the most traditional crops at the Mediterranean countries, and its cultivation is very relevant economically in Spain, the largest producer and exporter of olive oil in the world. Worldwide trade is very complex, and therefore a better comprehension of particular biochemical events such as changes in cuticular and cell wall composition along fruit maturation may prove helpful to improve the commercial competitiveness.

The composition and properties of fruit cuticle and cell wall may impact a number of aspects related to production, such as susceptibility to mechanical damages or pests, or the response to adverse climatic conditions. All of these factors play an important role on fruit characteristics, which are relevant both for manufacture of table olives and for olive oil production.

Compositional differences in fruit cuticle and cell walls were found between irrigated and rain-fed conditions for olives grown at the Protected Denomination of Origin (PDO) 'Les Garrigues', whereas very small irrigation-related differences were observed for olives picket at PDO 'Siurana'. Climatic conditions are much harsher at PDO 'Les Garrigues' than in PDO 'Siurana', and hence results are indicative of a possible role for fruit cuticle in plant adaptation to adverse environments.

The modifications in fruit cuticle along ripening were cultivar-dependent. Maslinic and oleanolic acids were the most abundant compounds among cuticular waxes (achieving in some cases up to 52 and 43 % over total waxes, respectively). Wax contents in monovarietal oils extracted from all nine olive cultivars considered was unrelated to the composition of cuticular waxes. Regarding the cutin composition, 18-hydroxyoctadecanoic and 16-hydroxyhexadecanoic were the predominant compounds. Furthermore, fruit surface microtopography also showed significant differences among all nine olive cultivars, and suggested a possible link to the response to some abiotic and biotic stress factors, such as olive fly infestation.

On the other hand, modifications in cell wall composition of fruit reflected the progressive solubilisation of their polysaccharide constituents. A comprehensive study on 'Arbequina' revealed a phase of sharp loss of fruit firmness at early stages of maturation, which paralleled the loss of neutral sugar. For all nine cultivars considered, high levels of pectin methylesterase activity and high calcium contents were found at early ripening stages, possibly related to low uronic acid loss arising from the reinforcement of the egg-box structures among polygalacturonans.

Results obtained in this Doctoral Thesis provide useful information on modifications in fruit cuticle and cell walls during ripening of olive fruit in response to different agronomic factors, as well as a comparison of cuticular properties with fruits and leaves of cherry laurel (*Prunus laurocerasus* L.), and with kiwifruit (*Actidinia spp.*).

TABLE OF CONTENTS

AGRAÏMENTS / AGRADECIMIENTOS/ ACKNOWLEDGEMENTS.....	IX
RESUM.....	XI
RESUMEN.....	XII
ABSTRACT.....	XIII
Introduction.....	17
A. Olive fruit and olive oil.....	19
B. Olive cultivars and PDO (Protected Designation of Origin) considered in the present Doctoral Thesis.....	22
C. The fruit cuticle: wax and cutin.....	27
D. Cell wall structure and ripening-related changes.....	31
E. Relation between cuticle and cell wall metabolism.....	34
F. References.....	34
Objectives.....	43
Plant material, methodology and work plan.....	47
A. Plan material.....	49
B. Methodology and work plan.....	50
Results.....	55
Chapter I: Insights into olive fruit surface functions: a comparison of cuticular composition, water permeability, and surface topography in nine cultivars during maturation.....	59
Chapter II: Ripening-related cell wall modifications in olive (<i>Olea europaea</i> L.) fruit: a survey of nine genotypes.....	95
Chapter III: Chemical and sensory characterization of nine Spanish monovarietal olive oils: an emphasis on wax esters.....	119
Chapter IV: Cuticle changes in 'Arbequina' olive fruit along on-tree ripening: the influence of irrigation and producing area.....	139
Chapter V: Firmness and cell wall changes during maturation of 'Arbequina' olive fruit grown at two Catalan Protected Designations of Origin: the impact of irrigation.....	175
Chapter VI: Compositional, structural and functional cuticle analysis of <i>Prunus laurocerasus</i> L. sheds light on cuticular barrier plasticity.....	203
General discussion.....	225
Conclusions.....	245
Future research.....	249
Annexes.....	253

Introduction

The olive (*Olea europaea* L.) is one of the most ancient crops cultivated by humans and, probably, one of the most iconic at the Mediterranean basin (Besnard, Terral and Cornille, 2018). The wild olive tree, a member of the *Oleaceae* family, is believed to have originated in Asia Minor, in whose forests occurs very abundantly, and from that area the olive crop would have spread to the Mediterranean countries (IOC <https://www.internationaloliveoil.org/>, 2020).

According to the Food and Agriculture Organization (FAO) of the United Nations, the last 40 years have witnessed a significant increase worldwide in olive tree cultivation area, which has duplicated between 1980 (5.1 million ha) and 2017 (10.6 million ha) with the concomitant boost in total olive production (11.2 to 20.9 million tons, respectively) (<http://www.fao.org/home/en/>, 2019). Even though 98% thereof pertains to countries in the Mediterranean countries, olives are also grown nowadays in different places around the world such as southern Africa, Australia, California, Japan, China or Argentina. Approximately 90% of total olive production is devoted to the olive oil industry, whereas barely 10% are used for the manufacturing of table olives. The exceptional organoleptic properties of olive oil, together with its healthy characteristics, are likely main reasons behind the overwhelmingly higher destination of olive fruit to oil extraction. Olive oil is purportedly a cardioprotective and antioxidant, and it also protects against cancer, osteoporosis and cognitive impairment due to high oleic acid content and to the presence of other constituents such as phenolic acids, flavonoids and squalene (Tripoli et al., 2006; Rodríguez-Morató et al., 2015). Provisional FAO data indicate that olive oil world production over the last three years (2018 to 2020) has been around 3,000,000 tones/year. The European Union produces up to 80% of total olive oil, with Spain, Greece and Italy, in that order, as the main manufacturers. Around 50% thereof is produced in Spain, where olive growing represents an important economic activity (IOC <https://www.internationaloliveoil.org/>, 2020). Nowadays, the olive growing sector is adapting the traditional crops to a more intensive production model, incorporating irrigation systems and mechanical harvesting where possible, with the purpose of obtaining higher productions with lower costs. Yet not all olive cultivars are fit for growing in ultra-high and high-density orchards, which leads to the globalization of some suitable cultivars such as ‘Arbequina’, while putting aside secondary and local varieties.

In Spain, the olive crop has a dominant character in many areas. The greatest extension (ha) of olive trees is found in Andalusia (61% of total olive growing area). Catalonia is the fourth region in terms of olive growing in Spain, olive crops occupying around 110,000 ha (Ninot et al., 2018) and representing the most important woody crop (39% of total area). Catalan olive producing areas are generally rain-fed conditions, corresponding mostly to Tarragona and Lleida (60% and 34%, respectively), and the rest to Barcelona and Girona (6% in total).

A. Olive fruit and olive oil

Olive fruit is an ellipsoidal or almost spherical drupe, contingent on the cultivar, with three well-defined parts (**Figure 1**): a stomatous epicarp (skin), a fleshy mesocarp (pulp or flesh), and a woody endocarp (stone) containing the seed.

Epicarp is the external and protective tissue of fruits. It contains 1-3% of drupe weight (Therios, 2009), and provides impermeability to water and protection against mechanical damage, infestations and rots. Cuticle is a fundamental part of the epicarp, and a key topic in the present Thesis. The mesocarp

Introduction

represents 70-80% of total weight of the whole ripe fruit. Oil accumulates in vacuoles of mesocarp cells, up to roughly 14 and 30% of total fruit weight in green and ripe olives, respectively.

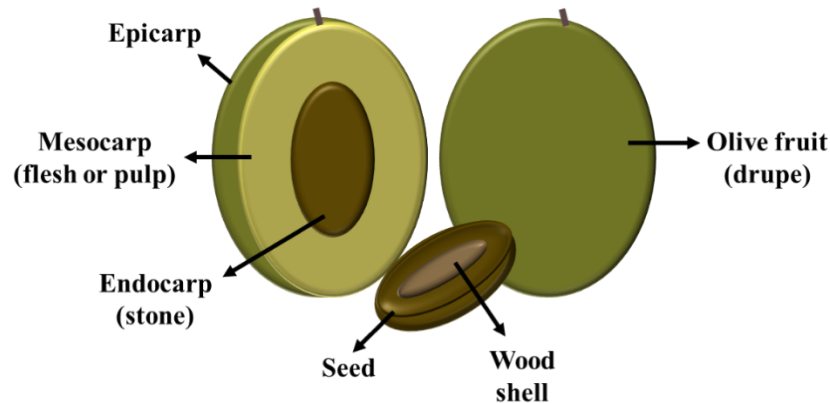


Figure 1. Simplified model of olive fruit cross-section (adapted from Juan et al., 2010).

Parenchymatic cells along with pectic and non-pectic polysaccharides (including fibre), proteins, sugars and phenolic compounds are constituents of the fleshy tissue of olive fruit, and will be addressed later in this document. The endocarp, which contains the seed (2-4% of the drupe weight), represents around 10-27 % of olive weight, depending on the cultivar.

Olive fruit displays a typical double sigmoidal growing pattern divided into three phases. Phase I, when the endocarp shows very active cell division until achieving its definitive size; phase II, when the seed develops within the endocarp; and phase III, when mesocarp cells expand to achieve final fruit size and physiologic maturity. In the latter phase, fruit surface colour changes from green at the immature stage to purplish-black when completely ripe. Some cultivars, though, remain green when ripe, while some other show coppery brown and even ivory hues at the same stage. Water content decreases during fruit ripening, whereas oil content and dry weight increase. Growth and ripening of the olive fruit growth take approximately 6 to 7 months, and the ripening period spans from early September to late January in the northern hemisphere, depending on cultivar and agronomic conditions (Therios, 2009).

In order to obtain table olives and olive oils with optimal sensory and chemical properties, several important factors should be considered. Firstly, (i) fruit maturity at harvest must be decided according to the production objectives (Famiani, Proietti and Nasini, 2005). For example, olive oil extracted from green olives is greener, bitterer and displays marked green, fruity and spicy flavour notes, which makes it excellent for fresh consumption by “native” consumers, whereas oil obtained from very ripe olives is sweeter, more yellow and less aromatic, more fit for consumers not used to olive oil (Inglese, 2011). Even though extraction is facilitated and higher oil yields can be obtained at a more advanced maturity stage, lower sensory, chemical and nutritional quality of oil ensues.

Secondly, (ii) harvesting system is also related to oil quality. Although mechanical harvest allows shortening the harvest period and facilitates the recollection at the appropriate maturity stage, the associated mechanical damage of fruit may lead to fermentation by a range of microorganisms, and hence to detrimental consequences on chemical and organoleptic characteristics of the oils. Trunk shakers are reportedly the mechanical harvesters producing the less damage (Tombesi et al., 1996).

Finally, (iii) defect-free fruit should be used for oil extraction, since infestations and rots may also affect negatively the quality and the shelf life potential of oil. Additional defects such as bruising or wrinkling will also compromise table olive quality. *Bactrocera oleae* (Rossi) (Diptera: Tephritidae), known as olive fly, is an important plague in olive crops. This olive fruit-affecting pest was detected in California for the first time, but it is currently spread all over the Mediterranean area, Africa, Asia and North and Central America (Nardi et al., 2005). The damage is characterized by tunnels in fruit pulp caused by the larvae, and can achieve 30% of crop production (Therios, 2009). The olive fly causes premature fruit fall, yield reduction and changes in the organoleptic properties (e.g. acidity) that decrease oil quality (Connor et al., 2014). The life cycle begins in winter when the pupal form of the olive fly is covered up several centimetres beneath the soil. During spring, depending on the weather conditions, the first generation of adults, fed on sugar and nitrogen compounds, arises from the pupal overwintering. In summer, after reaching sexual maturity, eggs are laid by the females under the olive fruit skin. One larva hatches from each egg after 2 - 4 days thereafter, and grows inside the fruit during 10 - 14 days, feeding with the pulp and thus causing fruit drop. Finally, the larva turns into the pupal form to survive at low temperatures, and the cycle restarts. In the Mediterranean basin, the insect presents two to five generations per year (Therios, 2009). Existing field studies (Gumusay et al., 1990; Iannotta et al., 1999) had hinted a relationship between fruit size and infestation susceptibility, larger cultivars being more prone, but posterior laboratory assays denied such a relationship (Kombargi et al., 1998). Olive fly can infest any olive cultivar, but the insect shows ovipositional and larval development preferences for certain varieties, which will influence the infestation rate and pattern, and how the pest will spread (Burrack and Zalom, 2008). The most common method used currently for olive fly control is treating with insecticide in bait or air spray, although environmentally more acceptable control methods can be also applied, such as γ -ray male sterilization (Economopoulos, 1972), pheromones and biological methods. Olives can be also afflicted by a range of fungal diseases, particularly *Camasporium dalmaticum* which causes considerable deterioration, especially in table olives.

Since most of harvested olives are intended for olive oil production, the quality characteristics of the oil are a relevant point to consider. In order to achieve high quality olive oil, it is important to prevent the alterations that the product could undergo, particularly lipolysis and oxidation. The lipolysis is the hydrolysis of the triglycerides induced by inappropriate temperature, moisture, enzymes and microorganisms. Lipolysis usually begins during on-tree fruit ripening, depending on cultivar, sanitary status, and environmental, climatic, soil and cultivation conditions, and will continue during harvesting and storage prior to oil extraction (Aparicio and Harwood, 2013). Additionally, fermentation processes may trigger free fatty acids which are precursors for oxidative pathways. Oxidation proceeds after oil extraction and, in general, during storage of the final product (Kiritsakis, 1990). Oil oxidation may happen in the dark (autoxidation process), or under the light (photooxidation process). Olive oils displaying low contents of polyunsaturated acids and high antioxidant (e.g. phenolics) levels will be resistant to autoxidation but susceptible to photooxidation. Taking into account all these considerations, it is very important to conduct all phases and processes, from the agronomic practices to olive oil storage, with the purpose of eventually obtaining the best possible quality olive oil, with no unpleasant flavours and odours. European Union (EU) regulations (EEC Regulation 2568/91 and amendments) compile the quality characteristics of the different grades established for olive oils and their byproducts, such as extra-virgin olive oil or olive pomace oil, based on different parameters. Acidity, peroxide value, K_{232} and K_{270} indices, wax contents and organoleptic attributes were the parameters of interest in the present Thesis.

B. Olive cultivars and PDO (Protected Designation of Origin) considered in the present Doctoral Thesis

B1. Cultivars

A total of nine autochthonous Spanish olive cultivars were studied in this Thesis. In alphabetical order, these cultivars were the following: ‘Arbequina’, ‘Argudell’, ‘Empeltre’, ‘Farga’, ‘Manzanilla’, ‘Marfil’, ‘Morrut’, ‘Picual’ and ‘Sevillena’. ‘Picual’ and ‘Manzanilla’ were selected as reference Spanish cultivars for olive oil and table olive production, respectively. ‘Arbequina’ is the main cultivar in Catalonia, and is employed for both purposes. ‘Argudell’, ‘Empeltre’, ‘Farga’, ‘Marfil’, ‘Morrut’, and ‘Sevillena’ were included as representatives of secondary and local cultivars.

‘Arbequina’ (Figure 2) is native to the Lleida area, and one of the most important cultivars in Spain. At present, this cultivar has also expanded to other olive-producing areas including Tarragona, Zaragoza and Huesca provinces, Andalusia, as well as other countries (Algeria, Argentina, Australia, Chile or USA). This genotype can be used in high density orchards, presents medium ripening pattern, medium vigour and high production, and displays small fruits grouped in bunches, although these characteristics may vary across different producing areas. Trees show great resistance to drought and cold, to *Verticillium* wilt and peacock spot (*Spilocaea oleaginea* Hughes), the most important fungus diseases in olive, but the fruits are susceptible to *Bactrocera oleae* (olive fly) infestation.



Figure 2. ‘Arbequina’ olive fruit at the green (a), turning (b) and ripe (c) stages collected at IRTA-Mas Bové (Constantí, Spain). The scale bar indicates 1 cm.

Fruits are small (about 2.0 g) and spherical, and are used for both table olive manufacturing and olive oil production, with high fat yields (around 21% of the extraction) (Tous and Romero, 1993). ‘Arbequina’ olive oil is characterized by green grass colour, softness in mouth, and sweet and fruity flavour with extraordinary fragrance. In comparison with other monovarietal olive oils, the concentration of phenolic compounds is lower, and so ‘Arbequina’ oil is not extremely bitter or spicy. Due to low phenolics content, it should be stored in the dark at low temperatures, since it is very prone to oxidise. The content of oleic acid is low-medium, but that of polyunsaturated acids is high, which confers fluidity to the oil (Tous and Franquet, 2019).

‘Argudell’ (Figure 3) is an important secondary olive variety in Girona province. The fruits are asymmetric and egg-shaped, small to medium size (approximately 2.2 g), display medium ripening pat-

tern, and are suitable for mechanic harvesting as they are easily detached from the tree. This olive cultivar is intended mainly for oil production as it contains high levels of good-quality fat, even though extraction is difficult (Tous and Romero, 1993; Rallo et al., 2005).



Figure 3. ‘Argudell’ olive fruit at the green (a), turning (b) and ripe (c) stages collected at IRTA-Mas Bové (Constantí, Spain). The scale bar indicates 1 cm.

‘Empeltre’ (Figure 4) is an important cultivar at the NE region of Spain (Aragon, Balearic Islands, Catalonia, Navarra, Valencian Community and La Rioja), although the extension of its producing area is smaller than that of other varieties such as ‘Arbequina’. This cultivar shows a very early ripening pattern, and it is devoted mainly to the manufacturing of table olives (black style). It is also very fit for the production of refined olive oil because of its soft taste and moderate bitterness due to low polyphenolics content (Abenoza et al., 2018). Fruits are medium-sized (around 2.6 g) and egg-shaped. ‘Empeltre’ is tolerant to *Verticillium* wilt, but susceptible to frost damage and fly olive (Tous and Romero, 1993).

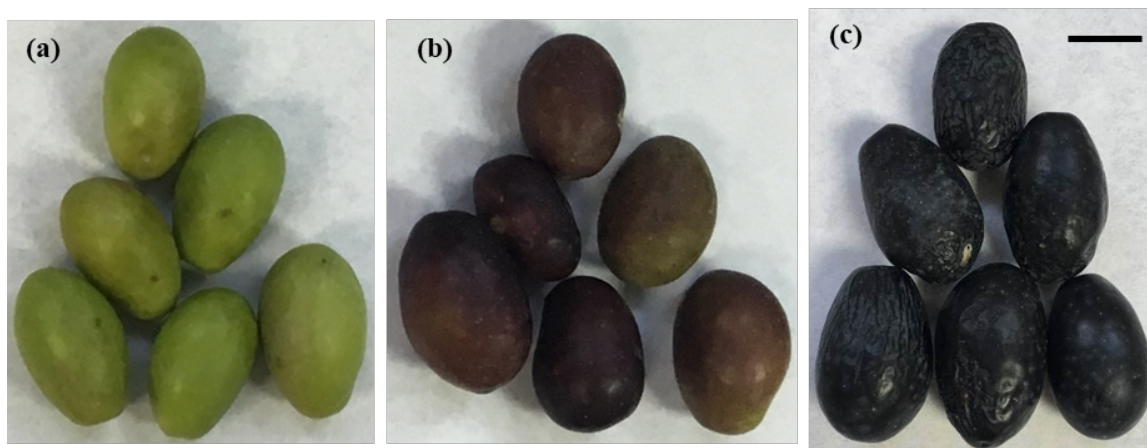


Figure 4. ‘Empeltre’ olive fruit at the green (a), turning (b) and ripe (c) stages collected at IRTA-Mas Bové (Constantí, Spain). The scale bar indicates 1 cm.

‘Farga’ (Figure 5) is a secondary cultivar in the Tarragona region and the north of the Valencian Community. This variety is able to adapt to a range of unfavourable environmental conditions, and this is probably the reason why huge specimens near 1,000 years old can be found (Arnan et al., 2012; Ninot et al., 2018). Fruits are outstretched and largely asymmetric, and display medium weight (approximately 2.4 g). Olives from this genotype show medium ripening pattern, and are used both for oil production and as table olives. Oil yield is high, but production is low and alternating, and fruit are susceptible to

Introduction

olive fly and to *Collectotrichum acutatum* (Tous and Romero, 1993; Ninot, Howad and Romero, 2019). Fruits show moreover high retention strength, which makes them inappropriate for mechanical harvest. ‘Farga’ oil is fruity with green notes, and contains high levels of oleic and phenolic acids, the latter being responsible for the bitter, spicy and slightly astringent flavour.

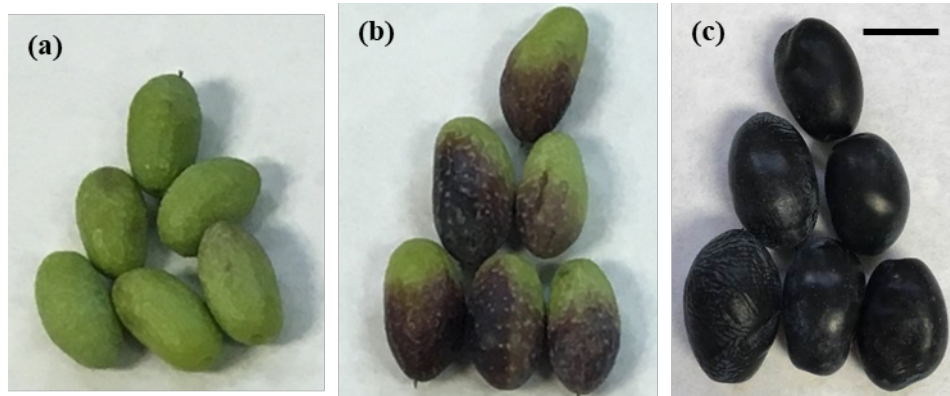


Figure 5. ‘Farga’ olive fruit at the green (a), turning (b) and ripe (c) stages collected at IRTA-Mas Bové (Constantí, Spain). The scale bar indicates 1 cm.

‘Manzanilla’ (Figure 6) is the most popular Spanish table olive, being California and Spain the most important producing areas. ‘Manzanilla’ fruit is large (about 4.4 g), spherical and symmetric (Hermoso et al., 2008). The genotype shows a very early ripening pattern, and production is best at warm locations with no winter frosts. Oil content is high (around 20 %) and the pit is small, which makes ‘Manzanilla’ the best dual-purpose variety in the world (Tous and Romero, 1993). The cultivar is suitable for high density orchards, but production is alternant and it is susceptible to frost damage, *Verticillium* wilt and olive fly (Therios, 2009).

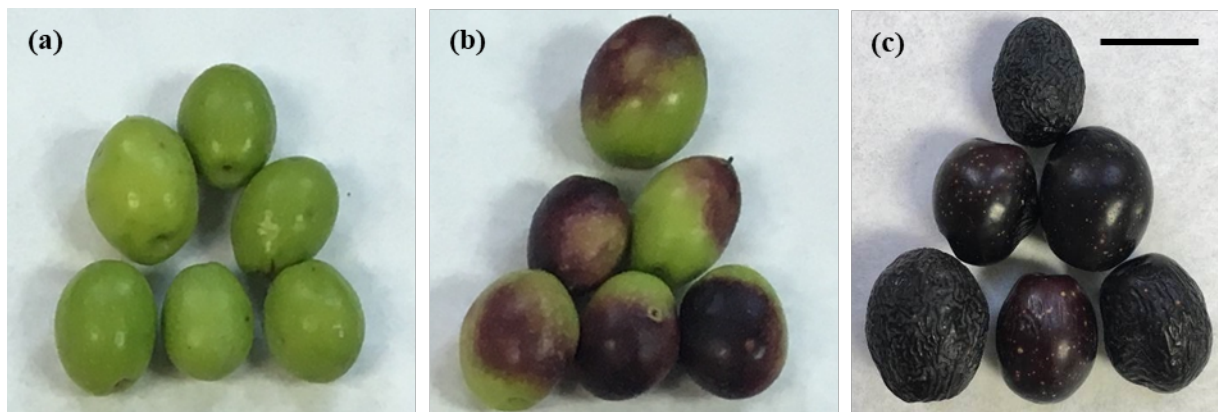


Figure 6. ‘Manzanilla’ olive fruit at the green (a), turning (b) and ripe (c) stages collected at IRTA-Mas Bové (Constantí, Spain). The scale bar indicates 1 cm.

‘Marfil’ is one of the few olive cultivars showing ivory skin colour when ripe (Figure 7). Native of the Tarragona area, it is a local cultivar usually grown between traditional olive orchards. White colour arises from the impairment of anthocyanin synthesis, and thus fruit turn from green to white in the course of ripening-related chlorophyll degradation. This cultivar is susceptible to olive fly and frost damage, but is tolerant to peacock spot. Fruit are outstretched and asymmetric in shape with small-medium weight (around 2.0 g), and ripen late in the season. They show low fruit removal force, which

allows the use of shakers for harvesting (Tous and Romero, 1998). ‘Marfil’ olives can be used for oil production as well as for table olive manufacturing. Oil content is not high, but it shows good quality characteristics, with similar fatty acid composition as in ‘Arbequina’ oil.

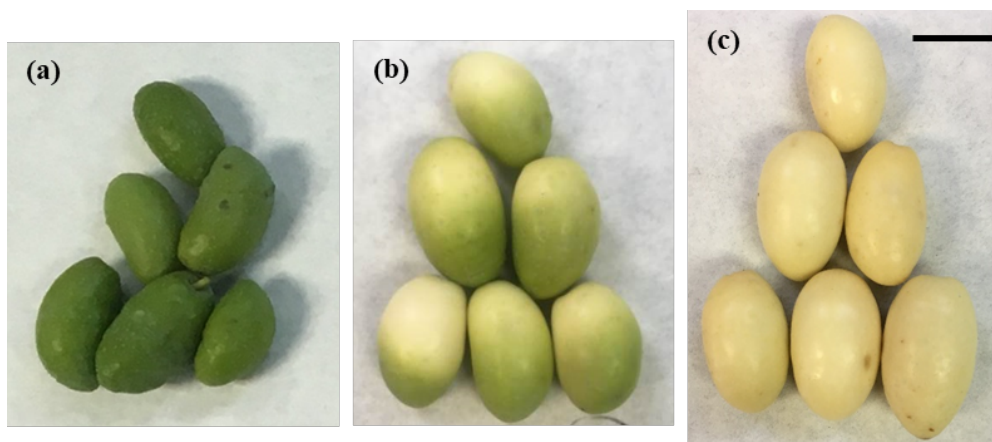


Figure 7. ‘Marfil’ olive fruit at the green (a), turning (b) and ripe (c) stages collected at IRTA-Mas Bové (Constantí, Spain). The scale bar indicates 1 cm.

‘**Morrut**’ (**Figure 8**) is a vigorous variety used for both oil production and olive table manufacturing, and is cultivated in Tarragona and Castelló. Oil yield is medium-high (around 21-23%) and the oil has low oxidative stability (Morelló, Romero and Motilva, 2004). Fruit ripen very late, and production is low and at alternate years. Olives are egg-shaped and show medium-high weight (about 3.9 g). The cultivar is susceptible to drought and to frost damage, but late ripening pattern protects fruit from olive fly infestation (Tous and Romero, 1993).



Figure 8. ‘Morrut’ olive fruit at the green (a), turning (b) and ripe (c) stages collected at IRTA-Mas Bové (Constantí, Spain). The scale bar indicates 1 cm.

‘**Pical**’ (**Figure 9**) represents around 20% of total olive growing extension in the world, and almost 50% thereof is located in Spain, particularly in the Andalusia region. ‘Pical’ displays very high oil yields (occasionally, up to 27%), leading to increasing production of this cultivar, which is used mainly for oil extraction. ‘Pical’ olives are large (approximately 3.7 g), elongated and slightly asymmetric in shape, and show medium ripening pattern. Oil is very bitter due to high phenolics content, which furthermore confer high oxidative stability and hence a long shelf life potential (Tous and Romero, 1993; Rallo et al., 2005).

Introduction

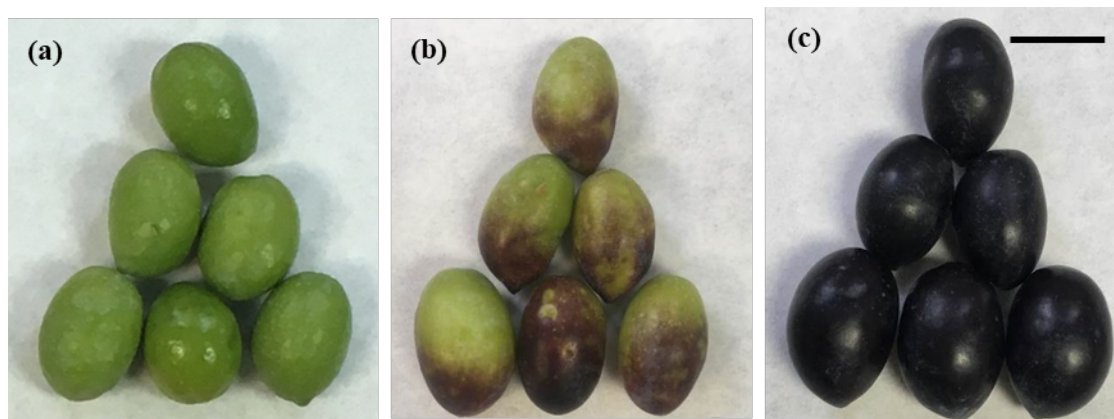


Figure 9. ‘Picual’ olive fruit at the green (a), turning (b) and ripe (c) stages collected at IRTA-Mas Bové (Constantí, Spain). The scale bar indicates 1 cm.

‘Sevillenca’ (Figure 10) is produced fundamentally in Tarragona, Castelló and Valencia. It is suitable for mechanical harvest, and displays an early ripening pattern. Fruit show high weight (about 3.4 g) and outstretched shape. The cultivar is resistant to *Verticillium* wilt and mild frosts, but susceptible to olive fly infestation and drought stress. Oil yields are around 22-24 %, and these olives are generally used for oil extraction, even though oleic acid content is usually low and the oil has low oxidative stability (Tous and Romero, 1993; Rallo et al., 2005).



Figure 10. ‘Sevillenca’ olive fruit at the green (a), turning (b) and ripe (c) stages collected at IRTA-Mas Bové (Constantí, Spain). The scale bar indicates 1 cm.

B2. PDO ‘Les Garrigues’ and PDO ‘Siurana’

The competitive scenario of olive oil production and consumers’ demands for high-quality, traditional food products have favoured the consolidation of Protected Designations of Origin (PDO) (regulated by EC Regulation 510/2006) as a key tool for the valorisation and certification of the area of origin of the product. Indeed, weather and edaphological conditions together with local agronomic practices are related to the chemical composition and characteristics of virgin olive oil (Camin et al., 2010; Mailer, Ayton and Graham, 2010; Casanovas, 2012; Romero, 2012). Therefore, the valorisation of oils produced in traditional areas entails a better understanding of physiological and biochemical characteristics of

additional autochthonous varieties such as ‘Argudell’, ‘Empeltre’, ‘Farga’, ‘Marfil’, ‘Morrut’ and ‘Sevillenca’, the secondary and local cultivars considered in this Thesis. Five different PDO for olive oil exist in Catalonia (Figure 11). In terms of total production, ‘Les Garrigues’ (Lleida province) and ‘Siurana’ (Tarragona province) are the most important ones, both of them recognised by the EU since 1996. PDO ‘Les Garrigues’ is characterized by cultivars ‘Arbequina’ (around 90 %) and ‘Verdiel’. For PDO ‘Siurana’, the most important varieties are ‘Arbequina’ (around 90 %) and ‘Morrut’. Other cultivars such as ‘Sevillenca’, ‘Empeltre’ or ‘Argudell’ also occupy significant production areas in Catalonia. The climate conditions at PDO ‘Les Garrigues’ are characterized by low annual rainfall and extreme temperatures, with frosts in winter and high temperatures in summer. As to PDO ‘Siurana’, the nearness to the Mediterranean Sea translates into higher rainfall, warmer temperatures in winter and chillier summers in comparison to those at PDO ‘Les Garrigues’.

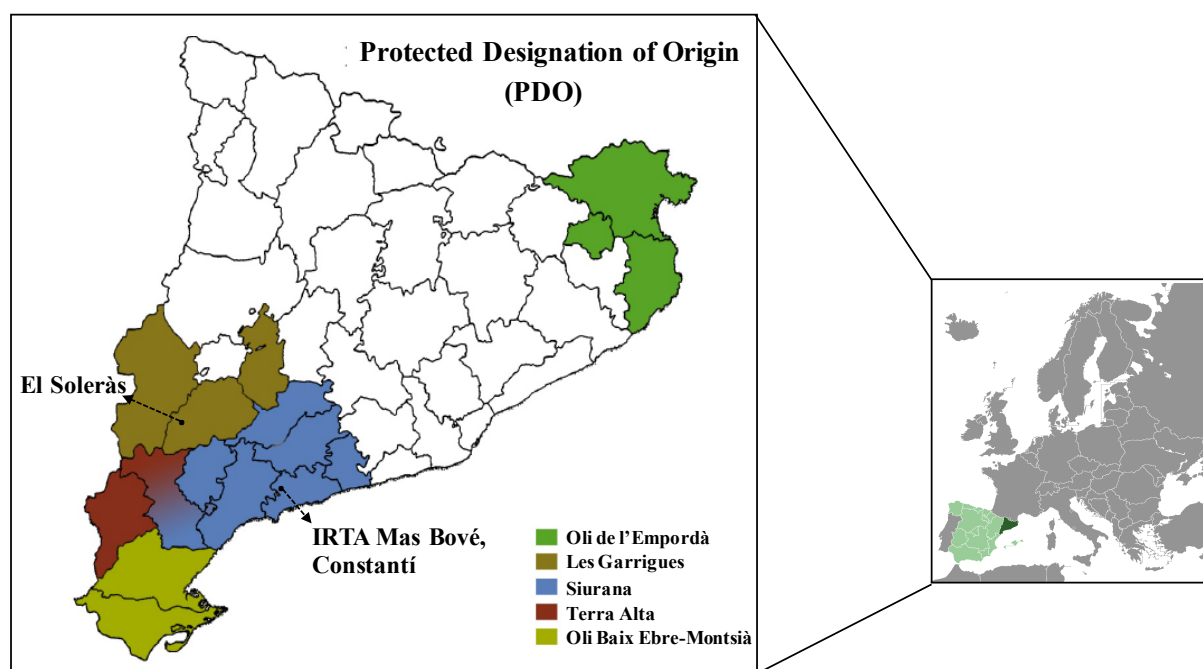


Figure 11. The Protected Designations of Origin (PDO) for extra-virgin olive oil in Catalonia (Spain).

C. The fruit cuticle: wax and cutin

The plant cuticle (Figure 12) is synthesized by the epidermal cells of aerial, non-lignified plant organs, including fruits, and constitutes an interface and a barrier against the environmental conditions surrounding the plant. Cuticular composition and structure varies across species, cultivars, organs and developmental stages, and they are also impacted by environmental conditions. Regardless of such differences, the plant cuticle is a hydrophobic layer which displays noticeable responsiveness to a variety of abiotic and biotic factors. Cuticular permeance to water modulates water loss, and the cuticle moreover protects against excessive UV irradiation, infestations and rots, and confers particular mechanical properties (Yeast and Rose, 2013; Lara, Belge and Goulao, 2014; Serrano et al., 2014; Jetter and Riederer, 2016). Understandably, fruit cuticle profoundly impacts fruit quality and postharvest shelf life potential (Martin and Rose, 2014).

Introduction

The quantity of cuticle per surface area reportedly ranges from 450-800 $\mu\text{g cm}^{-2}$ in leaves to 2000 $\mu\text{g cm}^{-2}$ in fruits (Heredia and Domínguez, 2014). The cuticle hence represents only a minor fraction of total mass of whole fruits or leaves. Even so, it plays a key role as a thermoregulator of the surrounded plant organ, as it allows to maintain internal temperature despite changes in the surrounding environment (Casado and Heredia, 2001; Heredia and Domínguez, 2014). For many horticultural crops, cuticle deposition decreases under high humidity. In plants adapted to water deficit conditions, the cuticle of fruits is generally well-developed (Baker and Procopiou, 2000; Xue et al., 2017), and its deposition in fruits can be affected by the interaction of light and temperature (McDonald, Nordby and McCollum, 1993; Léchaudel et al., 2013). Interestingly, cuticle composition rather than cuticle thickness determines susceptibility of fruit to pathogens (Reina-Pinto and Yephremov, 2009; Ziv et al., 2018).

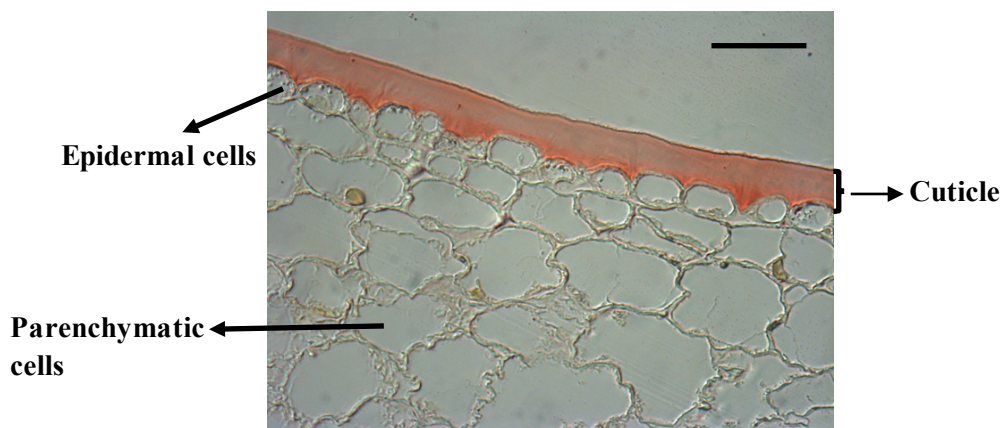


Figure 12. Sudan IV-stained cross-section of ‘Manzanilla’ olive pericarp at the ripe stage as observed under a bright-field microscope. The scale bar indicates 60 μm .

The mechanical behaviour of plant cuticles is biphasic; for this reason, cuticle deformation at low stress shows an elastic behaviour, whereas it is totally viscoelastic at high stress. Cuticle thickness is correlated with stiffness, but negatively correlated to cuticle deformation (Khanal and Knoche, 2017). This point is important, particularly for ripe fruits and also during post-harvest storage, when the pressure posed on the cuticle increases due to cell wall disruption. At that moment, therefore, stress is high and cuticle deformation is viscoelastic (Knoche et al., 2004; España et al., 2014). It is thus advisable to keep the fruits in low temperature and adequate relative humidity, since the cuticle turns more fluid at higher temperatures and relative humidity. Increased fluidity causes a decrease in cuticle resistance to the deformation, hence boosting water movement across the cuticle (Matas et al., 2005; Domínguez, Heredia-Guerrero and Heredia 2011).

The cuticle is composed of a cutin matrix, associated with a polysaccharide fraction derived from the epidermal cell walls, and impregnated and covered by waxes. Cutin is an insoluble polymeric matrix constituted by hydroxy-, carboxy-, and epoxy- C_{16} and C_{18} fatty acids, and esterified with a minor fraction of phenolic compounds (Domínguez et al., 2011; Serrano et al., 2014; Domínguez, Heredia-Guerrero and Heredia, 2015; Camacho-Vázquez et al., 2019). In general, the major cutin monomer representatives of the C_{16} -type are 9/10,16-dihydroxyhexadecanoic acid and 16-hydroxyhexadecanoic acid, and those of the C_{18} -type are 9,10,18-trihydroxyoctadecanoic acid and 9,10-epoxy,18-hydroxyoctadecanoic acid (**Figure 13**) (Franke et al., 2005; Nawrath and Porier, 2008; Graça and Lamosa, 2010).

A previous study on tomato (*Solanum lycopersicum*) (López-Casado et al., 2007) showed the great importance of the cutin matrix for viscoelastic behaviour (low elastic modulus), whereas cutin-associated polysaccharides are responsible for high elastic modulus (i. e. the stiffness) of cuticles.

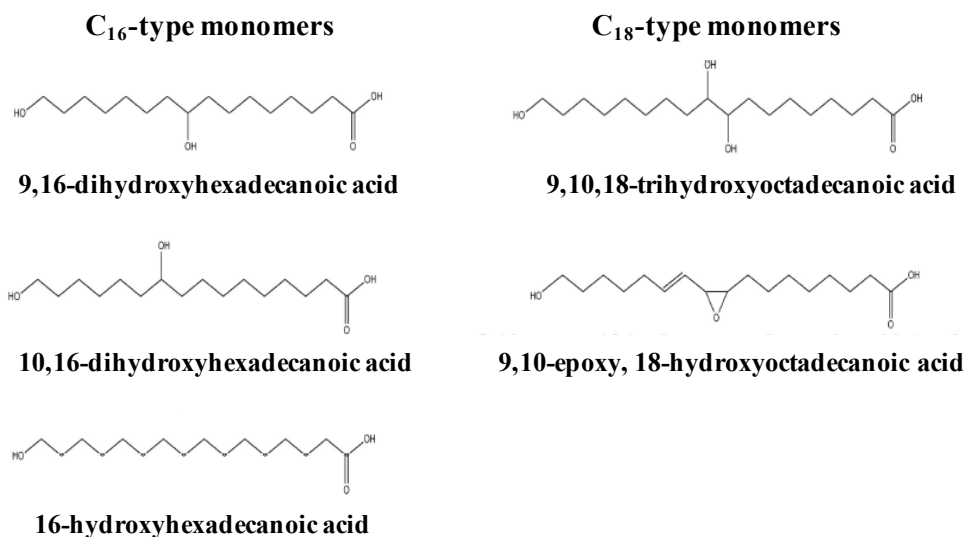


Figure 13. Major cutin components identified in fruit cuticles (adapted from Lara, Heredia and Domínguez, 2019).

Cuticular waxes, both in amorphous and in crystalline form, cover and are embedded into the cutin matrix. These compound family consist of a complex mixture of acyclic compounds and ring structures (pentacyclic triterpenoids). The aliphatic group comprises compounds with unbranched hydrocarbon chains at least 20 carbons long (fatty acids, alcohols, *n*-alkanes, aldehydes, and esters), originating from the elongation of C₁₆ and C₁₈ fatty acids (**Figure 14**) (Bianchi, 1995; Samuels, Kunst and Jetter, 2008; Kunst and Samuels, 2009; Buschhaus and Jetter, 2011). Although the specific wax compounds may vary along the ripening process, triterpenoids are the predominant compounds in fruits species such as olive (*Olea europaea*), grape (*Vitis vinifera*) persimmon (*Diospyros kaki*), and blueberry (*Vaccinium spp.*), in which only traces of *n*-alkanes are detectable. In contrast, both triterpenoids and *n*-alkanes are major compounds of cuticular waxes in tomato (*Solanum lycopersicum*), apple (*Malus x domestica*), Asian pear (*Pyrus spp.*), sweet cherry (*Prunus avium*), peach (*Prunus persica*) and pepper (*Capsicum annum*) (Trivedi et al., 2019).

One of the most important characteristics of the cuticular waxes is their capacity to provide mechanical support and resistance to pathogens, and to prevent fruit softening, minimizing the diffusional flow of water in the plant (Martin and Rose, 2014; Wang et al., 2014). This is related to cuticular wax composition features, such as the presence of alkanes and aldehydes, rather than to cuticle thickness (Riederer and Schreiber, 2001). Waxes contribute reportedly around 96 and 99.5 % against water loss across the cuticle in leaves of *Prunus laurocerasus* and *Pyrus communis*, respectively (Burghardt and Riederer, 2006). Contrarily, triterpenoids and sterols may increase water transpiration rates (Leide et al., 2007; Parsons et al., 2012; Moggia et al., 2016). Triterpenoids reinforce mechanical strength of cuticles in fruits such as persimmon or pitaya (dragon fruit), given their role as nanofillers into the cutin matrix (Tsubaki et al., 2013; Huang and Jiang, 2019). The antifungal activity of Asian pear fruit has been also associated with triterpenoids along with *n*-alkanes and fatty acids (Chen et al., 2014; Li et al., 2014). Besides, cuticular waxes are believed to confer protection against UV radiation (Pfundel, Agati and

Introduction

Cerovic, 2006), and the cuticle has been found to increase in response to high irradiation in many plant species (Shepherd and Griffiths, 2006; Tafolla-Arellano, Báez-Sañudo and Tiznado-Hernández, 2018). Regarding glossiness and brightness, cuticular waxes and the cutin matrix, respectively, determine these fruit traits (Ward and Nussinovitch, 1996; Petit et al., 2014), thus affecting consumer preferences. Moreover, cuticular waxes contribute to the lotus effect, due to their hydrophobic nature and nanostructure (Koch and Barthlott, 2009).

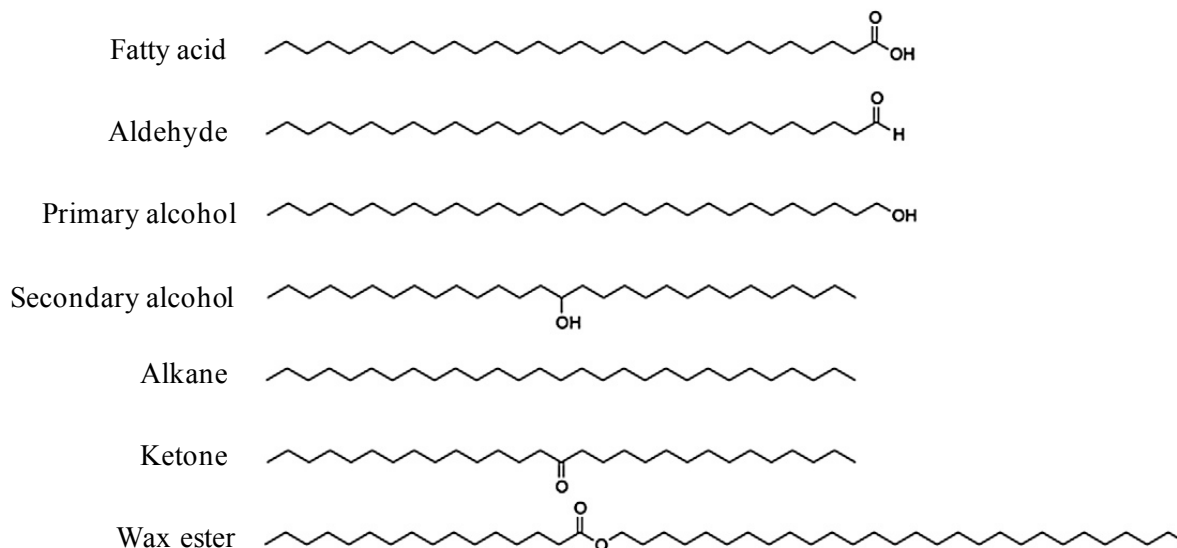


Figure 14. Major acyclic lipid classes of compounds of cuticular waxes of fruits (Yeats and Rose, 2013).

As far as olive oil production is concerned, cuticular waxes of fruit may be transferred to oil during the extraction process, and high concentrations of alcohols could cause increased wax content during oil storage. The evolution of oil properties during storage will depend on the initial content of reactive species in each cultivar, on the extraction system used to obtain the olive oil (Ranalli and Serraiocco, 1996; Alba et al., 1996; Boskou, 1998), and on the storage conditions (Christopoulo and Larazaki, 1997). Therefore, the wax profile could be used for the characterization of monovarietal oils. Furthermore, waxes provide turbidity to oil along storage and affect some sensory characteristics, such as fluidity, and it is thus important to take into consideration the composition of cuticular waxes in fruit before the extraction. Moreover, recent studies found that triterpenoids display important health-promoting properties, including anti-inflammatory, anticancer, antimicrobial and cardioprotective (Dzubak et al., 2006; Levi et al., 1999; Szakiel et al., 2012). Concerning cutin compounds, fatty acid monomers present in the tomato pomace waste can be used to produce packaging films after mixing with beeswax and alginate (Tedeschi et al., 2018). These findings imply that cuticular waxes and cutin monomers present in the olive oil industry waste (including the olive pomace) could be used for the extraction of bioactive and biodegradable products for the pharmaceutical and food industries, packaging, cosmetics and nanocoatings (Trivedi et al., 2019).

The cuticle components of olive fruit have not been studied in depth. Two previous works reported the characterization of cuticular waxes in fruit of ‘Coratina’ (Bianchi, Murelli and Vlahov, 1992) and of a selection of nine cultivars (‘Arbequina’, ‘Empeltre’, ‘Grossal Vimbodí’, ‘Llumet’, ‘Menya’, ‘Morrut’, ‘Palomar’, ‘Picual’ and ‘Sevillenca’) (Vichi et al., 2016). For ‘Arbequina’ uniquely, one recent study (Huang et al., 2017) analysed cutin monomers in addition to cuticular waxes of fruit. For other species,

studies focused on cuticle deposition during fruit development have generally found a progressive diminution of cuticle mass per unit of surface area as fruit expands to its final size (Lara et al., 2014). Hence, a better knowledge of cuticular composition and structure in olive fruit will be required in order to gain deeper insights on how these properties are related to water loss, susceptibility to mechanical damage, and proneness to infestations and rots. This information may have a practical interest for the olive producing sector.

D. Cell wall structure and ripening-related changes

Fruit softening is one of the most conspicuous ripening-related changes, and has profound implications for the postharvest and storage periods of fruits, including olives, and hence for growers and the fruit-related trade and industry. Firmness loss is a chief contributor to the textural changes that render the fruit palatable, but tissue softening also involves increased susceptibility to mechanical damages, pests and diseases, with the concomitant decrease in quality from which important economical losses may ensue (Wang et al., 2018). Firmness loss is largely related to cell wall metabolism, and therefore intensive research efforts have been invested in understanding this process and in investigating how optimal textural properties could be maintained after harvest, with the purpose of obtaining fruit products with higher quality and longer shelf life.

Briefly described, the plant cell wall comprises the middle lamella and the primary cell wall which is in contact with the plasma membrane (**Figure 15**). The middle lamella is the outer shell, composed by pectins and responsible for gluing the neighbouring cells together. The plasma membrane is a lipid bilayer with associated proteins, where certain sugars, amino acids and inorganic ions can also be found (Flint et al., 2012; Fry, 2017). The primary cell wall occurs between the middle lamella and the plasma membrane, and is composed of a cellulose scaffold interlinked with a variety of hemicelluloses (basically, xyloglucans) and embedded in an amorphous pectin matrix (Goulao and Oliveira, 2008).

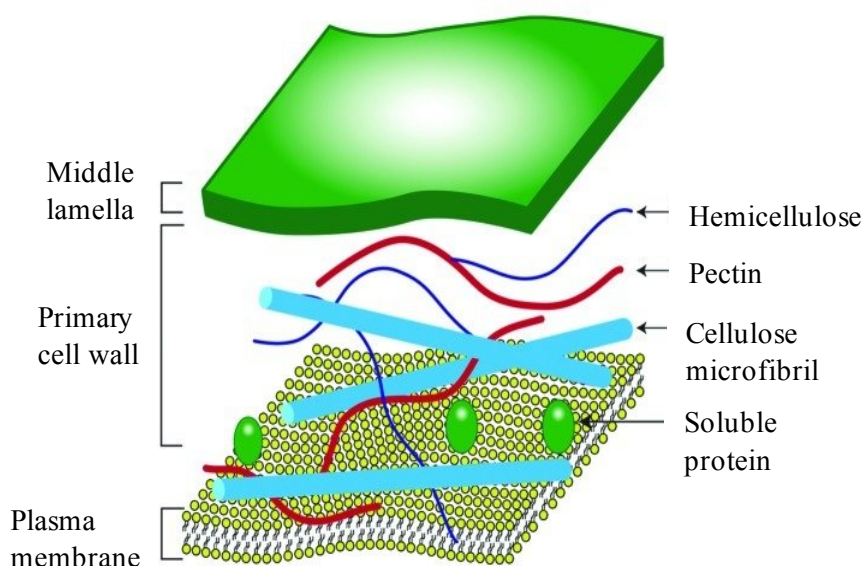


Figure 15. Simplified model of plant cell wall structure (Flint et al., 2012).

Introduction

In fruits, the pectin backbone is composed by homogalacturonans, comprised of α -(1,4)-linked D-galacturonic acid residues, frequently esterified to methyl groups, and branched rhamnogalacturonan I (α -D-galacturonosyl and rhamnosyl residues) displaying neutral sugars in the side-chains (**Figure 16**). In olive fruit, L-arabinosyl residues are a main component of rhamnogalacturonan I side-chains, whereas D-galactosyl residues are predominant in other fruit types (Kumar, Ali and Baboota, 2019; Wang et al., 2018). The pectin matrix plays a key role in defining the mechanical properties of fruits by preventing the aggregation and collapse of cell wall internal structure, and thus fruit softening (Koziol et al., 2017). The primary cell wall network also includes minor components such as phenolic compounds, proteins, enzymes and receptor-interacting molecules (Cosgrove, 2001).

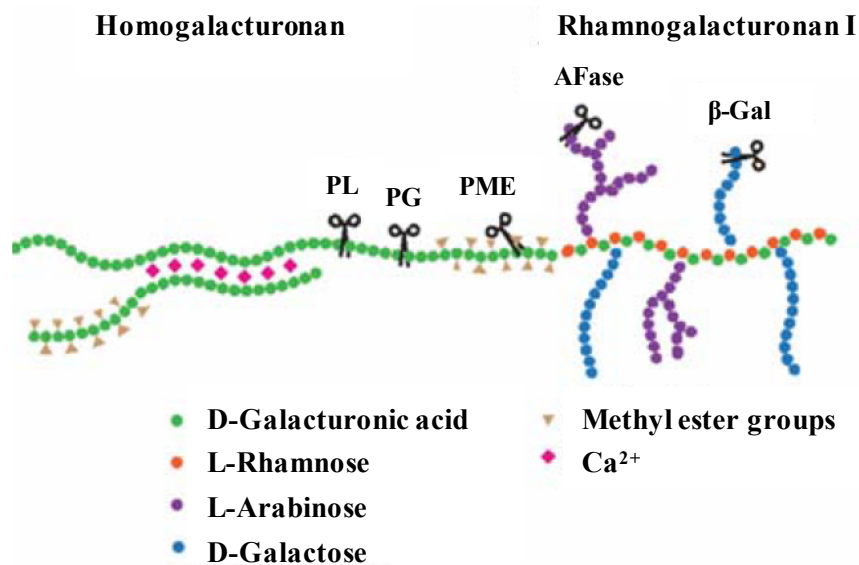


Figure 16. Model of pectin structure in fruits showing the main sugar component and link types, and some related enzymes (Wang et al., 2018).

*Abbreviations: AFase, α -L-arabinofuranosidase; β -Gal, β -galactosidase; PG, polygalacturonase; PL, pectate lyase; PME, pectin methylesterase.

During fruit ripening, the primary cell walls and middle lamellae undergo substantial disruption, which causes changes in cell wall structure and properties. These alterations are largely responsible for turgor and ripening-related firmness loss. This phenomenon involves polysaccharide solubilisation and rearrangements carried out by pectolytic and non-pectolytic enzymes. In some fruit species such as olive (Marsilio et al., 2000; González-Cabrera, Domínguez-Vidal and Ayora-Cañada, 2018), it can also include polysaccharide depolymerisation. For the present Thesis, a representative selection of pectolytic enzymes were considered, including polygalacturonase (*exo*-PG; EC 3.2.1.67 and *endo*-PG; EC 3.1.2.15), pectate lyase (PL; EC 4.2.2.2), pectin methylesterase (PME; EC 3.1.1.11), α -L-arabinofuranosidase (AFase; EC 3.2.1.55) and β -galactosidase (β -Gal; EC 3.2.1.23). PME, PG and PL are pectin backbone-acting enzymes, which release methyl groups esterified to the carboxyl moieties of galacturonic acid residues, hydrolyse previously de-esterified homogalacturonans, and release de-esterified pectin-backbone sugar monomers, respectively. PME demethylating action on galacturonans is required for subsequent PG and PL activity (Koziol et al., 2017). PME action can exert a dual effect on cell wall status, contingent upon additional factors: while it decreases the degree of methyl esterification of pectin hence facilitating PG and PL activity, it can also improve cell wall strength since demethylation exposes negatively charged carboxyl moieties which then can form calcium cross-bridges. A recent study on

'Arbequina' olives (Lara et al., 2018) suggested a more relevant action for PL and PME than for PG on ripening-related firmness loss. The action of backbone-acting enzymes is favoured by enzymes acting on pectin side-chains, such as AFase and β -Gal, as the removal of neutral sugars from pectin branches will result in increased size of pectin pores and aid the access of other enzymes to their pectin backbone substrates.

Non-pectolytic enzymes selected were the hemicellulose-acting endo-1,4- β -D-glucanase (EGase; EC 3.2.1.4) and β -xylosidase (β -Xyl; EC 3.2.1.37), which cleave the β -1,4 glucosidic linkages and release xylosyl residues from the xylan backbone, respectively (Goulao and Oliveira, 2008). Decreased yields of the cellulosic and hemicellulosic fractions observed during ripening of 'Hojiblanca' olives were associated to high EGase activity levels in ripe fruit (Jiménez et al., 2001), and these non-pectic fractions were suggested to undergo more intense modifications during fruit ripening than pectins.

Non-enzymatic mechanisms also take part in cell wall modifications. To our best knowledge, though, no published study has focused on these mechanisms in olive fruit. For other fruit species such as banana (*Musa spp.*), longan (*Dimocarpus Longan* Lour) and cherry fruit (*Prunus avium* L.) (Cheng et al., 2008; Duan et al., 2011; Belge et al., 2015), ascorbic acid (AA) and its derivatives have been shown to play an important role in the oxidative disassembly of cell wall polysaccharides. Therefore, a range of compounds (AA, phenolics) and properties (radical scavenging activity) related to oxidative processes were also analysed herein in order to obtain a more complete overview of cell wall modifications in ripening olive fruit.

For the study of ripening-related cell wall modifications, cell wall materials are usually extracted, fractionated and analysed. Extraction can be carried out in boiling ethanol, which allows the recovery of the alcohol-insoluble residue (AIR), which is then fractionated sequentially through further extraction in water, in a chelating solution and in basic solutions of increasing pH. This sequential process allows the separation of cell wall fractions ever more tightly bound, namely readily soluble materials, non-covalently-bound pectins, covalently-bound pectins and hemicelluloses. Subsequent sugar and uronic acid analyses of each fraction provide information on the solubilisation and disassembly processes. For 'Arbequina' olives, for instance, pectin side-chain removal during the final phase of fruit ripening was shown through decreased content of neutral sugars in the sodium carbonate-soluble fraction, enriched in covalently-bound pectins (Lara et al., 2018).

The mineral content is related to crop yield and to quality parameters in fruit (Netsby et al., 2014). For example, boron (B) deficiency could produce deformed fruits and a premature fall. Calcium (Ca), in turn, plays a key role in cell wall structure as it forms cross-bridges between adjacent demethylated galacturonic acid residues, which aid the reinforcement of cell walls and firmness preservation. Furthermore, a positive correlation may reportedly exist between olive fly infestation and the content of potassium (K) and iron (Fe) in different olive cultivars (Garantonakis et al., 2016). K and Ca are the most abundant minerals in olive fruit, followed by magnesium (Mg) and sodium (Na) (Nergiz and Engez, 2000; Fernández-Hernández et al., 2010). Mineral content in olive fruits, as in any other fruit, depends on several factors including climatic conditions, location, soil type, cultural practices, cultivar and maturity stage (López, García and Garrido, 2008; Sahan, 2010).

E. Relation between cuticle and cell wall metabolism

During the ripening and postharvest periods, disassembly of fruit cell walls poses great mechanical stress on the fruit cuticle to maintain fruit integrity. The cuticle so helps to establish and to maintain a functional and well-defined epidermis (Ingram and Nawrath, 2017). The concurrence of high epidermal cell density and cuticle thickness may help alleviating the mechanical stress, as this bring about higher cuticle resistance to deformation with a reduction of fruit cracking incidence (Correia et al., 2018; Jiang et al., 2019). Furthermore, fruit firmness levels are also associated with water loss in some species (Saladié et al., 2007; Paniagua et al., 2013), which hints a relationship to cuticle composition and structure. Thus, fruit softening may be related not only to cell wall modifications, but also to cuticle characteristics.

In order to find possible relationships between cuticle and cell wall composition and structure during olive fruit development, it is necessary to understand the physical and chemical modifications as affected by internal (cultivar and maturity stage) and external (growing area, agronomic practices, soil, temperature, water availability) factors potentially affecting quality indicators of fruit and oil. These data would also widen current understanding of cuticle impacts on susceptibility or resistance to olive fly infestation (Iannotta et al., 2007; Rizzo and Lombardo, 2007; Vichi et al., 2016) and to other pests and diseases. This knowledge should contribute to improve production, handling, manufacturing and commercialisation of olive fruit, olive oil and the rest of derived products.

F. References

- Alba J, Hidalgo F, Ruiz MA, Martinez F, Moyano MJ, Cert A, Pérez-Camino MC, Ruiz MV. 1996. Características de los aceites de oliva de primera y segunda centrifugación. *Grasas y Aceites*. 47, 163-181.
- Abenoza M, Raso J, Oria, R, Sánchez-Gimeno AC. 2018. Modulating the bitterness of ‘Empeltre’ olive oil by partitioning polyphenols between oil and water phases: Effect on quality and shelf life. *Food Sci. Technol. Int.* 25, 47-55.
- Aparicio R, Harwood J. 2013. *Handbook of olive oil: analysis and properties*. (ISBN 9781461477761).
- Arnan X, López BC, Martínez-Vilalta J, Estorach M, Poyatos R. 2012. The age of monumental olive trees (*Olea europaea*) in northeastern Spain. *Dendrochronologia*. 30, 11-14.
- Baker EA, Procopiou. 2000. The leaf and fruit cuticles of selected drought tolerant plants. *Acta Hort.* 527, 85-93.
- Belge B, Comabella E, Graell J, Lara I. 2015. Post-storage cell wall metabolism in two sweet cherry (*Prunus avium* L.) cultivars displaying different postharvest performance. *Food Sci. Technol. Int.* 21, 416-427.
- Besnard G, Terral JF, Cornille A. 2018. On the origins and domestication of the olive: A review and perspectives. *Ann. Bot.* 121, 385-403.
- Bianchi G, Murelli C, Vlahov G. 1992. Surface waxes from olive fruits. *Phytochemistry* 31, 3503-3506.

Bianchi G. 1995. Plant Waxes. In Waxes: chemistry, molecular biology and functions. (ISBN 97809514117157).

Boskou D. 1998. Química y tecnología del aceite de oliva. (ISBN 8489922063).

Burrack HJ, Zalom FG. 2008. Olive Fruit Fly (Diptera: Tephritidae) Ovipositional Preference and Larval Performance in Several Commercially Important Olive Varieties in California. *J. Econ. Entomol.* 101, 750-758.

Buschhaus C, Jetter R. 2011. Composition differences between epicuticular and intracuticular wax substructures: How do plants seal their epidermal surfaces? *J. Exp. Bot.* 62, 841-853.

Burghardt M, Riederer M. 2006. Cuticular transpiration. In *Biology of the plant cuticle*. Chapter 9. (ISBN 9781405132688).

Camacho-Vázquez C, Ruiz-May E, Guerrero-Analco JA, Elizalde-Contreras JM, Enciso-Ortiz EJ, Rosas-Saito G, López-Sánchez L, Kiel-Martínez AL, Bonilla-Landa I, Monribot-Villanueva JL, Olivares-Romero JL, Gutiérrez-Martínez P, Tafolla-Arellano JC, Tiznado-Hernandez ME, Quiroz-Figueroa FR, Birke A, Aluja M. 2019. Filling gaps in our knowledge on the cuticle of mangoes (*Mangifera indica*) by analyzing six fruit cultivars: Architecture/structure, postharvest physiology and possible resistance to fruit fly (Tephritidae) attack. *Postharvest Biol. Technol.* 148, 83-96.

Camin F, Larcher R, Nicolini G, Bontempo L, Bertoldi D, Perini M, Schlicht C, Schellenberg A, Thomas F, Heinrich K, Voerkelius S, Horacek M, Ueckermann H, Froeschl H, Wimmer B, Heiss G, Baxter B, Rossmann A, Hoogewerff J. 2010. Isotopic and elemental data for tracing the origin of European olive oils. *J. Agric. Food Chem.* 58, 570-577.

Casado C, Heredia A. 2001. Self-association of plant wax components: a thermodynamic analysis. *Biomacromolecules.* 2, 407-409.

Casanovas. 2012. Metabolismo de compuestos fenólicos y estudio de aceites de oliva singulares de la provincia de Lleida. PhD dissertation. Universidad de Lleida. Spain.

Chen S, Li Y, Bi Y, Yin Y, Ge Y, Wang Y. 2014. Solvent effects on the ultrastructure and chemical composition cuticular wax and its potential bioactive role against *Alternaria alternata* in Pinguoli pear. *J. Integr. Agric.* 13, 1137-1145.

Cheng G, Duan X, Shi J, Lu W, Luo Y, Jiang W, Jiang Y. 2008. Effects of reactive oxygen species on cellular wall disassembly of banana fruit during ripening. *Food Chem.* 109, 319-324.

Christopoulo E, Larazaki M. 1997. Variations in free and esterified alcohols of olive oils during storage. *Riv. Ital. Sostanze Grasse.* 74, 191-200.

Connor DJ, Gómez-del-Campo M, Rousseaux MC, Searles PS. 2014. Structure, management and productivity of hedgerow olive orchards: A review. *Sci. Hortic.* 169, 71-93.

Correia S, Schouten R, Silva AP, Gonçalves B. 2018. Sweet cherry fruit cracking mechanisms and prevention strategies: a review. *Sci. Hortic.* 240, 369-377.

Cosgrove, DJ. 2001. Wall structure and wall loosening. A look backwards and forwards. *Plant Physiol.* 125, 131-134.

Domínguez E, Heredia-Guerrero JA, Heredia A. 2011. The biophysical design of plant cuticles: An

Introduction

overview. *New Phytol.* 189, 938-949.

Domínguez E, Heredia-Guerrero JA, Heredia A. 2015. Plant cutin genesis: Unanswered questions. *Trends Plant Sci.* 20, 551-558.

Duan X, Zhang H, Zhang D, Sheng J, Lin H, Jiang Y. 2011. Role of hydroxyl radical in modification of cell wall polysaccharides and aril breakdown during senescence of harvested longan fruit. *Food Chem.* 128, 203-207.

Dzubak P, Hajduch M, Vydra D, Hustova A, Kvasnica M, Biedermann D, Markova L, Urban M, Sarek J. 2006. Pharmacological activities of natural triterpenoids and their therapeutic implications. *Nat. Prod. Rep.* 23, 394-411.

EC Regulation 510/2006. Protection of geographical indications and designations of origin for agricultural products and foodstuffs. *Off. J. Eur. Commun.* L93/12 31.3.2006.

Economopoulos AP. 1972. Sexual competitiveness of γ -ray sterilized males of *Dacus oleae*. Mating frequency of artificially reared and wild females. *Environ. Entomol.* 1, 490-497.

EEC Regulation 2568/91. Characteristics of olive oil and olive-residue oil and the relevant methods of analysis. *Off. J. Eur. Union.* L 266/9 16.10.2015.

España L, Heredia-Guerrero JA, Segado P, Benítez JJ, Heredia A, Domínguez E. 2014. Biomechanical properties of the tomato (*Solanum lycopersicum*) fruit cuticle during development are modulated by changes in the relative amount of its components. *New Phytol.* 202, 790-802.

Famiani F, Proietti P, Nasini L. 2005. Speciale Raccolta delle olive. *Olivo Olio.* 7, 32-51.

Food and Agricultural Organization of the United Nations (FAO). 2019. (<https://www.fao.org>).

Fernández-Hernández A, Mateos R, García-Mesa JA, Beltran G, Fernández-Escobar R. 2010. Determination of mineral elements in fresh olive fruits by flame atomic spectrometry. *Span. J. Agric. Res.* 8, 1183-1190.

Flint HJ, Scott KP, Duncan SH, Louis P, Forano E. 2012. Microbial degradation of complex carbohydrates in the gut. *Gut Microbes.* 3, 289-306.

Franke R, Briesen I, Wojciechowski T, Faust A, Yephremov A, Nawrath C, Schreiber L. 2005. Apoplastic polyesters in Arabidopsis surface tissues - A typical suberin and a particular cutin. *Phytochemistry.* 66, 2643-2658.

Fry SC. 2016. Cells. *Encycl. Appl. Plant Sci.* 1, 174-184.

Garantonakis N, Varikou K, Markakis E, Birouraki A, Sergentani C, Psarras G, Koubouris GC. 2016. Interaction between *Bactrocera oleae* (Diptera: Tephritidae) infestation and fruit mineral element content in *Olea europaea* (Lamiales: Oleaceae) cultivars of global interest. *Appl. Entomol. Zool.* 51, 257-265.

González-Cabrera M, Domínguez-Vidal A, Ayora-Cañada MJ. 2018. Hyperspectral FTIR imaging of olive fruit for understanding ripening processes. *Postharvest Biol. Technol.* 145, 74-82.

Goulao LF, Oliveira CM. 2008. Cell wall modifications during fruit ripening: when a fruit is not the fruit. *Trends Food Sci. Technol.* 19, 4-25.

Graça J, Lamosa P. 2010. Linear and branched poly(ω -hydroxyacid) esters in plant cutins. *J. Agric. Food Chem.* 58, 9666-9674.

Gümusay B, Ozilbey U, Ertem G, Oktar A. 1990. Studied on the susceptibility of some important table and oil olive cultivars of Aegean Region to olive fly (*Dacus oleae* Gmel.) in Turkey. *Acta Hortic.* 286, 359-361.

Heredia A, Domínguez E. 2014. The plant cuticle: a complex lipid barrier between the plant and the environment. An overview. In NATO Science for peace and security series A: Chemistry and biology. (ISSN 1874-6489).

Hermoso JF, Plana J, Romero A, Tous J. 2008. Performance of six olive oil cultivars in the south of Catalonia (Spain). *Acta Hortic.* 791, 333-337.

Huang H, Burghardt M, Schuster AC, Leide J, Lara I, Riederer M. 2017. Chemical composition and water permeability of fruit and leaf cuticles of *Olea europaea* L. *J. Agric. Food Chem.* 65, 8790-8797.

Huang H, Jiang Y. 2019. Chemical composition of the cuticle membrane of pitaya fruits (*Hylocereus polyrhizus*). *Agriculture.* 9, 1-10.

Iannotta N, Perri L, Tocci C, Zaffina F. 1999. The behaviour of different olive cultivars following attacks by *Bactrocera oleae* (Gmel). *Acta Hortic.* 474, 545-548.

Iannotta N, Noce ME, Ripa V, Scalercio S, Vizzarri V. 2007. Assessment of susceptibility of olive cultivars to the *Bactrocera oleae* (Gmelin, 1790) and *Camarosporium dalmaticum* (Thüm.) Zachos & Tzav. –Klon. attacks in Calabria (Southern Italy). *J. Environ. Sci. Health B.* 42, 789-793.

Inglese P. 2011. Factors affecting extra-virgin olive oil composition. *Hortic. Rev.* 38, 83-147.

Ingram G, Nawrath C. 2017. The roles of the cuticle in plant development: organ adhesion and beyond. *J. Exp. Bot.* 68, 5307-5321.

International Olive Council (IOC). 2020. (<https://www.internationaloliveoil.org/>).

Jetter R, Riederer M. 2016. Localization of the transpiration barrier in the epi- and intracuticular waxes of eight plant species: Water transport resistances are associated with fatty acyl rather than alicyclic components. *Plant Physiol.* 170, 921-934.

Jiang F, López A, Jeon S, Tonetto de Freitas S, Yu Q, Wu Z, Labavitch JM, Tian S, Powell ALT, Mitcham E. 2019. Disassembly of the fruit cell wall by the ripening-associated polygalacturonase and expansin influences tomato cracking. *Hortic. Res.* 6, 17.

Jiménez A, Rodríguez R, Fernández-Caro I, Guillén R, Fernández-Bolaños J, Heredia A. 2001. Olive fruit cell wall: degradation of cellulosic and hemicellulosic polysaccharides during the ripening. *J. Agric. Food Chem.* 49, 2008-2013.

Juan ME, Wenzel U, Daniel H, Planas JM. 2010. Olive fruit extracts and HT-29 human colon cancer cells. In *Olives and olive oil in health and disease prevention*. Chapter 145. (ISBN 978-0-12-374420-3).

Khanal BP, Knoche M. 2017. Mechanical properties of cuticles and their primary determinants. *J. Exp. Bot.* 68, 5351-5367.

Kiritsakis AK. 1990. *Olive oil*. (ISBN 0935315322).

Introduction

Knoche M, Beyer M, Peschel S, Oparlakow B, Bukovac MJ. 2004. Changes in strain and deposition of cuticle in developing sweet cherry fruit. *Physiol. Plant.* 120, 667-677.

Koch K, Barthlott W. 2009. Superhydrophobic and superhydrophilic plant surfaces: an inspiration for biomimetic materials. *Phil. Trans. R. Soc. A.* 367, 1487-1509.

Kozioł A, Cybulska J, Pieczywek PM, Zdunek A. 2017. Changes of pectin nanostructure and cell wall stiffness induced *in vitro* by pectinase. *Carbohydrate Polymers.* 161, 197-207.

Kombargi WS, Michelakis SE, Petrakis CA. 1998. Effect of olive surface waxes on oviposition by *Bactrocera oleae* (Diptera: Tephritidae). *J. Econ. Entomol.* 91, 993-998.

Kumar S, Ali J, Baboota S. 2019. Polysaccharide nanoconjugates for drug solubilization and targeted delivery. *Polysaccharide Carriers for Drug Delivery.* Elsevier Ltd. Amsterdam. p 443-475.

Kunst L, Samuels L. 2009. Plant cuticles shine: advances in wax biosynthesis and export. *Curr. Opin. Plant Biol.* 12, 721-727.

Lara I, Belge B, Goulao LF. 2014. The fruit cuticle as a modulator of postharvest quality. *Postharvest Biol. Technol.* 87, 103-112.

Lara I, Albrecht R, Comabella E, Riederer M, Graell J. 2018. Cell-wall metabolism of 'Arbequina' olive fruit picked at different maturity stages. *Acta Hort.* 1199, 133-138.

Lara I, Heredia A, Domínguez E. 2019. Shelf life potential and the fruit cuticle: the unexpected player. *Front. Plant Sci.* 10, 770.

Léchaudel M, López-Lauri F, Vidal V, Sallanon H, Joas J. 2013. Response of the physiological parameters of mango fruit (transpiration, water relations and antioxidant system) to its light and temperature environment. *J. Plant Physiol.* 170, 567-576.

Leide J, Hildebrandt U, Reussing K, Riederer M, Vogg G. 2007. The developmental pattern of tomato fruit wax accumulation and its impact on cuticular transpiration barrier properties: effects of a deficiency in a β -ketoacyl-coenzyme A synthase (LeCER6). *Plant Physiol.* 144, 1667-1679.

Levi F, Pasche C, La Vecchia C, Lucchini F, Franceschi S. 1999. Food groups and colorectal cancer risk. *Br. J. Cancer.* 79, 1283-1287.

Li Y, Yin Y, Chen S, Bi Y, Ge Y. 2014. Chemical composition of cuticular waxes during fruit development of Pingguoli pear and their potential role on early events of *Alternaria alternata* infection. *Funct. Plant Biol.* 41, 313-320.

López A, García P, Garrido A. 2008. Multivariate characterization of table olives according to their mineral nutrient composition. *Food Chem.* 106, 369-378.

López-Casado G, Matas AJ, Domínguez E, Cuartero J, Heredia A. 2007. Biomechanics of isolated tomato (*Solanum lycopersicum* L.) fruit cuticles: the role of the cutin matrix and polysaccharides. *J. Exp. Bot.* 58, 3875-3883.

Mailer RJ, Ayton J, Graham K. 2010. The influence of growing region, cultivar and harvest timing on the diversity of Australian olive oil. *J. Am. Oil Chem. Soc.* 87, 877-884.

- Marsilio V, Lanza B, Campestre C, De Angelis M. 2000. Oven-dried table olives: Textural properties as related to pectic composition. *J. Sci. Food Agric.* 80, 1271-1276.
- Martin LBB, Rose JKC. 2014. There's more than one way to skin a fruit: formation and functions of fruit cuticles. *J. Exp. Bot.* 65, 4639-4651.
- Matas AJ, López-Casado G, Cuartero J, Heredia A. 2005. Relative humidity and temperature modify the mechanical properties of isolated tomato fruit cuticles. *Am. J. Bot.* 92, 462-468.
- McDonald RE, Nordby HE, McCollum TG. 1993. Epicuticular wax morphology and composition are related to grapefruit chilling injury. *HortScience* 28, 311-312.
- Moggia C, Graell J, Lara I, Schmeda-Hirschmann G, Thomas-Valdés S, Lobos GA. 2016. Fruit characteristics and cuticle triterpenes as related to postharvest quality of highbush blueberries. *Sci. Hortic.* 2011, 449-457.
- Morelló JR, Romero MP, Motilva MJ. 2004. Effect of the maturation of the olive fruit on the phenolic fraction of drupes and oils from 'Arbequina', 'Farga', and 'Morrut' cultivars. *J. Agric. Food Chem.* 52, 6002-6009.
- Nardi F, Carapelli A, Dallai R, Roderick GK, Frati F. 2005. Population structure and colonization history of the olive fly, *Bactrocera oleae* (Diptera, Tephritidae). *Mol. Ecol.* 14, 2729-2738.
- Nawrath C, Porier Y. 2008. Pathways for the synthesis of the polyesters in plants: cutin, suberin, and polyhydroxyalkanoates. Pages 201-239. (ISSN 1755-0408).
- Nergiz C, Engez Y. 2000. Compositional variation of olive fruit during ripening. *Food Chem.* 69, 55-59.
- Netsby R, Lieten F, Pivot D, Lacroix CR, Tagliavini M. 2005. Influence of mineral nutrients on strawberry fruit quality and their accumulation in plant organs: a review. *Int. J. Fruit Sci.* 5, 139-156.
- Ninot A, Howad W, Aranzana MJ, Senar R, Romero A, Mariotti R, Baldoni L, Belaj A. 2018. Survey of over 4,500 monumental olive trees preserved on-farm in the northeast Iberian Peninsula, their genotyping and characterization. *Sci. Hortic.* 231, 253-264.
- Ninot A, Howad W, Romero A. 2019. Les varietats catalanes d'olivera. In *Quaderns agraris (Institució Catalana d'Estudis Agraris)*. 46, 7-36. (ISSN 0213-0319).
- Panigua AC, East AR, Hindmarsh JP, Heyes JA. 2013. Moisture loss is the major cause of firmness change during postharvest storage of blueberry. *Postharvest Biol. Technol.* 79, 13-19.
- Parsons EP, Popovskiy S, Lohrey GT, Lü S, Alkalai-Tuvia S, Perzelan Y, Paran I, Fallik E, Jenks MA. 2012. Fruit cuticle lipid composition and fruit post-harvest water loss in an advanced backcross generation of pepper (*Capsicum* sp.). *Physiol. Plantarum.* 146, 15-25.
- Petit J, Bres C, Just D, Garcia V, Mauxion J, Marion D, Bakan B, Joubès J, Domergue F, Rothan C. 2014. Analyses of tomato fruit brightness mutants uncover both cutin-deficient and cutin-abundant mutants and a new hypomorphic allele of GDSL lipase. *Plant Physiol.* 164, 888-906.
- Pfündel EE, Agati G, Cerovic ZC. 2006. Optical properties of plant cuticles. In *Biology of the plant cuticle*. Chapter 6. (ISBN 9781405132688).

Introduction

Rallo L, Barranco D, Caballero JM, Del Río C, Martín A, Tous J, Trujillo I. 2005. Variedades del olivo en España. (ISBN 8484761924).

Ranalli A, Serraiocco A. 1996. Evaluation of characteristics of olive oil produced by innovative or traditional processing technologies. Riv. Ital. Sostanze Grasse. 71, 303-315.

Reina-Pinto JJ, Yephremov A. 2009. Surface lipids and plant defenses. Plant Physiol. Biochem. 47, 540-549.

Riederer M, Schreiber L. 2001. Protecting against water loss: analysis of the barrier properties of plant cuticles. J. Exp. Bot. 52, 2023-2032.

Rizzo R, Lombardo A. 2007. Factors affecting the infestation due to *Bactrocera oleae* (Gmelin) in several Sicilian olive cultivars. In Proceedings of the 2nd International Seminar Olivebioteq. p 291-298.

Rodríguez-Morató J, Xicota L, Fitó M, Farré M, Dierssen M, de la Torre R. 2015. Potential role of olive oil phenolic compounds in the prevention of neurodegenerative diseases. Molecules. 20, 4655-4680.

Romero A. 2012. Caracterización y diferenciación de los aceites vírgenes de oliva de la comarca del Priorat (Tarragona), dentro del mercado global de aceites de la variedad 'Arbequina'. PhD dissertation. Universidad de Lleida, Spain.

Sahan Y. 2010. Some metals in table olives. In Olives and olive oil in health and disease prevention. Chapter 32. (ISBN 978-0-12-374420-3).

Saladié M, Matas AJ, Isaacson T, Jenks MA, Goodwin SM, Niklas KJ, Xiaolin R, Labavitch JM, Shackel KA, Fernie AR, Lytovchenko A, O'Neill MA, Watkins CB, Rose JKC. 2007. A reevaluation of the key factors that influence tomato fruit softening and integrity. Plant Physiol. 144, 1012-1028.

Samuels L, Kunst L, Jetter R. 2008. Sealing Plant Surfaces: Cuticular Wax Formation by Epidermal Cells. Annu. Rev. Plant Biol. 59, 683-707.

Shepherd T, Griffiths DW. 2006. The effects of stress on plant cuticular waxes. New Phytol. 171, 469-499.

Serrano M, Coluccia F, Torres M, L'Haridon F, Métraux J. 2014. The cuticle and plant defense to pathogens. Front. Plant Sci. 5, 274.

Szakiel A, Pączkowski C, Pensec F, Bertsch C. 2012. Fruit cuticular waxes as a source of biologically active triterpenoids. Phytochem. Rev. 11, 263-284.

Tafolla-Arellano JC, Báez-Sañudo R, Tiznado-Hernández ME. 2018. The cuticle as a key factor in the quality of horticultural crops. Sci. Hortic. 232, 145-152.

Tedeschi G, Benitez JJ, Ceseracciu L, Dastmalchi K, Itin B, Stark RE, Heredia A, Athanassiou A, Heredia-Guerrero JA. 2018. Sustainable fabrication of plant cuticle-like packaging films from tomato pomace agro-waste, beeswax, and alginate. ACS Sustain. Chem. Eng. 6, 14955-14966.

Therios I. 2009. Olives. In Crop production science in horticulture 18. (ISBN 9781845934583).

Tombesi A, Faminani F, Proietti P, Guelfi P. 1996. Manual, integrated and mechanical olive harvesting: efficiency and effects on trees and oil quality. Ezzaitouna, Revue scientifique de l'oléiculture et de l'oléotechnie. 2, 93-101.

Tous J, Romero A. 1993. Variedades del olive: con especial referencia a Cataluña. (ISBN 84-7664-376-4).

Tous J, Romero A. 1998. 'Marfil' olive. HortScience. 33, 162-163.

Tous J, Franquet JM. 2019. Olivo y aceites de calidad. (ISBN 9788417050955)

Tripoli E, Gianmarco M, Di Majo D, Gianmarco S, La Guardia M, Grescimanno M. 2006. The phenolic compounds of olive oil and human health. In Proceedings of the 2nd International Seminar Olivebioteq. Special Seminars and invited lectures. p 265-271.

Trivedi P, Nguyen N, Hykkerud AL, Häggman H, Martinussen I, Jaakola L, Karppinen K. 2019. Developmental and environmental regulation of cuticular wax biosynthesis in fleshy fruits. Front. Plant Sci. 10, 431.

Tsubaki S, Sugimura K, Teramoto Y, Yonemori K, Azuma J. 2013. Cuticular membrane of *Fuyu* Persimmon fruit is strengthened by triterpenoid nano-fillers. PLoS One 8, 1-13.

Vichi S, Cortés-Francisco N, Caixach J, Barrios G, Mateu J, Ninot A, Romero A. 2016. Epicuticular wax in developing olives (*Olea europaea*) is highly dependent upon cultivar and fruit ripeness. J. Agric. Food Chem. 64, 5985-5994.

Wang J, Sun L, Xie L, He Y, Luo T, Sheng L, Luo Y, Zeng Y, Xu J, Deng X, Cheng Y. 2016. Regulation of cuticle formation during fruit development and ripening in 'Newhall' navel orange (*Citrus sinensis* Osbeck) revealed by transcriptomic and metabolomic profiling. Plant Sci. 243, 131-144.

Wang D, Yeats TH, Uluisik S, Rose JKC, Seymour GB. 2018. Fruit softening: revisiting the role of pectin. Trends Plant Sci. 23, 302-310.

Ward G, Nussinovitch A. 1996. Gloss properties and surface morphology relationship of fruits. J. Food. Sci. 61, 973-977.

Xue D, Zhang X, Lu X, Chen G, Chen Z. 2017. Molecular and evolutionary mechanisms of cuticular wax for plant drought tolerance. Front. Plant Sci. 8, 621.

Yeats TH, Rose JKC. 2013. The formation and function of plant cuticles. Plant Physiol. 163, 5-20.

Ziv C, Zhao Z, Gao YG, Xia Y. 2018. Multifunctional roles of plant cuticles during plant-pathogen interactions. Front. Plant Sci. 9, 1088.

Objectives

The main objective of the current research was to characterize the cuticle and the cell wall composition of olive fruits as affected by different internal and external factors, as well as their impact on fruit quality attributes and on susceptibility to infestations and rots. A choice of relevant Spanish and Catalan cultivars were selected for the present Thesis and studied at different ripening stages, with particular focus on 'Arbequina' as the main cultivar in PDOs 'Les Garrigues' and 'Siurana'.

This information may be relevant for the conservation of currently underused secondary and local varieties.

An additional goal of the present Thesis was to evaluate how cuticular wax profiles of fruit may affect the wax profiles and other commercial quality characteristics of the corresponding monovarietal olive oils.

Therefore, the following specific objectives were defined:

1.1– To characterize and to compare cuticle composition and cell wall metabolism in fruit of nine olive cultivars ('Arbequina', 'Argudell', 'Empeltre', 'Farga', 'Manzanilla', 'Marfil', 'Morrut', 'Picual' and 'Sevillenca') at three different maturation stages (green, turning and ripe).

1.2– To carry out a more detailed characterization of cuticle and cell wall changes in 'Arbequina' fruit during ripening and over-ripening (September to January).

1.3– To evaluate the influence of agronomic factors (irrigation, growing area, producing season) on cuticle composition and cell wall metabolism in 'Arbequina' fruit.

1.4– To assess possible relationships between cuticle and cell wall characteristics and the susceptibility to infestations, rots, and other alterations of fruit.

1.5– To characterize wax profiles, sensory attributes and chemical quality parameters of monovarietal olive oil extracted from the nine cultivars considered, and to determine whether they may be affected by fruit cuticular wax composition.

1.6– To compare olive fruit cuticle composition and properties with those of fruit and leaves of *Prunus laurocerasus* L., an unrelated species. This complementary study was carried out in the course of a research stay at the University of Würzburg (Germany), with the purpose of illustrating species-related differences in cuticle features and of studying in detail the water-proofing properties of cuticles.

Plant material, methodology and work plan

The experimental work of the present Thesis was divided into three main experiments. **Experiment 1** consisted of a comparative study of cuticle and cell wall composition among nine olive cultivars at three different maturity stages. Moreover, the experiment was completed with a study of the characteristics of monovarietal oils obtained from olives collected at the usual maturity stage for oil production. **Experiment 2** was a study of changes in cuticle and cell wall composition in ‘Arbequina’ fruit during on-tree ripening as affected by irrigation, season-to-season variability and production area. Finally, **Experiment 3** was undertaken in the course of a research stay at the University of Würzburg, in which fruit and leaf cuticles of *Prunus laurocerasus* L. were analysed at three different maturity stages. Results from the latter experiment were aimed at comparing with olive results in order to obtain a wider overview of plant cuticles.

A. Plant material

For **Experiment 1**, olive fruits of nine cultivars (‘Arbequina’, ‘Argudell’, ‘Empeltre’, ‘Farga’, ‘Manzanilla’, ‘Marfil’, ‘Morrut’, ‘Picual’ and ‘Sevillena’) were used. All of them were harvested at the 2016/17 season from an experimental orchard located in IRTA-Mas Bové (Constantí, Tarragona, **Figure 17**), located within the geographical area covered by PDO ‘Siurana’. The orchard was established in 1991 with a plantation frame of 7 x 5 m, and was supported with drip irrigation. Olive oil from each cultivar was extracted at the 2018/19 season, and stored immediately at 4 °C until analysis.



Figure 17. Rain-fed ‘Arbequina’ olive tree grown at IRTA-Mas Bové (Constantí, Tarragona). November 11th 2018.

For **Experiment 2**, ‘Arbequina’ fruit samples were picked at two PDOs (‘Les Garrigues’ and ‘Siurana’) from rain-fed and irrigated orchards, during two consecutive productive seasons (2017/18 and 2018/19 seasons). Olives were collected periodically at eight time points between September and January of each season, from a commercial orchard located in El Soleràs (Lleida; PDO ‘Les Garrigues’) and from the same experimental orchard as in Experiment 1 (IRTA-Mas Bové, Constantí; PDO ‘Siurana’).

For **Experiment 3**, fruits and leaves of cherry laurel (*Prunus laurocerasus* L.) were harvested at the Botanical Garden at the Julius von Sachs Institute of Biological Science (University of Würzburg, **Figure 18**) in early September of year 2019.



Figure 18. Cherry laurel tree (*Prunus laurocerasus* L.) grown at the Botanical Garden (Julius von Sachs Institute of Biological Science, Würzburg, Germany), September 9th 2019.

B. Methodology and work plan

Table 1 shows the chronogram corresponding to the research activities carried out in the frame of this Thesis. Each experiment was split into different tasks. The experimental methodology used in each case is described in detail in the corresponding Chapter.

Table 1. Work plan of the experimental part carried out of the present thesis.

	2016-17	2017-18	2018-19	Chapter
Experiment 1: Study of nine cultivars				
Task 1.1 Fruit characterization				I, II, III
Task 1.2 Fruit cuticle				I
Task 1.3 Cell wall metabolism				II
Task 1.4 Monovarietal olive oils				III
Experiment 2: ‘Arbequina’ study				
Task 2.1 Fruit characterization				IV, V
Task 2.2 Fruit cuticle				IV
Task 2.3 Cell wall metabolism				V
Experiment 3: <i>Prunus laurocerasus</i> study				
Task 3.1 Fruit and leaf characterization				VI
Task 3.2 Fruit and leaf cuticle				

Experiment 1: A comparison of cuticle and cell wall composition in fruit of nine olive cultivars at three maturity stages. Determination of wax profiles in monovarietal olive oils.

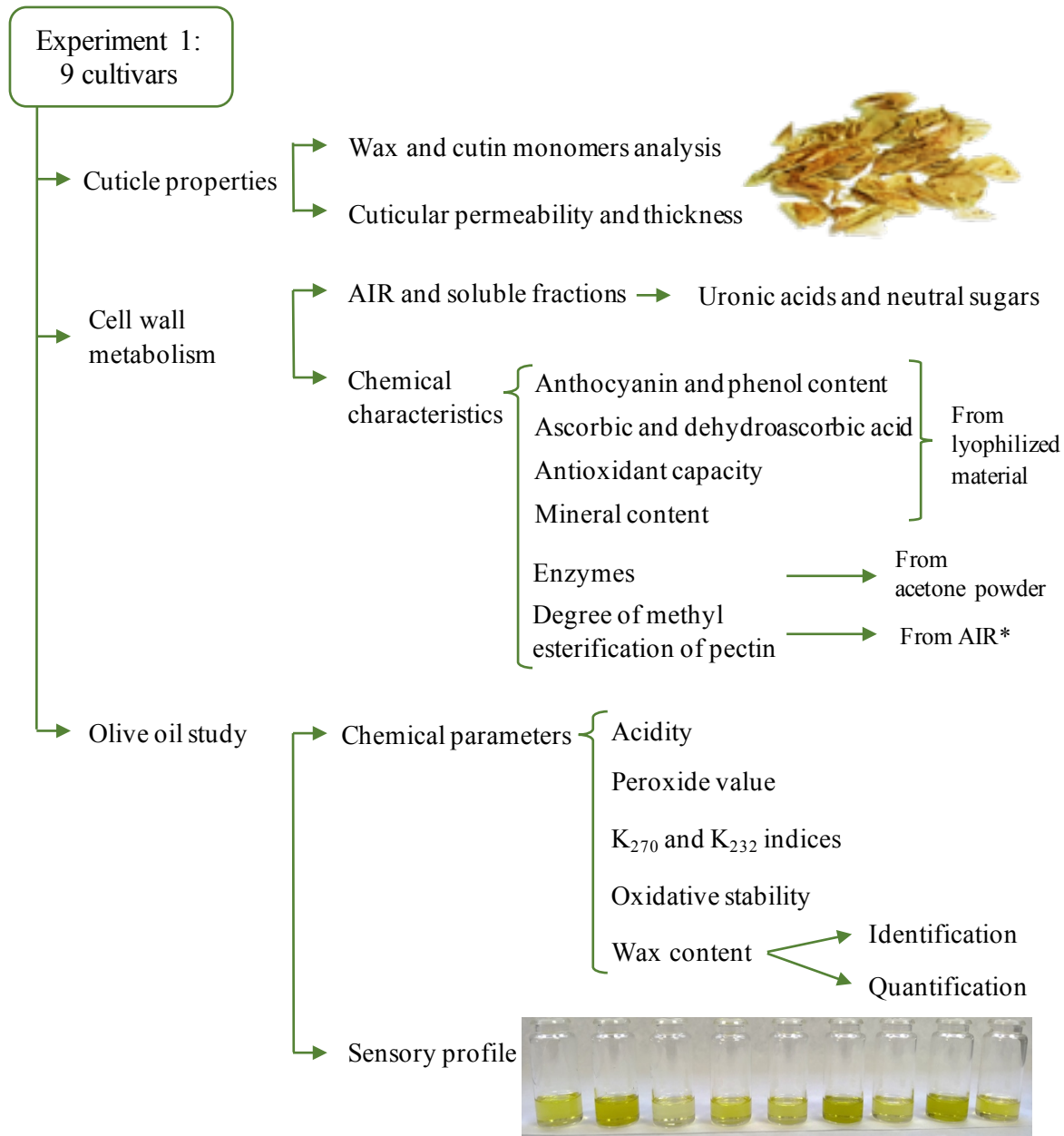


Figure 19. Diagram of the experimental work carried out for Experiment 1: Study of nine autochthonous olive cultivars at three different maturity stages. Upper image: Fruit cuticles isolated enzymatically from ‘Arbequina’ fruit. Bottom image: Samples of monovarietal oils extracted from ‘Arbequina’, ‘Argudell’, ‘Empeltre’, ‘Farga’, ‘Manzanilla’, ‘Marfil’, ‘Morrut’, ‘Picual’ and ‘Sevillenca’ olives, in that order. *Abbreviations: AIR, alcohol-insoluble residue.

Olive fruits from nine cultivars were picked at the green, turning and ripe stages. For ‘Manzanilla’, ‘Marfil’, and ‘Sevillenca’ cultivars, analysis at the turning stage was not possible, since owing to differing ripening patterns nor enough fruit at that maturity point were found at the sampling date. A diagram of the analyses undertaken is shown (Figure 19). For cuticle and cell wall characterization, fruit were picked in 2016. Samples for oil extraction and analysis were harvested in 2018.

For fruit characterization, the maturity index, weight, length, humidity, firmness and strength, olive oil yield, incidence of alterations, and toluidine blue (TB) test were determined (Task 1.1).

Fruit cuticle properties (Task 1.2) were determined from enzymatically isolated cuticles. Cuticular waxes were then extracted in chloroform, and thereafter identified and quantified using gas chromatography-mass spectroscopy (CG-MS) and gas chromatography with a flame ionization detector (CG-FID), respectively. Cutin was extracted from dewaxed cuticles through depolymerisation in methanol-HCl, and constituent monomers identified and quantified as for waxes. Finally, cuticle thickness was measured under a light microscope after Sudan IV staining, and water permeance was determined gravimetrically.

For the study of cell wall metabolism in all nine selected olive cultivars (Task 1.3), the alcohol-insoluble residue (AIR) was prepared, followed by sequential AIR fractionation as described in Chapter II. Uronic acid and neutral sugar contents were determined in each fraction. The degree of methyl esterification was analysed in AIR samples. Activity assays of cell wall-modifying enzymes (β -Xyl, EGase, PG, PL, PME, AFase, β -Gal) were undertaken on acetone powders (AP). The antioxidant capacity and the content of total anthocyanins, total phenolics, ascorbic acid and dehydroascorbic acid contents were analysed on samples of lyophilized fruit pericarp.

Finally, samples of monovarietal oils extracted from fruit of each cultivar were also analysed (Task 1.4). Acidity, peroxide values, K_{270} and K_{232} indices, oxidative stability, sensory profiles and wax contents and profiles were determined.

Experiment 2: Study of ‘Arbequina’ olive fruit during on-tree ripening and over-ripening: The influence of the irrigation regime and year-to-year variability.

The same determinations and analyses as in Experiment 1 were carried out on ‘Arbequina’ fruit harvested from irrigated and rain-fed orchards at two consecutive productive seasons (2017-18 and 2018-19) and at two PDOs (‘Les Garrigues’ and ‘Siurana’). Cuticle composition was characterized at both seasons. Cell wall metabolism and cuticle thickness were studied at the 2017-18 season uniquely.

Experiment 3: Cuticle properties of *Prunus laurocerasus* fruits and leaves. A comparison with the olive fruit.

Cuticle properties of fruit and leaves of *Prunus laurocerasus* were studied in order to provide a comparison with olive fruit, the focus of the present Thesis, and to gain better insights in the water-proofing properties of cuticles. Cherry laurel leaves were also included in the study in order to assess possible organ-related differences. This experiment was undertaken between September and December 2019, and the corresponding explanatory diagram is shown (**Figure 20**).

Fruit and leaf samples were first characterized in terms of fresh and dry weight, and surface area, and then morphological traits were calculated, namely water content, specific surface area and mass per surface area. For leaves, dry matter content, degree of succulence and degree of sclerophylly were also calculated (Task 3.1). For the profiling of cuticular waxes and cutin monomers, fruit and leaf cuticles were isolated enzymatically. Chloroform and boron trifluoride were used to extract cuticular waxes and cutin monomers, respectively. Both extraction procedures showed only minor differences with the methodology used for olive fruit. Identification and quantification were also carried out by GC-MS and GC-

FID, correspondingly, with slightly different chromatographic conditions as compared with the olive work (see **Chapter VI**). The melting point of waxes was determined by Fourier Transform Infrared (FTIR) spectroscopy. Cuticular permeability to water was determined gravimetrically by three different methods: (a) fruit cuticle permeability was determined by placing intact fruits at different temperatures, (b) on the envelope (stomata-free surface of the adaxial side) of intact leaves placed at 10, 25 and 40 °C, and (c) on isolated leaf cuticles mounted on transpiration chambers at 25 °C. Finally, cuticle thickness and the presence of stomata and wax crystals were assessed on the surface of cherry laurel cuticles through fluorescence microscopy and scanning electron microscopy (SEM), respectively (Task 3.2).

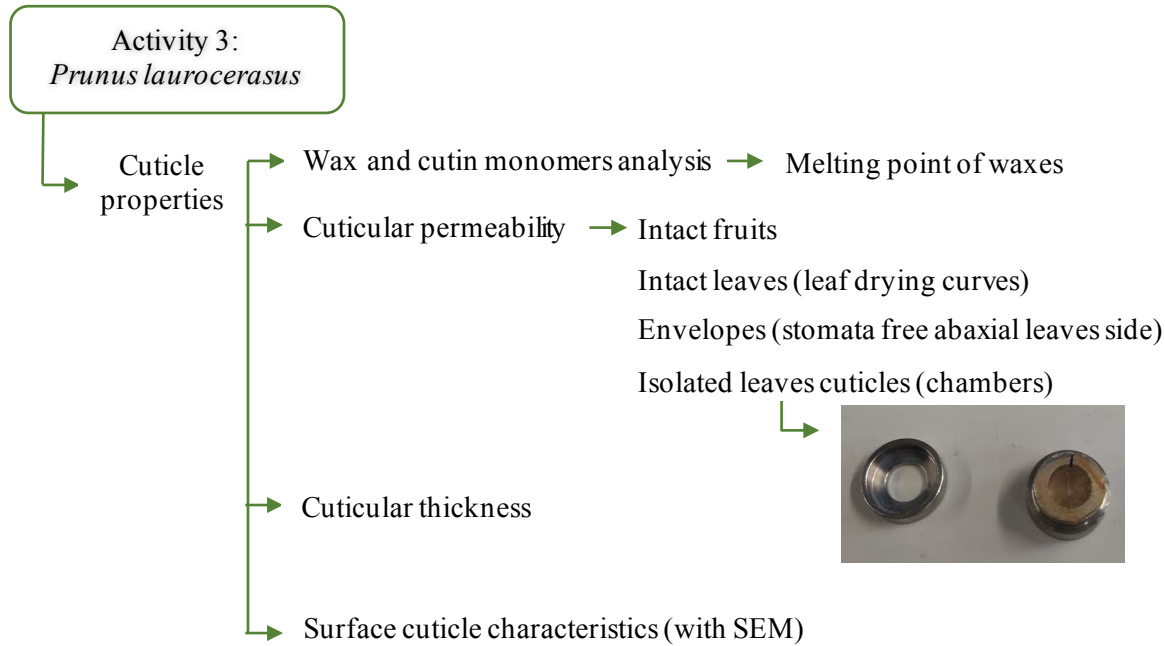


Figure 20. Diagram of the experimental work carried out for Experiment 3: Chemical and functional characterization of leaf and fruit cuticles of *Prunus laurocerasus*.

Results

SECTION I. A survey of nine olive cultivars

**Fruit cuticle and cell wall composition at three maturation stages.
Composition of waxes in nine monovarietal olive oils.**

Chapter I: Insights into olive fruit surface functions: a comparison of cuticular composition, water permeability, and surface topography in nine cultivars during maturation



ORIGINAL RESEARCH
published: 19 November 2019
doi: 10.3389/fpls.2019.01484



Insights Into Olive Fruit Surface Functions: A Comparison of Cuticular Composition, Water Permeability, and Surface Topography in Nine Cultivars During Maturation

Clara Diarte^{1,2}, Po-Han Lai³, Hua Huang^{4†}, Agustí Romero⁵, Tomás Casero¹, Ferran Gatiús¹, Jordi Graell^{1,2}, Vicente Medina^{1,6}, Andrew East⁷, Markus Riederer⁴ and Isabel Lara^{1,2*}

Frontiers in Plant Science (November 2019), 10, 1484. doi: 10.3389/fpls.2019.01484

Clara Diarte, Po-Han Lai, Hua Huang, Agustí Romero, Tomás Casero, Ferran Gatiús, Jordi Graell, Vicente Medina, Andrew East, Markus Riederer and Isabel Lara.

Abstract

Olive (*Olea europaea* L.) growing has outstanding economic relevance in Spain, the main olive oil producer and exporter in the world. Fruit skin properties are very relevant for fruit and oil quality, water loss, and susceptibility to mechanical damage, rots, and infestations, but limited research focus has been placed on the cuticle of intact olive fruit. In this work, fruit samples from nine olive cultivars ('Arbequina', 'Argudell', 'Empeltre', 'Farga', 'Manzanilla', 'Marfil', 'Morrut', 'Picual', and 'Sevillencia') were harvested from an experimental orchard at three different ripening stages (green, turning, and ripe), and cuticular membranes were enzymatically isolated from fruit skin. The total contents of cuticular wax and cutin significantly differed among cultivars both in absolute and in relative terms. The wax to cutin ratio generally decreased along fruit maturation, with the exception of 'Marfil' and 'Picual'. In contrast, increased water permeance values in ripe fruit were observed uniquely for 'Argudell', 'Morrut', and 'Marfil' fruit. The toluidine blue test revealed surface discontinuities on green samples of 'Argudell', 'Empeltre', 'Manzanilla', 'Marfil', and 'Sevillencia' fruit, but not on 'Arbequina', 'Farga', 'Morrut', or 'Picual'. No apparent relationship was found between water permeability and total wax coverage or the results of the toluidine blue test. The composition of cuticular waxes and cutin monomers was analysed in detail, and sections of fruit pericarp were stained in Sudan IV for microscopy observations. Skin surface topography was also studied by means of fringe projection, showing large differences in surface roughness among the cultivars, 'Farga' and 'Morrut' fruits displaying the most irregular surfaces. Cultivar-related differences in cuticle and surface features of fruit are presented and discussed.

Keywords: *Olea europaea* L.; cuticular wax; cutin; maturity stage; water permeance; skin surface topography

Except the vine, there is no plant which bears a fruit of as great importance as the olive.
Pliny the Elder (attributed)

1.1. Introduction

The olive (*Olea europaea* L.) tree is considered one of the oldest crops to have been domesticated by humans (Besnard, Terral and Cornille, 2018). Around 90% of the world production of olives is used for the production of olive oil, and the rest is employed for the manufacture of table olives¹. More than half of the total world olive production is grown in countries in the Mediterranean basin, Spain being the main olive oil producer and exporter in the world.

In Mediterranean areas, crops often develop under adverse environmental conditions, including restricted water availability, high temperatures, or elevated UV irradiation levels, which are expected to exacerbate in a scenario of global climate change. The performance of a given genotype under such conditions, as well as its resistance against pests and diseases, will be partly dependent upon the properties of fruit surface, which will act as the interface between the plant and the surrounding environment. Being the outer layer of the epidermis, the cuticle represents the first barrier against abiotic and biotic stress factors.

Plant cuticles are hydrophobic layers covering the epidermis of aerial, non-lignified plant organs, including the intact fruit. The cuticle scaffold is composed of the polyester cutin, an insoluble polymer matrix mostly containing hydroxy-, carboxy-, and epoxy-C₁₆ and C₁₈ fatty acids (Lequeu et al., 2003; Franke et al., 2005; Domínguez, Heredia-Guerrero and Heredia, 2011; Camacho- Vázquez et al., 2019). Different types of cuticular waxes, both in amorphous and crystalline form, and a variable amount of phenolics are integrated within or accumulate onto the surface of the cutin matrix (Samuels, Kunst and Jetter, 2008; Yeast and Rose, 2013; Lara, Belge and Goulao, 2014). The cuticle is considered to limit transpirational water loss to prevent the desiccation of the fruit, but it also confers or modulates relevant properties such as the susceptibility to mechanical damage, infestations, and rots (Kunst and Samuels, 2002; Lara et al., 2014; Martin and Rose, 2014; Serrano et al., 2014; Riederer et al., 2015; Wang et al., 2016).

In spite of these considerations, very few published studies have addressed the composition of cuticles of intact olive fruit. Most of them have focused uniquely on cuticular waxes (Bianchi, Murelli and Vlahov, 1992; Guinda et al., 2010; Vichi et al., 2016), whereas only one published study has also reported on cutin composition in fruit of this species (Huang et al., 2017). Compositional differences have been detected according to cultivar and maturation stage. These differences may relate to the water-proofing and mechanical properties of the cuticle, and thus be relevant for fruit resistance to abiotic and biotic stress-inducing factors.

In this study, olive fruit from nine oil- and table-cultivars differing in important quality traits were selected for the analysis of chemical composition and water permeability at three different maturity stages. With the purpose of widening the study on fruit surface differences across the considered genotypes, skin topography was non-destructively assessed by means of fringe projections (East et al., 2016). The bulk of results should help a better comprehension of the factors determining olive adaptations to the surrounding environment.

1.2.0. International Olive Council (IOC). (2018). Statistics (<http://www.internationaloliveoil.org/>).

1.2. Material and methods

1.2.1. Plant material and toluidine blue test

Fruit samples from nine olive (*Olea europaea* L.) autochthonous Spanish cultivars ('Arbequina', 'Argudell', 'Empeltre', 'Farga', 'Manzanilla', 'Marfil', 'Morrut', 'Picual', and 'Sevillanca') were hand-collected at an experimental orchard located at IRTA-Mas Bové (Constantí, Spain; 41°09' N, 1°12' E; altitude 100 m) from trees supplied with drip irrigation. Annual rainfall is 500 mm, and takes place mainly in April– May and September. Fertilization and cultural practices at the orchard are the usual in the producing area. Olives were picked at three different maturity stages (green, turning, and ripe) based on skin color during the usual harvest period (September to December) in 2016. Maturity index (0–7), fresh weight (g), flesh-to-stone ratio, and water content (% humidity) were determined on 50 fruits per cultivar and maturity stage. For the assessment of length and diameter (mm), 10 fruits were used (**Table 1**). Maturity index was scored on a 0–7 scale by subjectively categorizing each fruit within the sample according to skin and flesh color (Uceda and Frías, 1975); values indicate the weighted average of the 50 olives examined. Olive fly infestation was likewise assessed on 50 fruits per cultivar and maturity stage, by visually checking each fruit for egg deposition, and data shown as a percentage (**Supplementary Table S1**). In order to visualize possible discontinuities on fruit surface, samples of fresh olives at the green stage (10 fruits per cultivar) were stained in a toluidine blue (TB) solution (0.05%, w/v) for 2 h (Tanaka et al., 2004), rinsed, and allowed to dry in air. Since ripe 'Marfil' fruit turn white rather than black, the TB test was applied also to these samples.

1.2.2. Cuticle isolation

Disks of fruit exocarp (two disks per fruit) were excised with a cork borer. Thirty to 75 olives, depending on fruit size, were processed so to obtain around 100 cm² of skin per cultivar and maturity stage as described elsewhere (Belge et al., 2014a). Because not enough skin sample can be obtained from one individual olive fruit to enable further analysis of cuticle composition, excised skin disks were pooled into one sample of biological material. Exocarp samples were distributed in two tubes (50 cm² per tube) for the enzymatic isolation of cuticular membranes (CM). Disks were incubated at 37°C in cellulase/pectinase solution (0.2% (w/v) cellulase, 100 U ml⁻¹ pectinase, and 1 mM NaN₃ in 50 mM citrate buffer at pH 4.0 until no more material was released, and then washed in citrate buffer (50 mM, pH 4.0) until no material was left in suspension. After thoroughly rinsing in distilled water, CM disks were dried at 40°C, weighted, and then pooled and kept in hermetically capped vials until analysis. Cuticle yields were expressed per unit of fruit surface area (µg cm⁻²).

1.2.3. Extraction and analysis of cuticular wax

CM samples (20 mg/replicate × 3 technical replicates) were dewaxed in chloroform (2 mg mL⁻¹) for 24 h at room temperature, with constant shaking. Chloroform extraction was done three times, and the chloroform extracts were pooled, incubated 15 min in an ultrasonic bath and filtered. Dewaxed CM (DCM) were dried and kept in hermetically capped vials for subsequent analysis of cutin monomers. The chloroform extracts were concentrated at 40 °C using a rotatory evaporator, and waxes then transferred to a pre-weighed vial, dried in a vacuum concentrator at 40°C until complete dryness, and weighed to calculate total wax yields (µg cm⁻²). Dotriacontane (C32) was then added as an internal standard, and samples were derivatized during 15 min at 100 °C in N,O-bis(trimethylsilyl)trifluoroacetamide (BSTFA) and pyridine (3:2, v/v), in order to obtain trimethylsilyl (TMSi) ethers and esters from free hydroxyl and carboxyl groups, respectively.

Wax samples (1 μL) were injected in on-column mode into a gas chromatography-mass spectrometry (GC-MS) system for compound identification and quantification. This GC equipment (Agilent 7890N) was coupled with a quadrupole mass selective detector (Agilent 5973N) and equipped with a capillary column (DB 5 MS UI, 30 m \times 0.25 mm \times 0.25 μm ; SGE Europe Ltd., Milton Keynes, UK). Compounds were identified by comparison with their retention times with those of standards, and through their electron ionization-mass spectra using a mass spectral library (NIST 11 MS). Chromatographic conditions were as follows: oven was set at 100 $^{\circ}\text{C}$ for 1 min, then raised by 15 $^{\circ}\text{C min}^{-1}$ to 200 $^{\circ}\text{C}$, then by 5 $^{\circ}\text{C min}^{-1}$ to 310 $^{\circ}\text{C}$, and finally held 10 min at 310 $^{\circ}\text{C}$. Helium was used as the carrier gas at 1.0 ml min^{-1} . A flame ionization detector (FID) was used for quantitative analysis of cuticular waxes, in the same chromatographic conditions as described above excepting that, at the last step, the oven was held at 310 $^{\circ}\text{C}$ for 13 min and that a higher carrier gas flow (1.3 mL min^{-1}) was used. Data are expressed as a relative percentage (% over total waxes). Average chain length (ACL) of acyclic wax compounds was calculated as the weighted average number of carbon atoms, defined as

$$ACL = \frac{\sum C_n n}{\sum C_n}$$

where C_n is the percentage of each acyclic wax compound with n carbon atoms.

1.2.4. Extraction and analysis of cutin monomers

DCM samples (roughly 10 mg/replicate \times 3 technical replicates) were hydrolyzed for 2 h in 2 mL of 1 M HCl in 100% MeOH, esterified in the same solution during 2 h at 80 $^{\circ}\text{C}$, and added 2 mL saturated NaCl after cooling down. Cutin monomers were extracted three consecutive times in 2 ml hexane for 10 min using a mixer and centrifuged at 20 $^{\circ}\text{C}$. The collected supernatants were pooled and transferred into a pre-weighed vial, dried completely using a vacuum concentrator at 40 $^{\circ}\text{C}$, and then weighed to calculate total cutin yields ($\mu\text{g cm}^{-2}$). Heptadecanoate (C_{17}) and tricosanoate (C_{23}) were added as internal standards, and then samples were derivatized during 15 min at 100 $^{\circ}\text{C}$ in BSTFA and pyridine (3:2, v/v). Derivatized samples (1 μL) were finally injected in on-column mode into a GC-MS and a GC-FID system for compound identification and quantification, respectively, under the same chromatographic conditions as described above for the analysis of cuticular waxes.

1.2.5. Determination of cuticular transpiration

Transpiration from the whole fruit was determined gravimetrically from measures of water loss over time as described elsewhere (Huang et al., 2017). Eight to twelve olives per sample were sealed with paraffin wax on the pedicel area (melting point 65 $^{\circ}\text{C}$; Roth, Karlsruhe, Germany). To reduce the relative humidity until approximately zero, fruit samples were placed in boxes over silica gel (AppliChem, Darmstadt, Germany) and kept at 25 $^{\circ}\text{C}$ in an incubator (IPP 110, Memmert, Schwabach, Germany). Weight loss of the samples was monitored over time (five to six data points per individual sample) with an analytic electronic balance with ± 0.1 mg precision (MC-1 AC210S, Sartorius, Göttingen, Germany). Temperature inside the incubator was controlled continuously with a digital thermometer (Testoterm 6010, Lenzkirch, Germany) and the actual fruit temperature was measured using an infrared laser thermometer (Harbor Freight Tools, Calabasas, California). Transpiration rates (flux of water vapor; J in $\text{g m}^{-2}\text{s}^{-1}$) of the samples were calculated from changes in the fresh weight (ΔW in g) over time (Δt in s) and surface area (A in m^2) as indicated below:

$$J = \frac{\Delta W}{\Delta t \cdot A}$$

The permeance (P in m s^{-1}) was calculated from the transpiration rate (J) divided by the driving force:

$$P = \frac{J}{c_{wv}^* (a_{fruit} - a_{air})}$$

where c_{wv}^* was the water vapor content of air at saturation, obtained from tabulated values, a_{fruit} was the water activity in the fruit, which was assumed to be unity, and a_{air} was air water activity (that was close to zero).

1.2.6. Skin surface topography

Micro-topography of samples (25 olives per cultivar) was captured at two locations (180° apart) on the equatorial area of each individual fruit using fringe projection equipment (Primos™ Lite, Cranfield Image System, USA). Topography data were collected with an x-y resolution of $26.83 \mu\text{m}$ and z (vertical) resolution of $2 \mu\text{m}$. Subsequent calculations to extract surface roughness descriptive parameters (Lai et al., 2018) were conducted with the accompanying proprietary software package (Primos™ v5.8, Cranfield Image Systems, USA).

Surface roughness parameters studied in this work were Sa , Stm , Spm , Svm , Sk , and S (Gadelmawla et al., 2002). Sa is the arithmetic average height parameter, defined as the mean of the absolute deviation of roughness irregularities from the mean line. Stm describes the mean distance between the lowest valley and the highest peak at the measured area. Spm is defined as the mean of the maximum height peaks, and Svm is the mean of the maximum depth valleys. Sk measures peak-to-valley surface roughness after excluding the predominant peaks and valleys, and hence illustrates the core roughness depth. S is the only horizontal parameter, defined as the average spacing between profile peaks at the mean line in the profile measured.

1.2.7. Microscopy observations

Pericarp fruit samples were chopped to little cubes (roughly 2 mm per side) and fixed in a formaldehyde-acetic acid (FAA) solution [5% (v/v) formaldehyde and 5% (v/v) glacial acetic acid in 1:1 (v/v) ethanol-distilled water] for 12 h. Samples were dehydrated in aqueous solutions containing increasing ethanol concentrations up to 100% (v/v). Dehydrated samples were transferred to Eppendorf tubes for infiltration and polymerization in Technovit 7100® resin (Heraeus Kulzer GmbH, Wehrheim, Germany), and the resin was dried at 45°C for 24 h.

Resin-embedded samples were cut in $4\text{-}\mu\text{m}$ -thick sections using an ultramicrotome (Leica EM UC6, Leica Microsystems GmbH, Wetzlar, Germany), and subsequently stained on a slide for 15 min in a Sudan IV lysochrome solution [5% (w/v) in 85% (v/v) ethanol] in order to visualize the lipidic constituents of fruit cuticles. Excess staining was removed by rinsing in 50% (v/v) ethanol, and samples allowed to dry at room temperature. Olive pericarp sections were observed and photographed using a microscope (Leica DM4000 B) with a coupled camera (Leica DFC300 FX). Cuticle thickness was determined from five images obtained from five different fruit per cultivar and maturity stage with the Fiji image processing software (Schindelin et al., 2012).

1.2.8. Statistical analysis

The statistical analyses were conducted with the JMP® Pro 13 software. Results were calculated as means \pm standard deviations. Multifactorial analysis of variance (ANOVA) procedures were applied,

with cultivar and maturation stage as the factors, and means were compared with LSD test ($P \leq 0.05$). PCA was used to help the interpretation of the data set obtained, using the Unscrambler software, version 9.1.2 (CAMO ASA, Oslo, Norway). Data were centered and weighed by the inverse of the run as a validation procedure.

1.3. Results

Olive cultivars assessed in this study included some preferentially used for oil production ('Argudell', 'Picual', 'Sevillenca'), for manufacturing of table olives ('Empeltre', 'Manzanilla'), or for both purposes. The choice of genotypes comprised representatives of very early ('Empeltre', 'Manzanilla'), early ('Sevillenca'), medium ('Arbequina', 'Argudell', 'Farga', 'Picual'), and late ('Marfil', 'Morrut') ripening patterns (Tous and Romero, 1993), as well as a range of fruit sizes (**Table 1**). Due to differing ripening patterns, data corresponding to the turning stage are lacking for three cultivars ('Manzanilla', 'Marfil', and 'Sevillenca'), as not enough fruit material was found at the sampling dates. The highest flesh to stone ratios, weight, and water contents were found for 'Manzanilla', a very common table olive cultivar in Spain. The highest incidence of olive fly infestation was observed for 'Empeltre' and 'Manzanilla', which showed very high percentages of affected fruits, particularly in unripe olives (**Supplementary Table S1**).

1.3.1. Surface differences

Differences in surface characteristics were found among the nine olive cultivars assessed. Green fruits were stained with toluidine blue in order to visualize pores, cracks, or defects on the surface. Two groups of cultivars were revealed by the TB test: fruits of 'Argudell', 'Empeltre', 'Manzanilla', 'Marfil', and 'Sevillenca' were stained, whereas those of 'Arbequina', 'Farga', 'Morrut', and 'Picual' were not, even after leaving the fruit samples in the staining solution for several hours.

Differences in skin topography of green fruit among the cultivars were also detected. 'Farga' and 'Morrut' fruits showed the most irregular surface as shown by higher values of vertical roughness parameters (S_a , S_{tm} , S_{pm} , S_{vm} , and S_k). On the contrary, fruit of 'Sevillenca', 'Empeltre', 'Arbequina', and 'Argudell' had smoother skin surface than other cultivars based on lower values of vertical parameters together with higher horizontal roughness as shown by S_x , representative of peak-to-peak spacing (**Table 2**). 'Farga' samples displayed very different micro-topography and visual appearance as revealed by fringe projection data in comparison with other cultivars. In order to highlight the distinctive features of the surface of 'Farga' olives, a boxplot of S_a as the most common roughness parameter is provided (**Supplementary Figure S1**). Three-dimensional diagrams of raw data obtained from fringe projections, TB staining, and micrographs of Sudan IV-stained pericarp cross-sections for 'Farga' and 'Sevillenca' fruit are shown as an example to illustrate these differences (**Figure 1**), while results for the rest of cultivars assessed are presented as supplementary figures (**Supplementary Figures S2, S3, and S4** respectively). The surface of 'Sevillenca' green olives was not only smoother than that of 'Farga' at the same maturity stage, but also displayed significantly thicker cuticles (**Table 3** and **Figure 1**).

Table 1. Toluidine blue test and physical characteristics of olive fruit used in this study.

Cultivar	Maturity stage	Sampling date	Maturity Index	Weight (g)	F:S ratio*	Water content (%)	Length (mm)		Diameter (mm)		TB test*
'Arbequina'	Green	Sept 29	0.26	1.10	2.68	53.9	14.1	ab D	12.1	b CD	-
	Turning	Sept 29	2.14	1.27	3.18	55.2	13.4	b C	12.0	b B	ne
	Ripe	Nov 27	3.40	1.59	4.24	58.2	14.7	a D	13.0	a DE	ne
'Argudell'	Green	Sept 29	0.26	2.02	4.08	56.0	18.6	a C	13.9	b BC	+
	Turning	Nov 27	0.96	2.65	5.32	59.2	20.1	a B	15.3	ab A	ne
	Ripe	Nov 27	2.36	2.81	5.57	59.6	20.0	a BC	15.9	a B	ne
'Empeltre'	Green	Sept 29	0.48	3.18	4.05	56.1	23.7	a A	15.2	a B	+
	Turning	Sept 29	3.58	3.09	4.40	55.4	23.0	a A	15.0	a A	ne
	Ripe	Nov 27	5.00	3.13	4.00	49.3	24.1	a A	15.0	a BCD	ne
'Farga'	Green	Sept 29	0.36	1.28	2.47	54.8	16.9	b CD	10.8	b C	-
	Turning	Sept 29	2.04	1.74	3.18	58.7	19.0	a B	12.5	a B	ne
	Ripe	Nov 27	4.40	1.82	3.70	55.8	18.1	a C	12.0	a E	ne
'Manzanilla'	Green	Sept 29	0.12	4.57	8.31	70.1	24.0	a A	18.6	a A	+
	Ripe	Nov 27	5.88	4.65	7.68	66.6	23.9	a A	19.4	a A	ne
'Marfil'	Green	Sept 29	0.04	1.32	2.05	60.1	19.7	b BC	10.5	b C	+
	Ripe	Dec 12	0.96	1.98	3.95	53.6	21.6	a AB	13.3	a CDE	+
'Morrut'	Green	Sept 29	0.16	1.99	2.03	51.6	20.4	b BC	13.8	b BC	-
	Turning	Nov 27	1.04	2.34	2.52	51.1	20.4	b B	13.8	b A	ne
	Ripe	Jan 16	3.40	2.08	2.74	37.6	21.8	a AB	15.5	a BC	ne
'Picual'	Green	Sept 29	0.30	2.72	2.75	57.2	22.4	a AB	15.1	a B	-
	Turning	Nov 27	2.84	3.06	3.11	60.2	22.2	a AB	15.3	a A	ne
	Ripe	Nov 27	3.88	4.30	4.35	49.6	24.1	a A	17.3	a AB	ne
'Sevillenca'	Green	Sept 29	0.32	2.71	3.09	56.7	21.4	a ABC	14.1	a BC	+
	Ripe	Nov 27	3.16	3.32	4.97	52.0	22.1	a AB	15.5	a BC	ne

Values represent means of 50 fruits for maturity index, weight, F:S ratio, and water content, and of 10 fruits for length, diameter, and TB test. Different capital letters denote significant differences among the cultivars for a given maturation stage, and different lower-case letters stand for significant differences among maturation stages for a given cultivar, at $P \leq 0.05$ (LSD test). Fruit weight, F:S ratio, and water content were determined jointly for 50 fruits, and values reported represent the average of the 50 olives assessed. Maturity index values indicate the weighted average of the 50 olives within the sample (Uceda and Frías, 1975).

*Abbreviations: F:S ratio, flesh to stone ratio; TB test, toluidine blue test (Tanaka et al., 2004): stained and non-stained fruits are denoted respectively as + and -; ne, not evaluated.

Table 2. Surface roughness parameters (μm) measured in olive fruit at the green stage.

Cultivar	<i>Sa</i>		<i>Stm</i>		<i>Spm</i>		<i>Svm</i>		<i>Sk</i>		<i>S</i>	
‘Arbequina’	8.5	de	54.4	d	25.4	d	-29.0	a	27.0	de	839.4	a
‘Argudell’	8.5	de	58.4	d	27.8	d	-30.6	a	27.0	de	772.6	bc
‘Empeltre’	7.4	e	51.3	d	24.3	d	-27.1	a	23.5	e	818.2	ab
‘Farga’	20.6	a	98.7	a	49.8	a	-48.9	c	60.2	a	678.6	e
‘Manzanilla’	11.2	bc	76.5	bc	36.8	bc	-39.7	b	36.8	b	699.0	de
‘Marfil’	9.8	cd	69.1	c	33.4	c	-35.7	b	30.5	cd	735.1	cd
‘Morrut’	12.8	b	80.7	b	40.7	b	-40.0	b	39.3	b	654.8	e
‘Picual’	10.0	cd	72.7	bc	34.8	c	-37.9	b	32.1	c	678.5	e
‘Sevillenca’	7.4	e	51.4	d	24.7	c	-26.7	a	23.5	e	739.5	cd

Sa, *Stm*, *Spm* and *Svm* are related to vertical roughness, *Sk* represents core roughness, and *S* stands for horizontal roughness. Values represent means of 25 individual fruit per cultivar. Means followed by the different letters within a column are significantly different at $P \leq 0.05$ (LSD test).

1.3.2. Cuticle characteristics and changes along maturation

With the exception of ‘Arbequina’, cuticle yields (mg cm^{-2} surface area) did not change significantly along fruit maturation (**Table 3**). Total cuticle amounts at the green and the ripe stages ranged from 1.9 to 3.1 mg cm^{-2} and from 2.0 to 3.8 mg cm^{-2} , respectively. At both maturity stages, the lowest yields were observed for ‘Manzanilla’ fruit. Consistent with the lowest cuticle yields, ‘Manzanilla’ olives also displayed the lowest values for cuticle thickness, irrespective of maturity stage. Cuticle thickness remained steady along on-tree maturation in five (‘Argudell’, ‘Farga’, ‘Manzanilla’, ‘Marfil’, and ‘Picual’) out of the nine cultivars studied, while a significant decrease was observed for the rest of the genotypes (‘Arbequina’, ‘Empeltre’, ‘Morrut’, and ‘Sevillenca’) (**Table 3**).

Water permeance was determined in mature fruit of all nine cultivars studied. Two cultivar types could be defined according to permeability levels: a low-permeance group, including ‘Arbequina’, ‘Empeltre’, ‘Farga’, ‘Manzanilla’, ‘Picual’, and ‘Sevillenca’ and displaying water permeance values ranging from 7.21 (‘Manzanilla’) to 8.13 (‘Picual’) $\times 10^{-5} \text{ m s}^{-1}$, and a high-permeance cultivar set (‘Argudell’, ‘Marfil’, and ‘Morrut’) showing water permeance values above $11 \times 10^{-5} \text{ m s}^{-1}$ (**Table 3**). No changes in water permeance levels were observed along maturation for ‘Arbequina’, ‘Argudell’, or ‘Sevillenca’, while significant increases in mature as compared to green fruit were found for ‘Morrut’ and ‘Picual’ (38 and 19%, respectively).

Excepting ‘Marfil’ and ‘Picual’, wax yields decreased along maturation, both in absolute terms ($\mu\text{g cm}^{-2}$) and as a percentage over total cuticle (**Table 3**). Wax percentages ranged from 9.8% in ‘Farga’ mature fruit to 39.1% in ‘Empeltre’ green samples. When expressed as mass per surface area, yields ranged from roughly 230 $\mu\text{g cm}^{-2}$ in ‘Farga’ mature olives to over fivefold that much (1,284.5 $\mu\text{g cm}^{-2}$) in ‘Picual’ mature fruit, consistent with thicker cuticles in these samples (**Table 3**). More cultivar-to-cultivar variation was observed for cutin, both regarding yields and time-course changes along on-tree maturation. Total cutin yields decreased over fruit maturation in ‘Arbequina’ and ‘Farga’ fruits (approximately 23 and 18%, respectively), whereas they increased in ‘Picual’, ‘Argudell’, and ‘Empeltre’ fruits (by 38, 19, and 17%, in that order) and remained steady in the rest of the considered cultivars (‘Manzanilla’, ‘Marfil’, ‘Morrut’, and ‘Sevillenca’). Wax-to-cutin ratio declined with maturity stage in all cultivars with the exception of ‘Marfil’, owing to increased wax contents.

Table 3. Total cuticle amounts, cuticular wax and cutin yields, wax to cutin ratios, cuticle thickness and water permeance in olive fruit at the green, turning and ripe stages.

Cultivar	Maturity stage	Cuticle yield (mg cm ⁻²)		Wax yield (µg cm ⁻²)		Wax (%)		Cutin yield (µg cm ⁻²)		Cutin (%)		C ₁₆ /C ₁₈ *	Wax/ cutin ratio		Thickness (µm)		Permeance (× 10 ⁻⁵ m s ⁻¹)	
'Arbequina'	Green	3.1	a A	1163.6	a A	37.4	a AB	1205.4	a A	38.7	a A	0.41	0.97	a B	41.0	ab B	7.3	a B
	Turning	2.4	b DE	405.9	c D	16.7	c C	945.0	b BC	39.0	a A	0.33	0.43	c C	44.5	a A	7.9	a C
	Ripe	2.5	ab B	456.6	b D	18.5	b D	931.1	b BC	37.7	a AB	0.37	0.49	b EF	32.9	b BC	8.0	a B
'Argudell'	Green	2.9	a AB	649.4	a D	22.8	a E	846.9	b BC	29.8	b D	0.43	0.77	a C	35.0	a BC	11.2	a A
	Turning	3.6	a A	497.4	b C	13.7	c D	995.5	a B	27.4	b B	0.41	0.50	b C	34.2	a ABC	10.8	a A
	Ripe	2.7	a AB	453.5	b D	16.7	b DE	1021.4	a B	37.7	a AB	0.40	0.45	b F	36.3	a AB	11.9	a A
'Empeltre'	Green	2.3	a BCDE	903.6	a C	39.1	a A	722.7	b DE	31.3	a CD	0.35	1.26	a A	62.9	a A		na
	Turning	2.8	a CD	882.6	a A	31.6	b A	826.0	ab CD	29.6	a B	0.44	1.08	a A	38.7	b ABC		na
	Ripe	3.0	a AB	496.1	b CD	16.6	c DE	890.5	a BCD	29.9	a CD	0.38	0.56	b DE	32.9	b BC	7.4	B
'Farga'	Green	2.7	a ABCD	899.3	a C	34.0	a C	962.3	a B	36.4	a ABC	0.49	0.94	a BC	26.2	a C		na
	Turning	2.3	a E	564.6	b BC	24.9	b B	807.8	b CD	35.7	a A	0.44	0.70	b B	33.6	a BC		na
	Ripe	2.4	a B	229.7	c F	9.8	c F	789.1	b CD	33.5	a BC	0.37	0.29	c G	27.7	a BC	7.3	B
'Manzanilla'	Green	1.9	a E	566.3	a E	30.2	a D	620.1	a E	33.1	a BCD	0.44	0.92	a BC	25.5	a C		na
	Turning	na		na		na		na		na		na	na		28.5	a C		na
	Ripe	2.0	a B	364.7	b E	18.1	b D	527.5	a E	26.2	a D	0.43	0.69	b BC	25.7	a C	7.2	B
'Marfil'	Green	2.1	a CDE	320.2	b F	14.7	b F	810.0	a CD	37.3	a AB	0.29	0.40	b D	34.4	a BC		na
	Turning	na		na		na		na		na		na	na		32.8	a C		na
	Ripe	2.3	a B	581.0	a B	25.4	a B	756.1	a D	33.0	a BC	0.28	0.78	a AB	31.0	a BC	11.8	A
'Morrut'	Green	3.0	a A	994.8	a B	33.6	a C	933.9	a B	31.6	a CD	0.27	1.07	a B	44.4	a B	6.9	c B
	Turning	3.0	a BC	371.8	c D	12.2	c D	781.4	a D	25.7	b B	0.23	0.48	b C	32.2	b C	9.4	b B
	Ripe	2.8	a AB	437.5	b D	15.5	b E	886.1	a BCD	31.5	a CD	0.32	0.49	b EF	35.8	ab AB	11.1	a A
'Picual'	Green	2.7	a ABC	973.1	b BC	35.8	a BC	952.2	c B	35.1	a ABC	0.36	1.03	a B	37.0	a B	6.6	b B
	Turning	3.4	a AB	635.7	c B	19.0	b C	1230.9	b A	36.8	a A	0.32	0.52	c C	43.9	a AB	7.3	ab C
	Ripe	3.8	a A	1284.5	a A	33.5	a A	1543.9	a A	40.2	a A	0.33	0.83	b A	44.3	a A	8.1	a B
'Sevillena'	Green	2.1	a DE	693.0	a D	33.2	a C	668.6	a E	31.9	a CD	0.41	1.05	a B	40.6	a B	7.3	a B
	Turning	na		na		na		na		na		na	na		31.6	b BC	7.6	a C
	Ripe	2.4	a B	535.8	b BC	21.9	b C	834.8	a CD	34.2	a BC	0.36	0.65	b CD	30.8	b BC	7.3	a B

Cuticular membranes were isolated from skin samples (around 100 cm²) obtained from 30 to 75 olives, contingent upon fruit size. Wax and cutin data represent means of three technical replicates of this starting material. For cuticle thickness and water permeance, values represent means of five or 10 biological replicates, respectively (na, value not available). Different capital letters denote significant differences among the cultivars for a given maturity stage, and different lower-case letters stand for significant differences among maturity stages for a given cultivar, at $P \leq 0.05$ (LSD test).

* Abbreviations: Ratio of C₁₆ to C₁₈ cutin monomers.

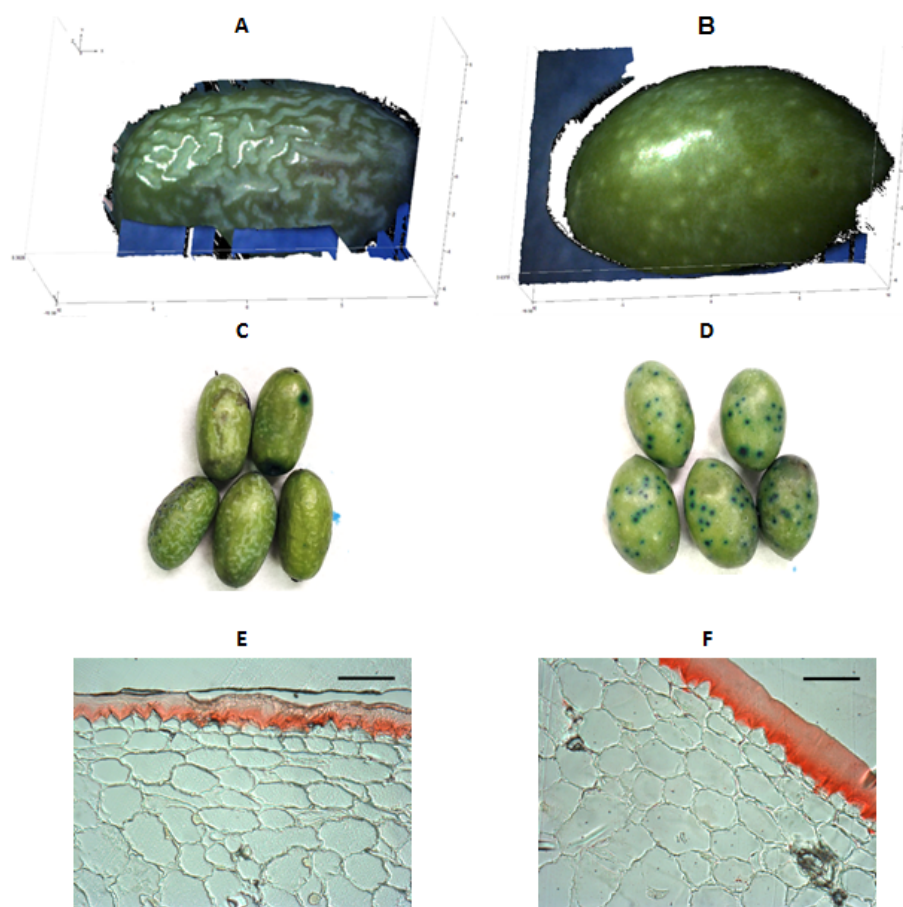


Figure 1. An example of fruit surface differences between two olive cultivars (left, ‘Farga’; right, ‘Sevillenca’) at the green stage. A, B: 3D-diagrams of raw data outputs from fringe projections. Blue and black areas represent background noise due to the shape and size of the olives, which did not cover the whole assessment window of the equipment. C, D: Toluidine Blue (TB) staining. E, F: Sudan IV-stained cross-sections of fruit pericarp observed under a bright-field microscope (bar: 60 µm).

1.3.3. Cuticular wax composition

Triterpenoids were the dominant fraction in cuticular waxes, relative percentages over total waxes ranging from 58 to roughly 81% (**Table 4**). For ‘Farga’, ‘Marfil’, and ‘Picual’ olives, the total amount of triterpenoids decreased with maturity by 15, 18, and 23%, respectively, whereas no significant changes were observed for the rest of the cultivars considered. Maslinic (27 to 52%, contingent on cultivar and maturity stage) and oleanolic (19 to 43%) acids were detected in the wax fraction obtained from all the samples, with very minor contents of ursolic acid being identified additionally in ‘Farga’, ‘Picual’, and ‘Sevillenca’ fruit (**Supplementary Table 2**). Relative contents of oleanolic acid decreased with maturity stage, while the amounts of maslinic acid generally showed limited changes, with the exception of ‘Farga’ and ‘Picual’ olives which displayed a sustained decline over maturation, and ‘Sevillenca’ samples for which, on the contrary, increased maslinic acid contents were found for the ripe as compared with the green stages.

Table 4. Relative amounts (% over total waxes) of wax compound types in cuticles isolated from olive fruit at the green, turning and ripe stages.

Cultivar	Maturity stage	ACL *		Acyclic/ cyclic ratio		Triterpenoids (%)		Fatty acids (%)		Fatty alcohols (%)		<i>n</i> -Alkanes (%)		Sterols (%)		Unidentified (%)	
‘Arbequina’	Green	25.2	a AB	0.30	a BC	63.7	a CDE	7.4	a B	8.0	a BC	3.7	a A	1.1	a A	16.2	a AB
	Turning	25.0	a A	0.25	a ABC	68.3	a AB	9.0	a C	4.7	a AB	3.1	ab A	0.4	a B	14.5	a B
	Ripe	24.6	a BC	0.26	a CDE	67.6	a AB	9.6	a C	5.7	a C	2.3	b CD	0.8	a BCD	14.0	a BC
‘Argudell’	Green	25.2	a AB	0.18	a D	70.0	a BCD	4.4	b CD	5.2	a D	3.2	a AB	0.9	a AB	16.4	a AB
	Turning	23.7	b B	0.21	a BC	64.7	a B	8.4	a CD	2.8	b B	2.6	a AB	1.1	a AB	20.5	a A
	Ripe	24.0	ab E	0.22	a DE	66.2	a AB	8.4	a C	3.4	b E	3.2	a BC	1.7	a A	17.1	a BC
‘Empeltre’	Green	24.9	a AB	0.17	a D	71.3	a BC	5.2	b BCD	5.1	ab D	2.2	a BC	0.9	ab AB	15.4	a BC
	Turning	24.8	a A	0.19	a BC	73.3	a A	5.8	b E	7.0	a A	0.6	b D	0.4	b B	12.8	a B
	Ripe	24.2	b DE	0.22	a DE	70.2	a A	9.3	a C	3.6	b DE	2.7	a BCD	1.2	a ABC	13.0	a BC
‘Farga’	Green	25.6	a A	0.20	b CD	73.5	a AB	6.9	b BC	6.0	a CD	2.0	ab CD	0.5	ab BC	11.1	b CD
	Turning	24.9	ab A	0.26	ab AB	70.6	a AB	11.0	a B	6.3	a A	1.3	b CD	0.4	b B	10.4	b B
	Ripe	24.4	b CD	0.33	a BC	62.9	b AB	12.7	a B	4.6	a CD	3.5	a B	0.8	a BCD	15.5	a BC
‘Manzanilla’	Green	25.0	a AB	0.41	a AB	63.1	a DE	13.0	a A	11.5	a A	0.5	b E	0.38	a CD	11.6	a CD
	Ripe	24.9	b B	0.49	a A	58.4	a B	15.8	a A	10.7	a A	2.0	a D	0.8	a BCD	12.4	a CD
‘Marfil’	Green	25.5	a A	0.19	b D	74.8	a AB	7.3	b B	5.8	b CD	1.0	b DE	0.6	a BC	10.6	a D
	Ripe	25.4	a A	0.40	a AB	61.6	b AB	11.9	a B	8.1	a B	4.8	a A	0.6	a CD	13.1	a BC
‘Morrut’	Green	23.9	b C	0.13	b D	70.7	a BCD	6.2	b BC	2.5	c E	0.5	b E	0.2	b CD	20.0	a A
	Turning	23.9	b B	0.31	a A	64.1	a B	15.2	a A	3.3	b B	2.0	a BC	1.5	a A	14.0	b B
	Ripe	24.7	a B	0.30	a CD	67.2	a AB	12.7	a B	5.0	a C	2.2	a CD	0.4	ab D	12.5	b C
‘Picual’	Green	24.6	a BC	0.09	b D	80.8	a A	2.8	c D	4.5	a DE	0.2	b E	nd	b D	11.7	b CD
	Turning	23.9	b B	0.17	a C	72.1	ab AB	6.7	a DE	3.3	a BC	2.2	a B	1.5	a A	14.2	b B
	Ripe	24.2	b DE	0.16	a E	61.9	b AB	4.6	b D	3.6	a DE	1.8	a D	1.2	a ABC	26.9	a A
‘Sevillena’	Green	25.5	a A	0.44	a A	61.5	a E	15.7	a A	9.9	a AB	1.7	a CD	0.9	a AB	10.4	b D
	Ripe	24.4	b CD	0.34	a BC	58.1	a B	15.1	a A	3.0	b E	2.3	a CD	1.5	a AB	20.1	a AB

Values represent means of three technical replicates (nd, non-detectable). Different capital letters denote significant differences among the cultivars for a given maturity stage, and different lower-case letters stand for significant differences among maturity stages for a given cultivar, at $P \leq 0.05$ (LSD test).

*Abbreviation: ACL, Average chain length of acyclic wax compounds.

Reduction of triterpenoid contents along maturation in ‘Farga’, ‘Marfil’, and ‘Picual’ fruits, together with an increment in fatty acids, led to increased acyclic to cyclic compounds ratios (**Table 4**). Augmented percentages of fatty acids, alcohols, and *n*-alkanes over total waxes during maturation also caused increased acyclic to cyclic compounds ratios in ‘Morrut’ samples, whereas the increase in fatty acids observed in ‘Argudell’ and ‘Empeltre’ was not important enough to significantly modify this ratio. Fatty acids and alcohols were the main types of acyclic compounds identified in cuticular waxes, with very minor percentages of *n*-alkanes, in contrast with reports for other fruit species, for which much higher *n*-alkane percentages in cuticular waxes have been reported (Belge et al., 2014a; Belge et al., 2014b). ‘Manzanilla’ and ‘Sevillena’ samples displayed the highest relative percentages of fatty acids and alcohols (**Table 4**). Among fatty acids, the most abundant compounds detected lignoceric (24:0) and cerotic (26:0) acids, while tetracosanol (C₂₄) and hexacosanol (C₂₆) were the predominant alcohols (**Supplementary Table S2**). The ACL of the acyclic compounds identified in the wax fraction decreased in the course of fruit maturation for most of the cultivars included in this work, with the exception of ‘Arbequina’ and ‘Marfil’, for which no significant differences were found, and ‘Morrut’ which showed an increase from the turning to the ripe stages (**Table 4**).

1.3.4. Cutin monomer composition

C₁₈-type monomers stood out quantitatively in cutin composition of the cultivars considered, representing around two thirds (68.7 to 76.2%) over total cutin monomers identified (**Supplementary Table 3**). The predominant compound type detected in the cutin fraction was hydroxy-fatty acids, relative percentages ranging 40 to 59% (**Table 5**). Among these, ω -hydroxy fatty acids and ω -hydroxy fatty acids with midchain hydroxyl groups were particularly abundant, mainly 18-hydroxyoctadecenoic and 16-hydroxyhexadecanoic acids. The relative percentage of 18-hydroxyoctadecenoic showed in general a moderate decline along maturation, ‘Picual’ samples displaying the highest contents of this cutin monomer (24.1, 21.5, and 22.5% at the green, turning, and black stage, respectively). A similar trend, with the exception of ‘Morrut’, was observed for 16-hydroxyhexadecanoic acid, ‘Manzanilla’ and ‘Picual’ fruits showing the highest amounts of this compound. The relative percentages of ω -hydroxy fatty acids with midchain hydroxyl groups remained steady throughout fruit maturation, ‘Farga’ samples showing the highest values (29.4% at the green stage) (**Table 5**). The predominant cutin monomer of this type was 9/10,16-dihydroxyhexadecanoic acid, which did not show noticeable variations during fruit maturation (**Supplementary Table S3**).

In terms of percentage over total cutin, α,ω -dicarboxylic (8.5 to 17.7%, depending on cultivar and maturity stage) and monocarboxylic (3.3 to 21.5%) fatty acids were also quantitatively important. With the exception of ‘Morrut’ fruits, the content of dicarboxylic fatty acids decreased along maturation, while that of monocarboxylic fatty acids was significantly augmented in all the cultivars analysed, excepting ‘Marfil’ (**Table 5**). Within the dicarboxylic fatty acids family, 9-octadecenedioic acid was the most abundant compound identified, the highest amounts being found for ‘Picual’ and ‘Morrut’ olives (16.9 and 16.5%, respectively), roughly twice those determined in ‘Empeltre’ fruit (**Supplementary Table 3**).

Table 5. Relative amounts (% over total cutin) of cutin monomer types in cuticles isolated from olive fruit at the green, turning and ripe stages.

Cultivar	Maturity stage	FA* (%)	α,ω -diFA (%)	α,ω -diFA, mcOH (%)	ω -OH FA (%)	ω -OH FA, mcOH (%)	α -OH FA (%)	Other OH FA (%)	Alcohols (%)	Unidentified (%)
'Arbequina'	Green	5.0 b BC	11.5 a D	2.6 a B	30.4 a BCD	21.5 a B	1.9 a B	nd C	2.0 ab D	25.2 a A
	Turning	18.0 a A	11.5 a B	2.1 ab B	28.3 ab B	16.0 b BC	0.9 b C	nd C	1.7 b BC	21.5 c ABC
	Ripe	16.4 a BC	9.6 a CD	2.0 b B	27.3 b B	18.3 ab BCD	1.2 ab C	nd B	2.3 a BC	23.0 b A
'Argudell'	Green	5.3 b BC	14.6 a B	1.4 a D	32.1 a BC	21.1 a B	1.4 a B	nd b C	3.0 a A	21.2 a CDE
	Turning	19.6 a A	10.9 b B	1.0 b CD	27.8 b B	18.1 a B	1.3 a BC	nd b C	2.4 a AB	19.0 b C
	Ripe	20.2 a A	11.1 b C	1.4 a C	24.8 b C	19.6 a ABC	1.7 a C	0.3 a A	2.6 a BC	18.4 b E
'Empeltre'	Green	4.7 b BC	11.7 a CD	3.6 a A	28.9 a CD	21.8 a B	5.7 a A	0.1 a B	1.5 a E	22.1 a BC
	Turning	5.9 b C	9.5 b C	3.9 a A	26.2 a B	27.1 a A	5.6 a A	0.2 a BC	1.7 a C	20.0 a ABC
	Ripe	13.1 a CDE	8.5 c D	3.4 a A	23.1 b C	22.6 a A	5.6 a A	0.3 a AB	1.8 a DE	21.6 a ABC
'Farga'	Green	6.0 c B	11.2 a D	1.9 a C	26.8 a D	29.4 a A	1.6 a B	nd b C	2.2 b CD	21.0 a CDE
	Turning	8.8 b C	11.2 a B	1.5 a BCD	28.4 a B	23.8 a A	2.0 a B	nd b C	2.7 a A	21.7 a AB
	Ripe	19.7 a AB	9.7 a CD	1.5 a C	24.1 a C	20.8 a AB	1.2 a C	0.2 a AB	2.5 ab BC	20.3 a CD
'Manzanilla'	Green	5.6 b BC	17.0 a A	1.3 a D	33.9 a B	18.3 a BCD	1.3 a B	0.1 a B	2.8 a AB	19.8 a DE
	Ripe	13.3 a CD	13.9 a B	1.3 a C	28.4 b B	18.6 a ABCD	1.3 a C	0.4 a A	3.3 a A	19.5 a DE
'Marfil'	Green	10.2 a A	16.9 a A	2.6 a B	32.2 a BC	12.5 a D	1.8 a B	0.2 b AB	1.9 a D	21.7 a BCD
	Ripe	11.1 a DEF	14.4 b B	3.0 a A	29.5 a B	14.9 a CD	4.5 b B	0.3 a AB	1.7 a E	20.6 CD
'Morrut'	Green	4.3 c BC	17.7 a A	2.0 a C	32.9 a BC	13.7 a CD	1.9 a B	0.2 a A	1.9 a D	25.4 a A
	Turning	17.1 a AB	15.3 b A	1.7 a BC	28.4 a B	11.5 a C	1.6 a BC	0.4 a A	1.8 ab BC	22.2 b A
	Ripe	9.7 b EF	17.3 ab A	1.4 a C	29.7 a B	16.0 a BCD	1.8 a C	0.4 a A	1.6 b E	22.2 b AB
'Picual'	Green	3.3 c C	17.6 a A	0.9 b D	40.1 a A	14.7 a BCD	1.6 a B	0.1 a B	2.6 a BC	19.1 b E
	Turning	13.9 a B	15.7 b A	0.8 b D	34.5 b A	12.7 a CD	1.0 a C	0.3 a AB	2.0 b BC	19.2 b BC
	Ripe	9.6 b F	15.7 b AB	1.2 a C	34.9 b A	14.1 a D	1.4 a C	0.1 a AB	2.1 b CD	20.9 a BCD
'Sevillena'	Green	5.4 b BC	13.6 a BC	2.3 a BC	31.1 a BCD	20.1 a BC	1.2 a B	0.1 a B	2.5 a BC	23.8 a AB
	Ripe	21.5 a A	11.3 b C	2.0 a B	24.3 b C	18.8 a ABCD	1.3 a C	0.3 a AB	1.8 b DE	18.7 b E

Values represent means of three technical replicates (nd, non-detectable). Different capital letters denote significant differences among the cultivars for a given maturity stage, and different lower-case letters stand for significant differences among maturation stages for a given cultivar, at $P \leq 0.05$ (LSD test).

*Abbreviations: FA, Monocarboxylic fatty acids; α,ω -diFA, α,ω -Dicarboxylic fatty acids; α,ω -diFA, mcOH, α,ω -Dicarboxylic fatty acids with mid-chain-hydroxy group; ω -OH FA, ω -Hydroxy fatty acids; ω -OH FA, mcOH, ω -Hydroxy fatty acids with mid-chain-hydroxy group; α -OH FA, α -Hydroxy fatty acids; Other OH FA, other hydroxy fatty acids.

1.4. Discussion

All olive samples used in this work were grown at the same orchard, under the same cultural practices. Therefore, the chemical composition differences in isolated fruit cuticles among the studied cultivars are not likely to reflect different environmental conditions, and might underlie the observed features of surface topography as well as the resistance of each variety to biotic and abiotic stress factors. Water permeance of olive fruit may be modulated by different cuticle-related factors, including the presence of surface discontinuities, total wax coverage, wax-to-cutin ratio, acyclic-to-cyclic waxes ratio (which would potentially provide more efficient barriers against water loss), and ACL of acyclic wax compounds. However, no consistent relationships were found among all these variables. The toluidine test as well as cuticle yields or thickness were also apparently unrelated to water permeance values. No apparent connection was observed either between the presence of discontinuities on fruit surface as revealed by the toluidine test and the susceptibility to infestation by olive fly (*Bactrocera oleae*): among the cultivars used in this work, ‘Empeltre’, ‘Farga’, ‘Manzanilla’, and ‘Sevillenca’ are characterized by severe incidence of infestation, while ‘Arbequina’, ‘Argudell’, ‘Marfil’, ‘Morrut’, and ‘Picual’ are less susceptible to this plague (Barrios et al., 2015), which do not agree with the groupings revealed by TB staining (**Table 1**).

However, our data suggest a relationship between TB staining results and descriptors of surface roughness. Vertical roughness parameters Stm , Spm , and Svm can be a good indicator for uneven surfaces and for surface cracks, which will normally have higher peaks and deeper valleys. An irregular surface can also display low horizontal roughness (S) values, because adjacent peaks would be close to each other. Among the olive cultivars considered herein, the lowest values for horizontal roughness were observed for ‘Farga’, ‘Morrut’, and ‘Picual’ samples, together with deeper valleys as shown by Svm (**Table 2**). Interestingly, when roughness parameters and TB staining data were used to characterize the samples by means of a PCA model, a good correlation was found between S , Svm , and TB test results (**Figure S5**). Eighty six percent of total variability was explained by the two first principal components (PC) alone. The plot shows that stained fruits displayed higher values for S and Svm , and the lowest for Sa , Stm , Spm , and Sk . Albeit to a lesser extent, a correlation was also found between roughness parameters and the incidence of fruit infestation by the olive fly (*B. oleae*). Higher percentage of infested fruits (**Supplementary Table S1**) was associated to high Svm values (**Supplementary Figure S5**), which might suggest that deeper irregularities on the surface may favor egg deposition.

Cuticle thickness values were higher than those reported for fruit from other olive cultivars, including ‘Gentile di Chieti’, ‘Carboncella’, ‘Dritta’, ‘Castiglionesa’, ‘Intosso’, and ‘Kalamata’ (Lanza and Di Serio, 2015). However, whereas that work found decreased cuticle thickness along maturation in all the cultivars assessed, a declining trend was observed in this study uniquely for ‘Arbequina’, ‘Empeltre’, ‘Morrut’, and ‘Sevillenca’, while cuticle thickness remained unchanged for the rest of cultivars considered. For tomato fruit (*S. lycopersicum* L.), cuticle thickness has been reported to increase during fruit development up to the mature green or breaker stage, and then to decrease thereafter until attaining full ripeness (Domínguez et al., 2008). Wide variation in thickness values has also been found among fruit species. Similar cuticle thickness has been reported for ripe tomato (*S. lycopersicum* L.), green and mature pepper (*Capsicum annuum* L.), and apple (*Malus pumila* L.) fruit in comparison with olive (Fernández, Osorio and Heredia, 1999), while that in mangoes (*Mangifera indica* L.) is reportedly thinner (Camacho-Vázquez et al., 2019).

A previous study on ‘Arbequina’ (Huang et al., 2017) did not find significant differences in water permeance of fruit at different maturity stages, the observed values averaging $9.5 \times 10^{-5} \text{ m s}^{-1}$. Similar results were found in the current study for ‘Arbequina’, but not for all the rest of varieties: changes in water permeance throughout fruit maturation were determined for five out of the nine cultivars studied, data indicating significant increases for ‘Morrut’ and ‘Picual’ samples, which incidentally displayed the highest loss in water content from the green to the ripe stages (27.1 and 13.3% for ‘Morrut’ and ‘Picual’, respectively) (**Table 1**). Water permeances observed in this study ranged from 6.6 to $11.9 \times 10^{-5} \text{ m s}^{-1}$, and were higher in comparison with those found for other fruit crops such as tomato (*S. lycopersicum* L.) and apple (*Malus domestica* Borkh), ranging respectively from 0.9 to $4.9 \times 10^{-5} \text{ m s}^{-1}$ (Leide et al., 2007; Leide et al., 2011) and from 4.6 to $5.3 \times 10^{-5} \text{ m s}^{-1}$ (Leide et al., 2018), but one order of magnitude lower than those observed for sweet cherry (*Prunus avium* L.) (1.4 to $3.7 \times 10^{-4} \text{ m s}^{-1}$) (Athoo, Winkler and Knoche, 2015).

With the exception of ‘Arbequina’, no significant changes in total cuticle yields were observed over maturation. Reports on changes in total cuticle yields ($\mu\text{g cm}^{-2}$) over fruit ripening of a model species such as tomato have been shown to be cultivar-dependent (Domínguez et al., 2008; España et al., 2014), while they were found to decrease over ripening of sweet cherry (Peschel et al., 2007). Contrarily to reports for tomato (Leide et al., 2007) or orange (*Citrus sinensis* Osbeck) (Wang et al., 2016) fruit, for which increased wax coverage was observed along maturation, the opposite was found in this work for olives, with the exception of ‘Marfil’ samples. In contrast, the proportions of the different wax fractions in olive fruit have been recently reported to be generally unrelated to sampling date, and to be largely cultivar-dependent (Vichi et al., 2016). Cutin yields were between 25.7 and 40.2%, and showed minor variations over fruit maturation. These cutin percentages over total cuticle were similar to those reported for some berries such as sea buckthorn (*Hippophaë rhamnoides* L.), cranberry (*Vaccinium oxycoccos* L.), or lingonberry (*Vaccinium vitis-idaea* L.), but much higher than those in black currant (*Ribes nigrum* L.) or bilberry (*Vaccinium myrtillus* L.) (8 and 6%, respectively) (Kallio et al., 2006). Stable cutin yields together with decreased wax coverage led to a significant decline in wax to cutin ratios (**Table 3**), in contrast with an earlier work on ‘Arbequina’, where no changes along fruit maturation were found (Huang et al., 2017). Both cutin yield and cutin percentage were inversely correlated to the observed olive fly egg deposition in the samples ($r = -0.59$ and $r = -0.57$ respectively), suggestive of a protective action of such compounds in the skin. This observation is in accordance with earlier suggestions that cultivar-related differences in olive fly egg deposition might be related to differential skin composition (Iannotta et al., 2007; Rizzo et al., 2007).

Triterpenes were the predominant cuticular wax compound type found in olive fruit as reported elsewhere (Lanza and Di Serio, 2015; Huang et al., 2017), and similarly to observations for other drupes such as sweet cherry (Peschel et al., 2007; Belge et al., 2014a) and peach (Belge et al., 2014b), as well as for blueberry (*Vaccinium spp.*) (Chu et al., 2016). Complete information on cuticle composition is available only for a handful of fruit species (reviewed in Lara, Belge and Goulao, 2015). Whereas the triterpenoid fraction of cuticular waxes is dominated by triterpenoid alcohols in orange, Asian pear (*Pyrus sinkiangensis* Yü and *Pyrus bretschneideri* Rehd) (Wu et al., 2017) as well as in fruit species within the *Solanaceae* family, triterpenoid acids predominate in grapes, olives, and *Rosaceae* fruit species. In fruit species in which triterpenoid acids are prevalent, the triterpenoid profile has been reported to consist uniquely of oleanolic acid (30% of total waxes) in mature grapes (*Vitis vinifera* L.) (Casado and Heredia, 1999), and of ursolic followed by oleanolic acid in peach and sweet cherry (Peschel et al., 2007; Belge et al., 2014a; Belge et al., 2014b). In olive fruit, the main triterpene compounds detected were maslinic and oleanolic acids, in agreement with previous works (Bianchi, 2003; Stiti, Triki and

Hartmann, 2007; Guinda et al., 2010). An inverse relationship between triterpenoid acids and olive fly egg deposition has been reported elsewhere (Kombargi, Michelakis and Petrakis, 1998). Triterpenoids also have reportedly an important role in the mechanical strength of fruit cuticles (Tsubaki et al., 2013; Wu et al., 2018), and have been shown to be related to weight loss and softening rates in blueberry (Moggia et al., 2016). In this work, however, no such relationship was observed between the incidence of olive fly infestation and triterpene content (**Table 4, Supplementary Table S1**). Contrarily, data show a positive correlation of triterpene acid levels to the percentage of affected fruit, with $r = 0.36$ and $r = 0.49$ for maslinic and oleanolic acids, respectively. Furthermore, when maturity stages were considered separately, high correlation coefficients were found for fruit at the turning stage (0.97 and 0.93 for maslinic and oleanolic acids, correspondingly). This may be relevant to understand resistance or tolerance to stress factors, as this physiological stage of the fruit coincides with environmental conditions which favor the development of pests and diseases (Vichi et al., 2016), and indeed olive fly infestation is particularly intense during the period of color change.

The profiles of fatty acids and fatty alcohols were in agreement with data reported by Huang et al., 2017, C_{24} and C_{26} being the most abundant compounds within both wax types. However, the percentage of *n*-alkanes over total waxes was very low in comparison with other fruit species: for example, *n*-alkanes accounted for 29.4% of total waxes in ‘Jesca’ peaches at harvest (Belge et al., 2014b), whereas in the present study the highest amount detected was 4.8% in ‘Marfil’ mature olives (**Table 4**). Accordingly, the ACL of acyclic wax compounds was lower than that found in other fruit species: ACL values were 28.8 to 29.9 in apple (Leide et al., 2018), sweet cherry (Athoo et al., 2015), and tomato (*S. lycopersicum* L.) (Leide et al., 2011).

C_{18} -type cutin monomers were 2 to 3.7 times more abundant than the C_{16} -type. Even so, 9/10,16-dihydroxyhexadecanoic was quantitatively the main ω -hydroxyacid with midchain hydroxyl groups identified in cutin samples, and an important compound in quantitative terms in cutin composition of all the olive cultivars considered herein. This compound has been reported to be prominent in cutin composition of mango (Camacho-Vázquez et al., 2019), a number of berries (Kallio et al., 2006; Järvinen, Kaimainen and Kallio, 2010), sweet cherry (Peschel et al., 2007), tomato (Leide et al., 2007), and pepper (*Capsicum* sp.) (Parsons et al., 2012). In contrast, cutin of mature persimmons (*Diospyros kaki* Thunb.) has been found to contain as much as 43.7% 9,10-epoxy-18-hydroxyoctadecanoic acid together with 17.4% 9/10,16-dihydroxyhexadecanoic acid (Tsubaki et al., 2013). In a great variety of plants, ω -hydroxy acids (either C_{16} or C_{18}) dominate cutin composition (Fich, Segerson and Rose, 2016), with agrees with results shown herein for olive fruit (**Table 5, Supplementary Table S3**).

1.5. Conclusions

This comparative study provided new insights in genotype-related differences in surface and cuticle features of olive fruit. Information on the chemical composition of both cuticular waxes and cutin in fruit of nine olive cultivars is reported for the first time, as well as water permeability at different maturity stages. Data on fruit micro-topography were also obtained by means of fringe projections, revealing genotype-related diversity of surface microstructure. Although water permeance of olive fruit might be controlled or fine-tuned by different cuticle-related traits, none of those considered herein appeared to suffice by itself to determine this trait, suggesting that additional properties of waxes and cutin, such as their physical structure or biomechanical properties, significantly influence the barrier functions of

plant cuticles. Even so, the bulk of results reported herein should establish the basis for a better comprehension of olive crop adaptations to the surrounding environment. Further research will be paramount to elucidate the role of cuticle properties in olive resistance to plagues, rots, and adverse environmental conditions. The comprehension of these relationships would be thus very relevant for improving orchard management.

1.6. References

- Athoo TO, Winkler A, Knoche M. 2015. Pedicel transpiration in sweet cherry fruit: mechanisms, pathways, and factors. *J. Am. Soc Hortic. Sci.* 140, 136-143.
- Barrios G, Mateu J, Ninot A, Romero A, Vichi S. 2015. Sensibilidad varietal del olivo a *Bactrocera oleae* y su incidencia en la gestión integrada de plagas. *Phytoma.* 268, 21-28.
- Belge B, Llovera M, Comabella E, Gatus F, Guillén P, Graell J, Lara I. 2014a. Characterization of cuticle composition after cold storage of ‘Celeste’ and ‘Somerset’ sweet cherry fruit. *J. Agric. Food Chem.* 62, 8722-8729.
- Belge B, Llovera M, Comabella E, Graell J, Lara I. 2014b. Fruit cuticle composition of a melting and a nonmelting peach cultivar. *J. Agric. Food Chem.* 62, 3488-3495.
- Besnard G, Terral JF, Cornille A. 2018. On the origins and domestication of the olive: a review and perspectives. *Ann. Bot.* 121, 385-403.
- Bianchi G, Murelli C, Vlahov G. 1992. Surface waxes from olive fruits. *Phytochemistry.* 31, 3503-3506.
- Bianchi G. 2003. Lipids and phenols in table olives. *Eur. J. Lipid Sci. Technol.* 105, 229-242.
- Camacho-Vázquez C, Ruiz-May E, Guerrero-Analco JA, Elizalde-Contreras JM, Enciso-Ortiz EJ, Rosas-Saito G, López-Sánchez L, Kiel-Martínez AL, Bonilla-Landa I, Monribot-Villanueva JL, Olivares-Romero JL, Gutiérrez-Martínez P, Tafolla-Arellano JC, Tiznado-Hernandez ME, Quiroz-Figueroa FR, Birke A, Aluja M. 2019. Filling gaps in our knowledge on the cuticle of mangoes (*Mangifera indica*) by analysing six fruit cultivars: Architecture/structure, postharvest physiology and possible resistance to fruit fly (Tephritidae) attack. *Postharvest Biol. Technol.* 148, 83-96.
- Casado CG, Heredia A. 1999. Structure and dynamics of reconstituted cuticular waxes of grape berry cuticle (*Vitis vinifera* L.). *J. Exp. Bot.* 50, 175-182.
- Chu W, Gao H, Cao S, Fang X, Chen H, Xiao S. 2016. Composition and morphology of cuticular wax in blueberry (*Vaccinium spp.*) fruits. *Food Chem.* 219, 436-442.
- Domínguez E, López-Casado G, Cuartero J, Heredia, A. 2008. Development of fruit cuticle in cherry tomato (*Solanum lycopersicum*). *Funct. Plant Biol.* 35, 403-411.
- Domínguez E, Heredia-Guerrero JA, Heredia A. 2011. The biophysical design of plant cuticles: an overview. *New Phytol.* 189, 938-949.
- East AR, Bloomfield C, Trejo Araya X, Heyes JA. 2016. Evaluation of fringe projection as a method to provide information about horticultural product surfaces. *Acta Hortic.* 1119, 189-196.

Results: Chapter I

España L, Heredia-Guerrero JA, Segado P, Benítez JJ, Heredia A, Domínguez E. 2014. Biomechanical properties of the tomato (*Solanum lycopersicum*) fruit cuticle during development are modulated by changes in the relative amounts of its components. *New Phytol.* 202, 790-802.

Fernández S, Osorio S, Heredia A. 1999. Monitoring and visualising plant cuticles by confocal laser scanning microscopy. *Plant Physiol. Biochem.* 37, 789-794.

Fich EA, Segerson NA, Rose JKC. 2016. The plant polyester cutin: biosynthesis, structure, and biological roles. *Annu. Rev. Plant Biol.* 67, 207-233.

Franke R, Briesen I, Wojciechowski T, Faust A, Yephremov A, Nawrath C, Schreiber L. 2005. Apoplastic polyesters in Arabidopsis surface tissues - A typical suberin and a particular cutin. *Phytochemistry.* 66, 2643-2658.

Gadelmawla ES, Koura MM, Maksoud TMA, Elewa IM, Soliman HH. 2002. Roughness parameters. *J. Mater. Process. Technol.* 123, 133-145.

Guinda A, Rada M, Delgado T, Gutiérrez-Adánez P, Castellano JM. 2010. Pentacyclic triterpenoids from olive fruit and leaf. *J. Agric. Food Chem.* 58, 9685-9691.

Huang H, Burghardt M, Schuster AC, Leide J, Lara I, Riederer M. 2017. Chemical composition and water permeability of fruit and leaf cuticles of *Olea europaea* L. *J. Agric. Food Chem.* 65, 8790-8797.

Iannotta N, Noce ME, Ripa V, Scalercio S, Vizzarri V. 2007. Assessment of susceptibility of olive cultivars to the *Bactrocera oleae* (Gmelin, 1790) and *Camarosporium dalmaticum* (Thüm.) Zachos & Tzav. –Klon. attacks in Calabria (Southern Italy). *J. Environ. Sci. Heal. B* 42, 789-793.

Järvinen R, Kaimainen M, Kallio H. 2010. Cutin composition of selected northern berries and seeds. *Food Chem.* 122, 137-144.

Kallio H, Nieminen R, Tuomasjukka S, Hakala M. 2006. Cutin composition of five finnish berries. *J. Agric. Food Chem.* 54, 457-462.

Kombargi WS, Michelakis SE, Petrakis CA. 1998. Effect of olive surface waxes on oviposition by *Bactrocera oleae* (Diptera: Tephritidae). *J. Econ. Entomol.* 91, 993-998.

Kunst L, Samuels AL. 2002. Biosynthesis and secretion of plant cuticular wax. *Prog. Lipid Res.* 42, 51-80.

Lai PH, Gwanpua SG, Bailey DG, Heyes JA, East AR. 2018. Skin topography changes during kiwifruit development. *Acta Hort.* 1218, 427-433.

Lanza B, Di Serio MG. 2015. SEM characterization of olive (*Olea europaea* L.) fruit epicuticular waxes and epicarp. *Sci. Hortic.* 191, 49–56.

Lara I, Belge B, Goulao LF. 2014. The cuticle as a modulator of postharvest quality. *Postharvest Biol. Technol.* 87, 103-112.

Lara I, Belge B, Goulao LF. 2015. A focus on the biosynthesis and composition of cuticle in fruits. *J. Agric. Food Chem.* 63, 4005-4019.

Leide J, Hildebrandt U, Reussing K, Riederer M, Vogg G. 2007. The developmental pattern of tomato fruit wax accumulation and its impact on cuticular transpiration barrier properties: effects of a deficiency in a β -ketoacyl-coenzyme A synthase (LeCER6). *Plant Physiol.* 144, 1667-1679.

Leide J, Hildebrandt U, Vogg G, Riederer M. 2011. The positional sterile (*ps*) mutation affects cuticular transpiration and wax biosynthesis of tomato fruits. *J. Plant Physiol.* 168, 871-877.

Leide J, de Souza AX, Papp I, Riederer M. 2018. Specific characteristics of the apple fruit cuticle: investigation of early and late season cultivars 'Prima' and 'Florina' (*Malus domestica* Borkh.). *Sci. Hortic.* 229, 137-147.

Lequeu J, Fauconnier M, Chammaï A, Bronner R, Blée E. 2003. Formation of plant cuticle: evidence of the peroxygenase pathway. *Plant J.* 36, 155-164.

Martin LBB, Rose JKC. 2014. There's more than one way to skin a fruit: formation and functions of fruit cuticles. *J. Exp. Bot.* 16, 4639-4651.

Moggia C, Graell J, Lara I, Schmeda-Hirschmann G, Thomas-Valdés S, Lobos GA. 2016. Fruit characteristics and cuticle triterpenes as related to postharvest quality of highbush blueberries. *Sci. Hortic.* 211, 449-457.

Parsons EP, Popovskiy S, Lohrey GT, Lü S, Alkalai-Tuvia S, Perzelan Y, Fallik E, Jenks MA. 2012. Fruit cuticle lipid composition and fruit post-harvest water loss in an advanced backcross generation of pepper (*Capsicum* sp.). *Physiol. Plant* 146, 15-25.

Peschel S, Franke R, Schreiber L, Knoche M. 2007. Composition of the cuticle of developing sweet cherry fruit. *Phytochemistry.* 68, 1017-1025.

Riederer M, Arand K, Burghardt M, Huang H, Riedel M, Schuster AC, Smirnova A, Jiang Y. 2015. Water loss from litchi (*Litchi chinensis*) and logan (*Dimocarpus logan*) fruits is biphasic and controlled by a complex pericarpal transpiration barrier. *Planta.* 242, 1207-1219.

Rizzo R, Lombardo A. 2007. Factors affecting the infestation due to *Bactrocera oleae* (Gmelin) in several Sicilian olive cultivars. In *Proceedings of the 2nd International Seminar Olivebioteq.* p 291-298

Samuels LA, Kunst L, Jetter R. 2008. Sealing plant surfaces: cuticular wax formation by epidermal cells. *Plant Biol.* 59, 68-707.

Schindelin JL, Arganda-Carreras I, Frise E, Kaynig V, Longair M, Pietzsch T, Preibisch S, Rueden C, Saafeld S, Schmid B, Tinevez JY, White DJ, Hartenstein V, Eliceiri K, Tomancak P, Cardona A. 2012. Fiji: an open-source platform for biological-image analysis. *Nat. Methods.* 9, 676-682.

Serrano M, Coluccia F, Torre M, L'Haridon F, Métraux JP. 2014. The cuticle and plant defense to pathogens. *Front. Plant Sci.* 5, 274.

Stiti N, Triki S, Hartmann MA. 2007. Formation of triterpenoids throughout *Olea europaea* fruit ontogeny. *Lipids.* 42, 55-67.

Tanaka T, Tanaka H, Machida C, Watanabe M, Machida Y. 2004. A new method for rapid visualization of defects in leaf cuticle reveals five intrinsic patterns of surface defects in *Arabidopsis*. *Plant J.* 37, 139-146.

Results: Chapter I

Tous J, Romero A. 1993. Variedades del olivo: con especial referencia a Cataluña. (ISBN 84-7664-376-4).

Tsubaki S, Sugimura K, Teramoto Y, Yonemori K, Azuma JI. 2013. Cuticular membrane of *Fuyu* persimmon fruit is strengthened by triterpenoid nano-fillers. *PLoS One*. 8, 1-13.

Uceda M, Frías L. 1975. Harvest dates. Evolution of the fruit of content, oil composition and oil quality. In Proceedings of II Seminario Oleícola Internacional. p125-130.

Vichi S, Cortés-Francisco N, Caixach J, Barrios G, Mateu J, Ninot A, Romero A. 2016. Epicuticular wax in developing olives (*Olea europaea*) is highly dependent upon cultivar and fruit ripeness. *J. Agric. Food Chem.* 64, 5985-5994.

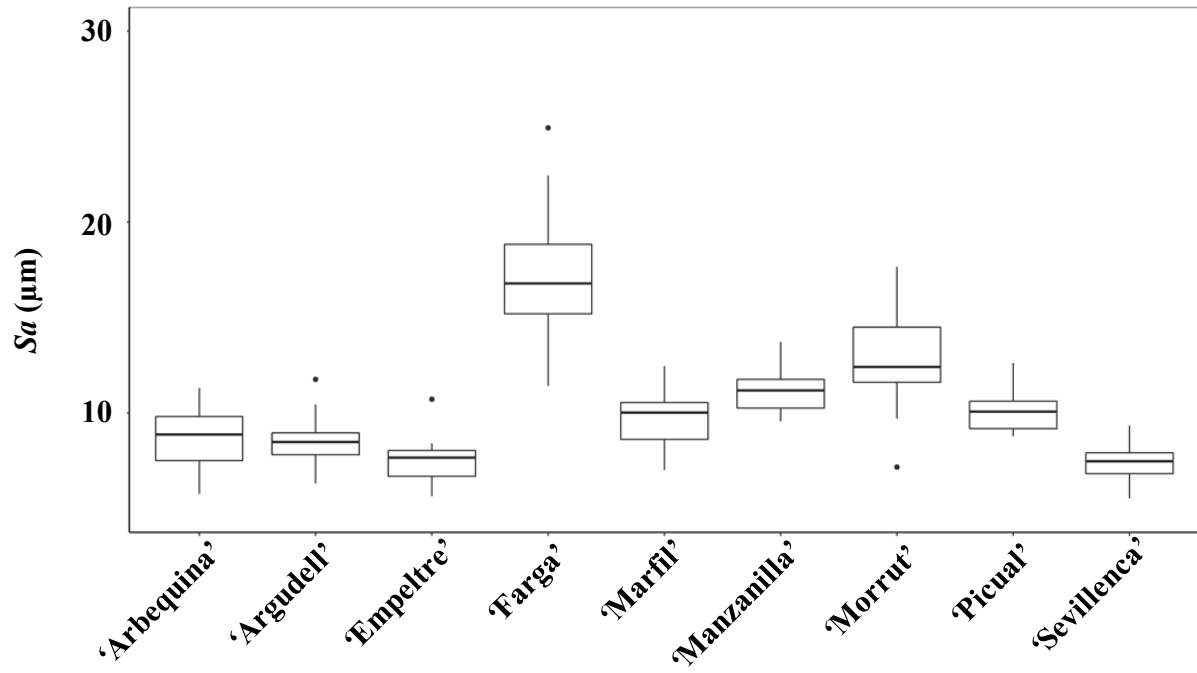
Wang J, Sun L, Xie L, He Y, Luo T, Sheng L, Luo Y, Zeng Y, Xu J, Deng X, Cheng Y. 2016. Regulation of cuticle formation during fruit development and ripening in 'Newhall' navel orange (*Citrus sinensis* Osbeck) revealed by transcriptomic and metabolic profiling. *Plant Sci.* 243, 131-144.

Wu X, Yin H, Chen Y, Li L, Wang Y, Hao P, Cao P, Qi K, Zhang S. 2017. Chemical composition, crystal morphology and key gene expression of cuticular waxes of Asian pears at harvest and after storage. *Postharvest Biol. Technol.* 132, 71-80.

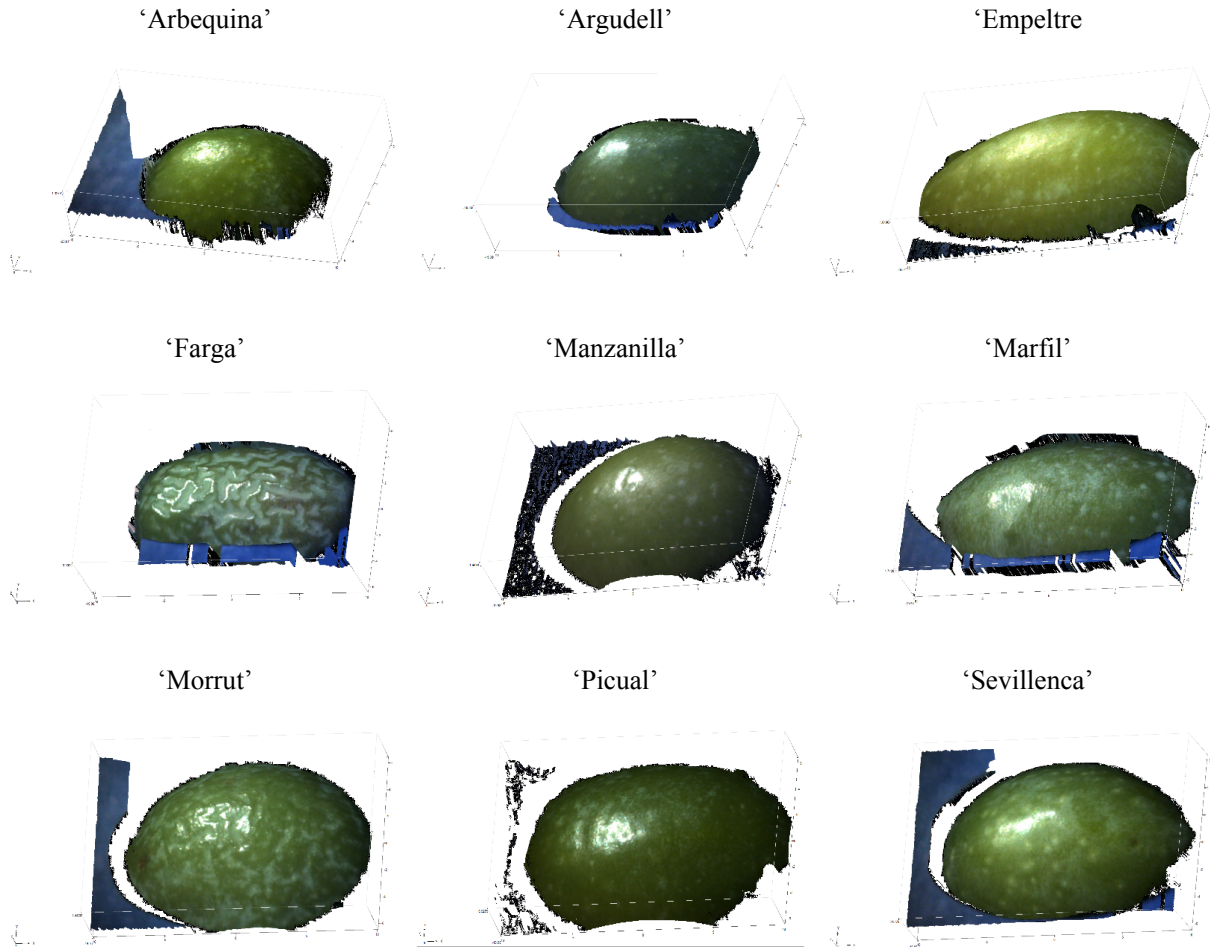
Wu X, Yin H, Shi Z, Chen Y, Qi K, Qiao X, Wang G, Cao P, Zhang S. 2018. Chemical composition and crystal morphology of epicuticular wax in mature fruits of 35 pear (*Pyrus spp.*) cultivars. *Front. Plant Sci.* 9, 1-14.

Yeast TH, Rose JKC. 2013. The formation of plant cuticle. *Plant Physiol.* 163, 5-20.

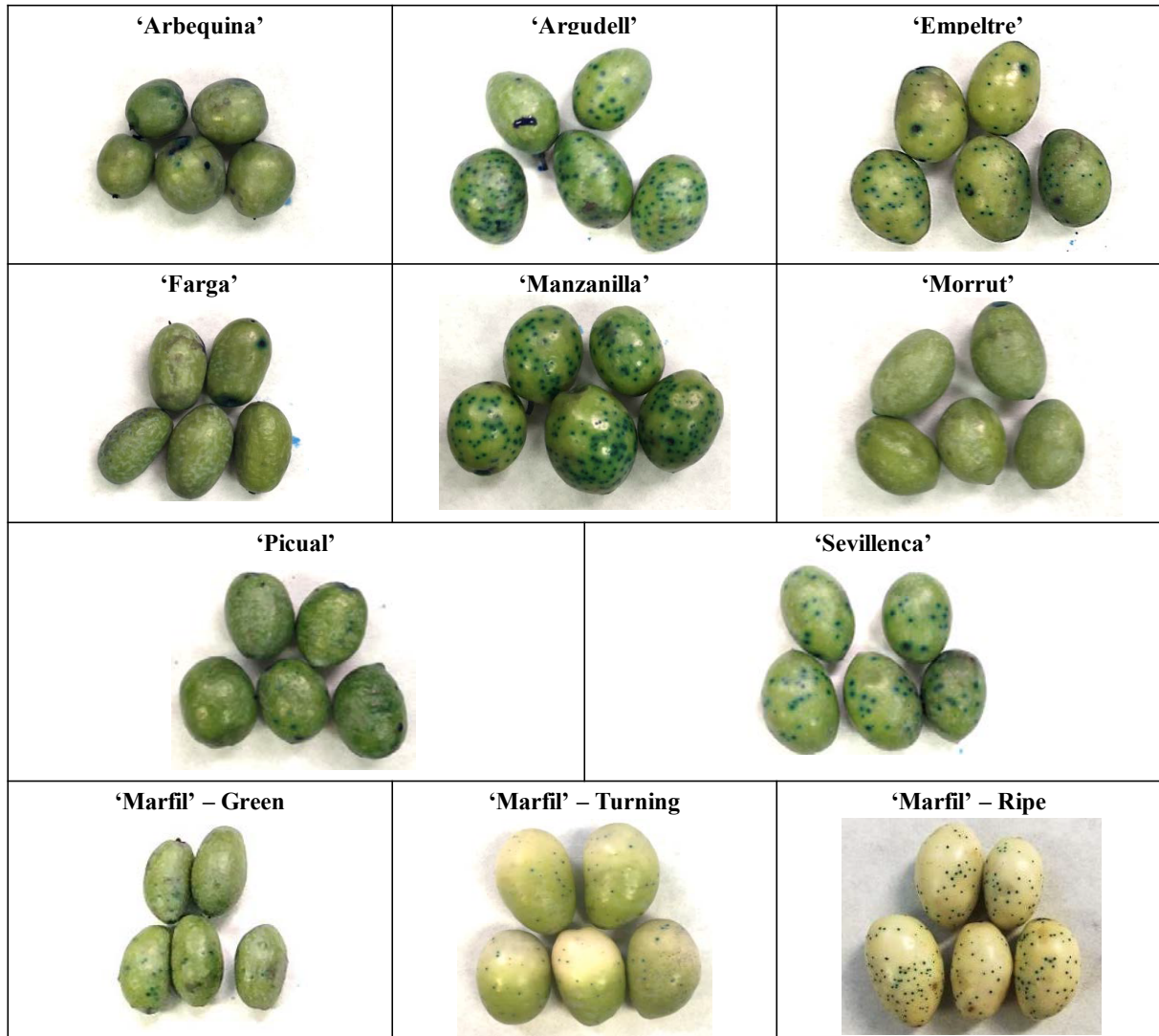
Supplementary material



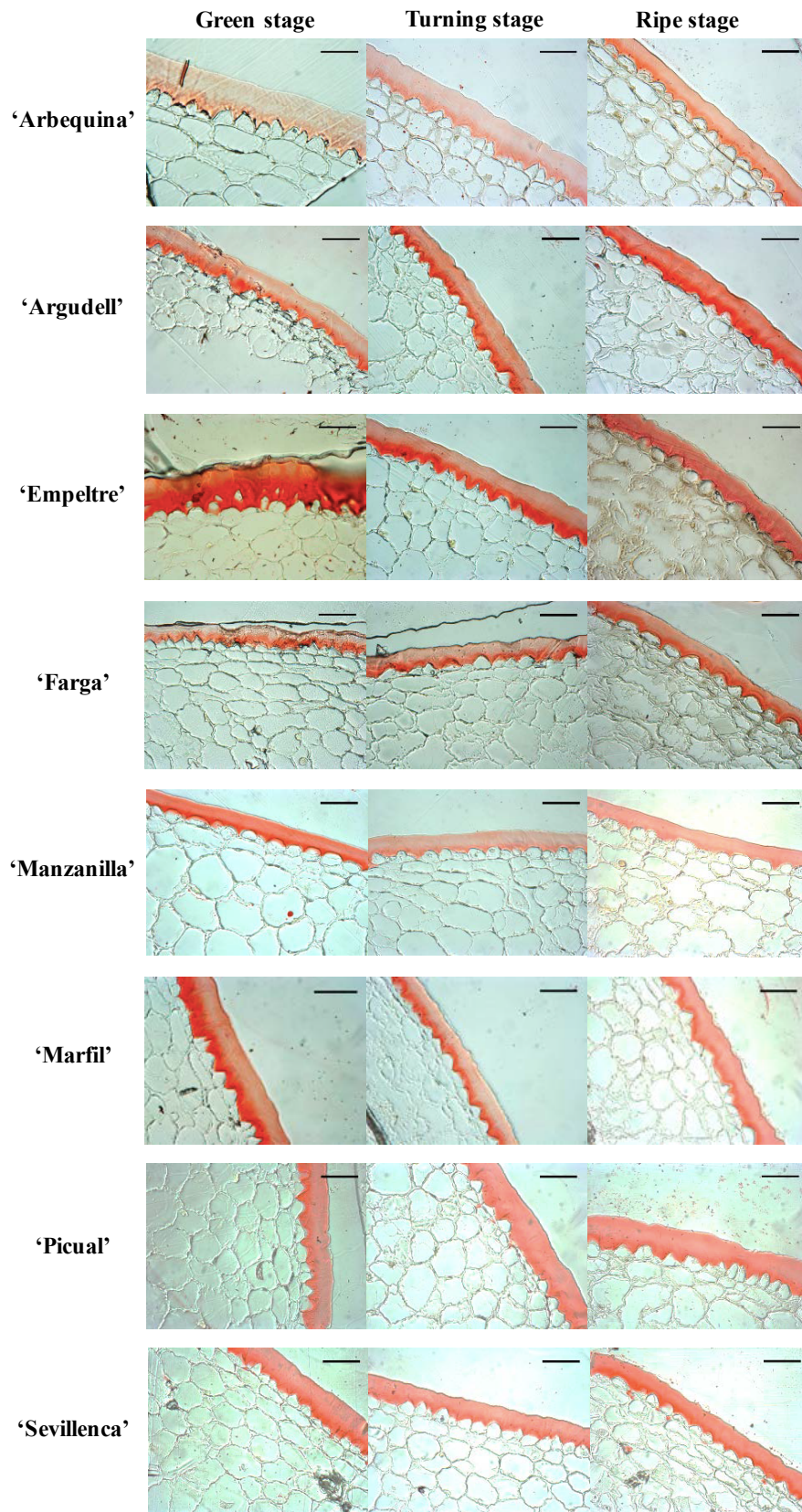
Supplementary Figure S1. Box plot of Sa of olive fruit surface at the green stage, as an example of differences in roughness parameters in the olive cultivars studied in this work. Sa is the arithmetic average height parameter, defined as the mean of the absolute deviation of roughness irregularities from the mean line.



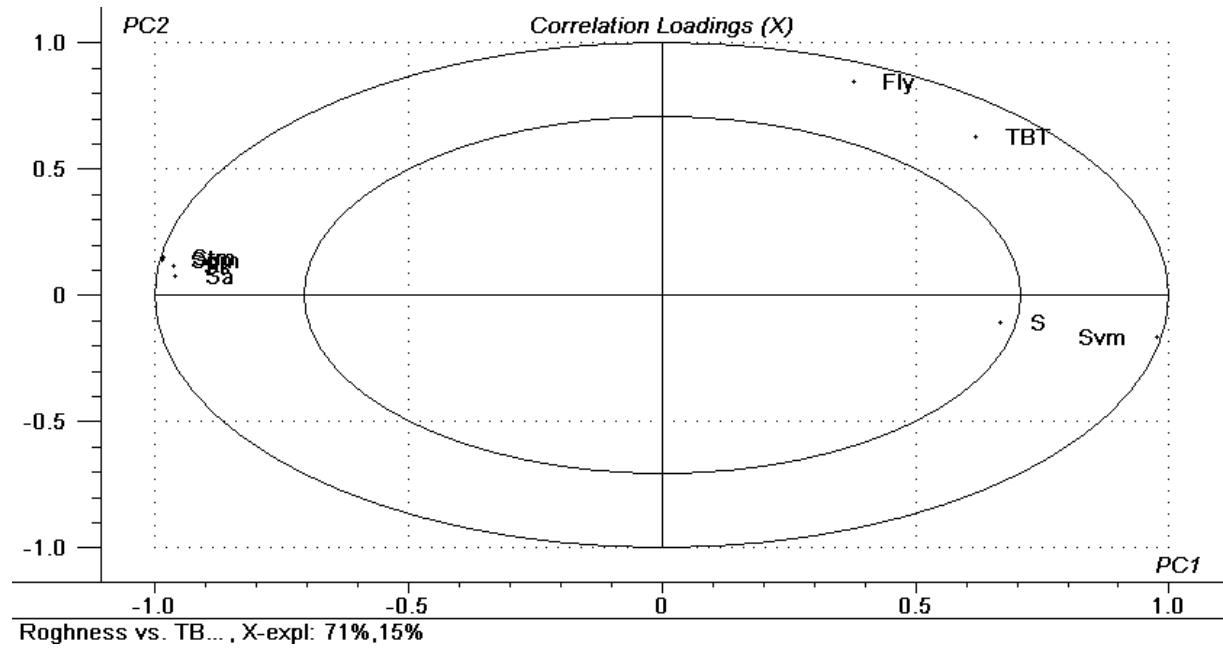
Supplementary Figure S2. 3D-diagrams of raw data outputs from fringe projections of olive fruits at the green stage. Blue and black areas represent background noise due to the shape and size of the olives, which did not cover the whole assessment window of the equipment.



Supplementary Figure S3. Toluidine Blue (TB) staining of olive fruits at the green stage. For 'Marfil' fruits, TB staining is shown for samples at three different maturity stages. Fruits were stained in a 0.05 % (w/v) TB solution for 2 h.



Supplementary Figure S4. Sudan IV-stained cross-sections of olive fruit pericarp at three maturity stages as observed under bright-field microscope. The scale bars indicate 60 μm.



Supplementary Figure S5. Correlation loadings plot of PC1 vs. PC2 corresponding to a Principal Component Analysis (PCA) model for surface roughness parameters, incidence (%) of olive fly infestation (Fly) and toluidine blue test (TBT) assessed in olive fruit at the green stage. *Sa*, *Stm*, *Spm* and *Svm* are related to vertical roughness, *Sk* represents core roughness, and *S* stands for horizontal roughness as defined in Materials and methods.

Supplementary Table S1. Indicence of infestation by *Bactrocera oleae* in olive fruits at the green, turning and ripe stages.

Cultivar	Maturity stage	Fly infestation (%)
‘Arbequina’	Green	0
	Turning	14
	Ripe	10
‘Argudell’	Green	12
	Turning	0
	Ripe	12
‘Empeltre’	Green	60
	Turning	76
	Ripe	24
‘Farga’	Green	4
	Turning	10
	Ripe	6
‘Manzanilla’	Green	56
	Ripe	20
‘Marfil’	Green	0
	Ripe	2
‘Morrut’	Green	6
	Turning	0
	Ripe	4
‘Picual’	Green	6
	Turning	6
	Ripe	8
‘Sevillenca’	Green	24
	Ripe	0

Values represent the percentage affected of fruits within sample of 50 olives.

Supplementary Table S2. Cuticular wax constituents (relative %) in cuticles isolated from olive fruit at the green, turning and ripe stages.

Cultivar	‘Arbequina’			‘Argudell’			‘Empeltre’		
Maturity stage	Green	Turning	Ripe	Green	Turning	Ripe	Green	Turning	Ripe
Fatty acids									
C20:0	0.20 ± 0.17	1.22 ± 0.03	0.90 ± 0.14	0.23 ± 0.21	1.56 ± 0.18	1.64 ± 0.49	nd	nd	0.99 ± 0.26
C20:1 (c13)	0.17 ± 0.15	1.09 ± 0.05	0.81 ± 0.07	0.21 ± 0.19	1.31 ± 0.11	1.44 ± 0.38	nd	nd	1.06 ± 0.19
C22:0	0.64 ± 0.09	1.02 ± 0.11	1.29 ± 0.13	0.64 ± 0.06	1.32 ± 0.13	1.43 ± 0.16	0.71 ± 0.12	0.74 ± 0.09	1.65 ± 0.03
C24:0	2.69 ± 1.50	1.33 ± 0.15	2.27 ± 0.03	1.73 ± 0.32	2.26 ± 0.17	1.68 ± 0.44	1.42 ± 0.17	1.49 ± 0.36	1.90 ± 0.28
C26:0	2.63 ± 0.49	3.09 ± 0.52	3.17 ± 0.07	1.58 ± 0.20	1.63 ± 0.03	1.67 ± 0.12	2.28 ± 0.33	2.63 ± 0.46	2.65 ± 0.30
C28:0	1.04 ± 0.22	1.27 ± 0.31	1.17 ± 0.13	0.00 ± 0.00	0.35 ± 0.00	0.50 ± 0.08	0.74 ± 0.09	0.96 ± 0.17	1.06 ± 0.15
n-Alkanes									
C20	0.60 ± 0.53	0.37 ± 0.02	0.31 ± 0.07	0.43 ± 0.40	0.30 ± 0.02	0.21 ± 0.05	0.27 ± 0.24	nd	0.20 ± 0.01
C21	nd	nd	nd	nd	0.23 ± 0.01	0.13 ± 0.12	nd	nd	nd
C22	0.63 ± 0.55	nd	nd	0.51 ± 0.47	nd	nd	0.45 ± 0.16	nd	nd
C25	0.62 ± 0.23	0.54 ± 0.47	0.57 ± 0.01	0.68 ± 0.31	0.73 ± 0.07	0.91 ± 0.23	0.73 ± 0.57	0.59 ± 0.34	0.90 ± 0.24
C26	0.84 ± 0.17	nd	0.47 ± 0.13	0.70 ± 0.07	0.57 ± 0.15	0.82 ± 0.15	0.70 ± 0.51	nd	0.81 ± 0.31
C27	0.43 ± 0.17	1.09 ± 0.27	0.95 ± 0.06	nd	0.43 ± 0.12	0.82 ± 0.13	nd	nd	0.81 ± 0.28
C34	0.61 ± 0.52	1.12 ± 0.66	nd	0.86 ± 0.97	0.31 ± 0.02	0.27 ± 0.07	nd	nd	nd
Fatty alcohols									
C22	1.43 ± 1.05	0.63 ± 0.08	0.73 ± 0.04	0.62 ± 0.07	0.49 ± 0.04	0.44 ± 0.04	1.09 ± 0.88	2.63 ± 0.63	0.52 ± 0.09
C24	1.25 ± 0.18	1.88 ± 0.59	2.31 ± 0.11	0.98 ± 0.11	1.59 ± 0.18	1.64 ± 0.19	1.00 ± 0.07	1.18 ± 1.04	1.99 ± 0.14
C26	3.83 ± 1.06	1.79 ± 0.58	1.99 ± 0.44	2.90 ± 0.66	0.69 ± 0.02	0.90 ± 0.18	2.41 ± 0.16	2.59 ± 0.61	1.04 ± 0.15
C28	1.44 ± 0.42	0.44 ± 0.40	0.70 ± 0.16	0.71 ± 0.18	nd	0.45 ± 0.16	0.63 ± 0.09	0.63 ± 0.15	nd
Sterols									
Squalene	0.76 ± 0.07	0.42 ± 0.38	0.41 ± 0.15	0.69 ± 0.17	0.51 ± 0.15	0.79 ± 0.11	0.63 ± 0.53	nd	0.71 ± 0.25
β-sitosterol	0.34 ± 0.31	nd	0.36 ± 0.01	0.21 ± 0.19	0.56 ± 0.16	0.89 ± 0.58	0.25 ± 0.22	0.44 ± 0.09	0.50 ± 0.12
Triterpenes									
Oleanolic acid	24.91 ± 3.40	23.70 ± 0.83	23.36 ± 1.13	29.59 ± 6.17	20.88 ± 0.66	21.68 ± 0.60	32.65 ± 1.25	33.94 ± 3.60	27.42 ± 0.37
Ursolic acid	nd	nd	nd	nd	nd	nd	nd	nd	nd
Maslinic acid	38.80 ± 10.83	44.55 ± 5.09	44.26 ± 2.00	40.39 ± 6.98	43.79 ± 0.77	44.55 ± 6.08	38.61 ± 0.73	39.38 ± 12.57	42.78 ± 2.18
Unidentified	16.15 ± 6.00	14.46 ± 1.36	13.96 ± 1.09	16.35 ± 0.99	20.48 ± 1.75	17.15 ± 2.99	15.41 ± 2.11	12.79 ± 5.65	13.00 ± 1.86

Supplementary Table S2 – Continued

Cultivar	'Farga'			'Manzanilla'			'Marfil'		
	Green	Turning	Ripe	Green	Turning	Ripe	Green	Turning	Ripe
Fatty acids									
C20:0	0.23 ± 0.21	0.74 ± 0.06	1.45 ± 0.11	0.17 ± 0.16	NA	0.79 ± 0.02	0.52 ± 0.03	NA	0.34 ± 0.04
C20:1 (c13)	0.21 ± 0.18	0.73 ± 0.05	1.57 ± 0.17	nd	NA	0.56 ± 0.00	0.80 ± 0.02	NA	0.63 ± 0.08
C22:0	0.67 ± 0.04	1.11 ± 0.13	1.67 ± 0.07	0.96 ± 0.23	NA	1.73 ± 0.12	0.49 ± 0.01	NA	1.00 ± 0.13
C24:0	2.25 ± 0.59	4.10 ± 0.48	3.04 ± 1.02	4.90 ± 1.18	NA	5.44 ± 0.57	1.00 ± 0.04	NA	2.86 ± 0.33
C26:0	2.55 ± 0.33	3.20 ± 0.53	3.41 ± 0.13	5.83 ± 1.43	NA	5.56 ± 0.74	3.52 ± 0.20	NA	4.66 ± 0.29
C28:0	0.99 ± 0.13	1.10 ± 0.18	1.58 ± 0.08	1.12 ± 0.29	NA	1.71 ± 0.14	0.98 ± 0.85	NA	2.44 ± 0.23
<i>n</i>-Alkanes									
C20	nd	nd	nd	nd	NA	nd	nd	NA	nd
C21	nd	nd	0.15 ± 0.13	nd	NA	nd	nd	NA	nd
C22	nd	nd	nd	nd	NA	nd	nd	NA	nd
C25	0.66 ± 0.17	0.61 ± 0.10	1.09 ± 0.09	0.53 ± 0.15	NA	0.71 ± 0.09	0.51 ± 0.03	NA	0.96 ± 0.13
C26	0.29 ± 0.31	nd	0.84 ± 0.15	nd	NA	0.45 ± 0.16	nd	NA	0.56 ± 0.09
C27	0.48 ± 0.23	0.21 ± 0.19	1.38 ± 0.20	nd	NA	0.79 ± 0.22	0.28 ± 0.01	NA	3.24 ± 0.29
C34	0.53 ± 0.91	0.47 ± 0.82	nd	nd	NA	nd	0.20 ± 0.02	NA	nd
Fatty alcohols									
C22	0.35 ± 0.03	0.53 ± 0.28	0.48 ± 0.03	2.70 ± 0.42	NA	1.03 ± 0.08	0.41 ± 0.02	NA	0.51 ± 0.06
C24	1.35 ± 0.28	2.10 ± 0.57	2.28 ± 0.02	1.63 ± 0.65	NA	3.58 ± 0.54	0.22 ± 0.02	NA	3.19 ± 0.43
C26	2.98 ± 0.48	2.66 ± 0.69	1.37 ± 0.01	5.88 ± 1.36	NA	4.77 ± 0.71	3.44 ± 0.43	NA	2.96 ± 0.23
C28	1.33 ± 0.19	1.03 ± 0.26	0.50 ± 0.01	1.29 ± 0.30	NA	1.31 ± 0.06	1.73 ± 0.25	NA	1.41 ± 0.05
Sterols									
Squalene	0.32 ± 0.38	0.18 ± 0.30	0.84 ± 0.16	nd	NA	0.48 ± 0.25	0.20 ± 0.17	NA	0.55 ± 0.12
β-sitosterol	0.22 ± 0.19	0.23 ± 0.20	0.00 ± 0.00	0.28 ± 0.26	NA	0.30 ± 0.02	0.35 ± 0.08	NA	nd
Triterpenes									
Oleanolic acid	32.79 ± 0.96	31.70 ± 1.03	28.20 ± 0.72	24.13 ± 1.63	NA	19.14 ± 1.04	42.55 ± 1.15	NA	28.48 ± 0.76
Ursolic acid	nd	nd	1.60 ± 1.32	nd	NA	nd	nd	NA	nd
Maslinic acid	40.74 ± 3.78	38.87 ± 5.55	33.09 ± 1.51	38.98 ± 9.04	NA	39.28 ± 8.41	32.20 ± 1.58	NA	33.13 ± 3.89
Unidentified	11.08 ± 0.59	10.40 ± 2.41	15.46 ± 0.89	11.60 ± 1.82	NA	12.37 ± 3.72	10.59 ± 0.85	NA	13.09 ± 1.58

Supplementary Table S2 – Continued

Cultivar	‘Morrut’			‘Picual’			‘Sevillena’		
	Green	Turning	Ripe	Green	Turning	Ripe	Green	Turning	Ripe
Fatty acids									
C20:0	0.20 ± 0.18	2.19 ± 0.16	0.88 ± 0.15	nd	1.20 ± 0.14	0.60 ± 0.04	nd	NA	1.75 ± 0.24
C20:1 (c13)	nd	1.37 ± 0.08	0.87 ± 0.08	nd	0.76 ± 0.09	0.41 ± 0.02	nd	NA	1.50 ± 0.23
C22:0	1.05 ± 0.18	2.03 ± 0.24	1.44 ± 0.17	0.58 ± 0.10	1.00 ± 0.19	0.84 ± 0.15	1.22 ± 0.13	NA	1.38 ± 0.03
C24:0	4.58 ± 0.88	4.65 ± 0.21	3.94 ± 0.93	1.34 ± 0.04	2.26 ± 0.77	1.29 ± 0.05	5.48 ± 0.83	NA	3.60 ± 0.52
C26:0	0.33 ± 0.30	4.18 ± 0.38	4.36 ± 0.63	0.92 ± 0.10	1.45 ± 0.27	1.10 ± 0.09	7.16 ± 1.24	NA	4.90 ± 0.54
C28:0	nd	0.79 ± 0.07	1.22 ± 0.12	nd	nd	0.34 ± 0.09	1.81 ± 0.30	NA	1.92 ± 0.46
<i>n</i>-Alkanes									
C20	nd	nd	nd	nd	nd	nd	nd	NA	nd
C21	nd	0.26 ± 0.03	nd	nd	0.13 ± 0.11	0.16 ± 0.14	nd	NA	0.28 ± 0.03
C22	nd	nd	nd	nd	nd	nd	nd	NA	nd
C25	0.46 ± 0.12	0.62 ± 0.05	0.63 ± 0.05	0.16 ± 0.14	0.75 ± 0.09	0.48 ± 0.07	0.29 ± 0.25	NA	0.72 ± 0.10
C26	nd	0.37 ± 0.15	0.29 ± 0.04	nd	0.63 ± 0.16	0.50 ± 0.17	0.24 ± 0.21	NA	0.48 ± 0.25
C27	nd	0.69 ± 0.19	1.27 ± 0.12	nd	0.70 ± 0.16	0.67 ± 0.18	nd	NA	0.82 ± 0.43
C34	nd	nd	nd	nd	nd	nd	1.17 ± 0.06	NA	nd
Fatty alcohols									
C22	0.71 ± 0.09	0.28 ± 0.14	0.49 ± 0.03	1.07 ± 0.53	0.67 ± 0.08	1.04 ± 0.68	3.15 ± 0.27	NA	0.33 ± 0.04
C24	1.20 ± 0.16	1.77 ± 0.15	1.97 ± 0.13	0.80 ± 0.09	1.07 ± 0.23	1.11 ± 0.19	1.26 ± 0.25	NA	1.37 ± 0.17
C26	nd	1.22 ± 0.10	1.98 ± 0.34	2.45 ± 0.15	1.59 ± 0.29	1.28 ± 0.14	3.74 ± 0.40	NA	0.76 ± 0.27
C28	0.56 ± 0.12	nd	0.56 ± 0.08	0.19 ± 0.16	nd	0.21 ± 0.02	1.69 ± 0.19	NA	0.48 ± 0.27
Sterols									
Squalene	nd	0.39 ± 0.16	nd	nd	0.61 ± 0.12	0.66 ± 0.16	0.60 ± 0.04	NA	0.62 ± 0.36
β-sitosterol	0.23	0.20	1.10 ± 0.93	0.36 ± 0.03	nd	0.85 ± 0.12	0.50 ± 0.04	NA	0.84 ± 0.57
Triterpenes									
Oleanolic acid	27.07 ± 2.38	21.00 ± 1.81	20.60 ± 0.89	29.06 ± 1.84	29.63 ± 1.79	24.74 ± 0.81	33.78 ± 1.10	NA	19.32 ± 1.02
Ursolic acid	nd	nd	nd	nd	nd	0.44 ± 0.47	1.22 ± 0.43	NA	nd
Maslinic acid	43.63 ± 7.18	43.13 ± 2.71	46.64 ± 1.79	51.71 ± 3.63	42.50 ± 3.53	36.73 ± 9.08	26.47 ± 4.20	NA	38.79 ± 6.01
Unidentified	19.97 ± 3.11	13.95 ± 0.67	12.51 ± 0.81	11.74 ± 1.77	14.20 ± 0.56	26.89 ± 8.74	10.43 ± 0.17	NA	20.13 ± 3.45

Values represent means of three replicates ± standard deviation (nd, non-detectable; NA, value not available).

Supplementary Table S3. Cutin constituents (relative %) in cuticles isolated from olive fruit at the green, turning and ripe stages.

Cultivar	‘Arbequina’			‘Argudell’			‘Empeltre’		
Maturity stage	Green	Turning	Ripe	Green	Turning	Ripe	Green	Turning	Ripe
Monocarboxylic fatty acids									
C16:0	0.92 ± 0.08	2.78 ± 0.11	2.46 ± 0.32	0.90 ± 0.04	3.17 ± 0.19	3.21 ± 0.70	0.59 ± 0.03	0.94 ± 0.56	1.73 ± 0.01
C16:1 (c9)	0.17 ± 0.03	0.33 ± 0.02	0.32 ± 0.04	0.15 ± 0.00	0.26 ± 0.01	0.35 ± 0.06	nd	nd	nd
C18:0	0.20 ± 0.03	0.39 ± 0.04	0.31 ± 0.04	0.20 ± 0.05	0.47 ± 0.05	0.52 ± 0.23	0.16 ± 0.03	0.42 ± 0.48	0.34 ± 0.01
C18:1 (c9)	1.84 ± 0.28	9.87 ± 0.74	8.46 ± 1.05	2.09 ± 0.12	9.31 ± 0.60	10.82 ± 1.99	1.55 ± 0.15	2.27 ± 1.27	6.86 ± 0.01
C18:1 (t9)	0.12 ± 0.02	0.48 ± 0.02	0.48 ± 0.05	0.12 ± 0.00	0.46 ± 0.03	0.64 ± 0.18	nd	0.25 ± 0.26	0.36 ± 0.01
C18:2 (c9,c12)	0.65 ± 0.11	2.23 ± 0.16	1.91 ± 0.24	0.70 ± 0.05	2.69 ± 0.23	2.94 ± 0.55	0.58 ± 0.04	0.76 ± 0.27	1.76 ± 0.01
C20:0	nd	nd	nd	nd	0.32 ± 0.05	0.23 ± 0.10	nd	nd	nd
C20:1 (c13)	nd	nd	nd	0.18 ± 0.00	nd	nd	nd	nd	nd
C22:0	0.58 ± 0.57	1.43 ± 0.24	1.88 ± 0.07	0.68 ± 0.38	1.68 ± 0.53	1.20 ± 0.27	1.03 ± 0.02	0.61 ± 0.13	1.44 ± 0.01
C24:0	0.53 ± 0.08	0.30 ± 0.03	0.30 ± 0.04	0.30 ± 0.06	0.66 ± 0.48	0.24 ± 0.03	0.35 ± 0.07	0.33 ± 0.09	0.29 ± 0.01
C26:0	nd	0.15 ± 0.13	0.22 ± 0.02	nd	0.61 ± 0.75	nd	0.38 ± 0.06	0.28 ± 0.02	0.36 ± 0.01
C28:0	nd	nd	nd	nd	nd	nd	nd	nd	nd
α,ω-Dicarboxylic fatty acids									
C16:0	0.81 ± 0.00	0.69 ± 0.06	0.68 ± 0.03	0.96 ± 0.11	0.78 ± 0.01	0.73 ± 0.06	0.79 ± 0.07	0.82 ± 0.11	0.61 ± 0.01
C18:1 (c9)	10.65 ± 1.40	10.76 ± 0.89	8.87 ± 1.45	13.61 ± 1.93	10.08 ± 0.15	10.38 ± 1.24	10.87 ± 0.36	8.66 ± 0.41	7.92 ± 0.01
α,ω-Dicarboxylic fatty acids with mid-chain-hydroxy group									
C18:0 (9,10-diOH)	2.63 ± 0.09	2.12 ± 0.31	1.97 ± 0.39	1.36 ± 0.05	0.95 ± 0.13	1.42 ± 0.25	3.58 ± 0.23	3.90 ± 0.95	3.40 ± 0.01
ω-Hydroxy fatty acids									
C16:0	7.96 ± 0.32	6.97 ± 0.54	7.02 ± 0.35	9.95 ± 0.41	8.79 ± 0.78	7.03 ± 0.65	6.12 ± 0.42	6.11 ± 0.60	4.98 ± 0.01
C18:0	4.00 ± 0.23	3.97 ± 0.31	4.02 ± 0.40	2.50 ± 0.38	3.55 ± 0.21	2.91 ± 0.33	5.07 ± 0.09	4.52 ± 0.33	4.23 ± 0.01
C18:1 (c9)	15.87 ± 2.04	15.58 ± 1.00	13.67 ± 1.79	17.79 ± 1.80	13.47 ± 0.48	13.14 ± 0.99	15.58 ± 0.98	13.40 ± 1.02	11.99 ± 0.01
C18:2 (c9,c12)	2.26 ± 0.30	1.82 ± 0.13	2.21 ± 0.49	1.85 ± 0.32	2.01 ± 0.17	1.37 ± 0.25	1.89 ± 0.23	1.85 ± 0.16	1.73 ± 0.01
C20:0	0.29 ± 0.08	nd	0.42 ± 0.04	nd	nd	0.33 ± 0.05	0.24 ± 0.08	0.32 ± 0.14	0.19 ± 0.01
ω-Hydroxy fatty acids with mid-chain-hydroxy group									
C16:0 (9/10,16-diOH)	18.91 ± 3.85	13.29 ± 2.19	15.86 ± 2.65	19.57 ± 2.63	17.26 ± 1.85	19.15 ± 5.02	16.73 ± 1.74	23.14 ± 5.72	19.03 ± 1.01
C18:0 (9,10,18-triOH)	2.57 ± 0.78	2.70 ± 0.12	2.40 ± 0.25	1.49 ± 0.10	0.85 ± 0.48	0.41 ± 0.08	5.08 ± 0.31	4.00 ± 0.46	3.58 ± 0.01

α -Hydroxy fatty acids

C22:0 (2-OH)	1.87 \pm 0.49	0.93 \pm 0.29	1.24 \pm 0.08	1.35 \pm 0.07	1.32 \pm 0.35	1.41 \pm 0.52	5.73 \pm 0.37	5.59 \pm 0.93	5.35 \pm 0.0
C24:0 (2-OH)	nd	nd	nd	nd	nd	0.25 \pm 0.19	nd	nd	0.21 \pm 0.

Other hydroxy fatty acids

C18:1 (c9, 12-OH)	nd	nd	nd	nd	nd	0.34 \pm 0.38	nd	nd	0.26 \pm 0.
C18:1 (c9, 17-OH)	nd	nd	nd	nd	nd	nd	0.12 \pm 0.10	0.18 \pm 0.11	nd

Fatty alcohols

C24	1.01 \pm 0.30	0.88 \pm 0.10	1.29 \pm 0.13	1.09 \pm 0.13	1.00 \pm 0.24	1.31 \pm 0.36	1.03 \pm 0.11	1.22 \pm 0.12	1.34 \pm 0.
C26	0.74 \pm 0.09	0.65 \pm 0.07	0.81 \pm 0.14	1.66 \pm 0.15	1.11 \pm 0.65	1.12 \pm 0.18	0.44 \pm 0.06	0.43 \pm 0.04	0.42 \pm 0.
C28	0.20 \pm 0.03	0.19 \pm 0.02	0.22 \pm 0.02	0.26 \pm 0.02	0.25 \pm 0.02	0.18 \pm 0.02	nd	nd	nd

Unidentified	25.23 \pm 0.78	21.50 \pm 0.55	22.97 \pm 0.76	21.23 \pm 1.15	18.96 \pm 1.18	18.39 \pm 0.81	22.08 \pm 0.56	20.00 \pm 3.08	21.61 \pm 0.
---------------------	------------------	------------------	------------------	------------------	------------------	------------------	------------------	------------------	----------------

Supplementary Table S3 – Continued

Cultivar	‘Farga’			‘Manzanilla’			‘Marfil’		
	Green	Turning	Ripe	Green	Turning	Ripe	Green	Turning	Ripe
Monocarboxylic fatty acids									
C16:0	0.66 ± 0.09	1.04 ± 0.11	1.98 ± 0.07	0.87 ± 0.26	NA	1.86 ± 0.28	2.00 ± 1.43	NA	1.34 ± 0.0
C16:1 (c9)	nd	nd	nd	nd	NA	nd	nd	NA	nd
C18:0	0.19 ± 0.02	0.23 ± 0.02	0.46 ± 0.03	0.31 ± 0.22	NA	0.55 ± 0.09	0.94 ± 0.96	NA	0.24 ± 0.0
C18:1 (c9)	2.51 ± 0.36	4.44 ± 0.46	12.41 ± 0.41	2.06 ± 0.70	NA	6.61 ± 1.17	3.84 ± 1.05	NA	6.03 ± 1.0
C18:1 (t9)	nd	0.17 ± 0.02	0.38 ± 0.01	nd	NA	0.36 ± 0.07	0.18 ± 0.05	NA	0.24 ± 0.0
C18:2 (c9,c12)	0.50 ± 0.07	0.89 ± 0.09	2.34 ± 0.19	0.60 ± 0.16	NA	1.33 ± 0.18	0.62 ± 0.22	NA	1.70 ± 0.0
C20:0	nd	nd	0.20 ± 0.03	nd	NA	0.27 ± 0.06	nd	NA	nd
C20:1 (c13)	nd	nd	nd	0.20 ± 0.01	NA	0.17 ± 0.01	0.16 ± 0.01	NA	nd
C22:0	1.52 ± 0.20	1.40 ± 0.62	1.43 ± 0.24	1.03 ± 0.08	NA	1.45 ± 0.90	1.77 ± 0.86	NA	1.00 ± 0.0
C24:0	0.38 ± 0.06	0.36 ± 0.06	0.26 ± 0.03	0.25 ± 0.04	NA	0.23 ± 0.05	0.42 ± 0.04	NA	0.23 ± 0.0
C26:0	0.25 ± 0.03	0.26 ± 0.01	0.26 ± 0.01	0.23 ± 0.02	NA	0.27 ± 0.02	0.30 ± 0.06	NA	0.31 ± 0.0
C28:0	nd	nd	nd	nd	NA	0.15 ± 0.02	nd	NA	nd
α,ω-Dicarboxylic fatty acids									
C16:0	0.75 ± 0.06	0.78 ± 0.05	0.60 ± 0.01	1.67 ± 0.22	NA	1.30 ± 0.10	1.88 ± 0.21	NA	1.34 ± 0.0
C18:1 (c9)	10.43 ± 1.46	10.45 ± 0.43	9.10 ± 0.36	15.29 ± 0.54	NA	12.59 ± 1.93	15.05 ± 0.61	NA	13.10 ± 0.0
α,ω-Dicarboxylic fatty acids with mid-chain-hydroxy group									
C18:0 (9,10-diOH)	1.93 ± 0.70	1.45 ± 0.09	1.46 ± 0.10	1.30 ± 0.24	NA	1.33 ± 0.12	2.61 ± 0.27	NA	2.98 ± 0.0
ω-Hydroxy fatty acids									
C16:0	7.19 ± 0.96	7.35 ± 0.26	5.91 ± 0.10	13.12 ± 0.49	NA	11.09 ± 0.13	7.86 ± 0.39	NA	6.01 ± 0.0
C18:0	3.99 ± 2.46	4.62 ± 0.22	4.00 ± 0.27	2.61 ± 1.34	NA	2.59 ± 0.67	2.49 ± 1.15	NA	4.51 ± 0.0
C18:1 (c9)	12.41 ± 2.20	13.32 ± 0.59	11.53 ± 0.13	16.04 ± 0.14	NA	12.67 ± 1.21	19.80 ± 0.37	NA	17.20 ± 0.0
C18:2 (c9,c12)	3.15 ± 0.28	3.14 ± 0.20	2.67 ± 0.26	1.79 ± 0.20	NA	1.77 ± 0.21	1.77 ± 0.11	NA	1.56 ± 0.0
C20:0	nd	nd	nd	0.36 ± 0.08	NA	0.31 ± 0.05	0.27 ± 0.02	NA	0.23 ± 0.0
ω-Hydroxy fatty acids with mid-chain-hydroxy group									
C16:0 (9/10,16-diOH)	27.42 ± 9.65	22.03 ± 2.43	19.00 ± 0.96	16.85 ± 2.33	NA	16.90 ± 3.38	9.36 ± 1.88	NA	11.66 ± 1.0
C18:0 (9,10,18-triOH)	1.98 ± 0.25	1.75 ± 0.15	1.78 ± 0.01	1.40 ± 0.20	NA	1.71 ± 0.12	3.09 ± 0.20	NA	3.26 ± 0.0

α -Hydroxy fatty acids

C22:0 (2-OH)	1.60 \pm 0.35	1.95 \pm 0.50	1.23 \pm 0.46	1.30 \pm 0.50	NA	1.10 \pm 0.50	1.75 \pm 0.91	NA	4.46 \pm 0.0
C24:0 (2-OH)	nd	nd	nd	nd	NA	0.23 \pm 0.05	nd	NA	nd

Other hydroxy fatty acids

C18:1 (c9, 12-OH)	nd	nd	0.17 \pm 0.01	nd	NA	0.22 \pm 0.21	nd	NA	0.14 \pm 0.0
C18:1 (c9, 17-OH)	nd	nd	nd	0.12 \pm 0.01	NA	0.17 \pm 0.04	0.16 \pm 0.01	NA	0.17 \pm 0.0

Fatty alcohols

C24	0.99 \pm 0.13	1.49 \pm 0.25	1.36 \pm 0.10	0.96 \pm 0.12	NA	1.39 \pm 0.31	0.54 \pm 0.19	NA	0.84 \pm 0.0
C26	0.84 \pm 0.16	0.91 \pm 0.09	0.87 \pm 0.14	1.61 \pm 0.03	NA	1.57 \pm 0.08	0.99 \pm 0.03	NA	0.62 \pm 0.0
C28	0.33 \pm 0.06	0.31 \pm 0.03	0.30 \pm 0.05	0.26 \pm 0.02	NA	0.30 \pm 0.02	0.40 \pm 0.02	NA	0.21 \pm 0.0

Unidentified	20.97 \pm 1.93	21.67 \pm 1.02	20.30 \pm 0.97	19.76 \pm 0.84	NA	19.49 \pm 1.06	21.73 \pm 2.31	NA	20.63 \pm 0.0
---------------------	------------------	------------------	------------------	------------------	----	------------------	------------------	----	-----------------

Supplementary Table S3 – Continued

Cultivar	‘Morrut’			‘Picual’			‘Sevillenca’		
	Green	Turning	Ripe	Green	Turning	Ripe	Green	Turning	Ripe
Monocarboxylic fatty acids									
C16:0	0.43 ± 0.01	1.73 ± 0.06	1.10 ± 0.16	0.38 ± 0.03	1.75 ± 0.35	1.16 ± 0.10	0.80 ± 0.03	NA	2.77 ± 0.0
C16:1 (c9)	nd	nd	nd	nd	nd	nd	nd	NA	nd
C18:0	0.18 ± 0.05	0.64 ± 0.04	0.29 ± 0.08	0.14 ± 0.02	0.49 ± 0.07	0.36 ± 0.03	0.18 ± 0.01	NA	0.56 ± 0.0
C18:1 (c9)	1.32 ± 0.03	10.09 ± 0.75	5.09 ± 0.70	1.13 ± 0.16	9.20 ± 1.97	6.14 ± 0.54	1.67 ± 0.05	NA	12.33 ± 0.0
C18:1 (t9)	nd	0.19 ± 0.04	0.15 ± 0.05	nd	0.26 ± 0.04	0.18 ± 0.02	nd	NA	0.39 ± 0.0
C18:2 (c9,c12)	0.69 ± 0.04	2.65 ± 0.22	1.69 ± 0.25	0.29 ± 0.02	0.92 ± 0.20	0.60 ± 0.04	0.72 ± 0.01	NA	3.37 ± 0.0
C20:0	nd	0.21 ± 0.04	0.17 ± 0.04	nd	0.12 ± 0.01	nd	nd	NA	nd
C20:1 (c13)	0.24 ± 0.02	0.18 ± 0.00	0.16 ± 0.02	0.23 ± 0.01	0.19 ± 0.01	0.19 ± 0.01	nd	NA	nd
C22:0	0.92 ± 0.56	0.92 ± 0.24	0.46 ± 0.22	0.88 ± 0.19	0.78 ± 0.31	0.77 ± 0.09	1.39 ± 0.17	NA	1.51 ± 0.0
C24:0	0.28 ± 0.02	0.24 ± 0.01	0.24 ± 0.04	0.21 ± 0.02	0.18 ± 0.01	0.21 ± 0.02	0.34 ± 0.02	NA	0.25 ± 0.0
C26:0	0.21 ± 0.02	0.23 ± 0.02	0.21 ± 0.02	nd	nd	nd	0.30 ± 0.03	NA	0.30 ± 0.0
C28:0	nd	nd	0.17 ± 0.03	nd	nd	nd	nd	NA	nd
α,ω-Dicarboxylic fatty acids									
C16:0	0.86 ± 0.07	0.72 ± 0.03	1.06 ± 0.04	0.74 ± 0.02	0.67 ± 0.07	0.63 ± 0.02	1.16 ± 0.12	NA	0.87 ± 0.0
C18:1 (c9)	16.88 ± 1.08	14.61 ± 0.75	16.20 ± 1.29	16.88 ± 0.53	15.04 ± 0.17	15.05 ± 0.34	12.39 ± 0.72	NA	10.39 ± 0.0
α,ω-Dicarboxylic fatty acids with mid-chain-hydroxy group									
C18:0 (9,10-diOH)	1.95 ± 0.40	1.68 ± 0.13	1.38 ± 0.48	0.90 ± 0.07	0.77 ± 0.05	1.19 ± 0.15	2.33 ± 0.23	NA	2.02 ± 0.0
ω-Hydroxy fatty acids									
C16:0	5.87 ± 0.84	4.88 ± 0.13	6.65 ± 0.66	12.01 ± 0.67	9.96 ± 0.86	9.12 ± 0.38	9.20 ± 0.59	NA	6.79 ± 0.0
C18:0	2.01 ± 0.96	2.47 ± 0.16	2.23 ± 0.17	2.50 ± 0.15	1.92 ± 0.30	2.26 ± 0.17	3.34 ± 0.13	NA	2.72 ± 0.0
C18:1 (c9)	23.54 ± 2.50	19.78 ± 0.59	19.55 ± 2.09	24.12 ± 0.54	21.48 ± 1.14	22.54 ± 1.11	16.46 ± 0.53	NA	13.46 ± 0.0
C18:2 (c9,c12)	1.28 ± 0.13	0.97 ± 0.01	1.06 ± 0.03	1.20 ± 0.12	0.93 ± 0.17	0.99 ± 0.13	1.82 ± 0.07	NA	1.38 ± 0.0
C20:0	0.22 ± 0.02	0.26 ± 0.01	0.24 ± 0.04	0.25 ± 0.05	0.19 ± 0.01	nd	0.23 ± 0.04	NA	nd
ω-Hydroxy fatty acids with mid-chain-hydroxy group									
C16:0 (9/10,16-diOH)	11.45 ± 2.36	9.39 ± 1.09	14.31 ± 5.18	13.60 ± 1.65	11.83 ± 0.39	13.68 ± 2.35	17.83 ± 1.00	NA	16.99 ± 0.0
C18:0 (9,10,18-triOH)	2.23 ± 0.26	2.13 ± 0.29	1.64 ± 0.39	1.14 ± 0.04	0.85 ± 0.09	0.44 ± 0.03	2.29 ± 0.31	NA	1.81 ± 0.0

α -Hydroxy fatty acids

C22:0 (2-OH)	1.87 \pm 0.43	1.52 \pm 0.30	1.63 \pm 0.06	1.60 \pm 0.62	0.83 \pm 0.31	1.41 \pm 0.34	1.20 \pm 0.31	1.87 NA	1.02 \pm 0.01
C24:0 (2-OH)	nd	0.12 \pm 0.10	0.16 \pm 0.06	nd	0.14 \pm 0.07	nd	nd	nd NA	0.24 \pm 0.01

Other hydroxy fatty acids

C18:1 (c9, 12-OH)	nd	0.20 \pm 0.16	0.18 \pm 0.13	nd	0.17 \pm 0.14	nd	nd	NA	0.30 \pm 0.01
C18:1 (c9, 17-OH)	0.22 \pm 0.01	0.19 \pm 0.02	0.19 \pm 0.03	0.13 \pm 0.00	0.12 \pm 0.01	0.11 \pm 0.01	0.12 \pm 0.01	NA	nd

Fatty alcohols

C24	0.99 \pm 0.14	1.22 \pm 0.11	1.05 \pm 0.05	1.02 \pm 0.16	0.80 \pm 0.05	1.01 \pm 0.17	1.03 \pm 0.19	NA	0.86 \pm 0.01
C26	0.78 \pm 0.12	0.55 \pm 0.01	0.58 \pm 0.12	1.39 \pm 0.11	1.11 \pm 0.03	1.11 \pm 0.09	1.06 \pm 0.02	NA	0.71 \pm 0.01
C28	0.16 \pm 0.02	nd	nd	0.15 \pm 0.01	0.13 \pm 0.01	nd	0.37 \pm 0.02	NA	0.23 \pm 0.01

Unidentified	25.42 \pm 1.04	22.23 \pm 0.43	22.17 \pm 1.26	19.10 \pm 0.34	19.17 \pm 1.01	20.86 \pm 0.27	23.79 \pm 0.45	NA	18.74 \pm 0.01
---------------------	------------------	------------------	------------------	------------------	------------------	------------------	------------------	----	------------------

Values represent means of three replicates \pm standard deviation (nd, non-detectable; NA, value not available).

Chapter II: Ripening-related cell wall modifications in olive (*Olea europaea* L.) fruit: a survey of nine genotypes

Food Chemistry 338 (2021) 127754



Contents lists available at ScienceDirect

Food Chemistry

journal homepage: www.elsevier.com/locate/foodchem

Ripening-related cell wall modifications in olive (*Olea europaea* L.) fruit: A survey of nine genotypes



Clara Diarte^{a,b}, Anna Iglesias^a, Agustí Romero^c, Tomás Casero^a, Antònia Ninot^c, Ferran Gatiús^a, Jordi Graell^{a,b}, Isabel Lara^{a,b,*}

^a Universitat de Lleida, Lleida, Spain

^b Postharvest Unit-XaRTA, AGROTÈCNIO, Lleida, Spain

^c IRTA-Mas Bové, Oliviculture, Oil Science and Nuts, Constantí, Spain

Food Chemistry (August 2021), 338, 127754. doi: 10.1016/j.foodchem.2020.127754

Clara Diarte, Anna Iglesias, Agustí Romero, Tomás Casero, Antònia Ninot, Ferran Gatiús, Jordi Graell and Isabel Lara.

Abstract

The production of olive (*Olea europaea* L.) is very important economically in many areas of the world, and particularly in countries around the Mediterranean basin. Ripening-associated modifications in cell wall composition and structure of fruits play an important role in attributes like firmness or susceptibility to infestations, rots and mechanical damage, but limited information on these aspects is currently available for olive. In this work, cell wall metabolism was studied in fruits from nine olive cultivars ('Arbequina', 'Argudell', 'Empeltre', 'Farga', 'Manzanilla', 'Marfil', 'Morrut', 'Picual' and 'Sevillena') picked at three maturity stages (green, turning and ripe). Yields of alcohol-insoluble residue (AIR) recovered from fruits, as well as calcium content in fruit pericarp, decreased along ripening. Cultivar-specific diversity was observed in time-course change patterns of enzyme activity, particularly for those acting on arabinosyl- and galactosyl-rich pectin side chains. Even so, fruit firmness levels were associated to higher pectin methylesterase (PME) activity and calcium contents. In turn, fruit firmness correlated inversely with ascorbate content and with α -L-arabinofuranosidase (AFase) and β -galactosidase (β -Gal) activities, resulting in preferential loss of neutral sugars from cell wall polymers.

Keywords: cell wall; cultivars; enzymes; firmness loss; maturity stage; minerals; *Olea europaea* L.

*O Love! What hours were thine and mine,
In lands of palm and southern pine,
In lands of palm, of orange-blossom,
Of olive, aloe, and maize and vine!*

Alfred, Lord Tennyson (*The Daisy*)

2.1. Introduction

Olive (*Olea europaea* L.) tree was one of the first crops to be domesticated by humans (Besnard, Terral and Cornille, 2018), and olive growing has outstanding economic relevance in countries around the Mediterranean basin. While the largest part of total production is devoted to oil extraction, a smaller amount thereof is intended for consumption as table olives, and hence fruit texture and mechanical properties are very relevant for the eating quality of the final product. Furthermore, high susceptibility of fruit to mechanical damage restricts the use of mechanical harvesting in table olive orchards, which hampers the reduction of production costs. In the case of cultivars used mainly for oil extraction, textural and mechanical factors may also influence extraction efficiency, while postharvest changes may have an impact on final oil quality (Vichi et al., 2009).

During the ripening process, textural changes occur which result from compositional and structural modifications in cell walls and middle lamellae. These changes arise largely from solubilisation and rearrangements of the constituent polysaccharides, carried out by pectolytic and non-pectolytic proteins (Goulao and Oliveira, 2008). Polysaccharide depolymerisation may also occur in some fruit species, including olive according to a few reports (Marsilio et al., 2000; González-Cabrera, Domínguez-Vidal, and Ayora-Cañada, 2018). Non-enzymatic factors may also contribute to ripening-related cell wall alterations, and experimental evidence of a role for ascorbic acid (AA) and its derivatives in the oxidative disassembly of cell wall polysaccharides has been found for banana (*Musa spp.*) (Cheng et al., 2008), longan (*Dimocarpus longan* Lour) (Duan et al., 2011) and sweet cherry (*Prunus avium* L.) (Belge et al., 2015).

In spite of the importance of ripening-associated modifications in cell wall composition and structure on key attributes such as firmness and susceptibility to mechanical damage, infestations or rots, very few published studies have addressed this topic during olive fruit maturation. Some information is however available for a few cultivars. For example, cell wall-related enzyme activities and cell wall gene expression levels have been reported to increase with maturity stage in ‘Hojiblanca’ (Fernández-Bolaños et al., 1997) and ‘Picual’ (Parra et al., 2013) fruit, respectively. Extensive solubilisation of cell wall materials occurred during ripening of ‘Koroneiki’ olives (Vierhuis et al., 2000). Similarly, ripening ‘Negrinha do Douro’ fruit showed progressive cell-to-cell separation and strong losses of arabinosyl residues resulting in noticeable firmness diminution (Mafra et al., 2001). Accordingly, substantial loss of neutral sugars from pectins was observed for ‘Arbequina’ olives during fruit ripening, linked to the progressive increase in α -L-arabinofuranosidase (AFase) activity (Lara et al., 2018). We were therefore interested in broadening these studies on a wider choice of cultivars, in order to improve current understanding of the biochemical mechanisms underlying texture changes in olive fruit during maturation.

2.2. Materials and methods

2.2.1. Plant material

Fruits of nine local Spanish olive cultivars (‘Arbequina’, ‘Argudell’, ‘Empeltre’, ‘Farga’, ‘Manzanilla’, ‘Marfil’, ‘Morrut’, ‘Picual’ and ‘Sevillanca’) were hand-collected in 2016 at three different maturity stages based on skin colour (green, turning and ripe) from trees supplied with support irrigation grown at an experimental orchard located at IRTA-Mas Bové (Constantí, Spain, 41° 09’N; 1° 12’E). Picking period was September to December. The main part of total annual rainfall in the producing area

(500 mm in 2016) took place during spring (April-May). Cultural practices and fertilization were the standard ones used in commercial orchards around the sampling site. The selected cultivars included oil- and table-olive representatives of very early ('Empeltre', 'Manzanilla'), early ('Sevillenca'), medium ('Arbequina', 'Argudell', 'Farga', 'Picual') and late ('Marfil', 'Morrut') ripening patterns (Tous & Romero, 1993).

The maturity index (0-7) was determined on 50 olives per cultivar and maturity stage based on the visual evaluation of fruit skin and flesh colour according to the usual practice by the olive industry, and values indicate the weighted average of the 50 fruits assessed. Oil content was determined jointly on 50 fruits per cultivar and maturity stage by nuclear magnetic resonance (NMR) spectroscopy after drying samples in the oven at 105 °C till constant weight. For the evaluation of fruit firmness, a penetration test was run on 10 olives per cultivar and maturity stage with an INSTRON texture analyser (Model 3344, Instron, Bucks, UK) equipped with a 1-mm diameter cylindrical probe descending at 1 mm s⁻¹. The maximum strength (N) and deformation (mm) to achieve surface breakage were recorded. Fruit skin colour was also assessed on 10 fruits with a desktop colorimeter (Chroma Meter CR-300, Minolta Corp., Osaka, Japan) using CIE illuminant D₆₅ with 8-mm aperture diameter and 10° observation angle. Results were expressed as CIELAB colour space coordinates (L*, a*, b*). The incidence of some alterations (olive fly infestation, infection by *Camarosporium dalmaticum*, bruised and wrinkled fruits) was also assessed visually on 50 fruits per cultivar and maturity stage, and data shown as a percentage.

2.2.2. Determination of mineral content

Fifty olives per cultivar and maturity stage were washed in 1% (v/v) Triton X-100, rinsed in deionised water (Fernández-Hernández et al., 2010) and pitted. Flesh samples were then vacuum-dried in a lyophilizer (Telstar[®] Cryodos, Azbil Group, Tokyo, Japan), milled and kept at -80 °C until analysis.

A muffle furnace (Carbolite CWF 1100, Carbolite Gero Ltd., Hope, UK) was used to obtain the ashes from lyophilized samples: temperature was raised during 12 h to 550 °C, kept at 550 °C for 12 h and then cooled down to room temperature. In order to hydrolyse pyrophosphates formed during incineration, samples were submitted to dry digestion in 6 mL of an aqueous HCl solution (1:1, v/v), and then kept in a sand bath at 70 °C until complete dryness. Finally, samples were resuspended in Milli-Q[®] water and filtered through Whatman[®] 40 ashless paper prior to injection into an inductively coupled plasma-mass spectrometry (ICP-MS) equipment (Agilent 7700X, Agilent Technologies Inc., Santa Clara, CA, USA) for quantification (mg kg⁻¹ DW) of boron (B), magnesium (Mg), potassium (K), calcium (Ca), manganese (Mn) and iron (Fe) contents.

2.2.3. Extraction, fractionation and analysis of cell wall materials

Cell wall materials were extracted as the alcohol-insoluble residue (AIR) as described in Voragen et al., 1983. Destoned olive fruit samples (50 g) were homogenised in 80% (v/v) ethanol in a domestic blender to obtain a 10% (w/v) suspension, and then heated at 80 °C for 20 minutes. After cooling down to room temperature, samples were filtered through Miracloth[®] (Merck Life Science S.L.U., Madrid, Spain). The solid residue was shaken three times in 80% ethanol for 30 minutes, then 5 minutes in 96% ethanol, and finally 5 minutes in acetone, and filtered through Miracloth[®] after each step. The final solid residue was dried at 50 °C and stored at -20 °C until fractionation and analysis. AIR yields were expressed as g 100 g⁻¹ fresh weight (FW).

The methodology for AIR fractionation was modified from a previous work (Lefever et al., 2004). AIR samples (0.5 g) were extracted sequentially in distilled water, 0.1 % (w/v) sodium oxalate (pH 5.6),

0.05 mol L⁻¹ sodium carbonate and 4 mol L⁻¹ potassium hydroxide to obtain the water-, sodium oxalate-, sodium carbonate- and potassium hydroxide-soluble fractions (W_{sf} , $NaOx_{sf}$, Na_2CO_{3sf} and KOH_{sf} , respectively). After each fractionation step, the supernatant was concentrated in a rotary evaporator and precipitated by adding 96% (w/v) ethanol. The sediment was then washed three times in water, and dried at 50 °C to determine fraction yields. Each extraction was done in triplicate, and yields given as g 100 g⁻¹ AIR.

Total sugar and uronic acid contents were analysed respectively by the phenol-sulfuric acid assay (Dubois et al., 1956) and the *m*-hydroxyphenyl method (Blumenkratz and Asboe-Hansen, 1973). Neutral sugar amount was calculated by subtracting the content of uronic acids from that of total sugars. Results were given as g 100 g⁻¹.

The degree of methyl esterification of pectins was determined according to Klavons and Bennet, 1986, with some modifications. Methyl groups were removed by adding 1 mL 1 M KOH and 5 mL Milli-Q[®] water to AIR samples (15 mg), which were then kept at room temperature for 2 h. After neutralising with 0.49 mol L⁻¹ H₃PO₄, released methanol was oxidised enzymatically (1 U mL⁻¹ alcohol oxidase) before adding 2 mL 0.02 mol L⁻¹ pentane-2,4-dione and incubating at 60 °C for 2 h. When mixture cooled down, the absorbance at 412 nm was read. The degree of methyl esterification was calculated as the molar ratio (%) of methanol to uronic acid content.

2.2.4. Cell wall-related enzyme activities

Enzyme activities were determined on acetone powder (AP) obtained from fruit pericarp samples as described by Fernández-Bolaños et al., 1997, with small modifications. Briefly, flesh tissue samples were homogenised in cold acetone (10% suspension, w/v) with a domestic blender and filtered. The solid residue was washed three times in acetone, filtered, allowed to dry at room temperature, and stored at -20 °C. Enzyme assays were carried out in triplicate on AP samples (100 mg) mixed in 1 mL of the appropriate extraction buffer.

Extraction buffers and activity assays for α -L-arabinofuranosidase (AFase; EC 3.2.1.55), β -galactosidase (β -Gal; EC 3.2.1.23), pectin methylesterase (PME; EC 3.1.1.11), polygalacturonase (exo-PG; EC 3.2.1.67 and endo-PG; EC 3.1.2.15), pectate lyase (PL; EC 4.2.2.2), endo-1,4- β -D-glucanase (EGase; EC 3.2.1.4) and β -xylosidase (β -Xyl; EC 3.2.1.37) were as described in Ortiz, Graell and Lara 2011, and references therein. Total protein content in the extracts was determined with the Bradford, 1976 method, using BSA as a standard, and data expressed as specific activity (U mg protein⁻¹).

2.2.5. Antioxidant properties

All analyses were undertaken on lyophilised pericarp tissue. Radical scavenging activity (RSA) was determined by the 2,2-diphenyl-1-picrylhydrazyl (DPPH) assay, in which the antioxidant ability of sample extracts is expressed as the percentage of DPPH reduction in comparison with the control (DPPH without sample). Total phenolics were extracted in methanol, quantified colorimetrically, and results given as mg gallic acid equivalents g⁻¹ DW. Anthocyanin content was estimated as cyanidin-3-rutinoside equivalents in extracts obtained from lyophilised tissue and expressed as mg cyanidin equivalents g⁻¹ DW. All procedures were as described elsewhere (Lara, Camats and Comabella, 2015).

The contents of total (TAA) and reduced (AA) ascorbic acid were measured with the colorimetric ascorbate assay (Gillespie and Ainsworth, 2007), and data given as nmol g⁻¹ dry weight (DW). Dehydroascorbic acid (DHA) content was taken as the difference between those in TAA and AA.

2.2.6. Statistical analysis

Means were submitted to multifactorial analysis of variance (ANOVA), with cultivar and maturation stage as the factors, and separated by LSD test ($p \leq 0.05$). JMP[®] Pro 13 and Sigma Plot 11.0 (Systat Software Inc.) software packages were used for statistical analyses. In order to relate dependent Y -variables to a set of potentially explanatory X -variables, partial least square regression (PLSR) was employed as a predictive method. The Unscrambler version 9.1.2 software (CAMO ASA, Oslo, Norway) was used for PLSR model development. Data were weighed by the inverse of the standard deviation of each variable and full cross-validation was run as a validation procedure.

2.3. Results and discussion

Physical characteristics of olive fruits used in this study are shown (**Table 1**). Additional phenotypical data including fruit size and water content are also included as supplementary material (**Supplementary Table S1**). Colour parameters showed increasing values of a^* along maturation accompanied by concomitant decreases in those of b^* and L^* , which reflect the progressive shift in fruit surface colour from green to purple or black hues. Maturity indices (MI) ranged between 0.04 and 5.88, contingent upon cultivars and harvest date. In accordance with colour changes, total anthocyanins increased significantly along fruit maturation (**Supplementary Table S2**) with the exception of ‘Marfil’ samples, which turn white rather than black owing to blockage of anthocyanin synthesis. The highest levels were observed for ripe ‘Manzanilla’ fruits ($8.0 \text{ mg g}^{-1} \text{ DW}$), while they were unsurprisingly very low in ripe ‘Marfil’ samples ($0.3 \text{ mg g}^{-1} \text{ DW}$).

Fruits softened significantly along ripening as indicated both by a decrease in the maximum strength required to induce surface breakage (henceforth, “firmness”) and by augmented deformation values indicative of increasing skin elasticity, excluding ‘Morrut’ samples for which no significant differences were observed in the latter indicator. ‘Marfil’ fruits displayed the largest differences in firmness levels between the green and the ripe stages (73.8%), while ripe ‘Empeltre’ olives lost only 36.9% firmness in relation with values at the green stage: these fruits showed the lowest firmness levels when sampled in September (**Table 1**) consistent with their very early ripening pattern (Tous and Romero, 1993). Both ‘Empeltre’ and ‘Manzanilla’ fruits suffered from the most severe incidence of *Bactrocera oleae* infestation (**Supplementary Table S3**).

Some chemical characteristics related to antioxidant properties were also assessed in fruit samples (**Supplementary Table S2**). The content of total phenols ranged from $12.3 \text{ mg g}^{-1} \text{ DW}$ (ripe ‘Sevillena’ samples) to $49.9 \text{ mg g}^{-1} \text{ DW}$ (green ‘Morrut’ fruits). A previous study on cultivars ‘Dhokar’ and ‘Chemlali’ reported increased content of total phenolics along fruit ripening (Jemai, Bouaziz and Sayadi, 2009).

Table 1. Maturity indicators and physical characteristics of olive fruits at the green, turning and ripe stages.

Cultivar	Maturity stage	Sampling date	Maturity index	Oil content (g 100g ⁻¹ DW)	L*	a*	b*	Maximum strength (N)	Deformation (mm)
'Arbequina'	Green	Sept 29	0.26	39.3	38.11 a BC	-9.23 c A	23.16 a CD	6.39 a CD	0.94 b A
	Turning	Sept 29	2.14	43.3	28.34 b BC	4.12 b B	10.17 b B	4.01 b A	1.03 b CD
	Ripe	Nov 27	3.40	52.2	21.88 c B	11.01 a A	2.62 c B	2.99 c A	1.38 a B
'Argudell'	Green	Sept 29	0.26	39.8	29.84 a F	-9.97 b AB	16.19 b E	6.60 a BC	0.58 b D
	Turning	Nov 27	0.96	48.0	32.69 a B	-7.98 b D	19.23 a A	3.72 b A	1.13 a BC
	Ripe	Nov 27	2.36	50.1	16.76 b C	2.32 a B	-1.04 c C	2.55 c BC	1.03 a CD
'Empeltre'	Green	Sept 29	0.48	45.9	38.24 a B	-9.76 c AB	25.49 a B	4.04 a F	0.87 c AB
	Turning	Sept 29	3.58	45.5	18.45 b D	3.37 a B	-0.13 b C	2.57 b C	1.20 b B
	Ripe	Nov 27	5.00	56.1	17.88 b C	-0.02 b BC	-1.83 c C	2.55 b BC	1.68 a A
'Farga'	Green	Sept 29	0.36	36.4	35.56 a CD	-10.53 b ABC	21.76 a CD	6.29 a CD	0.64 b
	Turning	Sept 29	2.04	40.9	26.27 b C	-0.08 a C	8.82 b B	4.02 b A	0.80 ab E
	Ripe	Nov 27	4.40	51.2	16.35 c C	-0.20 a C	-1.85 c C	2.14 c DE	0.87 a D
'Manzanilla'	Green	Sept 29	0.12	45.0	34.12 a DE	-10.94 b BC	21.33 a D	5.96 a D	0.87 b AB
	Ripe	Nov 27	5.88	50.6	17.64 b C	1.71 a BC	-1.52 b C	2.37 b CD	1.25 a B
'Marfil'	Green	Sept 29	0.04	46.1	50.26 b A	-13.91 b D	30.97 a A	7.57 a A	0.69 b C
	Ripe	Dec 12	0.96	34.2	66.39 a A	-3.27 a D	20.79 b A	1.98 b E	1.03 a D
'Morrut'	Green	Sept 29	0.16	27.0	35.00 b D	-10.48 c ABC	21.18 a D	7.15 a AB	0.83 a B
	Turning	Nov 27	1.04	37.2	38.73 a A	-5.12 b D	21.36 a A	3.21 b B	0.96 a D
	Ripe	Jan 16	3.40	45.0	22.12 c B	10.28 a A	1.72 b B	2.70 c B	0.95 a D
'Picual'	Green	Sept 29	0.30	35.6	32.01 a EF	-10.83 c BC	21.17 a D	6.92 a BC	0.86 c AB
	Turning	Nov 27	2.84	48.6	15.59 b D	7.71 a A	0.64 b C	2.97 b BC	1.49 b A
	Ripe	Nov 27	3.88	55.4	17.32 b C	1.14 b BC	-1.74 c C	2.59 c BC	1.69 a A
'Sevillena'	Green	Sept 29	0.32	43.8	35.73 a BCD	-11.67 b C	23.91 b BC	5.26 a E	0.68 b CD
	Ripe	Nov 27	3.16	57.0	17.71 b C	0.14 a BC	-1.85 a C	2.26 b D	1.24 a BC

Maturity indices represent the weighted average of 50 olives. Oil content was determined jointly for 50 fruits, and values reported represent the average of the 50 olives assessed. For CIELAB colour parameters, maximum strength and deformation, values represent means of 10 olives assessed individually. Different capital letters denote significant differences among the cultivars for a given maturity stage, and different lower-case letters stand for significant differences among maturity stages for a given cultivar, at $P \leq 0.05$ (LSD test).

Abbreviation: L, a*, b*: coordinates of CIELAB colour space.

In this work, though, this increasing trend was observed for ‘Farga’ uniquely. In contrast, results indicate cultivar-related differences in the evolution of total phenols: while no significant changes were found for ‘Manzanilla’ and ‘Marfil’, contents decreased along fruit ripening in fruit samples from the rest of the cultivars assessed (**Supplementary Table S2**). Total amount of phenolics showed no apparent relationship with RSA in fruit samples. RSA levels were very high in all cases, ranging from 79.2% to as much as 98.9%. RSA was particularly high in ‘Marfil’, ‘Manzanilla’ and ‘Morrut’ fruits, with values above 90% regardless of maturity stage (**Supplementary Table S2**). Limited ripening-related variation in RSA was found, with the exception of ‘Farga’ and ‘Marfil’ samples, for which significant increases were observed, in agreement with reports on ‘Dhokar’ and ‘Chemlali’ olives (Jemai et al., 2009). Ascorbic acid (AA) is a major antioxidant buffer in plant apoplasts (Pignocchi and Foyer, 2003). Because of increased permeability of cell membranes along fruit ripening, ascorbate is released into the apoplast (Fry, 1998), where it can be oxidised to dehydroascorbic acid (DHA). DHA has to be returned back to the cytosol for subsequent reduction. In five out of the nine cultivars considered in this study (‘Empeltre’, ‘Farga’, ‘Manzanilla’, ‘Morrut’ and ‘Picual’), AA levels detected in fruit pericarp increased with maturity stage. In contrast, significant decreases were found along maturation for ‘Marfil’ and ‘Sevillanca’, while limited change was observed for ‘Arbequina’ and ‘Argudell’ (**Supplementary Table S2**). The observation of increased AA contents along maturation is interesting in the light of a previous work showing that D-galacturonic acid released as a consequence of cell wall solubilisation may be a major precursor for ascorbic acid biosynthesis in fruits (Agius et al., 2003). In this work, indeed, firmness loss along fruit maturation was paralleled by decreased yields of insoluble cell wall materials and by progressive solubilisation of cell wall constituents as shown by higher yields of the water-soluble fraction in more mature samples (**Table 2**). These ripening-related cell wall modifications were hence considered more in detail.

2.3.1. Cell wall modifications along fruit ripening

With the exception of ‘Empeltre’, AIR yields decreased significantly throughout fruit maturation (**Table 2**), in agreement with earlier reports on ‘Hojiblanca’ and ‘Negrinha do Douro’ olives (Jiménez et al., 2001; Mafra et al., 2001). When AIR were fractionated further, the percentage of water-soluble materials (W_{sf}) over total AIR was generally found to increase over ripening, reflecting progressive solubilisation of cell wall polymers. In contrast, no consistent trends in change dynamics over fruit ripening were observed across all nine cultivars considered regarding yields of the chelator-soluble ($NaOx_{sf}$), the sodium carbonate-soluble (Na_2CO_{3sf}) or the potassium-soluble (KOH_{sf}) fractions, enriched in non-covalently linked pectins, covalently-linked pectins and matrix glycans, respectively (**Table 2**).

When the content in neutral sugars was analysed in AIR, little variations were found over fruit ripening (**Table 3**), which suggest that sugars were reallocated among AIR fractions. Indeed, substantial loss of neutral sugars along fruit ripening was shown for the KOH-soluble fraction, sometimes paralleled by significant increases in neutral sugar content in the Na_2CO_3 -soluble fraction. These rearrangements might account for the erratic trends in fraction yields observed during fruit ripening (**Table 2**).

The analysis of uronic acid percentage in the different AIR fractions isolated showed significant decreases in the water-soluble fraction during fruit ripening (**Table 4**). Together with the observation that total W_{sf} yields increased with maturity stage (**Table 2**), this finding clearly suggests that neutral sugars, rather than uronic acids, were solubilised preferentially from cell wall polymers.

Table 2. Yield of alcohol-insoluble residue (AIR) (g 100 g⁻¹ FW), degree of methyl esterification of pectins (% , molar ratio), yields of AIR fractions (g 100 g⁻¹ AIR) and of the final insoluble residue (g 100 g⁻¹ FW) isolated from olive fruits at the green, turning and ripe stages.

Cultivar	Maturity stage	AIR	d.e.	AIR fractions						Final insoluble residue				
				W _{sf}	NaOx _{sf}	Na ₂ CO _{3sf}	KOH _{sf}							
'Arbequina'	Green	7.8	56.9	b DEF	0.7	b D	2.6	b C	0.9	c D	1.8	b EF	7.31	a D
	Turning	7.6	49.8	b D	2.5	a A	5.0	ab D	1.7	b C	2.4	a CD	6.72	b D
	Ripe	3.6	64.8	a B	3.5	a CD	7.8	a B	2.3	a BCD	0.9	c E	3.08	c G
'Argudell'	Green	12.3	77.9	b B	1.1	b D	7.6	b AB	0.9	a D	2.0	b DEF	10.90	a B
	Turning	11.4	93.1	a A	1.5	a A	9.2	a A	2.0	a C	2.7	ab BC	9.62	b C
	Ripe	8.4	78.4	b A	1.3	ab G	8.5	b B	2.2	a BCD	3.4	a BC	7.12	c B
'Empeltre'	Green	5.1	88.5	a A	4.1	ab A	3.7	b C	3.3	a AB	4.5	b A	4.26	b F
	Turning	3.8	48.9	b D	1.9	b A	5.8	b CD	3.8	a A	4.7	ab A	3.21	c F
	Ripe	6.4	31.9	c D	6.7	a A	8.7	a AB	3.4	a ABC	5.5	a A	4.82	a E
'Farga'	Green	8.6	52.1	b EF	2.9	b B	6.3	a B	2.8	a BC	4.1	a AB	7.20	a D
	Turning	5.0	58.2	b CD	2.5	b A	6.7	a BC	2.7	a BC	3.5	a B	4.26	b E
	Ripe	4.0	71.2	a AB	5.2	a B	6.5	a B	1.5	b CD	3.3	a BC	3.36	c F
'Manzanilla'	Green	4.0	62.4	a CDE	2.0	b C	8.8	a A	4.6	a A	3.3	a BC	3.25	a G
	Ripe	3.0	67.5	a AB	4.0	a C	11.9	a A	4.9	a A	2.3	a D	2.30	b I
'Marfil'	Green	7.93	49.8	a F	1.9	a C	6.6	b B	3.6	a AB	4.1	b AB	6.64	a E
	Ripe	3.5	50.9	a C	2.4	a EF	9.7	a AB	3.7	a AB	5.3	a A	2.78	b H
'Morrut'	Green	15.2	70.0	a BC	1.1	b D	9.0	b A	1.3	a CD	1.1	b F	13.29	a A
	Turning	12.7	76.6	a B	2.0	a A	10.2	a A	1.9	a C	1.7	b D	10.69	b A
	Ripe	6.2	74.3	a AB	2.0	a F	8.5	b B	1.7	a BCD	2.7	a CD	5.31	c D
'Picual'	Green	8.4	58.3	b DEF	1.1	b D	8.7	a A	3.1	a ABC	2.9	a CD	7.07	b D
	Turning	11.6	68.1	ab BC	2.3	a A	7.5	b B	3.4	a AB	1.6	b D	9.90	a B
	Ripe	7.3	76.5	a AB	2.5	a EF	7.8	ab B	3.1	a ABCD	1.4	b E	6.24	c C
'Sevillenca'	Green	10.1	62.7	a CD	1.1	b D	7.6	a AB	2.1	a BCD	2.3	b DE	8.75	a C
	Ripe	9.7	67.5	a AB	2.9	a DE	8.0	a B	1.1	a D	3.7	a B	8.17	b A

Alcohol-insoluble residue (AIR) was recovered jointly from approximately 50 g fruit pericarp, obtained from 15 to 50 olives contingent upon fruit size. Degree of esterification values and fraction yields represent means of three replicate determinations. Different capital letters denote significant differences among the cultivars for a given maturity stage, and different lower-case letters stand for significant differences among maturity stages for a given cultivar, at $P \leq 0.05$ (LSD test).

*Abbreviations: AIR, Alcohol-insoluble residue; d.e., degree of methyl esterification of pectins; W_{sf}, water-soluble fraction; NaOx_{sf}, sodium oxalate-soluble fraction; Na₂CO_{3sf}, sodium carbonate-soluble fraction; KOH_{sf}, potassium hydroxide-soluble fraction.

Table 3. Neutral sugar content (g 100⁻¹ g) in the alcohol-insoluble residue (AIR), and in AIR fractions isolated from olive fruits at the green, turning and ripe stages.

Cultivar	Maturity stage	AIR _{sf}		AIR fractions			
				Na ₂ CO _{3sf}		KOH _{sf}	
‘Arbequina’	Green	12.62	a A	nd		28.11	a D
	Turning	7.38	b DE	2.80	b C	20.68	b E
	Ripe	13.33	a AB	10.05	a DE	11.70	c D
‘Argudell’	Green	12.82	a A	3.62	a D	29.32	b D
	Turning	13.72	a AB	8.56	a B	35.40	a C
	Ripe	14.42	a A	7.70	a E	29.01	b A
‘Empeltre’	Green	13.68	a A	16.33	a C	39.33	a C
	Turning	11.61	a BC	14.67	a A	42.14	a B
	Ripe	13.47	a AB	5.68	b E	28.42	b A
‘Farga’	Green	12.24	a A	4.98	b D	20.86	c E
	Turning	10.41	a CD	18.01	a A	48.02	a A
	Ripe	10.84	a BC	5.53	b E	29.17	b A
‘Manzanilla’	Green	14.40	a A	14.92	a C	39.54	a C
	Ripe	14.38	a A	13.07	a CD	24.51	b B
‘Marfil’	Green	2.06	b C	19.92	b C	58.44	a A
	Ripe	9.92	a C	29.06	a A	19.36	b C
‘Morrut’	Green	14.71	a A	8.73	b D	43.40	a B
	Turning	14.96	a A	16.44	a A	36.20	b C
	Ripe	13.11	a ABC	15.68	a C	21.97	c BC
‘Picual’	Green	5.84	a BC	26.51	a B	39.72	a C
	Turning	6.77	a E	16.30	b A	28.42	b D
	Ripe	6.50	a D	16.24	b C	23.91	b B
‘Sevillenca’	Green	8.23	b B	36.29	a A	19.19	a E
	Ripe	11.04	a BC	21.36	b B	13.22	b D

Values represent means of three replicates (nd, non-detectable). Different capital letters denote significant differences among the cultivars for a given maturity stage, and different lower-case letters stand for significant differences among maturity stages for a given cultivar, at $P \leq 0.05$ (LSD test).

*Abbreviations: AIR, alcohol-insoluble residue; Na₂CO_{3sf}, sodium carbonate-soluble fraction; KOH_{sf}, potassium hydroxide-soluble fraction.

For some of the cultivars considered (‘Arbequina’, ‘Argudell’, ‘Manzanilla’, ‘Morrut’, ‘Picual’ and ‘Sevillenca’), this is also supported by the observation of augmented proportions of uronic acids in the chelator-soluble fraction of more mature samples (Table 4). Substantial uronic acid losses from the Na₂CO₃-soluble fraction were found during ‘Arbequina’ fruit ripening, in accordance with a previous report (Lara et al., 2018). This trend was observed also for ‘Morrut’, ‘Picual’ and ‘Sevillenca’ fruits, suggesting a link to firmness loss.

2.3.2. Cell-wall modifying enzyme activities along fruit ripening

Changes in cell wall fraction yields and composition suggested important losses of neutral sugars from cell wall polymers along ripening, and thus pointed out to a relevant role for enzyme activities acting on pectin side-chains. Because arabinose stands out quantitatively in olive fruit pectins (Mafra et al., 2001), levels of AFase activity were considered. AFases remove arabinosyl residues from galacturonans, and so contribute to cell wall disassembly by promoting pectin solubilisation and by facilitating the access of other enzymes to their galacturonan backbone substrate.

Table 4. Uronic acid content (g 100⁻¹ g) in the alcohol-insoluble residue (AIR) and in AIR fractions isolated from olive fruits at the green, turning and ripe stages.

Cultivar	Maturity stage	AIR		AIR fractions							
				W _{sf}		NaOx _{sf}		Na ₂ CO _{3sf}		KOH _{sf}	
‘Arbequina’	Green	8.25	a CD	6.88	a D	2.96	b B	34.93	a A	1.95	b DE
	Turning	6.46	b BC	1.71	b C	3.20	a AB	17.46	b A	1.94	b A
	Ripe	8.67	a B	1.93	b F	4.36	a A	11.01	c BC	3.03	a C
‘Argudell’	Green	9.43	b BC	20.55	a A	0.73	b DE	8.90	a CD	2.64	a B
	Turning	10.98	a A	11.80	b A	1.13	a C	8.75	a C	1.98	b A
	Ripe	6.86	c CD	12.93	b A	1.83	a EF	8.81	a D	2.40	ab D
‘Empeltre’	Green	6.16	ab E	1.66	b E	3.78	a A	10.38	a BC	2.68	a B
	Turning	6.91	a B	2.66	a C	3.54	ab A	11.80	a B	2.16	ab A
	Ripe	4.38	b G	0.30	c G	2.45	b CD	12.25	a B	2.00	b E
‘Farga’	Green	6.90	a DE	2.14	a E	4.04	a A	11.44	b B	1.66	b EF
	Turning	5.56	b C	0.47	b D	4.07	a A	11.03	b B	2.45	a A
	Ripe	6.20	ab DE	1.49	a FG	2.75	b C	15.80	a A	2.44	a D
‘Manzanilla’	Green	14.27	a A	8.39	a D	0.77	b D	6.88	a D	2.49	b BC
	Ripe	12.79	a A	2.33	b EF	3.54	a B	5.49	a EF	4.54	a A
‘Marfil’	Green	14.00	a A	9.41	a CD	2.84	a B	8.64	b CD	2.41	a BC
	Ripe	7.25	b C	5.16	b C	1.94	b DEF	10.53	a C	2.58	a D
‘Morrut’	Green	5.55	a E	13.31	a BC	0.50	b E	8.10	a D	3.25	a A
	Turning	3.95	b D	10.69	a A	1.33	a C	5.08	b D	2.43	b A
	Ripe	5.71	a EF	6.84	b B	1.54	a FG	4.85	b F	2.38	b D
‘Picual’	Green	10.37	a B	17.27	a AB	1.30	c C	8.20	a D	1.51	c F
	Turning	6.69	b B	6.86	b B	2.01	b BC	5.04	b D	2.53	b A
	Ripe	6.13	b DE	3.52	c DE	2.21	a CDE	5.02	b F	4.04	a B
‘Sevillena’	Green	8.34	a CD	15.96	a B	0.98	b D	11.22	a B	2.11	a CD
	Ripe	4.97	b FG	3.62	b D	1.14	a G	6.61	b E	1.28	b F

Values represent means of three replicates. Different capital letters denote significant differences among the cultivars for a given maturity stage, and different lower-case letters stand for significant differences among maturity stages for a given cultivar, at $P \leq 0.05$ (LSD test).

*Abbreviations: AIR, alcohol-insoluble residue; W_{sf}, water-soluble fraction, NaOx_{sf}, oxalate-soluble fraction; Na₂CO_{3sf}, sodium carbonate-soluble fraction; KOH_{sf}, potassium hydroxide-soluble fraction.

AFase activity levels in ‘Arbequina’ as well as in ‘Empeltre’, ‘Farga’, ‘Manzanilla’ and ‘Sevillena’ fruits increased significantly with maturity stage (**Table 5**), as reported previously for ‘Arbequina’ (Lara et al., 2018). However, genotype-related differences existed as to time-course changes in AFase activity, since no variation or even decreased activity levels were observed for the rest of the cultivars considered. Even though galactose is less abundant in cell walls of olive fruit (Mafra et al., 2001), β -Gal-catalysed removal of galactosyl residues might also contribute to the reallocation of neutral sugars to the water-soluble fraction and to pectin rearrangements during ripening. The change patterns observed for this enzyme activity were also variable across the nine olive cultivars assessed, significant ripening-associated increases being found for ‘Arbequina’, ‘Argudell’, ‘Manzanilla’ and ‘Marfil’ uniquely (**Table 5**).

Table 5. Specific activity (U mg⁻¹ protein) of cell wall-related enzymes in acetone powders obtained from the pericarp of olive fruits at the green, turning and ripe stages.

Cultivar	Maturity stage	Non-pectolytic				Pectolytic									
		β-Xyl		EGase		PG		Backbone-acting PL		PME		Side chain-acting AFase		β-Gal	
‘Arbequina’	Green	0.032	a D	0.178	a E	0.681	a F	1.040	a D	60.373	a CD	0.049	b BC	0.109	c CD
	Turning	0.041	a B	0.131	b C	0.455	b E	0.613	b C	11.777	b C	0.071	a BC	0.159	b BC
	Ripe	0.033	a A	0.088	b D	0.201	c D	0.373	c E	9.871	b CD	0.068	a C	0.271	a C
‘Argudell’	Green	0.088	a A	1.396	a BC	9.891	a C	5.073	a AB	167.170	a B	0.079	a A	0.395	ab AB
	Turning	0.053	b A	0.690	b A	2.432	b C	2.034	b C	22.981	b BC	0.087	a A	0.183	b B
	Ripe	0.024	c B	0.512	b C	2.356	b C	1.428	b CD	9.840	b CD	0.061	b CD	0.557	a B
‘Empeltre’	Green	0.030	a D	0.262	ab E	1.142	ab F	0.829	ab D	24.344	a DE	0.040	b CD	0.244	a BCD
	Turning	0.032	a BC	0.423	a B	1.650	a D	2.048	a C	26.174	a B	0.043	b C	0.147	b BC
	Ripe	0.023	a B	0.119	b D	0.641	b D	1.100	b CD	3.480	b D	0.061	a CD	0.049	c D
‘Farga’	Green	0.013	b E	0.159	a E	0.958	a F	2.190	a C	5.644	b E	0.026	c E	0.124	a CD
	Turning	0.018	b D	0.141	a C	0.640	b E	1.619	b C	23.704	a BC	0.043	b C	0.102	a CD
	Ripe	0.030	a A	0.071	b D	0.305	c D	0.970	c CDE	16.944	a B	0.105	a A	0.099	a CD
‘Manzanilla’	Green	0.034	a D	1.441	a B	5.691	a D	2.807	a C	24.275	a DE	0.037	b DE	0.049	b D
	Ripe	0.009	b CD	0.101	b D	0.789	b D	1.547	b C	11.963	b BC	0.104	a A	2.158	a A
‘Marfil’	Green	0.032	a D	0.828	b C	3.889	b E	2.940	a C	816.837	a A	0.033	a DE	0.085	b D
	Ripe	0.011	b CD	2.285	a A	9.700	a A	2.424	a B	45.134	b A	0.033	a E	0.132	a CD
‘Morrut’	Green	0.049	a C	1.919	a A	12.562	a B	4.778	a B	182.640	a B	0.056	b B	0.605	a A
	Turning	0.029	b C	0.564	b AB	3.430	b B	2.649	b B	92.093	b A	0.070	a B	0.074	b D
	Ripe	0.007	c D	0.084	b D	0.628	c D	0.749	c DE	7.984	c CD	0.041	c E	0.523	a B
‘Picual’	Green	0.061	a B	1.042	a CD	16.109	a A	5.843	a A	86.326	a C	0.049	a BC	0.329	ab BC
	Turning	0.034	b BC	0.660	b A	4.861	c A	3.436	b A	27.886	b B	0.048	a C	0.572	a A
	Ripe	0.029	b AB	0.735	b B	7.070	b B	3.370	b A	38.710	b A	0.055	a D	0.127	b CD
‘Sevillenca’	Green	0.039	a CD	0.371	a E	3.408	a E	4.890	a AB	24.470	a DE	0.080	b A	0.168	a BCD
	Ripe	0.015	b C	0.129	b D	0.743	b D	2.554	b B	11.818	a BC	0.090	a B	0.129	a CD

Values represent means of three replicates. Different capital letters denote significant differences among the cultivars for a given maturity stage, and different lower-case letters stand for significant differences among maturity stages for a given cultivar, at $P \leq 0.05$ (LSD test). *Abbreviations: β-Xyl, β-xylosidase; EGase, endo-1,4-β-D-glucanase; PG, polygalacturonase; PL, pectate lyase; PME, pectin methylesterase; AFase, α-L-arabinofuranosidase; β-Gal, β-galactosidase.

For eight out of the nine cultivars considered, the highest levels of PME activity corresponded to green fruits (**Table 5**), and accordingly the degree of methyl esterification of pectins was generally lower in these samples in comparison with ripe fruits (**Table 2**). The declining trend observed for PME activity during ripening suggests an early role in cell wall modifications leading to olive fruit softening, in agreement with previous works (Mafra et al., 2001; Lara et al., 2018). PME modulates cell wall structure in different ways. On a side, PME demethylating action may favour cell wall reinforcement through the establishment of calcium bridges between free carboxyl groups (Goulao and Oliveira, 2008). Yet PME action also leads to lowered pH in the apoplast, thus providing a regulatory mechanism for additional cell wall-related enzymes. Negatively charged polyuronides will also favour pectin hydration and may thus modify protein diffusion and activity (Grignon and Sentenac, 1991). Furthermore, PME-catalysed cleavage of methyl groups from α -D-GalUA-rich polymers is a requirement for subsequent action of other pectolytic enzymes such as PG and PL, which will remove demethylated residues uniquely, respectively through hydrolysis or β -elimination.

With the exception of ‘Marfil’, PG and PL activity assays showed reduced activity levels along olive ripening (**Table 5**). Even though the time-course trend was similar across cultivars, noticeable variation in specific activity levels were observed, ranges spanning from 16.1 (green ‘Picual’) to 0.2 (ripe ‘Arbequina’) unit mg^{-1} protein for PG, and from 5.8 (green ‘Picual’) to 0.4 (ripe ‘Arbequina’) unit mg^{-1} protein for PL (**Table 5**). It has been suggested (Jiménez et al., 2001) that degradation of cell wall polysaccharides during ripening of ‘Hojiblanca’ olives may be sequential, the metabolism of pectic polysaccharides being more active at the onset of the ripening process, while neutral polysaccharides would be metabolised more intensively at subsequent stages. This would be consistent with data herein showing opposite trends for enzyme activities acting on the pectin backbone (PG, PL, PME) and those acting on the neutral sugar-rich sidechains (AFase, β -Gal). This would also agree with the apparently preferential loss of neutral sugars along ripening (**Tables 2, 3**).

Two non-pectolytic enzyme activities, β -Xyl and EGase, were also analysed. Results revealed a general decreasing trend in activity values during fruit ripening. This observation may be reflecting an early role in cell wall modifications. For some of the cultivars assessed, lower β -Xyl activity levels were observed in samples displaying higher yields of KOH_{sf} , the cell wall fraction enriched in the matrix glycan substrates of those enzymes (**Table 2**). Even so, it should be pointed out that fraction yields were expressed as a percentage over AIR, and hence variations in other AIR fractions as well as in total AIR isolated will also affect the relative KOH_{sf} proportions observed. Additionally, certain amount of tightly-bound cell wall polymers may have not been extracted in KOH and have so remained in the final insoluble residue. Actually, yields of the insoluble residue remaining after sequential AIR extraction decreased over fruit ripening, expressed both as a percentage over AIR ($\text{g } 100 \text{ g}^{-1} \text{ AIR}$) and as a percentage over FW ($\text{g } 100 \text{ g}^{-1} \text{ FW}$) (**Table 2**). This would be in accordance with the observation of sharp decreases in the content of xylose, a quantitatively prominent sugar component of olive cell walls, in the final residue during ripening of ‘Negrinha do Douro’ olives (Mafra et al., 2001), as well as with increased W_{sf} yields over ripening found herein (**Table 2**).

2.3.3. Other potential factors: mineral content and antioxidant status

In addition to related enzyme activities, some studies have suggested a role for ascorbic acid in fruit ripening-associated cell wall disassembly and firmness loss (Cheng et al., 2008; Duan et al., 2011; Belge et al., 2017). As a consequence of increasing cell membrane permeability upon fruit ripening, ascorbate is released into the apoplast, leading to the generation of hydroxyl ($\bullet\text{OH}$) radicals (Fry, 1998). At phys-

iological ranges, ascorbate can favour the oxidative scission of plant cell wall polysaccharides, and xyloglucans are reportedly more susceptible than pectins to ascorbate-induced scission (Fry, 1998), which might relate to the observed decline in yields of the insoluble residue during ripening (**Table 2**).

Evidence also exists that mineral deficiency may impact cell wall integrity through metabolic changes eventually affecting cell wall expansion, plant growth, crop yield and quality of the final product (Goulao, Fernandes and Amâncio, 2017). Therefore, the content of some minerals in fruit samples was also studied. The highest contents observed corresponded to potassium (K), calcium (Ca) and magnesium (Mg) (**Supplementary Table S4**). In general, boron (B) concentrations observed were higher than those reported for other olive cultivars including ‘Amfissis’, ‘Chondrolia Chalkidikis’ and ‘Picholine’ (Chatzissavvidis, Therios and Antonopoulou, 2004; Tekaya et al., 2014). Magnesium (Mg) and potassium (K) contents were also higher than those reported for other cultivars (Nergiz and Engez, 2000; Fernández-Poyatos, Ruiz-Medina and Llorent-Martínez, 2019). In contrast, manganese (Mn) concentrations recorded were lower than those in other cultivars grown in Spain (Fernández-Hernández et al., 2010), while those of iron (Fe) were roughly as in earlier reports (Llorent-Martínez et al., 2014). The presence of Fe in green olives intended for manufacturing as table olives is considered undesirable, as this mineral sets up complexes with polyphenols naturally present in the fruit, which causes skin to blacken (Fernández-Poyatos et al., 2019), and from this point of view the low Fe levels in green ‘Manzanilla’ and ‘Morrut’ fruits would indicate that these cultivars are more suitable for this purpose than the rest of assessed cultivars.

A clear, general trend among cultivars was recognisable for Ca uniquely, which decreased with fruit ripening. Calcium content ranged widely from 306.0 to 1837.6 mg kg⁻¹DW (ripe ‘Morrut’ and green ‘Marfil’, respectively). The observation that it generally decreased along ripening is interesting in the light of its role in the preservation of fruit firmness and other quality-related aspects (reviewed in Lara, 2013). With the purpose of obtaining a global overview of the relationships among the many variables assessed, a partial least square regression (PLSR) model was developed, in which data on cell wall fractions, enzyme activities, ascorbate and mineral content were used as the set of *X*-variables potentially explaining firmness levels of fruit samples. The corresponding correlation loadings plot (**Figure 1**) shows that the two first principal components (PC) of the model accounted for up to 85% of total variability in fruit firmness. Firmness was associated to higher levels of PME activity and Ca concentrations, AIR yields, and content of neutral sugars in the KOH_{sf}. The association between PME activity and Ca levels to fruit firmness agrees with a reinforcing role for this enzyme activity at early stages of fruit ripening. Moreover, the mode of PME action on pectins, and hence the distribution of free carboxyl groups, is dependent on apoplastic pH (Denès et al., 2000). In the apoplast of unripe fruits, with pH values close to neutrality, the enzyme acts through a single chain, multiple attack mechanism, leading to a blockwise distribution of de-esterified residues which confers pectins higher calcium affinity. In the presence of high calcium contents (**Supplementary Table S4**) this would result in cell wall stiffening and favour firmness retention as shown herein (**Figure 1**).

Higher firmness levels were also associated to high levels of PG and PL activities (**Figure 1**). However, it should be noted that high activities by themselves may be of little significance for actual cell wall disassembly. Factors such as cell wall porosity, apoplastic pH or cell wall hydration status may limit their activity or access to their pectin backbone substrate.

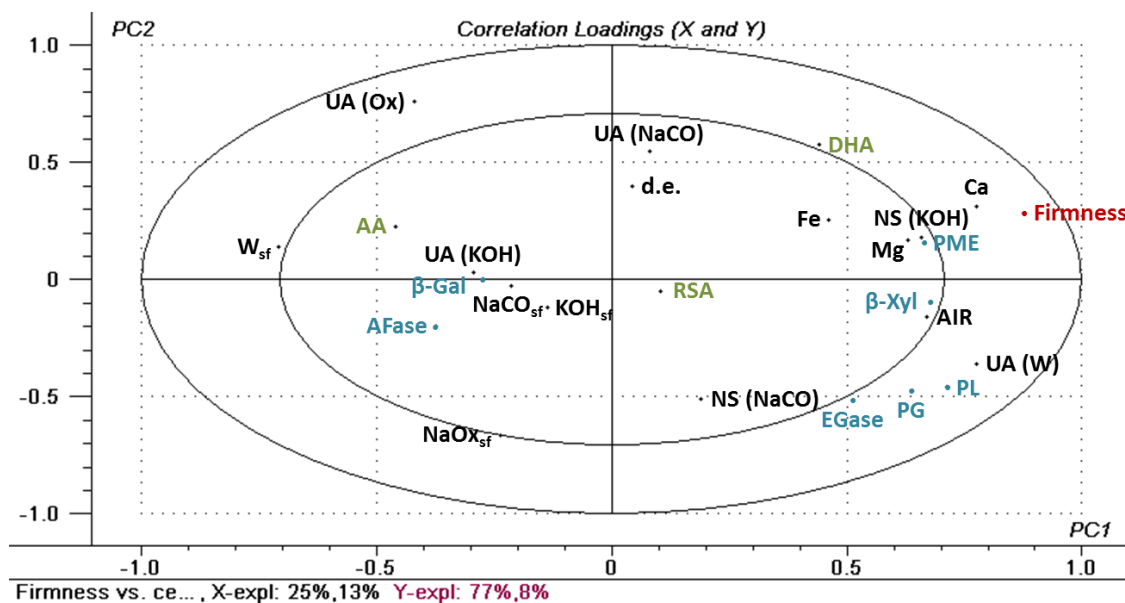


Figure 1. Correlation loadings plot of PC1 vs. PC2 corresponding to a PLSR model for fruit firmness (Y variable) vs. cell wall composition, enzyme activities, ascorbate and mineral contents (X variables) of olive fruits. *Abbreviations: AIR, alcohol-insoluble residue; d.e., degree of methyl esterification of pectins; Wsf, NaOXsf, NaCOsf and KOHsf, yields of water-, sodium oxalate-, sodium carbonate- and potassium hydroxide-soluble fractions, respectively; UA(W), UA(Ox), UA (NaCO) and UA (KOH), uronic acid contents in Wsf, NaOXsf, NaCOsf and KOHsf, respectively; NS (NaCO) and NS (KOH), neutral sugar contents in NaCOsf and KOHsf, respectively; d.e., degree of methyl esterification of pectins; β -Xyl, β -xylosidase; EGase, endo-1,4- β -D-glucanase; PG, polygalacturonase; PL, pectate lyase; PME, pectin methylesterase; AFase, α -L-arabinofuranosidase; β -Gal, β -galactosidase; Ca, Fe, Mg, content of calcium, iron and magnesium; AA, reduced ascorbic acid; DHA, dehydroascorbic acid; RSA, radical scavenging activity.

Indeed, AFase and β -Gal activities were inversely correlated to fruit firmness, which suggest that the presence of highly branched sidechains in pectins of green fruits restricted actual PG and PL action in spite of high activity levels. Enzyme activity assays are usually performed in optimal conditions of pH, temperature and concentrations of substrates and cofactors, which often do not correspond with the real *in mureo* conditions. Hence, *in vitro* activity may not match the actual *in planta* activity, and so some caution should be exerted when interpreting activity assay results. Furthermore, such data generally represent the joint activities of several isoforms, and change patterns in the activity of the ripening-specific isozyme(s) may be masked within total activity recorded.

Firmer fruits also showed higher percentage of uronic acids in the water-soluble fraction, which reflects the decrease in the uronic acids:neutral sugar ratio in this fraction as sugars become progressively solubilized as ripening proceeds. This is in agreement with the observation that the content of neutral sugars in the KOH_{sf} was also associated to higher fruit firmness (**Figure 1**). The KOH_{sf} is enriched in polysaccharides collectively termed hemicelluloses, which among others include xyloglucans, xylans, glucomannans and arabinoxylans. The xyloglucan backbone is constituted of β -1,4-linked glucose residues, displays xylose- and galactose-rich sidechains, and forms cell wall-strengthening cross-links with cellulose. Decreasing trends for β -Xyl and EGase activities (**Table 5**), which act on these non-pectic polymers, may indicate an early role in the onset of ripening-related cell wall changes.

Ascorbic acid content was inversely correlated to fruit firmness and to PME (**Figure 1**). This is also interesting on the basis of previous studies reporting that (a) de-esterified pectin is more susceptible than

methyl-esterified pectin to ascorbate-induced scission (Dumville and Fry, 2003), and that (b) galacturonic acid released from cell walls is an important precursor for L-ascorbic acid biosynthesis in fruits (Agius et al., 2003). Higher susceptibility of de-esterified pectins to ascorbate would hint at an additional mechanism by which PME could impact on ripening-related firmness loss.

2.4. Conclusions

The comparative study reported herein pointed out a relevant role for some cell wall-related enzyme activities in the process of ripening-associated softening of olive fruit. Even though cultivar-specific diversity was observed in time-course trends of activity changes, some common patterns in ripening-related cell wall modifications were found. Progressive solubilisation of cell wall polysaccharides was reflected in increased yields of the water-soluble fraction. Fruit firmness in green fruits was associated to higher levels of PME activity and calcium levels, suggesting that the formation of egg-box structures between pectic polysaccharides led to cell wall reinforcement. Data also suggest that neutral sugars rather than uronic acids were lost from cell wall polymers, in agreement with the observation that AFase and β -Gal activities were correlated inversely with fruit firmness. Ascorbate levels might also play an aiding role in cell wall disassembly. A better comprehension of these ripening-associated modifications may allow improving orchard management and produce handling for the enhancement of fruit quality.

2.5. References

- Agius F, González-Lamothe R, Caballero JL, Muñoz-Blanco J, Botella MA, Valpuesta V. 2003. Engineering increased vitamin C levels in plants by overexpression of a D-galacturonic acid reductase. *Nat. Biotechnol.* 21, 177-181.
- Belge B, Comabella E, Graell J, Lara I. 2015. Post-storage cell wall metabolism in two sweet cherry (*Prunus avium* L.) cultivars displaying different postharvest performance. *Food Sci. Technol.* 21, 416-427.
- Belge B, Goulao LF, Comabella E, Graell J, Lara I. 2017. Refrigerated storage and calcium dips of ripe ‘Celeste’ sweet cherry fruit: Combined effects on cell wall metabolism. *Sci. Hortic.* 219, 182-190.
- Besnard G, Terral JF, Cornille A. 2018. On the origins and domestication of the olive: a review and perspectives. *Ann. Bot.* 121, 385-403.
- Blumenkrantz N, Asboe-Hansen G. 1973. New method for quantitative determination of uronic acids. *Anal. Biochem.* 54, 484-489.
- Bradford MM. 1976. A rapid and sensitive method for the quantitation of microgram quantities of protein utilizing the principle of protein-dye binding. *Anal. Biochem.* 72, 248-254.
- Chatzissavvidis CA, Therios IN, Antonopoulou C. 2004. Seasonal variation of nutrients concentration in two olive (*Olea europaea* L.) cultivars irrigated with high boron water. *J. Hortic. Sci. Biotechnol.* 79, 683-688.
- Cheng G, Duan X, Shi J, Lu W, Luo Y, Jiang W, Jiang Y. 2008. Effects of reactive oxygen species on cellular wall disassembly of banana fruit during ripening. *Food Chem.* 109, 319-324.

Results: Chapter II

Denès JM, Baron MA, Renard CMGC, Péan C, Drilleau JF. 2000. Different action patterns for apple pectin methylesterase at pH 7.0 and 4.5. *Carbohydr. Res.* 327, 385-393.

Duan X, Zhang H, Zhang D, Sheng J, Lin H, Jiang Y. 2011. Role of hydroxyl radical in modification of cell wall polysaccharides and aril breakdown during senescence of harvested longan fruit. *Food Chem.* 128, 203-207.

Dubois M, Gilles KA, Hamilton JK, Rebers PA, Smith F. 1956. Colorimetric method for determination of sugars and related substances. *Anal. Chem.* 28, 350-356.

Dumville JC, Fry SC. 2003. Solubilisation of tomato fruit pectins by ascorbate: a possible non-enzymic mechanism of fruit softening. *Planta.* 217, 951-961.

Fernández-Bolaños J, Heredia J, Vioque B, Castellano JM, Guillén R. 1997. Changes in cell-wall-degrading enzyme activities in stored olives in relation to respiration and ethylene production - Influence of exogenous ethylene. *Z. Lebensm. Unters. Forch.* 204, 293-299.

Fernández-Hernández A, Mateos R, Garcia-Mesa JA, Beltran G, Fernández-Escobar R. 2010. Determination of mineral elements in fresh olive fruits by flame atomic spectrometry. *Span. J. Agric. Res.* 8, 1183-1190.

Fernández-Poyatos MP, Ruiz-Medina A, Llorent-Martínez EJ. 2019. Phytochemical profile, mineral content, and antioxidant activity of *Olea europaea* L. cv. Cornezuelo table olives. Influence of *in vitro* simulated gastrointestinal digestion. *Food Chem.* 297, 124933.

Fry SF. 1998. Oxidative scission of plant cell wall polysaccharides by ascorbate-induced hydroxyl radicals. *Biochem. J.* 332, 507-515.

Gillespie KM, Ainsworth EA. 2007. Measurement of reduced, oxidized and total ascorbate content in plants. *Nat. Protoc.* 2, 871-874.

González-Cabrera M, Domínguez-Vidal A, Ayora-Cañada MJ. 2018. Postharvest Biol. Technol. 145, 74-82.

Goulao LF, Oliveira CM. 2008. Cell wall modifications during fruit ripening: when a fruit is not the fruit. *Trends Food Sci. Technol.* 19, 4-25.

Goulao LF, Fernandes JC, Amânci S. 2017. How the depletion in mineral major elements affects grapevine (*Vitis vinifera* L.) cell wall. *Front. Plant Sci.* 8, 1439.

Grignon C, Sentenac H. 1991. pH and ionic conditions in the apoplast. *Annu. Rev. Plant Physiol. Plant Mol. Biol.* 42, 103-128.

Jemai H, Bouaziz M, Sayadi S. 2009. Phenolic composition, sugar contents and antioxidant activity of Tunisian sweet olive cultivar with regard to fruit ripening. *J. Agric. Food Chem.* 57, 2961-2968.

Jiménez A, Rodríguez R, Fernández-Caro I, Guillén R, Fernández-Bolaños J, Heredia A. 2001. Olive fruit cell wall: degradation of pectic polysaccharides during ripening. *J. Agric. Food Chem.* 49, 409-415.

Klavons JA, Bennet RD. 1986. Determination of methanol using alcohol oxidase and its application to methyl ester content of pectins. *J. Agric. Food Chem.* 34, 597-599.

Lara I. 2013. Preharvest sprays and their effects on the postharvest quality of fruit. *Stewart Postharvest Rev.* 9, 1-12.

Lara I, Camats JA, Comabella E, Ortiz A. 2015. Eating quality and health-promoting properties of two sweet cherry (*Prunus avium* L.) cultivars stored in passive modified atmosphere. *Food Sci. Technol.* 21, 133-144.

Lara I, Albrecht R, Comabella E, Riederer M, Graell J. 2018. Cell-wall metabolism of ‘Arbequina’ olive fruit picked at different maturity stages. *Acta Hort.* 1199, 133-138.

Lefever G, Vieuille M, Delage N, d’Harlingue A, de Monteclerc J, Bompeix G. 2004. Characterization of cell wall enzyme activities, pectin composition, and technological criteria of strawberry cultivars (*Fragaria x ananassa* Duch). *Food Chem. Toxicol.* 69, 221-226.

Llorent-Martínez EJ, Fernández-de Córdova ML, Ortega-Barrales P, Ruiz-Medina A. 2014. Quantitation of metals during the extraction of virgin olive oil from olives using ICP-MS after microwave-assisted acid digestion. *J. Am. Oil Chem. Soc.* 91, 1823-1830.

Mafra I, Lanza B, Reis A, Marsilio V, Campestre C, De Angelis M, Coimbra MA. 2001. Effect of ripening on texture, microstructure and cell wall polysaccharide composition of olive fruit (*Olea europaea*). *Physiol. Plant.* 111, 439-447.

Marsilio V, Lanza B, Campestre C, De Angelis M. 2000. Oven-dried table olives: textural properties as related to pectic composition. *J. Sci. Food Agric.* 80, 1271-1276.

Nergiz C, Engez Y. 2000. Compositional variation of olive fruit during ripening. *Food Chem.* 69, 55-99.

Ortiz A, Graell J, Lara I. 2011. Preharvest calcium applications inhibit some cell wall-modifying enzyme activities and delay cell wall disassembly at commercial harvest of ‘Fuji Kiku-8’ apples. *Postharvest Biol. Technol.* 62, 161-167.

Parra R, Paredes MA, Sánchez-Calle IM, Gómez-Jiménez MC. 2013. Comparative transcriptional profiling analysis of olive ripe-fruit pericarp and abscission zone tissues shows expression differences and distinct patterns of transcriptional regulation. *BMC Genomics.* 14, 866-886.

Pignocchi C, Foyer CH. 2003. Apoplastic ascorbate metabolism and its role in the regulation of cell signalling. *Curr. Plant Biol.* 6, 379-389.

Tekaya M, Mechri B, Cheheb H, Attia F, Chraief I, Ayachi M, Boujneh D, Hammami M. 2014. Changes in the profiles of mineral elements, phenols, tocopherols and soluble carbohydrates of olive fruit following foliar nutrient fertilization. *LWT.* 59, 1047-1053.

Tous J, Romero A. 1993. *Variedades del olivo: con especial referencia a Cataluña.* (ISBN 8476643764).

Vichi S, Romero A, Gallardo-Chacón J, Tous J, López-Tamames E, Buixaderas S. 2009. Influence of olives’ storage conditions on the formation of volatile phenols and their role in off-odor formation in the oil. *J. Agric. Food Chem.* 57, 1449-1455.

Results: Chapter II

Vierhuis E, Schols HA, Beldman G, Voragen AGJ. 2000. Isolation and characterisation of cell wall material from olive fruit (*Olea europea* cv. Koroneiki) at different ripening stages. *Carbohydr. Polym.* 43, 11-21.

Voragen FGJ, Timmers JPJ, Linssen JPH, Schols HA, Pilnik W. 1983. Methods of analysis for cell-wall polysaccharides of fruit and vegetables. *Z. Lebensm. Unters. Forch.* 177, 251-256.

Supplementary material

Supplementary Table S1. Phenotypical data of olive fruits used in this study.

Cultivar	Maturity stage	Weight (g)	F:S ratio *	Water content (%)	Length (mm)	Diameter (mm)
'Arbequina'	Green	1.10	2.68	53.9	14.1 ab D	12.1 b CD
	Turning	1.27	3.18	55.2	13.4 b C	12.0 b B
	Ripe	1.59	4.24	58.2	14.7 a D	13.0 a DE
'Argudell'	Green	2.02	4.08	56.0	18.6 a C	13.9 b BC
	Turning	2.65	5.32	59.2	20.1 a B	15.3 ab A
	Ripe	2.81	5.57	59.6	20.0 a BC	15.9 a B
'Empeltre'	Green	3.18	4.05	56.1	23.7 a A	15.2 a B
	Turning	3.09	4.40	55.4	23.0 a A	15.0 a A
	Ripe	3.13	4.00	49.3	24.1 a A	15.0 a BCD
'Farga'	Green	1.28	2.47	54.8	16.9 b CD	10.8 b C
	Turning	1.74	3.18	58.7	19.0 a B	12.5 a B
	Ripe	1.82	3.70	55.8	18.1 a C	12.0 a E
'Manzanilla'	Green	4.57	8.31	70.1	24.0 a A	18.6 a A
	Ripe	4.65	7.68	66.6	23.9 a A	19.4 a A
'Marfil'	Green	1.32	2.05	60.1	19.7 b BC	10.5 b C
	Ripe	1.98	3.95	53.6	21.6 a AB	13.3 a CDE
'Morrut'	Green	1.99	2.03	51.6	20.4 b BC	13.8 b BC
	Turning	2.34	2.52	51.1	20.4 b B	13.8 b A
	Ripe	2.08	2.74	37.6	21.8 a AB	15.5 a BC
'Picual'	Green	2.72	2.75	57.2	22.4 a AB	15.1 a B
	Turning	3.06	3.11	60.2	22.2 a AB	15.3 a A
	Ripe	4.30	4.35	49.6	24.1 a A	17.3 a AB
'Sevillena'	Green	2.71	3.09	56.7	21.4 a ABC	14.1 a BC
	Ripe	3.32	4.97	52.0	22.1 a AB	15.5 a BC

Values represent means of 50 fruits for weight, F:S ratio and water content, and of 10 fruits for length and diameter. Fruit weight, F:S ratio and water content were determined jointly for 50 fruits, and values reported represent the average of the 50 olives assessed. For length and diameter data, different capital letters denote significant differences among the cultivars for a given maturation stage, and different lower-case letters stand for significant differences among maturation stages for a given cultivar, at $P \leq 0.05$ (LSD test).

* Abbreviation: F:S ratio, flesh to stone ratio.

Supplementary Table S2. Some chemical characteristics of olive fruits at the green, turning and ripe stages.

Cultivar	Maturity stage	Anthocyanins (mg g ⁻¹ DW)	Phenolics (mg g ⁻¹ DW)	RSA (%)	AA (nmol g ⁻¹ DW)	DHA (nmol g ⁻¹ DW)
'Arbequina'	Green	0.4 b CD	27.6 a EF	94.4 a A	0.16 a A	0.11 a B
	Turning	0.7 b C	20.8 c D	88.2 b AB	0.13 b B	0.06 b D
	Ripe	2.5 a C	23.0 b CD	89.3 ab BC	0.16 a D	0.06 b AB
'Argudell'	Green	0.4 c CDE	37.8 a C	88.8 a BC	0.14 a B	0.02 b G
	Turning	0.6 b C	33.6 ab B	90.7 a AB	0.11 c C	0.04 a E
	Ripe	0.8 a D	33.1 b B	89.7 a BC	0.12 b E	0.04 ab CD
'Empeltre'	Green	0.3 c DE	26.8 a EF	88.7 a BC	0.08 b E	0.11 a B
	Turning	1.0 b A	21.0 b CD	81.2 b C	0.09 b D	0.11 a A
	Ripe	3.6 a B	20.7 b D	91.3 a AB	0.17 a CD	0.07 b A
'Farga'	Green	0.6 c A	25.2 b FG	82.4 c D	0.11 b CD	0.09 a CD
	Turning	0.8 b BC	19.6 c D	86.2 b BC	0.14 b AB	0.08 a C
	Ripe	3.7 a B	31.2 a B	90.5 a B	0.29 a B	0.06 b AB
'Manzanilla'	Green	0.6 b A	42.3 a B	93.5 a AB	0.11 b CD	0.06 a EF
	Ripe	8.0 a A	41.9 a A	91.1 a AB	0.33 a A	0.06 a AB
'Marfil'	Green	0.4 a CDE	22.3 a G	92.8 b AB	0.16 a A	0.20 a A
	Ripe	0.3 b D	22.7 a CD	98.9 a A	0.08 b F	0.05 b BCD
'Morrut'	Green	0.4 b DC	49.9 a A	93.2 a AB	0.10 b D	0.07 b DE
	Turning	0.7 b C	38.5 b A	91.7 a A	0.11 b C	0.09 a B
	Ripe	2.2 a C	24.3 c C	91.6 a AB	0.18 a C	0.05 c BC
'Picual'	Green	0.3 c E	34.1 a D	88.3 a BC	0.12 c C	0.09 a BC
	Turning	0.9 b AB	24.1 b C	87.1 a AB	0.15 b A	0.08 ab C
	Ripe	2.4 a C	24.7 b C	79.2 a D	0.17 a CD	0.06 b AB
'Sevillena'	Green	0.5 b AB	28.1 a E	84.3 a CD	0.14 a B	0.05 a F
	Ripe	1.9 a C	12.3 b E	81.8 a CD	0.10 b F	0.03 b D

Values represent means of three replicates. Different capital letters denote significant differences among the cultivars for a given maturity stage, and different lower-case letters stand for significant differences among maturity stages for a given cultivar, at $P \leq 0.05$ (LSD test).

*Abbreviations: RSA, radical-scavenging capacity; AA, reduced ascorbic acid; DHA, dehydroascorbic acid.

Supplementary Table S3. Incidence of defects and disorders in olive fruits at the green, turning and ripe stages.

Cultivar	Maturity stage	Fly ^a (%)	Fungus ^b (%)	Bruised (%)	Wrinkled (%)
'Arbequina'	Green	0	0	0	0
	Turning	14	0	0	0
	Ripe	10	0	6	0
'Argudell'	Green	12	100	0	0
	Turning	0	34	8	0
	Ripe	12	34	0	0
'Empeltre'	Green	60	0	0	0
	Turning	76	0	0	0
	Ripe	24	0	6	22
'Farga'	Green	4	0	0	100
	Turning	10	0	0	100
	Ripe	6	0	2	6
'Manzanilla'	Green	56	100	0	0
	Ripe	20	8	6	44
'Marfil'	Green	0	0	4	0
	Ripe	2	0	78	0
'Morrut'	Green	6	0	0	100
	Turning	0	0	18	6
	Ripe	4	2	18	0
'Picual'	Green	6	0	0	0
	Turning	6	0	4	0
	Ripe	8	0	0	2
'Sevillenca'	Green	24	0	0	0
	Ripe	0	0	16	28

Values represent the percentage of affected fruits within a sample of 50 olives.

^a Infestation by *Bactrocera oleae*.

^b Infection by *Camarosporium dalmaticum*.

Supplementary Table 4. Mineral content (mg kg⁻¹ DW) in olive fruits at the green, turning and ripe stages.

Cultivar	Maturity stage	Boron (B)		Calcium (Ca)		Iron (Fe)		Magnesium (Mg)		Manganese (Mn)		Potassium (K)	
'Arbequina'	Green	20.85	a A	1167.93	a C	5.24	a BC	397.27	a EF	4.96	b B	18039.28	a B
	Turning	16.34	c A	775.41	c A	5.36	a BC	356.30	a C	5.37	a A	18445.57	a A
	Ripe	17.50	b A	864.24	b A	4.58	a C	372.63	a CD	5.40	a A	20171.60	b A
'Argudell'	Green	12.55	ab BCD	846.94	a D	6.37	a B	511.41	a ABC	4.57	a BC	16831.24	a BCD
	Turning	11.36	b B	750.94	b AB	5.87	a B	526.42	a A	4.70	a B	17629.81	a A
	Ripe	13.01	a B	737.58	b B	5.61	a B	509.93	a A	4.50	a C	16767.58	a B
'Empeltre'	Green	15.73	a B	521.16	a F	6.13	a B	383.96	a EF	3.75	a D	17497.64	a BC
	Turning	15.36	a A	506.48	a C	4.88	a C	383.15	a BC	3.81	a C	16362.33	a A
	Ripe	9.93	b CD	381.36	b DEF	5.55	a B	379.88	a CDE	3.11	b F	17379.98	a B
'Farga'	Green	8.48	ab D	689.16	a E	6.55	a B	523.13	a AB	5.64	a A	25893.75	a A
	Turning	9.99	a B	541.46	b C	7.33	a A	432.41	b B	4.71	b B	18340.79	b A
	Ripe	7.65	b D	458.40	b CD	6.81	a A	385.64	b CD	3.96	c D	17169.67	b B
'Manzanilla'	Green	9.65	a CD	685.86	a E	4.56	a C	350.84	a F	3.24	b E	14031.45	b CD
	Ripe	13.21	a B	711.18	a B	5.13	a BC	434.71	a B	4.87	a B	22449.74	a A
'Marfil'	Green	9.68	a CD	1837.64	a A	12.81	a A	552.95	a A	4.45	a C	25367.38	a A
	Ripe	12.70	a BC	413.00	b DE	4.61	b C	400.51	b BC	3.42	a EF	12680.52	b C
'Morrut'	Green	13.61	a BC	903.23	a D	4.44	b C	432.33	a DE	3.32	a DE	13389.29	a D
	Turning	17.13	a A	573.03	b C	3.90	c D	394.22	a BC	3.67	a C	15603.07	a A
	Ripe	13.03	a B	306.01	c F	5.49	a B	345.77	a D	3.32	a F	16528.14	a B
'Picual'	Green	16.82	a AB	1299.97	a B	6.30	a B	475.72	a BCD	4.70	a BC	18206.73	a B
	Turning	15.06	b A	691.40	b B	3.96	a D	332.13	b C	3.41	b C	16966.15	a A
	Ripe	13.94	b B	367.07	c EF	4.44	a C	299.38	b E	3.28	b F	16444.52	a B
'Sevillenca'	Green	14.08	a B	827.86	a D	5.09	b BC	439.66	a CDE	3.57	a DE	19181.58	a B
	Ripe	15.41	a AB	530.41	b C	7.06	a A	401.15	b BC	3.75	a DE	20046.42	a A



Values represent the means of two replicates per cultivar and maturity stage. Different capital letters denote significant differences among the cultivars for a given maturity stage, and different lower-case letters stand for significant differences among maturity stages for a given cultivar, at $P \leq 0.05$ (LSD test).

Chapter III: Chemical and sensory characterization of nine Spanish monovarietal olive oils: an emphasis on wax esters



Article

Chemical and Sensory Characterization of Nine Spanish Monovarietal Olive Oils: An Emphasis on Wax Esters

Clara Diarte ^{1,2}, Agustí Romero ³ , María Paz Romero ^{2,4}, Jordi Graell ^{2,4} and Isabel Lara ^{1,2,*} 

¹ Chemistry Department, Universitat de Lleida, 25198 Lleida, Spain; clara.diarte@udl.cat

² AGROTÈCNIO-CERCA Center, 25198 Lleida, Spain; mariapaz.romero@udl.cat (M.P.R.); jordi.graell@udl.cat (J.G.)

³ Oliviculture, Oil Science and Nuts, Institut de Recerca i Tecnologia Agroalimentàries (IRTA), IRTA Mas Bové, 43120 Constantí, Spain; agusti.romero@irta.cat

⁴ Food Technology Department, Universitat de Lleida, 25198 Lleida, Spain

* Correspondence: isabel.lara@udl.cat; Tel: +34-973-702526

Agriculture (February 2021), 11, 170. doi: 10.3390/agriculture11020170

Clara Diarte, Agustí Romero, María Paz Romero, Jordi Graell and Isabel Lara

Abstract

Olive oil is an essential part of the so-called “Mediterranean diet”, purportedly one of the healthiest gastronomic traditions in the world. The wax content in olive oil is regulated under European Union directives, and it is used as a purity parameter for extra-virgin and virgin olive oils. The wax profile may also help the characterization of monovarietal olive oils. In this study, monovarietal oils were extracted from the fruits of nine native Spanish olive varieties (‘Arbequina’, ‘Argudell’, ‘Empeltre’, ‘Farga’, ‘Manzanilla’, ‘Marfil’, ‘Morrut’, ‘Picual’ and ‘Sevillanca’), and their chemical and sensory attributes were determined. Total wax content in oil was cultivar-dependent and ranged widely between 26 (‘Manzanilla’) and 144 mg kg⁻¹ (‘Arbequina’), while it was negligible in ‘Picual’ oil. The wax ester fraction was comprised largely of phytol-containing diterpene esters, with phytyl vaccinate and phytyl arachidate being the most common components of this non-polar fraction in all nine olive oils assessed. A direct relationship between phytyl esters and the sensory perception of “ripe fruit” notes was also observed.

Keywords: Chemical properties; *Olea europaea*; olive oil; phytyl esters; sensory attributes; wax

(...) *oleum saporis egregii, dum viride est, intra annum corrumpitur.*

Lucius Iunius Moderatus, a.k.a. *Columella*

De re rustica (Book V)

3.1. Introduction

Olive (*Olea europaea* L.) oil is one of the key products characterising the Mediterranean diet and displays matchless characteristics as a food fat regarding organoleptic, chemical and health-promoting attributes. High contents of monounsaturated fatty acids and the presence of phenolic acids reportedly confer olive oil valuable antioxidant and anti-cancer properties, as well as protective activity against heart diseases, osteoporosis and cognitive impairment (Tripoli et al., 2006; Rodríguez-Morató et al., 2015; Condelli et al., 2015). The European Union (EU) is the main olive- and olive oil-producing area in the world and has established official standards and analytical methods for the classification of olive oils according to their physical, chemical and sensory characteristics (Commission Regulation (EEC) No 2568/91 and amendments). According to EU regulations, the acidity of extra-virgin olive oil should not exceed 0.8% and the total wax content should be below 150 mg kg⁻¹. For peroxide value, K₂₃₂ and K₂₇₀, which are used as indicators of oxidative processes, the legal limits are 20 mEq O₂ kg⁻¹, 2.50 and 0.22, respectively. As for sensory attributes, the official requirements include freedom from defects and the presence of fruity notes. Epidermal cells of fruits and other aerial, non-lignified plant organs produce and secrete cuticular waxes, an important component of the cuticle surrounding and protecting the organ. Cuticular waxes comprise a mixture of aliphatic very-long-chain fatty acid (VLCFA) derivatives and variable amounts of triterpenoids and phenylpropanoids (Kunst and Samuels, 2009).

During the mechanical extraction of olive oil, a part of cuticular waxes from the intact fruit may be transferred into the oil in small quantities, which might affect some quality and purity characteristics of the product. For example, cuticular waxes in olive fruit are particularly rich in triterpenoid acids, with relative percentages over total waxes ranging from 58% to roughly 81% (Diarte et al., 2019), contingent upon cultivar and maturity stage Vichi et al., 2016). The presence of particular compounds in olive oil could provide information on the cultivar and extraction method employed and, thus, be helpful as a tool to authenticate oil origin (Samaniego-Sánchez et al., 2010; Taticchi et al., 2019). Similarly, leaf admixture in extra-virgin olive oils may lead to significantly different *n*-alkane profiles in comparison with oils free from leaf material (Mihailova, Abbado and Pedentchouk, 2015), as *n*-alkanes present in olive leaves display higher average chain lengths (ACLs) than those in fruits (Mihailova et al., 2015; Huang et al., 2017). Moreover, when oil is extracted in an organic solvent such as *n*-hexane, wax esters contained in the olive paste are transferred in high quantities to the product (Giuffrè, 2014), and hence, wax ester contents will be higher in crude pomace olive oil than in virgin olive oils. Additional pre- and post-harvest factors that may impact wax concentration in olive oil include maturity stage of the fruit, environmental conditions, harvesting period or centrifuge procedures during oil extraction (Mele et al., 2018). The amount of waxes in olive oil will also depend on olive fruit integrity and will be higher in oil obtained from soft and degrading fruit tissues (Biedermann and Bongartz, 2008). Accordingly, olive oils of inferior quality contain more waxes than high-quality oils; wax content in extra-virgin olive oil should not exceed 150 mg kg⁻¹ (Commission Regulation (EEC) No 2568/91), while that in refined or lampante oils ranges from 300 to 350 mg kg⁻¹. Consequently, it is possible to detect frauds in extra-virgin and virgin olive oils, for example adulterations with lower-quality oils such as refined olive pomace oil or cheaper vegetable oils (Grob et al., 1994; Hodaifa et al., 2012). Wax ester content is, hence, a helpful indicator of the purity and high quality of olive oils, such as cold-pressed extra-virgin olive oil (Reiter and Lorbeer, 2001).

Wax esters found in olive oil are generally long, straight-chain fatty alcohols esterified with fatty acids, but wax esters containing a phytol (a diterpenic alcohol) group have been reported, and the C40 wax ester has been shown to contain phytol behenate (Mariani and Venturi, 2002). More recent research

confirmed that although phytyl esters dominated the wax ester fraction in olive oil, these could be accompanied by variable amounts of geranylgeraniol esters (Biederman and Bongartz, 2008). A few previous studies have analysed the wax esters in monovarietal olive oils from different Spanish and Italian cultivars (Aragón et al., 2011; Giuffrè, 2013; Mariani, Lucci and Conte, 2018). In the present study, wax ester profile was determined in monovarietal olive oils obtained from nine different cultivars ('Arbequina', 'Argudell', 'Empeltre', 'Farga', 'Manzanilla', 'Marfil', 'Morrut', 'Picual' and 'Sevillanca'). 'Marfil' is the only white-skinned olive cultivar in Spain, while the rest were chosen on the basis of their importance in the producing area. The chemical and sensory attributes of the oil samples were also determined.

3.2. Materials and methods

3.2.1. Plant material and oil extraction

Monovarietal olive oils were obtained mechanically from defect-free fruits of nine native Spanish varieties ('Arbequina', 'Argudell', 'Empeltre', 'Farga', 'Manzanilla', 'Marfil', 'Morrut', 'Picual' and 'Sevillanca'), harvested on 3 December 2018 at the IRTA-Mas Bové experimental orchard in Constantí (41° 90' N, 1° 12' E; altitude 100 m), within the geographical area covered by the Protected Designation of Origin 'Siurana'. The annual rainfall in 2018 was 310 mm, and the trees were supplied with drip irrigation. Fertilization and cultural practices were as usual in the surrounding producing area. Maturity indices at harvest (50 olives per cultivar) were determined visually according to skin and flesh colour on a 0–7 scale according to standard procedures (Uceda and Frías, 1975), and results were expressed as the weighted average of the 50 fruits within each sample. Oil was extracted immediately after harvest with an Abencor[®] system (MC2 Ingeniería y Sistemas, S.L., Seville, Spain), which involves mechanical extraction in a hammer mill, followed by mixing of the paste under controlled temperature to increase oil extraction efficiency and then by centrifuging to eventually separate the oil from water and solid residues. The olive oils were stored at 4 °C for 4 months in the dark until analysis. Acidity, peroxide values, K_{232} and K_{270} indices, wax esters and sensory profiles were determined in the oil samples according to official methods as briefly described below (Commission Regulation (EEC) No 2568/91).

3.2.2. Chemical characterization

All procedures were carried out in triplicate. For the determination of free fatty acid content, samples (5 g) of olive oil were dissolved in 50 mL diethyl ether and 95% ethanol (1:1, v/v) and titrated with ethanolic potassium hydroxide (0.1 mol L⁻¹ KOH in 95% ethanol). Acidity was expressed as the percentage of oleic acid.

For the analysis of peroxide value, oil samples (2 g) were mixed with 10 mL chloroform, 15 mL acetic acid and 1 mL saturated potassium iodide and allowed to react for 5 min in the dark at room temperature. Distilled water (75 mL) was then added, and free iodine titrated with 0.01 N sodium thio-sulphate. Results were given as milliequivalents (mEq) active oxygen kg⁻¹ oil.

Specific extinction coefficients of oil oxidation products (K_{232} and K_{270}) were determined by UV spectrophotometry (JenwayTM 6715 series, Cole-Palmer[®], Stone, Staffordshire, UK) on filtered samples (0.1 and 0.2 g, respectively) dissolved in 25 and 10 mL cyclohexane, respectively.

Oxidative stability was also assessed through the Rancimat method, an accelerated aging test measuring the increase in conductivity of deionized water (60 mL) as a consequence of the absorption of

volatile secondary compounds produced in the course of fatty acid oxidation. Oil samples (3 g) were loaded onto the Rancimat equipment (743 Rancimat, Metrohm AG, Switzerland) at 120 °C and with a 20 mL min⁻¹ air flow rate. Stability data were expressed as hours.

3.2.3. Wax ester profiles

For the analysis of wax contents, olive oil samples (500 mg) were added to 2 mL *n*-hexane and lauryl arachidate as the internal standard. The mixture was pre-purified through a silica gel column and eluted with *n*-hexane/ethyl ether (99:1, v/v). The percolated sample (180 mL) was evaporated completely under vacuum, resuspended in 2 mL *n*-heptane and injected (1 L) for subsequent analysis of total wax contents in a gas chromatograph equipped with a flame ionization detector (GC-FID) (Agilent 7890N, Santa Clara, CA, USA) and a capillary column (ZB-1HT, 15 m 0.32 mm 0.25 m; Zebron™ Phenomenex Inc., Torrance, CA, USA). The chromatographic conditions were adapted from the official method: the oven program was initially set at 80 °C, and this temperature was raised by 30 °C min⁻¹ to 250 °C, then by 5 °C min⁻¹ to 340 °C, and was then held for 15 min at this final temperature. Helium was used as the carrier gas at a flow rate of 4 mL min⁻¹. The injector and detector were held at 80 and 340 °C, respectively. Total wax contents were expressed as mg kg⁻¹ oil, and the reported data represent the average of three replicates. The identification of individual wax compounds was carried out in a gas chromatography–mass spectrometry (GC-MS) system coupled with a quadrupole mass selective detector (Agilent 5973N, Santa Clara, CA, USA). The capillary column and the chromatographic conditions were the same as in the GC-FID analyses. The mass spectra obtained from samples were compared with those from a mass spectral library (NIST 11 MS, Gaithersburg, MD, USA). The concentration of each detected ester was given as mg kg⁻¹ oil.

3.2.4. Sensory analysis

The sensory analysis was carried out by the Official Tasting Panel of Virgin Olive Oils of Catalonia (Panell de Tast Oficial d'Olis Verges d'Oliva de Catalunya), according to European Union Standard Methods (Commission Regulation (EEC) No 2568/91). This panel is accredited under ISO 17025 and is recognized by the International Olive Oil Council. Each oil sample was analysed by eight tasters who scored the official sensory descriptors using a 10-cm scale anchored on zero. In addition, the presence of secondary sensory attributes and defects was determined by the percentage of panellists able to perceive each odour note using an open generic profile (Romero, Tous and Guerrero, 1999; Guerrero, Romero and Tous, 2001). Finally, the median intensities of sensory attributes were used for the calculation of the global sensory score on a 0–9 scale (0, very bad quality; 9, highest quality) with an algorithm developed by IRTA (Romero et al., 1999). Global scores facilitate the comparison of the sensory quality of different samples. As a reference, global sensory scores for olive oils within the extra-virgin category should be at least 6.5 points.

3.3. Results and discussion

3.3.1. Physicochemical and organoleptic quality characteristics

The physicochemical parameters of all nine monovarietal olive oils assessed are shown in **Table 1**. The nine olive cultivars used for oil extraction display different ripening patterns (Tous and Romero, 1993), with ‘Manzanilla’, ‘Empeltre’ and ‘Sevillanca’ being the earliest varieties to attain maturity, whereas the rest of cultivars ripen later. In contrast, ‘Marfil’ olives were still quite green when harvested

in early December and just beginning to turn white, this being the only white-skinned olive cultivar in Spain. These differences in ripening patterns were reflected in the different maturity indices found in each case at the picking date (**Table 1**).

Table 1. Weight and maturity index of olives used for oil extraction and chemical characteristics of monovarietal oils studied.

Cultivar	Weight (g)	Maturity index	Acidity (% oleic acid)		Peroxide value (mEq O ₂ kg ⁻¹)		K ₂₃₂ index		K ₂₇₀ index		Oxidative stability (h)	Wax content* (mg kg ⁻¹)		
‘Arbequina’	1.69	2.4	0.14	h	6.89	d	1.68	c	0.07	f	8.53	d	143.97	a
‘Argudell’	3.10	3.2	0.16	g	9.40	a	1.94	b	0.11	c	8.34	d	51.20	c
‘Empeltre’	1.41	5.0	0.64	b	3.76	h	1.81	bc	0.06	g	8.27	d	65.95	b
‘Farga’	2.20	3.6	0.21	e	5.52	f	1.67	c	0.08	e	8.53	d	60.04	b c
‘Manzanilla’	5.79	6.4	0.51	c	4.44	g	1.53	d	0.10	d	22.11	b	25.85	d
‘Marfil’	1.98	1.9	0.18	f	7.35	c	2.12	a	0.13	a	17.45	c	35.30	d
‘Morrut’	2.98	3.1	0.45	d	2.57	i	1.68	c	0.08	e	8.45	d	68.77	b
‘Picual’	3.61	2.3	0.14	h	8.89	b	1.70	c	0.13	a	33.24	a	nd	
‘Sevillenca’	4.04	4.7	1.60	a	5.74	e	1.81	bc	0.12	b	4.43	e	67.87	b

Maturity index (0-7) and weight represent the average of 50 olives. Values for the rest of parameters represent means of three technical replicates (nd, non-detectable). Different letters within each column denote significant differences among the different monovarietal olive oils at $P \leq 0.05$ (LSD test).

*Wax content data comprise C₄₂, C₄₄ and C₄₆ aliphatic compounds uniquely (EEC No. 2568/91).

In all cases, oil was extracted at once after harvest, hence limiting fermentative and oxidative processes. Based on the analytical parameters considered herein, all the monovarietal oils studied could be classified as extra-virgin olive oils according to European Union regulations (Commission Regulation (EEC) No 2568/91), with the exception of ‘Sevillenca’ oil due to its high acidity values (1.6%) exceeding the regulated limit (0.8%). On this basis, ‘Sevillenca’ oil had to be classified as virgin olive oil, for which the maximum acidity value is higher (2.0%). This agrees with the “fusty” defect detected by the panelists, possibly contributing to the low global sensory score of ‘Sevillenca’ oil in comparison to the rest of the monovarietal oils evaluated (**Table 2**). On the contrary, ‘Arbequina’ and ‘Picual’ oils contained the lowest acidity (0.14%).

Peroxide values ranged from 2.56 (‘Morrut’ oil) to 9.40 (‘Argudell’ oil) mEq O₂ kg⁻¹. As regards the K₂₃₂ index, ‘Marfil’ and ‘Manzanilla’ oils were statistically different in comparison with the rest and showed the highest (2.12) and the lowest (1.53) values, respectively. Peroxide value and K₂₃₂ are indicators of primary oxidation in olive oil, consisting in the addition of oxygen to fatty acids at the double bond position to form peroxides, and thus, these data confirm the good quality of the oils considered in the present study. This fact was corroborated by the K₂₇₀ values, which ranged within values below the legal limit (from 0.06 in ‘Empeltre’ to 0.13 in ‘Marfil’ and ‘Picual’ oils) and hence illustrated the absence of secondary oxidation, which would produce volatile compounds affecting oil taste and off-flavour, in accordance with the lack of rancidity found during sensory analyses. The wide range of values observed for each parameter, together with previous reports for other cultivars (Bengana et al., 2013; Alvarruiz et al., 2015), suggests these attributes be largely cultivar-specific.

Table 2. Sensory attributes of nine Spanish monovarietal olive oils.

Cultivar	Fruity	Bitter	Pungent	Global sensory score
‘Arbequina’	4.40	2.55	3.40	6.6
‘Argudell’	4.65	3.15	3.60	7.0
‘Empeltre’	4.10	2.70	3.25	6.7
‘Farga’	5.05	2.85	3.80	6.8
‘Manzanilla’	4.30	4.05	4.45	6.5
‘Marfil’	5.75	4.70	5.15	7.6
‘Morrut’	4.35	3.45	3.90	7.0
‘Picual’	6.15	5.20	5.15	7.4
‘Sevillenca’	3.75	3.45	4.30	6.1

Sensory scores are expressed on a 10-cm (0, no perception, to 9, strongest perception). Values represent the median of 8 trained panellists from an official panel (*Panell de Tast Oficial d’Olis Verges d’Oliva de Catalunya*).

Oxidative stability showed considerable variation across all nine monovarietal oils considered and ranged widely from 4.43 (‘Sevillenca’) to 33.24 h (‘Picual’). These data might be related to the content of phenolics, which enhance oxidative stability (Vázquez, Janer and Janer, 1975), and in which olive oil from ‘Picual’ is particularly rich (García et al., 2003) while that from ‘Sevillenca’ is reportedly not (Vichi et al., 2019). Accordingly, ‘Manzanilla’ and ‘Marfil’ oils also showed high stability against oxidation (22.11 and 17.45 h, respectively) in agreement with previous reports on high phenolic levels in oils obtained from these varieties (Aloiaiesh et al., 2018; Ninot, Howad and Romero, 2019). The rest of the olive oils analysed had similar oxidative stability values (roughly 8.50 h). Although total phenolics in oil samples were not assessed in this study, data obtained in previous producing seasons for oils extracted from the same cultivars at the same experimental orchard (**Supplementary Table S1**) support a relationship between higher contents of total phenolics and superior oxidative stability (**Table 1**).

The analysis of sensory attributes indicated the lowest fruitiness scores for ‘Sevillenca’ virgin olive oil, together with a “fusty” defect (some tasters reported “winy” as well). Extra-virgin oils obtained from the rest of the varieties showed no sensory defects, which is an additional indicator of their high-quality character (**Table 2, Figure 1**). ‘Picual’, ‘Marfil’ and, to a lesser extent, ‘Manzanilla’ oils were perceived as particularly bitter and pungent (**Table 2, Figure 1**). It has been suggested that bitter and pungent sensations are highly correlated to the total content of phenolics (Morelló, Romero and Motilva, 2004; Servili et al., 2004; Baldioli et al., 1996). This agrees with data obtained in preceding years at IRTA-Mas Bové, showing that ‘Marfil’ and ‘Picual’ oils also displayed the highest contents of total phenolics (**Supplementary Table S1**). ‘Picual’ and ‘Marfil’ oils also scored higher than the rest regarding fruity and green notes (**Figure 1**), while ‘Empeltre’ oil was, in contrast, one of the softest, as indicated by low bitterness (2.70) and pungency (3.25). For ‘Empeltre’, a relationship has been observed between low phenolic contents in oil and low scores (2 to 4) for fruitiness, bitterness and pungency (Abezona et al., 2018), which results in a soft olive oil.

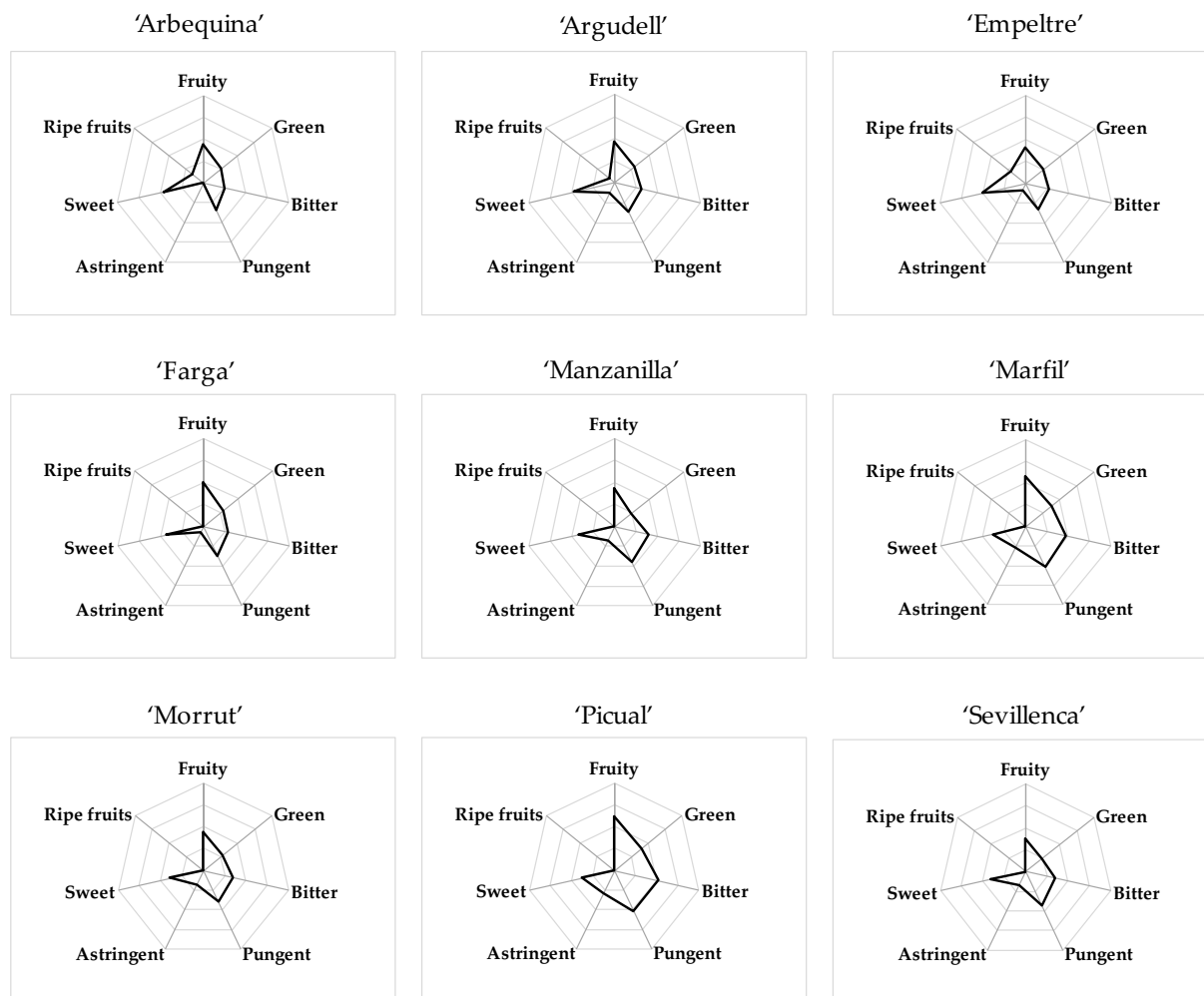


Figure 1. Radar chart of sensory parameters of nine monovarietal olive oils. Sensory attributes were scores on a 10-cm scale (chart centre, 0; outer heptagon, 10). Values represent the median of eight trained panellists from an official panel (Panell de Tast Oficial d'Olis Verges d'Oliva de Catalunya).

3.3.2. Wax content and wax ester profiles

Olive oil waxes are used as a purity parameter. For the determination of wax content in high-quality (extra-virgin or virgin) olive oils, and according to European Union olive oil regulation (Commission Regulation (EEC) No 2568/91), only C_{42} , C_{44} and C_{46} esters are considered. The wax content of all of the monovarietal olive oils studied herein was below the regulated limit, established at 150 mg kg^{-1} (**Table 1**). This is important, as the formation of wax esters continues during the shelf life of olive oils, and thus, the initial wax content has a significant impact on the subsequent evolution of the product. The results showed a wide range of wax content levels among the nine olive oils analysed, suggesting that this parameter could be cultivar-dependent, as reported previously for Italian olive oils (Giuffrè, 2013). Only 'Arbequina' oil approached (144 mg kg^{-1}) the maximum established value (**Table 1**), with the wax content being two to fourfold higher than that in the rest of the samples. These data are in agreement with earlier observations by Aragón et al., 2011 that monovarietal 'Arbequina' olive oil displayed one of the highest wax contents in comparison with oils obtained from other cultivars.

The typically small size of the ‘Arbequina’ fruit as compared with other genotypes suggests that the high wax content in oil extracted from this cultivar might have arisen from the larger fruit surface area relative to fruit volume, and indeed, a negative correlation ($r = 0.74$) was found in this work between wax content in oil and fruit weight (Figure 2). This trend, though, did not hold for all the studied cultivars, particularly for ‘Marfil’, which displayed low wax content in oil together with an average fruit weight below 2 g (Table 1). ‘Arbequina’ fruits also exhibit considerable cuticle and cuticular wax contents per surface area together with high cuticle thickness by the usual time when they are harvested for oil extraction (Diarte et al., 2019). For these reasons, legal regulation of wax content may prove controversial among olive oil producers and traders, as some genotypes may naturally display higher concentrations and thus easily reach values close to or above the legal limits.

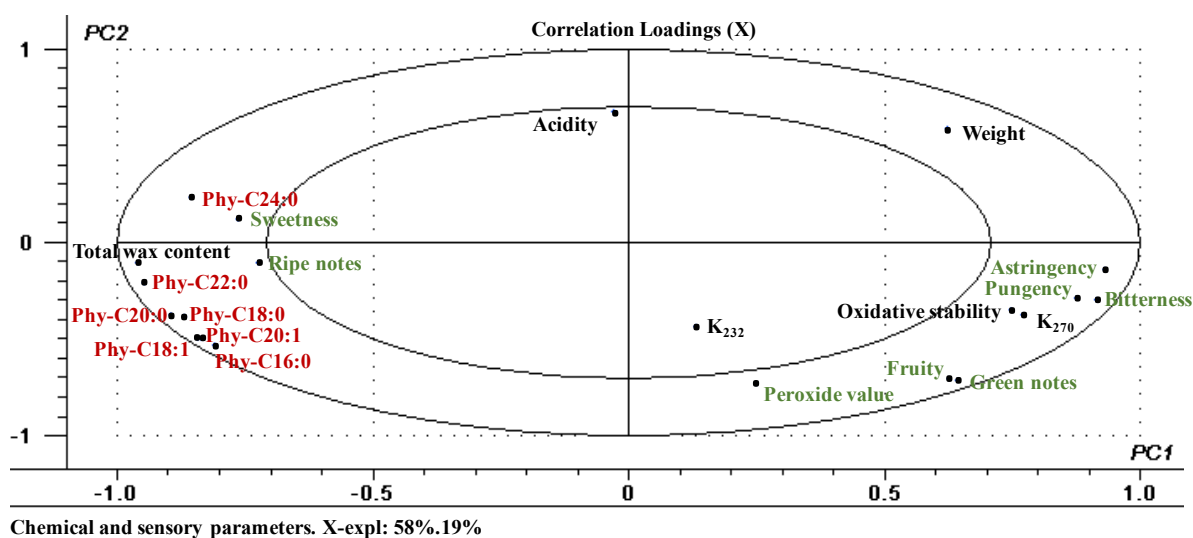


Figure 2. Correlation loadings plot of PC1 vs. PC2 corresponding to a Principal Component Analysis (PCA) model for chemical and sensory parameters assessed in nine monovarietal olive oils. *Abbreviations: Phy-C16:0, phytol palmitate; Phy.C18:0, phytol stearate; Phy-C18:1, phytol vaccinate; Phy-C20:0, phytol arachidate; Phy-C20:1, phytol eicosenate; Phy-C22:0, phytol behenate; Phy-C24:0, phytol lignocerate.

The wax ester types identified in the olive oils were in the range of C_{36} to C_{44} (Table 3). In quantitative terms, C_{38} and C_{40} esters were prominent, whereas the concentrations of C_{36} and C_{44} esters were less important. For ‘Picual’ oil, though, C_{36} , C_{42} and C_{44} esters were undetectable, consistent with the observation that the total wax content as defined by European Union regulations (Commission Regulation (EEC) No 2568/91) was negligible in this oil (Table 1). This finding agrees with previous reports for monovarietal ‘Picual’ oil (Samaniego-Sánchez et al., 2010), showing that wax content was not high, even though in that work, low concentrations of C_{36} , C_{42} and C_{44} esters could be identified and quantified. C_{46} esters are present in negligible quantities in extra-virgin and virgin olive oils (Mariani et al., 2018a), and accordingly, no C_{46} esters were detected in this work. The absence of C_{46} esters also could be attributed partially to their possible co-elution with sterol compounds, which would pose further difficulty in their identification. Indeed, the mass spectra retrieved in this work suggested that some signals detected at the last part of the chromatograms might correspond to sterol-type compounds (see Supplementary Figure S1 for an example).

GC-MS results revealed that the wax compounds identified in the non-polar fraction corresponded to diterpene esters composed of phytol groups esterified to different fatty acids, including palmitic

(16:0), stearic (18:0), vaccenic (18:1), arachidic (20:0), eicosenoic (20:1), behenic (22:0) and lignoceric (24:0) acids (**Table 3**). Low concentrations of geranylgeraniol esters, also diterpenic compounds, have been occasionally identified in olive oils (Biedermann and Bongartz, 2008; Mariani et al., 2018b), but none were detected in the present study, maybe in connection with the experimental difficulty of retrieving the mass spectra when compound concentration is very low (Reiter and Lorbeer, 2001). Diterpenic esters are basically found in the pulp of the olive, and it has been suggested that the official methodology for the analysis of wax content as established by the European Union may cause them to elute together with cuticular wax esters (Biedermann and Bongartz, 2008). Even so, no diterpenes were detected in the cuticular waxes of olive fruits (Diarte et al., 2019). Additionally, the olive oils analysed in this work were extracted by mechanically crushing the fruits and then centrifuging the olive paste, and no solvents whatsoever were used for the extraction. The presence of phytol fatty acid esters might be related to fruit ripening-associated chlorophyll degradation (Krauß and Vetter, 2018). In agreement, phytol fatty acid esters were detected in red and yellow, but not in green, bell pepper fruits (Krauß, Hammann and Vetter, 2016), indicating that they accumulated mainly during fruit ripening.

Table 3. Wax compound types (mg kg^{-1}) identified in nine Spanish monovarietal oils.

Cultivar	Ester C36		Ester C38			Ester C40			Ester C42		Ester C44			
	Phy-C16:0		Phy-C18:0	Phy-C18:1		Phy-C20:0	Phy-C20:1		Phy-C22:0		Phy-C24:0			
‘Arbequina’	61.09	a	92.95	a	434.46	a	307.84	a	150.46	a	117.05	a	26.92	a
‘Argudell’	18.73	b	22.79	bc	117.99	b	95.43	b	45.78	bc	40.09	b	11.11	d
‘Empeltre’	15.78	b	27.09	b	132.96	b	95.63	b	42.96	bc	48.15	b	17.87	c
‘Farga’	10.82	c	19.28	c	86.97	c	79.31	c	37.18	cd	40.51	b	19.53	c
‘Manzanilla’	4.38	d	13.83	d	32.01	de	32.33	d	8.26	e	11.94	d	7.29	e
‘Marfil’	19.25	b	22.46	bc	125.59	b	77.00	c	48.77	b	26.59	c	8.71	de
‘Morrut’	8.54	c	23.64	bc	65.96	c	79.40	c	29.04	d	45.22	b	23.55	b
‘Picual’	nd		1.51	e	2.79	e	2.21	e	nd		nd		nd	
‘Sevillena’	7.88	cd	20.76	c	56.24	cd	86.08	bc	29.06	d	46.96	b	20.90	bc

Values represent means of three technical replicates (nd, non-detectable). Different letters within each row denote significant differences among the different monovarietal olive oils at $P \leq 0.05$ (LSD test). Abbreviations: Phy-C16:0, phytol palmitate; Phy-C18:0, phytol stearate; Phy-C18:1, phytol vaccinate; Phy-C20:0, phytol arachidate; Phy-C20:1, phytol eicosenate; Phy-C22:0, phytol behenate; Phy-C24:0, phytol lignocerate.

In all the analysed oil samples, phytol vaccinate and phytol arachidate dominated the wax ester fraction. Both compounds also stood out quantitatively among diterpene esters identified in monovarietal Kalamata olive oil (Reiter and Lorbeer, 2001). ‘Arbequina’ oil displayed the highest phytol vaccinate concentration ($434.46 \text{ mg kg}^{-1}$), in agreement with previous studies showing that this ester represented about 8–10% of total phytol wax esters detected in oil from this cultivar (Mariani et al., 2018a). The concentrations of phytol vaccinate in the nine monovarietal olive oils considered herein amounted for as much as 21–38% of total phytol esters. In ‘Picual’, this compound practically amounted to around 43%, although this percentage corresponded to a concentration of only 2.79 mg kg^{-1} . The high content of phytol vaccinate is noticeable, taking into account that oleic acid ($18:1 \Delta^9$), not vaccenic acid ($18:1 \Delta^{\text{trans-11}}$), is the most common $18:1$ fatty acid component of olive oil triacylglycerols (around 70% and 3% in extra-virgin oil, respectively) (Rotondo et al., 2020). Additionally, unsaturated fatty acids are common in triacylglycerols present in olive oil, but in contrast, a substantial percentage (47% to 68%) of fatty acid constituents of diterpene esters identified herein were saturated (Table 3). These data agree

with previous reports (Mariani et al., 2018a) and suggest the presence of a dedicated biosynthetic pathway for these esters.

The data were used to characterize the oil samples by means of a PCA model, and the corresponding correlation loadings plot (**Figure 2**) shows that the two first principal components (PC1 and PC2) explained up to 77% of sample variability. Samples were separated mainly along PC1, which accounted alone for 58% of total variability. An interesting association was found between phytyl esters and the perception of “ripe fruit” notes in the sensory analysis. Phytyl ester content has been suggested as a feasible marker for the maturity stage of bell pepper fruits (Krauβ et al., 2016). The PCA model also revealed that the sensory perceptions of bitterness, pungency and “fruity” and “green” notes were associated to oxidative stability and K_{270} and correlated negatively to the wax content and the perception of “ripe” notes. In contrast, acidity and primary oxidation indicators (peroxide value and K_{232}) were apparently unrelated to wax ester content or the sensory perception of “sweet” and “ripe fruit” notes.

3.4. Conclusions

The bulk of results reported in this study illustrate the existence of cultivar-related differences in wax contents and profiles of monovarietal olive oils. The highest concentration of waxes was found for ‘Arbequina’ oil, which was at least twofold the amount observed for the rest of the monovarietal oils studied in this work, while, conversely, ‘Picual’ oil displayed the lowest wax contents. The data also show the relevance of phytyl esters as the main components of the wax ester fraction in extra-virgin and virgin olive oils and confirm vaccenic acid as a major fatty acid constituent thereof. In contrast, the data do not support the hypothesis that cuticular waxes may be transferred to the oil during mechanical extraction, as no relationship was found between wax profiles in olive oils and those in the fruit cuticle. On the basis of the data, diterpenic esters in extra-virgin and virgin olive oils appear a promising topic for future investigations, with a focus on improving the knowledge of the metabolic origins of phytol and of less common fatty acids. A wider range of cultivars and agronomic conditions should be considered for such future studies.

3.5. References

Abenoza M, Raso J, Oria R, Sánchez-Gimeno AC. 2018. Modulating the bitterness of Empeltre olive oil by partitioning polyphenols between oil and water phases: Effect on quality and shelf life. *Food Sci. Technol. Int.* 25, 47-55.

Alowaiesh B, Singh Z, Fang Z, Kailis SG. 2018. Harvest time impacts the fatty acid compositions, phenolic compounds and sensory attributes of Frantoio and Manzanilla olive oil. *Sci. Hortic.* 2018, 234, 74-80.

Alvarruiz A, Álvarez-Ortí M, Mateos B, Sena E, Pardo JE. 2015. Quality and composition of virgin olive oil from varieties grown in Castilla-La Mancha (Spain). *J. Oleo Sci.* 64, 1075-1082.

Aragón A, Toledano RM, Cortés JM, Villén J, Vázquez A. 2011. Wax ester composition of monovarietal olive oils from Designation of Origin (DO) “Campos de Hellin”. *Food Chem.* 129, 71-76.

Baldioli M, Servili M, Perreti G, Montedoro GF. 1996. Antioxidant activity of tocopherols and phenolic compounds of virgin olive oil. *J. Am. Oil Chem. Soc.* 1996, 73, 1589-1593.

Bengana M, Bakhouch A, Lozano-Sánchez J, Amir Y, Youyou A, Segura-Carretero A, Fernández-Gutiérrez A. 2013. Influence of olive ripeness on chemical properties and phenolic composition of Chemlal extra-virgin olive oil. *Food Res. Inter.* 54, 1868-1875.

Biedermann M, Bongartz A. 2008. Fatty acid methyl and ethyl esters as well as wax esters for evaluating the quality of olive oils. *Eur. Food Res. Technol.* 228, 65-74.

Condelli N, Caruso MC, Galgano D, Russo D, Milella L, Favati F. 2015. Prediction of the antioxidant activity of extra virgin olive oils produced in the Mediterranean area. *Food Chem.* 177, 233-239.

Diarte C, Lai P, Huang H, Romero A, Casero T, Gatius F, Graell J, Medina V, East A, Riederer M, Lara I. 2019. Insights into olive fruit surface functions: A comparison of cuticular composition, water permeability, and surface topography in nine cultivars during maturation. *Front. Plant Sci.* 10, 1484.

García A, Brenes M, García P, Romero C, Garrido A. 2003. Phenolic content of commercial olive oils. *Eur. Food Res. Technol.* 216, 520-725.

Giuffrè AM. 2013. Influence of harvest year and cultivar on wax composition of olive oils. *Eur. J. Lipid Sci. Technol.* 115, 549-555.

Giuffrè AM. 2014. Wax ester variation in olive oils produced in Calabria (southern Italy) during olive ripening. *J. Am. Oil Chem. Soc.* 91, 1355-1366.

Grob K, Giuffrè AM. 1994. Leuzzi, U.; Mincione, B. Recognition of adulterated oils by direct analysis of the minor components. *Fat Sci. Technol.* 96, 286-290.

Guerrero L, Romero-Aroca A, Tous J. 2001. Importance of generalised procrustes analysis in sensory characterisation of virgin olive oil. *Food Qual. Prefer.* 12, 515-520.

Hodaifa G, Martínez Nieto L, Lozano JL, Sánchez S. 2012. Changes of the wax content in mixture of olive oil as determined by gas chromatography with flame ionization detector. *J. AOAC Int.* 95, 1720-1724.

Huang H, Burghardt M, Schuster AC, Leide J, Lara I, Riederer M. 2017. Chemical composition and water permeability of fruit and leaf cuticles of *Olea europaea* L. *J. Agric. Food Chem.* 65, 8790-8797.

Krauß S, Hammann S, Vetter W. 2016. Phytol fatty acid esters in pulp of bell pepper (*Capsicum annuum*). *J. Agric. Food Chem.* 64, 6306-6311.

Krauß S, Vetter W. 2018. Phytol and phytol fatty acid esters: Occurrence, concentration, and relevance. *Eur. J. Lipid Sci. Technol.* 120, 1700387.

Kunst, L.; Samuels, A.L. 2009. Plant cuticles shine: Advances in wax biosynthesis and export. *Curr. Opin. Plant Biol.* 12, 721-727.

EEC Regulation 2568/91. Characteristics of olive oil and olive-residue oil and the relevant methods of analysis. *Off. J. Eur. Union.* L 266/9 16.10.2015.

Mariani C, Venturi S. 2002. Sulla struttura delle cere degli oli delle olive. *Riv. Ital. Sostanze Grasse* 79, 49-57.

Mariani C, Lucci P, Conte L. 2018a. Identification of phytol vaccinate as a major component of wax ester fraction of extra virgin olive oil. *Eur. J. Lipid Sci. Technol.* 120, 1800154.

Mariani C, Cesa S, Ingallina C, Mannina L. 2018b. Identification of tetrahydrogeraniol and dihydrogeranylgeraniol in extra virgin olive oil. *Grasas Aceites.* 69, e263.

Mele MA, Islam MZ, Kang H, Giuffrè AM. 2018. Pre-and post-harvest factors and their impact on oil composition and quality of olive fruit. *Emir. J. Food Agric.* 30, 592-603.

Mihailova A, Abbado D, Pedentchouk N. 2015. Differences in n-alkane profiles between olives and olive leaves as potential indicators for the assessment of olive leaf presence in virgin olive oils. *Eur. J. Lipid Sci. Technol.* 117, 1480-1485.

Morelló JR, Romero MP, Motilva MJ. 2004. Effect of the maturation process of olive fruit on the phenolic fraction of drupes and oils from Arbequina, Farga and Morrut cultivars. *J. Agric. Food Chem.* 52, 6002-6009.

Ninot A, Howad W, Romero A. 2019. Les varietats catalanes d'olivera. In *Quaderns agraris (Institució Catalana d'Estudis Agraris)*. 46, 7-36. (ISSN 0213-0319).

Reiter B, Lorbeer E. 2001. Analysis of the wax ester fraction of olive oil and sunflower oil by gas chromatography and gas chromatography-mass spectrometry. *J. Am. Oil Chem. Soc.* 78, 881-888.

Rodríguez-Morató J, Xicota L, Fitó M, Farré M, Dierssen M, de la Torre R. 2015. Potential role of olive oil phenolic compounds in the prevention of neurodegenerative diseases. *Molecules.* 20, 4655-4680.

Romero A, Tous J, Guerrero L. 1999. El análisis sensorial del aceite de oliva virgen. In *Introducción al análisis sensorial de los alimentos*. (ISBN 8483380528).

Rotondo A, La Torre GL, Dugo G, Cicero N, Santini A, Salvo A. 2020. Oleic acid is not the only fatty ester in olive oil. *Foods.* 9, 384.

Samaniego-Sánchez C, Quesada-Granados JJ, López-García de la Serrana H, López-Martínez MC. 2010. β -Carotene, squalene and waxes determined by chromatographic method in Picual extra virgin olive oil obtained by a new cold extraction system. *J. Food Compos. Anal.* 23, 671-676.

Servili M, Selvaggini R, Esposto S, Taticchi A, Montedoro GF, Morozzi G. 2004. Health and sensory properties of virgin olive oil hydrophilic phenols: Agronomic and technological aspect of production that affect their occurrence in the oil. *J. Chromatogr. A.* 1054, 113-127.

Taticchi A, Selvaggini R, Esposto S, Sordini B, Veneziani G, Servili M. 2019. Physicochemical characterization of virgin olive oil obtained using an ultrasound-assisted extraction at an industrial scale: Influence of olive maturity index and malaxation time. *Food Chem.* 289, 7-15.

Tous J, Romero A. 1993. *Variedades del olivo: con especial referencia a Cataluña*. (ISBN 84-7664-376-4).

Tripoli E, Gianmarco M, Di Majo D, Gianmarco S, La Guardia M, Grescimanno M. 2006. The phenolic compounds of olive oil and human health. In *Proceedings of the 2nd International Seminar Olivebioteq. Special Seminars and invited lectures*. p 265-271.

Uceda M, Frías L. 1975. Harvest dates. Evolution of the fruit of content, oil composition and oil quality. In Proceedings of II Seminario Oleícola International. p125-130.

Vázquez Roncero A, Janer del Valle C, Janer del Valle ML. 1975. Polifenoles naturales y estabilidad del aceite de oliva. *Grasas Aceites*. 26, 14-18.

Vichi S, Cortés-Francisco N, Caixach J, Barrios G, Mateu J, Ninot A, Romero A. 2016. Epicuticular wax developing olives (*Olea europaea*) is highly dependent upon cultivar and fruit ripeness. *J. Agric. Food Chem.* 64, 5985-5994.

Vichi S, Tres A, Quintanilla-Casa B, Bustamante J, Guardiola F, Martí E, Hermoso JF, Ninot A, Romero A. 2019. Catalan virgin olive oil protected designations of origin: Physicochemical and major sensory attributes. *Eur. J. Lipid Sci. Technol.* 121, 1800130.

Supplementary material

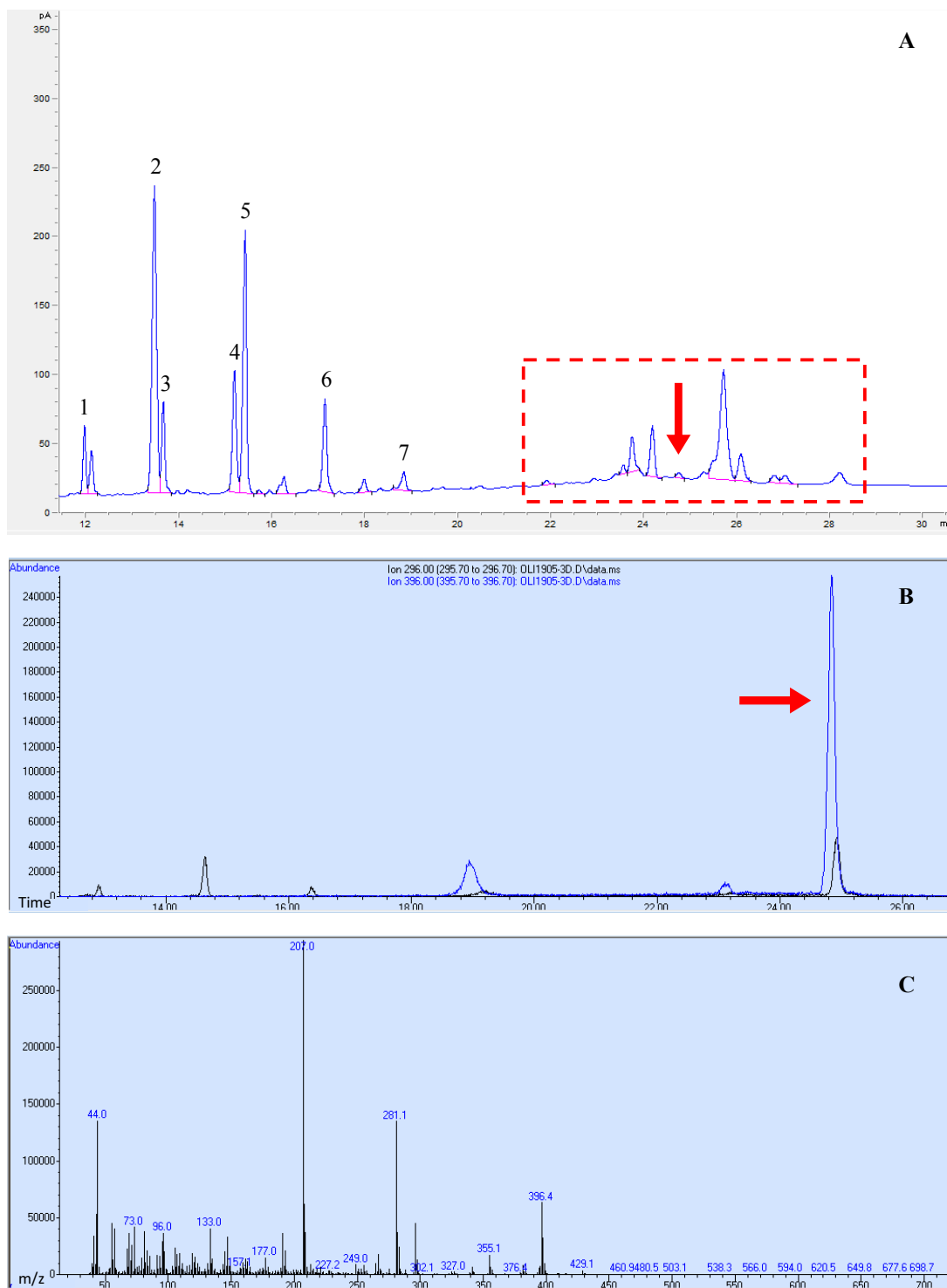
Supplementary Table S1. Average contents of total phenolics (TPC) in nine Spanish monovarietal oils (IRTA-Mas Bové experimental station, period 1993-1998).

Cultivar	TPC (mg caffeic acid kg⁻¹)
'Arbequina'	201
'Argudell'	280
'Empeltre'	238
'Farga'	202
'Manzanilla'	321
'Marfil'	727
'Morrut'	325
'Picual'	509
'Sevillena'	187

TPC were determined by Folin-Ciocalteu assay according to Singleton, Orthofer and Lamuela-Raventós (1999).

Reference:

Singleton VL, Orthofer R, Lamuela-Raventós RM. 1999. Analysis of total phenols and other oxidation substrates and antioxidants by means of Folin-Ciocalteu reagent. *Method Enzymol.* 299, 152-178.



Supplementary Figure S1. (A) GC-FID chromatogram from ‘Arbequina’ olive oil wax esters (peak assignment: 1, phytyl palmitate; 2, phytyl vaccinate; 3, phytyl stearate; 4, phytyl eicosenoate; 5, phytyl arachidate; 6, phytyl behenate; 7 phytyl lignocerate). The dotted box indicates the area of the chromatogram where some signals appear which might correspond to sterol-type compounds. The arrow points to a signal eluting at 24.9 minutes, as an example of such a compound. (B) Abundance of the ions 296 and 396 for different compounds, corresponding respectively to the molar mass of the phytol group and of cerotic acid. The arrow points to the same signal as in panel (A). (C) Fragmentation pattern for signal obtained at minute 24.9.

SECTION II. A focus on ‘Arbequina’ olive fruit

Fruit cuticle and cell wall composition of ‘Arbequina’ olives over maturation at two Protected Designation of Origin (PDO) (‘Les Garrigues’ and ‘Siurana’) and the effect of irrigation.

Chapter IV: Cuticle changes in ‘Arbequina’ olive fruit along on-tree ripening: the influence of irrigation and producing area

(Manuscript)

Clara Diarte, Anna Iglesias, Agustí Romero, Vicente Medina, Jordi Graell, and Isabel Lara

Abstract

Olive (*Olea europaea* L.) fruit and derived products play a pivotal role in the Mediterranean diet, to which they contribute their gastronomic value and their health-promoting properties. The fruit cuticle constitutes the interface between the plant and the surrounding environment, and it modulates relevant traits such as water loss, mechanical resistance and susceptibility to plagues and rots. Hence a better knowledge of fruit cuticle properties and the impact thereupon of agronomic factors could help improving olive grove management. In this work, time-course changes in fruit cuticle yields and composition were assessed during on-tree ripening of ‘Arbequina’ olives obtained from irrigated or rain-fed trees grown at two different geographical areas in Catalonia (NE Spain). For olives produced at El Soleràs, a location characterized by low annual rainfall, cold winters and hot dry summers, significantly higher wax contents over total cuticle were observed for rain-fed (229 to 621 g cm⁻², contingent upon picking date) than for irrigated (198 to 554 g cm⁻²) fruits, in agreement with their proposed role as a barrier against water loss. Contrarily, limited irrigation-related differences were found for fruit samples obtained from Mas Bové (233 to 522 g cm⁻² and 223 to 513 g cm⁻² in rain-fed and irrigated conditions, respectively), where climatic conditions are usually milder. Compositional differences in cuticular waxes were also detected between irrigated and rain-fed olives. In contrast to cuticular waxes, data do not support an association of cuticle barrier properties with either total cuticle or cutin loads.

Keywords: ‘Arbequina’; cuticular wax, cutin, irrigation, *Olea europaea* L., production area

Olea prima arborum omnium est.

Lucius Iunius Moderatus, a.k.a. *Columella*
De Arboribus

4.1. Introduction

‘Arbequina’ is the most important olive (*Olea europaea* L.) cultivar in Catalonia (NE Spain), where it represents over 50% of total olive cultivated area (Ninot et al., 2015). ‘Arbequina’ fruit are used both for oil production and for manufacturing as tables olives. From its original growing region, ‘Arbequina’ production has outspread to other areas of the world, where its groves occupy a total surface of around 60,000 ha (Tous, 2017). Vigor and productive characteristics of the tree make this cultivar suitable for high density planting (Ninot et al., 2019) and for mechanical harvesting, thereby reducing the cost of the final product.

Olive trees usually grow in Mediterranean-type climates, where the plant must withstand adverse environmental conditions, increasingly harsher and more stress-inducing due to global climate change. Consequently, it is important to understand the plant-environment interactions. Leaf and fruit cuticles play important roles in plant protection against the surrounding conditions, including the restriction of uncontrolled water loss which would challenge plant survival (Riederer and Schreiber, 2001).

The plant cuticle is a hydrophobic layer covering the aerial, non-lignified plant organs including fruits. Cuticles consist mainly of an insoluble polymeric cutin matrix, rich in hydroxy-, carboxy- and epoxy-C₁₆ and C₁₈ fatty acid derivatives and embedded with waxes. The wax fraction, present both in amorphous and crystalline form, is composed of very long-chain aliphatic as well as cyclic compounds (Buschhaus and Jetter, 2011; Domínguez, Heredia-Guerrero and Heredia, 2011; Belge et al., 2014; Lanza and Di Serio, 2015; Camacho-Vázquez, et al., 2019; Trivedi et al., 2019). Cuticle constituents are exported and assembled on the external side of the epidermis, hence acting as the first barrier against abiotic (UV radiation, water availability, high temperatures, mechanical injuries) and biotic (plagues and rots) stressors (Lara et al., 2019). The limitation of transpirational water loss, which helps protecting plants against desiccation, is one of the important functions exerted by the plant cuticle (Lara, Belge and Goulao, 2014; Riederer et al., 2015; Wang et al., 2016; Romero and Rose, 2019).

To date, only a handful of published studies have addressed cuticle composition of intact olive fruit, and most of them have focused on cuticular waxes (Bianchi, 2003; Vichi et al., 2016). Two studies uniquely have reported cutin composition of olive fruit cuticles (Huang et al., 2017; Diarte et al., 2019). These studies revealed that triterpenoid acids (maslinic and oleanolic acids) account for over 65% of cuticular waxes of ‘Arbequina’ fruit, followed by lower amounts of fatty acids, fatty alcohols, *n*-alkanes and sterols, while cutin composition is predominated by C₁₈ fatty acids and hydroxy fatty acids. Even though the main chemical families of cuticle constituents remained the same throughout fruit ripening, significant differences were found in their relative percentages over total cuticle (Huang et al., 2017; Diarte et al., 2019), which may impact cuticle properties and fruit attributes. Given the relevant roles attributed to plant cuticles on the resistance to biotic and abiotic stressors, the question arises whether an important environmental factor such as water availability may also modulate the profiles of cuticular components in the fruit. This knowledge may also aid the improvement of grove management.

In this study, time-course changes in cuticle composition of ‘Arbequina’ olive fruits were assessed during on-tree ripening in irrigated or rain-fed conditions. Fruit samples were obtained from two different producing areas in Catalonia, covered respectively by Protected Designations of Origin (PDO) ‘Les Garrigues’ and ‘Siurana’.

4.2. Material and methods

4.2.1. Plant material and toluidine (TB) test

‘Arbequina’ olive fruit samples were hand-collected at regular intervals during the 2017-2018 producing season, from mid-September to mid-January. Fruit samples were picked from a commercial orchard located in El Soleràs (41°24'N; 0°39'E), within PDO ‘Les Garrigues’. Samples were also obtained from the IRTA-Mas Bové experimental grove in Constantí (41°09' N; 1°12' E), within PDO ‘Siurana’. In both areas, olive trees either remained rain-fed or were supplied with drip irrigation from April to October (207 and 325 L week⁻¹ tree⁻¹ in El Soleràs and Mas Bové, respectively). Total rainfall and temperatures (maximum, minimum and average) at both producing sites during 2017 are shown in **Table 1**. Maturity indices (0-7) were determined on 50 olives per sampling date and irrigation regime according to skin and flesh colour as described by Uceda and Frías (1975); values represent the weighted average of fruits within each sample. Fresh weight (g), flesh to stone ratio and humidity (%) were determined jointly on 50 fruits per sampling date and irrigation regime, and results were divided by 50 to obtain the average value in each case. Fruit length and diameter were determined individually on ten olives using a digital calliper, and data expressed as mm. In order to assess the presence of discontinuities on fruit surface, 10 fresh olives per sampling date (as long as fruit remained green) were stained in a toluidine blue (TB) solution (0.05%, w/v) for 2 h (Tanaka et al., 2004); presence or absence of staining were denoted respectively as + or -.

4.2.2. Cuticle isolation

Fruit cuticle was isolated from around 100 cm² olive skin per sampling date and irrigation regime. Skin disks (2 disks/fruit) were excised with a cork borer from 50 to 75 olives, depending on fruit size at each maturation stage, and distributed into two replicate tubes (50 cm²/replicate) for the enzymatic isolation of cuticular membranes (CM). CM isolation was carried out at 37 °C in 50 mM citrate at pH

Table 1. Rainfall and temperatures at both olive-producing sites in 2017.

	Jan	Feb	Mar	Apr	May	Jun	Jul	Aug	Sep	Oct	Nov	Dec	Total rainfall (mm)
El Soleràs (PDO ‘Les Garrigues’)	20.2	9.6	77.8	14.8	34.0	47.0	13.0	2.9	48.0	33.0	9.6	8.1	318.0
Absolute Max T (°C)	15.4	16.6	25.8	27.8	33.5	37.0	37.5	38.7	30.2	28.4	22.1	17.7	
Average Max T (°C)	8.0	13.5	18.1	20.8	25.8	31.2	32.4	32.1	25.4	23.5	14.8	9.5	
Average T (°C)	4.2	8.6	11.8	13.9	18.7	24.1	25.4	25.3	19.2	17.3	9.3	5.1	
Average Min T (°C)	0.4	3.7	5.5	7.1	11.5	17.0	18.4	18.6	12.9	11.1	3.7	0.7	
Absolute Min T (°C)	-5.3	0.2	0.2	2.2	5.0	11.9	12.0	10.8	7.2	6.5	-1.8	-4.2	
Rainfall (mm)	23.9	33.2	72.8	17.1	35.2	15.5	31.5	20.0	28.0	46.8	10.5	5.4	
Mas Bové (PDO ‘Siurana’)	18.2	20.5	23.9	23.6	28.2	32.7	32.2	36.1	31.8	28.3	23.4	21.3	339.9
Absolute Max T (°C)	13.2	16.3	18.7	19.4	23.7	28.5	29.3	29.6	24.9	23.7	18.1	14.8	
Average Max T (°C)	7.1	10.8	12.1	13.3	17.9	23.0	24.2	24.2	20.1	17.9	10.8	8.5	
Average T (°C)	1.3	5.6	6.0	6.7	11.3	16.9	18.8	19.1	14.3	12.4	4.3	2.3	
Average Min T (°C)	-7.0	-0.9	2.8	2.3	6.1	12.6	13.0	13.1	7.2	6.5	-1.6	-3.7	
Absolute Min T (°C)													
Rainfall (mm)													

Abbreviations: Max T and Min T, maximum and minimum temperature, respectively.

4.0, in the presence of 0.2% (w/v) cellulase, 100 U mL⁻¹ pectinase and 1 mM of NaN₃ to prevent microbial growth. When no more material release was apparent, CM disks were washed in citrate buffer (50 mM, pH 4.0), then in distilled water, and finally dried at 40 °C, weighted, pooled and kept in hermetically capped vials until further analysis. Cuticle yields were expressed per unit of surface area (mg cm⁻²).

4.2.3. Extraction and analysis of cuticular wax

CM samples (20 mg/replicates × 3 replicates) were extracted in chloroform (2 mg mL⁻¹) with constant shaking during 24 h at room temperature. Chloroform extraction of each sample was carried out three consecutive times, and the resulting extracts were pooled and incubated for 15 min in an ultrasonic bath. The dewaxed cuticular membranes (DCM) were then dried and kept in hermetically capped vials for subsequent cutin monomer analysis. The chloroform extracts were filtered, concentrated in a rotatory evaporator at 40 °C, and transferred to a pre-weighed vial for vacuum concentration until complete dryness. The vials were then weighted, and total wax yields expressed as µg cm⁻². For wax analysis, ethers and esters were transformed to free hydroxyl and carboxyl groups, respectively, by derivatisation with *N,O*-bis(trimethylsilyl)trifluoroacetamide (BSTFA) in the presence of pyridine (3:2, v/v) and dotriacontane (C₃₂) as the internal standard, with shaking during 15 min at 100 °C.

Samples (1 µL) were injected into a gas chromatography-mass spectrometry (GC-MS) system (Agilent 7890N) equipped with a quadrupole mass selective detector (Agilent 5973N) and a capillary column (DB 5 MS UI, 30 m × 0.25 mm × 0.25 µm; SGE Europe Ltd., Milton Keynes, UK) in on-column mode. The oven was set initially at 100 °C for 1 min, and temperature was raised thereafter by 15 °C min⁻¹ to 200 °C, then by 5 °C min⁻¹ to 310 °C, and finally held at this temperature for 10 min. Helium was used as the carrier gas at 1.0 mL min⁻¹. Wax compounds were identified by comparison of their retention times with those of standards and by matching their electron ionization-mass spectra with those retrieved from a mass spectral library (NIST 11 MS). For quantitative analysis, a flame ionization detector (FID) was used under the same chromatographic conditions as for GC-MS, excepting that helium flow was 1.3 mL min⁻¹ and that, at the final step, the oven was kept at 310 °C for 13 min. Results were expressed as relative percentage (% over total waxes). The average chain length (ACL) of the acyclic wax compounds was also calculated as the weighted average number of carbon atoms by the following equation:

$$ACL = \frac{\sum C_n n}{\sum C_n}$$

where C_n is the percentage of each acyclic wax compound with *n* carbon atoms.

4.2.4. Extraction and analysis of cutin monomers

For hydrolysis of cutin monomers, DCM samples (roughly 10 mg/replicate × 3 replicates) were added 2 mL 1M HCL in 100% MeOH and esterified in this solution during 2 h at 80 °C. After cooling down to room temperature, 2 mL saturated NaCl were added, and the cutin monomers were then extracted three consecutive times in 2 mL hexane during 10 min with shaking at 20 °C and finally centrifuged. The supernatants from all three extractions were pooled and dried under vacuum at 40 °C in a pre-weighed vial. The vials containing the dry samples were weighted to calculate total cutin yields (µg cm⁻²). Procedures for compound derivatisation, identification (GC-MS) and quantification (GC-FID), were as described above for wax analysis, with the exception that heptadecanoate (C₁₇) and tricosanoate (C₂₃) were used as internal standard.

4.2.5. Microscopy observations

Pericarp cubes (1-2 mm) were chopped from fruit samples and fixed in a formaldehyde-acetic acid (FAA) solution (5% (v/v) formaldehyde and 5% (v/v) glacial acetic acid in 1:1 (v/v) ethanol-distilled water) for 12 h. For sample dehydration, the FAA solution was changed with different solutions of increasing ethanol concentrations up to 100 %. Dehydrated samples were then transferred to Eppendorf tubes for infiltration and polymerization in Technovit 7100[®] resin (Heraeus Kulzer GmbH, Wehrheim, Germany) and dried during 24 h at 45 °C.

Resin-embedded samples were cut with an ultramicrotome (Leica EM UC6, Leica Microsystems GmbH, Wetzlar, Germany) into 4 µm-thick slices, and then stained with the lysochrome Sudan IV (5% (w/v) in 85% (v/v) ethanol) to visualize the lipidic constituents of the olive cuticles. Lysochrome excess was removed by rinsing in 50% (v/v) ethanol, and the stained samples were dried at room temperature. Images were obtained by an optic microscope (Leica DM4000 B) coupled with a camera (Leica DFC300 FX). To measure cuticle thickness, 5 images per sample were taken with the Fiji image processing software (Schindelin et al., 2012).

4.2.6. Statistical analysis

Results were expressed as means ± standard deviations. The JMP[®] Pro 13 software was used to conduct the statistical analysis. Multifactorial analysis of variance (ANOVA) was carried out with irrigation regime and maturity stage as the factors, and means were compared with the LSD test ($p \leq 0.05$). Principal component analysis (PCA) was also applied to assess possible relationships among the different factors studied.

4.3. Results and discussion

4.3.1. The impact of irrigation on physical characteristics of fruits

Physical characteristics of fruits were assessed after recollection (**Table 2, Supplementary Table S1**). Phenotypic data show that water availability had an impact on the development of ‘Arbequina’ fruit. For olives grown at El Soleràs, weight and size were higher for irrigated than for rain-fed samples, in agreement with higher water content. Different studies have shown that lower water content increases oil concentration in olive fruits, resulting in higher oil extraction yields (Inglese, 2011; Ben-Gal et al., 2021). Furthermore, total contents of phenolic compounds was lower in olives grown under irrigation (see **Table 1 in Chapter IV** of this Thesis), in accordance with previous reports (Berenguer et al., 2006; Gómez-Rico et al., 2007; Morales-Sillero. et al 2013; Mechri et al., 2020), hence suggesting better health-promoting properties for olive fruits and olive oil produced in rain-fed conditions. Consistent with higher water content, flesh-to-stone ratio was also higher in fruits picked from irrigated trees. Furthermore, toluidine blue (TB) test (**Table 2, Supplementary Figure S1**) revealed the existence of pores on the surface of fruit from irrigated trees, while for rain-fed samples these were visible in fruit picked during the first two weeks of October uniquely. TB test for rain-fed fruit was negative thereafter, coincident with the combined occurrence of warm temperature episodes (absolute maximum temperature of

Table 2. Physical characteristics and toluidine blue test of ‘Arbequina’ olives picked at El Soleràs (PDO ‘Les Garrigues’) in 2017-2018 season.

Sampling date	Irrigation regime	Weight (g)	Length (mm)	Diameter (mm)	F:S ratio	Water content (%)	TB test
Sept 18	Irrigated	1.23 e A	14.18 d A	12.66 f A	3.80 c A	67.02 b A	-
Oct 3		1.62 cd A	15.51 bc A	14.00 cde A	4.57 b A	69.15 a A	+
Oct 16		1.81 bc A	16.01 a A	14.77 a A	5.55 a A	66.67 b A	+
Oct 30		1.86 ab A	15.60 abc A	14.08 cd A	5.58 a A	66.44 b A	+
Nov 13		2.02 a A	15.90 ab A	14.52 ab A	4.69 b A	60.71 c A	+
Nov 28		1.84 ab A	15.48 bc A	14.21 bc A	4.46 b A	54.99 d A	ne
Dec 11		1.58 d A	15.20 c A	13.68 de A	4.55 b A	44.92 e A	ne
Jan 15		1.59 d A	15.42 c A	13.61 e A	3.61 c A	41.92 f A	ne
Sept 18	Rain-fed	1.08 d B	12.90 c B	11.63 e B	3.19 e B	60.18 ab A	-
Oct 3		1.38 b A	13.54 b B	12.12 cd B	3.65 cd B	61.85 a B	+
Oct 16		1.23 c B	13.32 bc B	11.86 de B	3.63 cd B	48.94 c B	+
Oct 30		1.42 b B	13.73 b B	12.53 bc B	4.48 a B	57.78 b B	-
Nov 13		1.52 a B	14.59 a B	12.96 ab B	3.86 bc A	47.33 c B	-
Nov 28		1.28 c B	14.49 a B	12.69 ab B	3.41 de B	43.92 d B	ne
Dec 11		1.57 a A	14.40 a B	12.59 abc B	4.01 b B	39.28 e B	ne
Jan 15		1.54 a A	14.32 a B	13.04 a B	3.45 de A	39.44 e B	ne

Values represent means of two 10-fruit replicates. Different capital letters denote significant differences between irrigated and rain-fed olives for a given sampling date, and different lower-case letters stand for significant differences among sampling dates for a given irrigation regime, at $P \leq 0.05$ (LSD test). For the TB test, 10 olives per sampling date were assessed, and stained and non-stained fruits are denoted respectively as + and -.

*Abbreviations: F:S ratio, flesh to stone ratio; TB test, toluidine blue test (Tanaka et al., 2004); ne, not evaluated.

28.4 °C in October) and lower rainfall as compared with September, which dropped further during the subsequent months (**Table 1**). These observations suggest that TB test results might be reflecting the impact of water scarcity, and indeed the presence of cuticular irregularities has been associated with water loss and solute absorption (Fernández and Eichert, 2009; Fernández, Sotiropoulos and Brown, 2013). This trend could not be confirmed due to ripening-related colour change of fruit samples which prevented the assessment of TB staining in black fruit. The significant differences in fruit weight and water content between irrigated and rain-fed fruit, though, were apparent after mid-October, coincident with positive TB test for the latter (**Table 2**). The determination of permeability to water of fruit cuticle may help dissecting these aspects in future studies.

Physical characteristics were also determined for irrigated and rain-fed fruits produced in Mas Bové, within PDO ‘Siurana’ (Supplementary Table S1). Flesh-to-stone ratio and water content of fruit picked at this location were lower than those in fruits from El Soleràs, although annual rainfall was similar (**Table 1**). TB test results (**Supplementary Table S1, Supplementary Figure S1**) showed the same trends as for fruits from El Soleràs, discontinuities being observable on the surface of fruit from irrigated trees for as long as it was possible to visualise test results while, in contrast, pores were visible on rain-fed samples only during the first two weeks of October. For clarity, this discussion will focus preferentially on olives produced at El Soleràs, while data for fruits from Mas Bové are shown as supplementary material (**Supplementary Tables S1 to S4**).

4.3.2. The impact of irrigation on fruit cuticle characteristics

No clear trend was observed for total cuticle, wax and cutin along fruit maturation (**Table 3, Supplementary Table S2**). For olives harvested from El Soleràs (PDO ‘Les Garrigues’), a noticeable peak in total cuticle yield (3.8 mg cm⁻²) was found at mid-October in rain-fed fruits (**Table 3**), coincident with the period when TB test was positive in these samples (**Table 2**). With this exception, no remarkable differences in total cuticle yields were observed during the experimental period between irrigated and rain-fed fruits, values ranging from 1.7 to 3.8 mg cm⁻². An increasing trend was observed for cutin yields throughout maturation of rain-fed olives, which ranged from 403.8 to 753.0 µg cm⁻² (roughly 17-35 % over total cuticle). Similar cutin yields were generally found irrespective of irrigation, with the exception of November, when cutin amounts per surface area were significantly higher in rain-fed than in irrigated fruits (**Table 3**). Contrarily, wax yields were significantly higher in rain-fed (228.5 to 621.2 µg cm⁻²) than in irrigated (197.8 to 553.5 µg cm⁻²) olives during most of the experimental time, and represented respectively 8.9-37.1 % and 8.5-20.0 % over total cuticle. Disparities in wax loads were reflected in wax-to-cutin ratios, which were also generally higher for rain-fed samples (**Table 3**). These data are in accordance with reports on other species, including litchi (*Litchi chinensis*), longan (*Dimocarpus longan*) (Riederer et al., 2015) and Arabidopsis (Patwari et al., 2019), suggesting a relationship between cuticular waxes and barrier properties under water deficiency conditions. Previous studies on the fruit cuticle of ‘Arbequina’ olives reported higher wax and cutin yields than those found in the present work (Huang et al., 2017; Diarte et al., 2019), which reflects year-to-year variation and highlights the convenience of repeating these studies over a range of producing seasons. When compared with other fruit species, data obtained herein also reflect interspecific variation in total cuticle, wax and cutin yields: for example, similar wax load but lower cutin yields were obtained for peach fruit cuticles (Belge et al., 2019), whereas lower yields of cuticle, cuticular wax and cutin were found for sweet cherry (Belge et al., 2014) and pitaya (Huang and Jiang, 2019) in comparison with ‘Arbequina’ olives.

Table 3. Cuticle, cuticular wax and cutin yields, wax to cutin ratio and cuticle thickness of ‘Arbequina’ olives picked at El Soleràs (PDO ‘Les Garrigues’) in 2017-2018 season.

Sampling date	Irrigation regime	Cuticle yield (mg cm ⁻²)		Wax yield (µg cm ⁻²)		Wax (%)		Cutin yield (µg cm ⁻²)		Cutin (%)		Wax/ cutin ratio		Thickness (µm)	
Sept 18	Irrigated	2.8	a A	553.4	a A	20.0	a A	667.4	a A	24.1	bc A	0.83	b B	36.0	b B
Oct 3		2.1	cd B	293.7	c A	13.9	b A	416.2	c A	19.6	de A	0.71	bc A	43.6	a A
Oct 16		2.2	cd B	197.8	d B	9.2	c B	539.1	b A	25.0	bc A	0.37	de B	39.8	ab A
Oct 30		2.1	cd A	271.1	c B	13.2	b B	387.0	c A	18.8	de A	0.70	bc B	40.2	ab A
Nov 13		1.7	e A	302.0	bc A	20.0	a A	303.8	d B	18.3	e A	0.99	a A	38.6	ab A
Nov 28		2.0	d A	274.0	c B	16.1	b B	422.2	c B	21.5	cd B	0.65	c B	41.3	ab A
Dec 11		2.3	bc A	340.3	b B	14.9	b B	691.3	a A	30.2	a A	0.49	d B	41.4	ab A
Jan 15		2.5	ab A	215.3	d A	8.5	c A	630.8	a A	25.0	b A	0.34	e A	44.9	a A
Sept 18	Rain-fed	2.4	c A	558.1	a A	21.8	b A	403.8	d A	17.2	c A	1.38	a A	53.7	a A
Oct 3		2.7	b A	280.9	cd A	10.4	d B	467.2	cd A	17.4	c A	0.60	d A	46.5	abc A
Oct 16		3.8	a A	477.3	b A	22.1	b A	603.6	b A	15.8	c B	0.79	cd A	49.3	ab A
Oct 30		2.2	c A	406.7	b A	18.1	bc A	408.0	d A	18.2	c A	1.00	bc A	42.8	bcd A
Nov 13		2.2	c A	321.6	c A	16.1	c B	461.8	cd A	21.2	c A	0.70	cd A	36.5	d A
Nov 28		1.9	d A	621.2	a A	33.4	a A	562.4	bc A	30.2	ab A	1.10	ab A	38.8	cd A
Dec 11		1.7	d B	618.9	a A	37.1	a A	590.9	b A	35.5	a A	1.05	b A	40.6	cd A
Jan 15		2.6	b A	228.5	d A	8.9	d A	753.0	a A	29.3	b A	0.30	e B	38.5	cd A

Cuticular membranes were isolated from skin samples (around 95 cm²) obtained from 50 to 75 olives, contingent upon ‘Arbequina’ fruit size. Wax and cutin data represent means of three technical replicates of this starting material. For cuticle thickness values represent means of four biological replicates. Different capital letters denote significant differences among irrigated and rain-fed samples for a given sampling date, and different lower-case letters stand for significant differences among sampling date and irrigation regime at $P \leq 0.05$ (LSD test).

When olives harvested from Mas Bové (PDO ‘Siurana’) were analysed, similar trends in total cuticle and cutin yields were observed as for fruits from El Soleràs, no remarkable differences in total cuticle being observed between irrigated and rain-fed fruits, while cutin yields were generally higher for the latter (**Supplementary Table S2**). In contrast, no clear impact of irrigation on wax content or wax percentage was apparent, which might have arisen from milder temperatures in this geographical area (**Table 1**). In agreement with the observations for olives picked from El Soleràs, increasing cutin yields were found during fruit maturation, which in combination with decreasing wax amounts per surface area resulted in lower wax-to-cutin ratios in more mature fruits possibly contributing to lower water contents (**Table 3, Supplementary Table S2**). Whereas no maturity stage-related differences in cuticular permeability to water were detected in a previous study throughout maturation of rain-fed ‘Arbequina’ olives produced at El Soleràs (Huang et al., 2017), no significant changes in total amount of cuticular waxes or wax-to-cutin ratios were either detected in that study. However, wax-to-cutin ratio in leaves more than doubled that in fruits, while cuticular water permeance of fruits was roughly five-fold higher than that of leaves, which indicates a relevant role of waxes on barrier properties of the plant organ surface.

Cuticle thickness has been found to decrease during ripening of ‘Arbequina’ fruit picked from trees grown at the same experimental grove in Mas Bové (Diarte et al., 2019). Accordingly, a decreasing trend in fruit cuticle thickness was observed herein during maturation of olives produced at Mas Bové for both irrigated and rain-fed samples (**Supplementary Table S2, Supplementary Figure S2**), while no irrigation-related differences were found. As to fruit samples picked from El Soleràs, and with the exception of the mid-September sampling, no differences were observed either in cuticle thickness in response to irrigation. In contrast, whereas a moderately decreasing trend was found for rain-fed samples, no significant differences in fruit cuticle thickness were observed during maturation of olives from irrigated trees (**Table 3, Supplementary Figure S2**). Water availability at early stages of fruit development has been suggested to impact cuticle thickness, which agrees with low rainfall and high temperatures recorded at El Soleràs during July and August (**Table 1**) and suggests that fruit cuticle was thicker in response to more stressful environmental conditions. Previous studies on *Arabidopsis* leaves (Kosma et al., 2003) concluded that the deposition of cuticular waxes and cuticle thickness increased in response to water deficit conditions. Yet, a recent survey of published literature on the role of fruit epidermis as a barrier against water stress (Zarrouk et al., 2018) concluded that cuticular waxes, rather than cuticle thickness, are pivotal against water loss. The composition of cuticular waxes was hence analysed in detail.

4.3.3. Wax composition of ‘Arbequina’ olive fruit cuticles

The wax fraction was comprised of cyclic and acyclic compounds. Cyclic compounds included large amounts of triterpenoids and minor contents of sterols. As to acyclic waxes, the main chemical families identified were fatty acids, fatty alcohols and *n*-alkanes. The acyclic to cyclic ratios ranged between 0.15 and 0.29 for fruits picked from El Soleràs (**Table 4**) and between 0.13 and 0.38 for those obtained from Mas Bové (**Supplementary Table S3**), and no irrigation-related differences were generally detected at either production site. However, an increasing trend along fruit maturation was observed. An increasing trend was also reported for rain-fed ‘Arbequina’ fruits produced at El Soleràs (Huang et al., 2017), even though values were higher in that previous study (0.27, 0.38 and 0.47 for green, turning and black fruit, correspondingly), while Diarte et al. (2019) did not find significant maturity-related differences. The detected differences are indicative of shifts in the proportions of the different wax compound families throughout fruit maturation. In the present work, higher percentages of triterpenoids and lower

Table 4. Composition of wax constituents (relative % over total waxes) in cuticle isolated from ‘Arbequina’ olives picked at El Soleràs (PDO ‘Les Garrigues’) in 2017-2018 season.

Sampling date	Irrigation regime	ACL*		Acyclic/cyclic ratio		Triterpenoids (%)		Fatty acids (%)		Fatty alcohols (%)		<i>n</i> -Alkanes (%)		Sterols (%)		Unidentified (%)	
Sept 18	Irrigated	24.3	abc A	0.17	c A	71.7	a A	7.4	c A	3.70	d A	1.0	cd A	0.9	ab A	15.3	abc A
Oct 3		24.0	e B	0.20	bc A	69.0	ab A	9.6	abc A	3.60	d B	1.0	cd B	0.8	b A	16.1	ab A
Oct 16		24.0	de A	0.24	abc A	65.2	b A	10.2	ab A	3.94	d A	1.8	a A	1.1	a A	17.7	a A
Oct 30		24.3	ab A	0.28	a A	65.8	ab A	11.5	a A	6.13	ab A	1.1	c A	0.8	ab A	14.6	bcd A
Nov 13		24.1	cde A	0.26	ab A	66.6	ab A	11.2	a A	5.41	bc A	1.0	cd A	0.8	b A	15.0	abc A
Nov 28		24.3	ab A	0.24	abc A	70.4	ab A	8.7	bc A	7.38	a A	1.1	cd A	0.6	b A	11.8	d A
Dec 11		24.4	a A	0.26	ab A	67.8	ab A	10.2	ab A	5.77	bc A	1.4	b A	0.6	b A	14.1	bcd A
Jan 15		24.2	bcd B	0.23	abc A	70.4	ab A	10.6	ab A	4.51	cd B	0.8	d A	0.8	b A	12.8	cd A
Sept 18	Rain-fed	24.4	b A	0.17	cd A	69.8	b A	7.1	c A	3.81	de A	1.4	a A	0.9	a A	17.0	ab A
Oct 3		24.8	a A	0.29	a A	62.4	c A	10.1	a A	6.61	a A	1.3	a A	0.7	ab A	18.8	a A
Oct 16		24.2	bc A	0.17	cd A	72.0	ab A	8.1	bc A	4.14	cde A	0.4	b B	0.6	b A	14.7	bc A
Oct 30		23.9	d B	0.21	bc A	70.0	b A	9.7	ab A	5.04	bcd A	0.4	b B	0.9	a A	13.9	bc A
Nov 13		23.3	e B	0.20	bcd A	70.6	b A	9.8	a A	3.66	e B	0.5	b B	0.8	ab A	14.7	bc A
Nov 28		24.1	bcd A	0.15	d B	76.9	a A	6.6	c B	5.08	bc A	0.3	b B	0.9	ab A	10.2	d A
Dec 11		24.0	cd A	0.18	cd A	72.6	ab A	7.9	c A	4.26	cde A	0.7	b B	0.8	ab A	13.7	bc A
Jan 15		24.3	b A	0.24	ab A	69.1	b A	10.0	a A	6.15	ab A	0.6	b A	0.6	b A	13.6	c A

Cuticular membranes were isolated from skin samples (around 95 cm²) obtained from 50 to 75 olives, contingent upon ‘Arbequina’ fruit size. Values represent means of three technical replicates. Different capital letters denote significant differences among irrigated and rain-fed samples for a given sampling date, and different lower-case letters stand for significant differences among sampling date and irrigation regime at $P \leq 0.05$ (LSD test).

*Abbreviations: ACL, Average chain length of acyclic wax compounds.

relative amounts of fatty alcohols and *n*-alkanes over total waxes were detected in comparison with those previous reports.

As mentioned above, triterpenoids were the main cuticular wax compounds identified in olive fruit cuticles in agreement with previous studies (Bianchi, Murelli and Vlahov, 1992; Guinda et al., 2010; Lanza and Di Serio, 2015; Huang et al., 2017; Diarte et al., 2019). Relative amounts of triterpenoids (ranging 62.4 to 76.9%) remained largely unchanged along fruit maturation, in agreement with previous reports on ‘Arbequina’ olive (Huang et al., 2017; Diarte et al., 2019), and no significant differences were detected between irrigated and rain-fed samples picked from El Soleràs (**Table 4**). The fate of particular compound families is cultivar-specific, and may show variability across genotypes: for example, triterpenoid content decreased significantly during maturation of ‘Picual’ olives (Diarte et al., 2019) and was lower in response to water stress (Jiménez-Herrera, Pacheco-López and Peragón, 2019). Therefore, caution should be exerted in order to avoid generalisation of the available information to other genotypes, as each individual cultivar will need to be examined on a case-by-case basis (Vichi et al., 2016; Diarte et al., 2019). Environmental factors should be considered as well: for example, ‘Picual’ olives analysed by Jiménez-Herrera et al. (2019) were produced in Jaén (south Spain), where climatic conditions during summer are more extreme (higher temperatures and lower rainfall) than in Mas Bové where olives analysed in Diarte et al. (2019) were picked. In the present work, though, even if the proportion of triterpenoids over total waxes was similar regardless of irrigation (**Table 4**), wax yields were lower in irrigated samples (**Table 3**), meaning that triterpenoid concentration was higher in fruits from rain-fed trees if expressed in absolute terms ($\mu\text{g cm}^{-2}$ fruit surface). The most abundant identified triterpenoids were maslinic and oleanolic acids (**Supplementary Table S5**), in agreement with previous studies (Bianchi et al., 1992; Guinda et al., 2010; Huang et al., 2017; Diarte et al., 2019).

As regards acyclic wax compounds, the weighted average chain length (ACL) in olives picked from El Soleràs was similar for irrigated and rain-fed fruits, and ranged respectively from 24.0 to 24.4 and from 23.3 to 24.8 (**Table 4**). At two sampling points uniquely, namely those spanning the first half of November, and coincident with lowered rainfall at the production site (**Table 1**), were significant differences between irrigated and rain-fed fruits detected. These ACL values were lower than those reported in a previous report on ‘Arbequina’ olives picked from the same orchard (Huang et al., 2017) for which ACL values ranged 25.8 to 27.3 contingent on maturity stage. Similar ACL values, ranging between 23.7 and 25.0, were found for olives produced in Mas Bové regardless of irrigation (**Supplementary Table S3**), which were similar to those reported elsewhere for irrigated samples collected from that site (Diarte et al., 2019). Discrepancies may reflect year-to-year variability owing to variations in climatic conditions, as well as environmental differences (climatic, edaphic) across producing sites.

For both producing locations, the percentage of fatty acids in olive fruit cuticles was similar (6.6-11.5% and 6.0-15.4% over total waxes for samples from El Soleràs and Mas Bové, respectively). Fatty acid percentages increased in general terms along fruit maturation, while no significant differences were detected in response to irrigation (**Table 4, Supplementary Table S3**). No irrigation-related differences in the amounts of fatty alcohols (below 10% in all cases) were observed either. Cerotic acid (26:0) predominated quantitatively among the detected fatty acids, while hexacosanol (C_{26}) was the most abundant fatty alcohol, followed by tetracosanol (C_{24}) and octacosanol (C_{28}) (**Supplementary Table S5**). No clear time-course change trend along fruit maturation was observed for these compounds.

Finally, and regarding *n*-alkanes, relative amounts (% over total waxes) were higher in irrigated than in rain-fed fruits produced in El Soleràs (**Table 4**), in which heptacosane (C_{27}) was not detectable (**Supplementary Table S5**). This was unexpected, since *n*-alkanes have been often related to the water-

proofing functions of the plant cuticle through the ability to establish crystalline structures which would help restrict water loss (Grncarevic and Radler 1997; Leide et al., 2007; Leide et al., 2011). Even so, the very low percentages detected for this wax fraction (around 1% or lower) may indicate that their role in the prevention of water loss from olive fruits may be less important than in other olive organs or in other fruit species. For example, *n*-alkane amounts in ‘Arbequina’ leaves were found to be around four-fold higher than those in fruits, and leave cuticles were moreover observed to display much lower water permeability (Huang et al., 2017). The concentrations of *n*-alkanes in the cuticle of olive fruits have been consistently reported to be much lower than those found for other fruit species (reviewed in Lara et al., 2014; Belge et al., 2014, 2019). Alkane amounts in cuticles of fruits picked from Mas Bové were similarly low as in olives from El Soleràs, but in contrast no irrigation-related differences were detected (**Supplementary Table S3**).

4.3.4. Cutin monomers composition of ‘Arbequina’ olive fruit cuticles

Cutin monomers were also analysed. Overall, cutin composition in olives picked from El Soleràs showed limited variation in response to irrigation (**Table 5**). C₁₈-type predominated over C₁₆-type monomers, in some instances even doubling the percentages of C₁₆ compounds (**Table 5**). The predominant chemical family of cutin monomers identified was ω -hydroxy fatty acids, which accounted for 23.5-29.5% and 25.9-29.7% over total cutin in irrigated and rain-fed samples, correspondingly (**Supplementary Table S6 A and B**). Monocarboxylic fatty acids and ω -hydroxy fatty acids displaying midchain hydroxy groups (ω -OH FA mcOH) were also prominent among the detected cutin monomer types. The highest percentages over total cutin corresponded to 18-hydroxy-octadecenoic acid and 9/10,16-dihydroxy-hexadecanoic acid, which were hence the predominant cutin monomers identified in olive fruit samples (**Supplementary Table S6A and B**). In addition to the mentioned ω -hydroxy acids, considerable relative amounts of the dicarboxylic *cis*-9-octadecenoic α,ω -diacid were detected, which increased along fruit ripening, particularly in fruits picked from irrigated trees, to achieve around 11% over total cutin. The monocarboxylic oleic acid (18:1 Δ^9) was more abundant in irrigated than in rain-fed samples, percentages over total cutin ranging respectively from 6.7 to 14.5% and from 4.8 to 9.2%. Although the main monomer types identified were the same as in previous reports on ‘Arbequina’ olives (Huang et al., 2017; Diarte et al., 2019), some quantitative discrepancies were detected in comparison with Huang et al. (2017), who reported much higher relative amounts (% over total cutin) of ω -OH FA mcOH monomers. Likewise cuticular waxes, considerable variability in cutin monomer types and relative abundance has been observed across fruit species and cultivars (Kallio et al., 2006; Järvinen, Kaimainen and Kallio, 2010; Peschel et al., 2007; Belge et al., 2014; Lara et al., 2014; Belge et al., 2019). Additionally, much of the published literature on fruit cuticles has focused preferentially on waxes, and hence many knowledge gaps exist on cutin composition of fruit species.

With regard to cutin composition of fruit samples obtained from Mas Bové, similar trends were observed as for samples from El Soleràs (**Supplementary Table S4**). The quantitatively prominent cutin monomers 9/10,16-dihydroxy-hexadecanoic acid and 16-hydroxy-hexadecanoic did not display any noticeable changes regardless of irrigation or maturity stage, whereas relative amounts of 18-hydroxy-octadecenoic acid and *cis*-9-octadecenoic α,ω -diacid increased along fruit maturation as observed for samples from El Soleràs, in contrast with previous reports (**Supplementary Table S6**) (Diarte et al., 2019).

Even though cutin yields displayed an increasing trend during fruit maturation of ‘Arbequina’ olives (**Table 3, Supplementary Table S2**), the time-course change pattern of the different cutin monomer

Table 5. Composition of cutin monomers (relative % over total cutin) in cuticle isolated from ‘Arbequina’ olive fruit picked at El Soleràs (PDO ‘Les Garrigues’) in 2017-2018 season.

Sampling date	Irrigation regime	C ₁₆ /C ₁₈ *	FA	α,ω -diFA (%)	α,ω -diFA, mcOH (%)	ω -OH FA (%)	ω -OH FA, mcOH (%)	α -OH FA (%)	Alcohols (%)	Unidentified (%)								
Sep 15	Irrigated	0.81	21.35	ab A	4.39	d A	1.97	a A	23.48	c A	19.39	a A	1.25	ab A	1.82	cd A	26.34	a A
Oct 4		0.55	21.88	ab A	9.34	bc A	1.14	bc B	27.76	ab A	12.48	bc A	0.63	b A	1.64	d A	25.14	ab A
Oct 17		0.49	27.32	a A	8.52	c B	1.17	bc A	26.47	bc A	12.13	bc A	0.82	ab A	1.70	d A	21.86	d B
Oct 31		0.45	23.47	ab A	10.73	ab A	0.99	c B	28.63	ab A	10.28	c B	0.80	ab B	1.91	bcd B	23.18	d B
Nov 14		0.49	17.58	bc A	10.97	a A	1.01	c A	29.52	a A	11.84	c A	0.88	ab B	2.05	abc B	26.17	a A
Nov 29		0.62	13.42	c A	11.15	a A	1.93	a A	28.00	ab A	18.18	a A	1.73	a A	2.23	ab A	23.36	cd A
Dec 12		0.51	13.45	c A	12.04	a A	1.78	ab A	29.37	a A	14.97	b B	1.23	ab A	2.18	abc A	24.98	abc A
Jan 16		0.43	19.57	b A	12.21	a A	1.20	bc A	28.35	ab A	11.60	c A	1.19	ab A	2.39	a A	23.48	bcd B
Sep 15	Rain-fed	0.66	13.45	bc A	7.37	d A	2.00	a A	27.06	a A	16.97	ab A	1.48	ab A	2.08	ab A	29.58	a A
Oct 4		0.55	16.42	ab A	10.44	abc A	1.68	a A	28.26	a A	14.21	bc A	0.75	c A	1.72	c A	26.52	bc A
Oct 17		0.45	19.95	a B	10.67	abc A	1.66	a A	27.50	a A	10.75	c B	0.88	bc A	1.83	bc A	26.76	bc A
Oct 31		0.48	16.26	b B	9.84	bc A	2.05	aA	26.65	a A	13.69	bc A	1.39	ab A	2.15	a A	27.97	ab A
Nov 14		0.54	16.62	ab A	9.46	bc B	1.51	a A	27.82	a A	15.33	bc A	1.66	a A	2.20	a A	25.41	c A
Nov 29		0.56	11.77	c A	11.67	a A	1.68	a A	29.74	a A	14.81	bc A	1.12	abc A	2.17	a A	27.03	bc A
Dec 12		0.70	13.30	bc A	9.12	cd B	1.90	a A	25.88	a B	20.30	a A	1.27	abc A	2.16	a A	26.08	bc A
Jan 16		0.50	15.68	b A	11.00	ab A	1.42	a A	26.84	a A	14.89	bc A	1.26	abc A	2.30	a A	26.62	bc A

Cuticular membranes were isolated from skin samples (around 95 cm²) obtained from 50 to 75 olives, contingent upon ‘Arbequina’ fruit size. Values represent means of three technical replicates. Different capital letters denote significant differences among the cultivars for a given maturity stage, and different lower-case letters stand for significant differences among maturation stages for a given cultivar, at $P \leq 0.05$ (LSD test).

*Abbreviations: C₁₆/C₁₈, Ratio of C₁₆/C₁₈ cutin monomers; FA, Monocarboxylic fatty acids; α,ω -diFA, α,ω -Dicarboxylic fatty acids; α,ω -diFA, mcOH, α,ω -Dicarboxylic fatty acids with midchain hydroxy group; ω -OH FA, ω -Hydroxy fatty acids; ω -OH FA, mcOH, ω -Hydroxy fatty acids with midchain hydroxy group; α -OH FA, α -Hydroxy fatty acids; Other OH FA, other hydroxy fatty acids.

types detected was not the same in all cases, albeit the relative percentages over total cutin at each sampling point did not show important changes. This suggests that the metabolic pathways involved in the biosynthesis, transport and assembly of cutin monomers were affected differentially during the process.

4.3.5. PCA model

Because of the large dataset obtained, principal component analysis was used to help visualising relationships among the variables and factors considered. A preliminary PCA model including Mas Bové data did not reveal any clear irrigation-related separation among samples, possibly because of less harsh environmental conditions in this producing area (**Table 1**). Therefore, and because irrigation effects on the physical characteristics were much more apparent for olives obtained from El Soleràs (**Table 2**), only these samples were included in the model, which accounted for 60% of total variability (**Figure 1**).

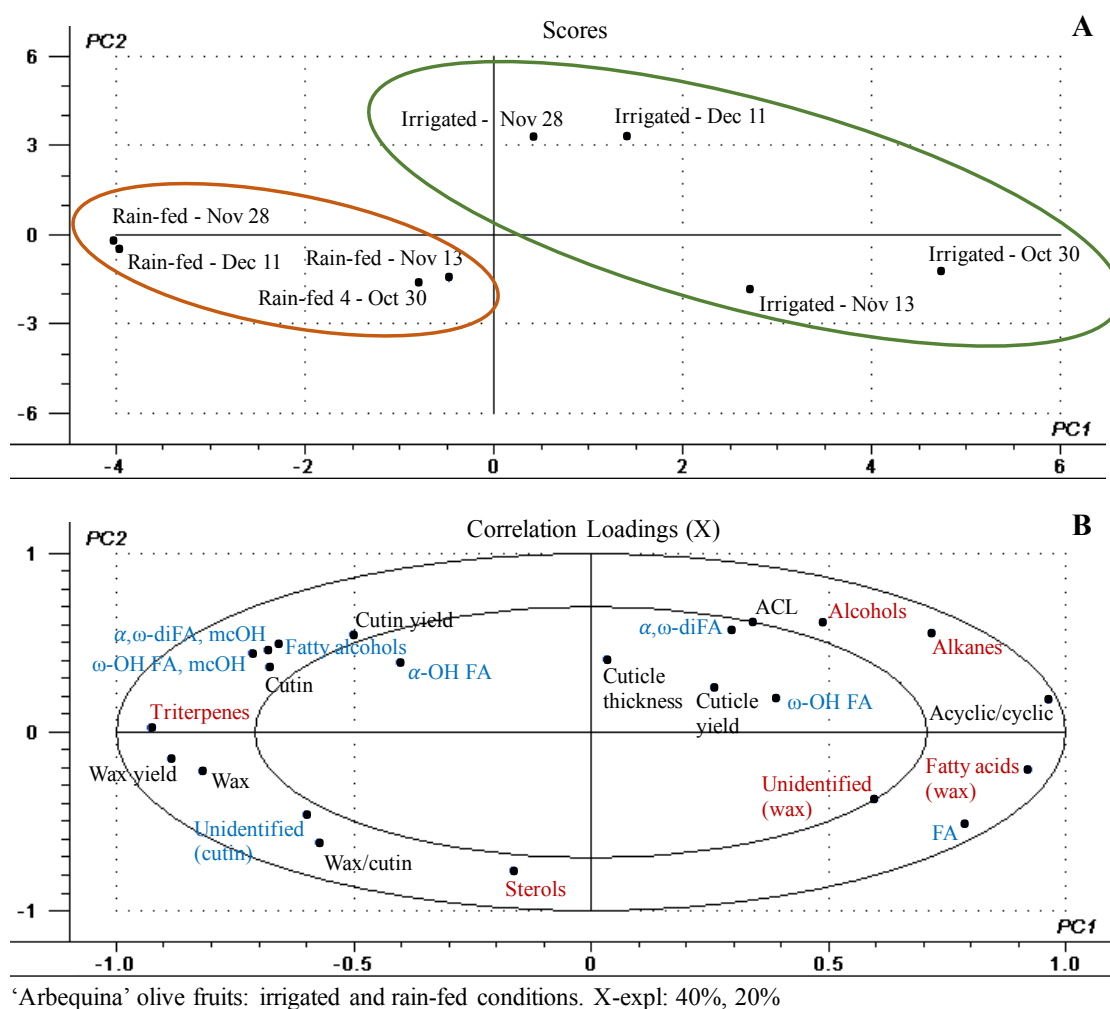


Figure 1. Scores (A) and correlation loadings (B) plots of PC1 vs. PC2 corresponding to a Principal Component Analysis (PCA) model for cuticle composition of fruits collected from El Soleràs (PDO ‘Les Garrigues, NE Spain) at advanced maturity stages in 2017.

*Abbreviations: FA, Mono Monocarboxylic fatty acids; α,ω -diFA, α,ω -Dicarboxylic fatty acids; α,ω -diFA, mcOH, α,ω -Dicarboxylic fatty acids with midchain hydroxy group; ω -OH FA, ω -Hydroxy fatty acids; ω -OH FA, mcOH, ω -Hydroxy fatty acids with midchain hydroxy group; α -OH FA, α -Hydroxy fatty acids.

The scores plot for this model (**Figure 1A**) shows that irrigated and rain-fed samples separated along principal component 1 (PC1). In turn, the correlation loadings plot (**Figure 1B**) showed that triterpene content, wax yields and the acyclic to cyclic ratio of cuticular waxes were the variables having most weight for sample differentiation. In contrast, the plot confirmed that cuticle thickness and, to a lesser extent, total cuticle yield, which were located close to the plot centre, were of little significance for plant response to water scarcity.

4.4. Conclusions

‘Arbequina’ olives grown in El Soleràs showed significant differences in phenotypical and cuticular characteristics in response to irrigation, while limited impact was observed for fruit samples obtained from Mas Bové. These observations suggest that environment conditions, and hence the production site, are important factors modulating the responses to water scarcity. The obtained dataset suggests that total load and composition of cuticular waxes play the main role in determining the water-proofing properties of the olive fruit cuticle, while cuticle thickness or total cuticle yields are less relevant in this regard. Future studies will help dissect these relationships, and the resulting knowledge may aid the improvement of grove management for the production of high-quality table olives and olive oils.

4.5. References

- Belge B, Llovera M, Comabella E, Gatiús F, Guillén P, Graell J, Lara I. 2014. Characterization of cuticle composition after cold storage of “Celeste” and “Somerset” sweet cherry fruit. *J. Agric. Food Chem.* 62, 8722-8729.
- Belge B, Goulao LF, Comabella E, Graell J, Lara I. 2019. Postharvest heat and CO₂ shocks induce changes in cuticle composition and cuticle-related gene expression in ‘October Sun’ peach fruit. *Post-harvest Biol. Technol.* 148, 200-207.
- Ben-Gal A, Ron Y, Yermiyahu U, Zipori I, Naoum S, Dag A. 2021. Evaluation of regulated deficit irrigation strategies for oli olives: A case study for two modern Israeli cultivars. *Agric. Water Manag.* 245, 106577.
- Berenguer MJ, Vossen PM, Grattan SR, Connel JH, Polito VT. 2006. Tree irrigation levels for optimum chemical and sensory properties of olive oil. *HortScience.* 41, 427-432.
- Bianchi G, Murelli G, Vlahov G. 1992. Surface waxes from olive fruits. *Phytochemistry.* 31, 3503-3506.
- Bianchi G. 2003. Lipids and phenols in table olives. *Eur. J. Lipid Sci. Technol.* 105, 229-242.
- Buschhaus C, Jetter R. 2011. Composition differences between epicuticular and intracuticular wax substructures: How do plants seal their epidermal surfaces? *J. Exp. Bot.* 62, 841-853.
- Camacho-Vázquez C, Ruiz-May E, Guerrero-Analco JA, Elizalde-Contreras JM, Enciso-Ortiz EJ, Rosas-Saito G, López-Sánchez L, Kiel-Martínez AL, Bonilla-Landa I, Monribot-Villanueva JL, Olivares-Romero JL, Gutiérrez-Martínez P, Tafolla-Arellano JC, Tiznado-Hernández ME, Quiroz-Figueroa FR, Birke A, Aluja M. 2019. Filling gaps in our knowledge on the cuticle of mangoes (*Mangifera indica*)

by analyzing six fruit cultivars: Architecture/structure, postharvest physiology and possible resistance to fruit fly (Tephritidae) attack. *Postharvest Biol. Technol.* 148, 83-96.

Diarte C, Lai PH, Huang H, Romero A, Casero T, Gatiús F, Graell J, Medina V, East A, Riederer M, Lara I. 2019. Insights into olive fruit surface functions: a comparison of cuticular composition, water permeability, and surface topography in nine cultivars during maturation. *Front. Plant Sci.* 19, 1484.

Domínguez E, Heredia-Guerrero JA, Heredia A. 2011. The biophysical design of plant cuticles: An overview. *New Phytol.* 189, 938-949.

Fernández V, Eichert T. 2009. Uptake of hydrophilic solutes through plant leaves: current state of knowledge and perspectives of foliar fertilization. *Crit. Rev. Plant Sci.* 28, 36-68.

Fernández V, Sotiropoulos T, Brown P. 2013. Foliar Fertilization: scientific principles and field practices. (ISBN 979-10-92366-00-6).

Grncarevic M, Radler F. 1967. The effect of wax components on cuticular transpiration model experiments. *Planta.* 75, 23-27.

Gómez-Rico A, Salvador MD, Moriana A, Pérez D, Olmedilla N, Ribas F, Fregapane G. 2007. Influence of different irrigation strategies in a traditional Cornicabra cv. olive orchard on virgin olive oil composition and quality. *Food Chem.* 100, 568-578.

Guinda A, Rada M, Delgado T, Gutiérrez-Adán P, Castellano JM. 2010. Pentacyclic triterpenoids from olive fruit and leaf. *J. Agric. Food Chem.* 58, 9685-9691.

Huang H, Burghardt M, Schuster AC, Leide J, Lara I, Riederer M. 2017. Chemical Composition and Water Permeability of Fruit and Leaf Cuticles of *Olea europaea* L. *J. Agric. Food Chem.* 65, 8790-8797.

Huang H, Jiang Y. 2019. Chemical composition of the cuticle membrane of pitaya fruits (*Hylocereus polyrhizus*). *Agriculture.* 9, 250.

Inglese P. 2011. Factors affecting extra-virgin olive oil composition. *Hortic. Rev.* 38, 83-147.

Järvinen R, Kaimainen M, Kallio H. 2010. Cutin composition of selected northern berries and seeds. *Food Chem.* 122, 137-144.

Jiménez-Herrera R, Pacheco-López B, Peragón J. 2019. Water stress, irrigation and concentrations of pentacyclic triterpenes and phenols in *Olea europaea* L. cv. Picual olive trees. *Antioxidants.* 8, 294.

Kallio H, Nieminen R, Tuomasjukka S, Hakala M. 2006. Cutin composition of five Finnish berries. *J. Agric. Food Chem.* 54, 457-462.

Kosma DL, Bourdenx B, Bernard A, Parsons EP, Lü S, Joubès J, Jenks MA. 2003. The impacts of water deficiency on leaf cuticle lipids of *Arabidopsis*. *Plant Physiol.* 151, 1918-1929.

Lanza B, Di Serio MG. 2015. SEM characterization of olive (*Olea europaea* L.) fruit epicuticular waxes and epicarp. *Sci. Hortic.* 191, 49-56.

Lara I, Belge B, Goulao LF. 2014. The fruit cuticle as a modulator of postharvest quality. *Postharvest Biol. Technol.* 87, 103-112.

Lara I, Heredia A, Domínguez E. 2019. Shelf life potential and the fruit cuticle: the unexpected player. *Front. Plant Sci.* 10, 770.

Leide J, Hidelbrandt U, Reussing K, Riederer M, Vogg G. 2007. The developmental pattern of tomato fruit wax accumulation and its impact on cuticular transpiration barrier properties: effects of a deficiency in β -Ketoacyl-Coenzyme A synthase (LeCER6). *Plant Physiol.* 144, 1667-1679.

Leide J, Hildebrandt U, Vogg G, Riederer M. 2011. The *positional sterile (ps)* mutation affects cuticular transpiration and wax biosynthesis of tomato fruits. *J. Plant Physiol.* 168, 871-877.

Mechri B, Tekaya M, Hammami M, Chehab H. 2020. Effects of drought stress on phenolic accumulation in greenhouse-grown olive trees (*Olea europaea*). *Biochem. Syst. Ecol.* 92, 104112.

Morales-Sillero A, García JM, Torre-Ruiz JM, Montero A, Sánchez-Ortiz A, Fernández JE. 2013. Is the productive performance of olive trees under localized irrigation affected by leaving some roots in drying soil? *Agric. Water Manag.* 123, 79-92.

Ninot A, Hermoso JF, Martí E, Rovira M, Batlle I, Romero A. 2015. Recuperació i conservació de varietat autòctones d'olivera. Dossier Tècnic, L'oli d'oliva a Catalunya. Ed. Direcció general d'alimentació, qualitat i indústries agroalimentàries. Catalonia, Spain. 80, 6-16.

Ninot A, Howad W, Romero A. 2019. Les varietats catalanes d'olivera. In *Quaderns agraris (Institució Catalana d'Estudis Agraris)*. 46, 7-36. (ISSN 0213-0319).

Patwari P, Salewski V, Gutbrod K, Kreszies T, Dresen-Scholz B, Peisker H, Steiner U, Meyer AJ, Schreiber L, Dörmann P. Surface wax esters contribute to drought tolerance in *Arabidopsis*. *Plant J.* 98, 727-744.

Peschel S, Frank R, Schreiber L, Knoche M. 2007. Composition of the cuticle of developing sweet cherry fruit. *Phytochemistry.* 68, 1017-1025.

Riederer M, Schreiber L. 2001. Protecting against water loss: analysis of the barrier properties of plant cuticles. *J. Exp. Bot.* 52, 2023-2032.

Riederer M, Arand K, Burghardt M, Huang H, Riedel M, Schuster AC. 2015. Water loss from litchi (*Litchi chinensis*) and longan (*Dimocarpus logan*) fruits is biphasic and controlled by a complex pericarpal transpiration barrier. *Planta.* 242, 1207-1219.

Romero P, Rose JKC. 2019. A relationship between tomato fruit softening, cuticle properties and water availability. *Food Chem.* 295, 300-310.

Schindelin JL, Arganda-Carreras I, Frise E, Kaynig V, Longair M, Pietzsch T. 2012. Fiji: an open-source platform for biological-image analysis. *Nat. Methods.* 9, 676-682.

Tanaka T, Tanaka H, Machida C, Watanabe M, Machida Y. 2004. A new method for rapid visualization of defects in leaf cuticle reveals five intrinsic patterns of surface defects in *Arabidopsis*. *Plant J.* 37, 139-146.

Tous J. 2017. The influence of growing region and cultivar on olives and olive oil characteristics and on their functional constituents. In *Olives and olive oil as functional foods: bioactivity, chemistry and processing*. Chapter 4. (ISBN 9781119135340).

Trivedi P, Nguyen N, Hykkerud AL, Häggman H, Martinussen I, Jaakola L. 2019. Developmental and environmental regulation of cuticular wax biosynthesis in fleshy fruits. *Front. Plant Sci.* 10, 431.

Uceda M, Frías L. 1975. Harvest dates. Evolution of the fruit of content, oil composition and oil quality. In *Proceedings of II Seminario Oleícola International*. p125-130.

Vichi S, Cortés-Francisco N, Caixach J, Barrios G, Mateu J, Ninot A. 2016. Epicuticular wax in developing olives (*Olea europaea*) is highly dependent upon cultivar and fruit ripeness. *J. Agric. Food Chem.* 64, 5985-5994.

Wang J, Sun L, Xie L, He Y, Luo T, Sheng L. 2016. Regulation of cuticle formation during fruit development and ripening in ‘Newhall’ navel orange (*Citrus sinensis* Osbeck) revealed by transcriptomic and metabolic profiling. *Plant Sci.* 243, 131-144.

Zarrouk O, Pinheiro C, Misra CS, Fernández V, Chaves MM. 2018. Fleshy fruit epidermis is a protective barrier under water stress. In *Water scarcity and sustainable agriculture in semiarid environment*. Chapter 20. (ISBN 978-0-12-813164-0).

Supplementary material

Supplementary Table S1. Physical characteristics and toluidine blue test of ‘Arbequina’ olives picked at Mas Bové (PDO ‘Siurana’) in 2017-2018 season.

Sampling date	Irrigation regime	Weight (g)	Length (mm)	Diameter (mm)		F:S ratio*	Water content (%)	TB test	
Sep 15	Irrigated	1.14	13.42	c B	11.56	d B	2.20	50.73	-
Oct 4		1.47	13.93	bc B	12.29	c A	2.41	50.79	+
Oct 17		1.35	13.94	bc B	12.32	c B	2.27	45.41	+
Oct 31		1.45	14.55	ab A	13.22	a A	2.87	59.13	+
Nov 14		1.50	14.35	ab A	13.11	ab A	3.24	54.08	+
Nov 29		1.41	14.34	ab A	12.69	abc A	2.58	48.67	ne
Dec 12		1.68	14.10	b A	12.50	bc A	3.86	45.85	ne
Jan 16		1.79	15.01	a A	13.27	a A	3.00	39.75	ne
Sep 15	Rain-fed	1.29	14.59	a A	12.65	bc A	2.73	55.28	-
Oct 4		1.46	14.94	a A	12.83	abc A	3.03	54.90	+
Oct 17		1.62	15.20	a A	13.47	a A	2.77	53.73	+
Oct 31		1.54	15.00	a A	13.20	ab A	4.18	56.46	-
Nov 14		0.92	12.49	b B	10.92	e B	3.64	48.27	-
Nov 29		1.22	13.21	b B	11.54	de B	3.16	47.92	ne
Dec 12		1.69	14.60	a A	12.22	cd A	3.63	43.05	ne
Jan 16		1.60	15.52	a A	13.31	ab A	4.31	39.75	ne

Values represent means of 50 fruits for weight, F:S ratio and water content, and of 10 fruits for length, diameter and TB test. Different capital letters denote significant differences among irrigated and rain-fed samples for a given sampling date, and different lower-case letters stand for significant differences among sampling date and irrigation regime at $P \leq 0.05$ (LSD test).

*Abbreviations: F:S ratio, flesh to stone ratio; TB test, toluidine blue test (Tanaka et al., 2004): stained and non-stained ‘Arbequina’ fruits are denote respectively as + and -; ne, not evaluated.

Supplementary Table S2. Cuticle, cuticular wax and cutin yields, wax to cutin ratio and cuticle thickness of ‘Arbequina’ olives picked at Mas Bové (PDO ‘Siurana’) in 2017-2018 season.

Sampling date	Irrigation regime	Cuticle yield (mg cm ⁻²)	Wax yield (µg cm ⁻²)	Wax (%)	Cutin yield (µg cm ⁻²)	Cutin (%)	Wax/ cutin ratio	Thickness (µm)
Sep 15	Irrigated	2.2 b A	510.5 a A	22.9 ab A	432.7 b A	19.4 bc A	1.4 a A	44.2 a A
Oct 4		2.2 b A	522.2 a A	23.9 a A	424.4 b A	19.4 bc A	1.2 a A	41.0 a B
Oct 17		3.1 a A	284.9 cd A	9.2 e B	405.2 bc A	13.1 e B	0.7 c A	41.1 a A
Oct 31		2.0 b A	274.3 cd B	13.9 d A	228.2 d B	11.6 e B	1.2 a A	41.7 a A
Nov 14		2.1 b A	232.8 d B	11.1 e B	339.5 c B	16.2 d B	0.7 c A	41.8 a A
Nov 29		2.2 b A	373.3 b A	16.8 c A	404.6 bc B	18.2 cd B	0.9 b A	38.1 ab A
Dec 12		2.1 b A	401.0 b A	21.2 b A	428.5 b A	20.7 b B	0.9 b A	37.0 ab A
Jan 16		1.9 b B	304.7 c A	16.2 cd A	514.5 a B	27.3 a A	0.6 c A	32.9 b A
Sep 15	Rain-fed	2.4 a A	512.9 a A	21.3 a B	400.8 b A	16.7 d A	1.3 a A	46.1 ab A
Oct 4		2.5 a A	373.7 b B	16.1 b B	419.1 b A	17.0 d A	0.9 ab A	50.5 a A
Oct 17		2.1 b B	266.0 d A	12.8 c A	500.6 b A	24.2 abc A	0.5 bc A	37.4 cd A
Oct 31		2.1 b A	318.2 c A	15.3 b A	417.8 b A	20.1 bcd A	0.8 bc A	40.3 bcd A
Nov 14		2.2 b A	328.9 c A	15.1 b A	408.8 b A	18.8 cd A	0.8 bcA	43.2 abcd A
Nov 29		2.6 a A	324.7 c B	12.6 c B	750.2 a A	29.1 a A	0.4 c B	44.5 abc A
Dec 12		1.8 c A	371.9 b A	20.1 a A	464.0 b A	25.1 ab A	0.8 bc A	43.7 abcd A
Jan 16		2.4 a A	223.4 e B	9.0 d B	712.3 a A	29.3 a A	0.3 c B	36.8 d A

Cuticular membranes were isolated from skin samples (around 95 cm²) obtained from 50 to 75 olives, contingent upon ‘Arbequina’ fruit size. Wax and cutin data represent means of three technical replicates of this starting material. For cuticle thickness values represent means of four biological replicates. Different capital letters denote significant differences among irrigated and rain-fed samples for a given sampling date, and different lower-case letters stand for significant differences among sampling date and irrigation regime at $P \leq 0.05$ (LSD test).

Supplementary Table S3. Composition of wax constituents (relative % over total waxes) in cuticle isolated from ‘Arbequina’ olives picked at Mas Bové (PDO ‘Siurana’) in 2017-2018 season.

Sampling date	Irrigation regime	ACL*		Acyclic/cyclic ratio		Triterpenoids (%)		Fatty acids (%)		Fatty alcohols (%)		<i>n</i> -Alkanes (%)		Sterols (%)		Unidentified (%)	
Sep 15	Irrigated	24.7	ab A	0.18	c A	70.3	ab B	7.5	cd A	4.2	d A	1.2	b A	1.0	a A	15.8	a A
Oct 4		24.5	bc A	0.19	c A	69.7	abc A	8.0	cd B	4.4	cd A	0.9	b A	0.9	a A	16.0	a A
Oct 17		23.8	d A	0.23	bc A	66.7	bc A	10.3	b A	4.2	d A	0.9	b A	1.0	a A	16.8	a A
Oct 31		24.1	cd B	0.19	bc A	72.6	a A	9.5	bc A	4.1	d B	0.7	b A	0.9	a A	12.2	b A
Nov 14		24.1	cd A	0.26	ab A	66.0	bc B	11.4	ab A	5.0	bc B	0.8	b A	0.6	a A	16.0	a A
Nov 29		24.6	b A	0.17	c A	74.3	a A	6.5	c A	5.4	ab A	0.6	b A	1.1	a A	12.2	b A
Dec 12		25.0	a A	0.32	a A	66.6	bc A	13.2	a A	6.1	a A	1.9	a A	1.2	a A	10.9	b A
Jan 16		24.5	b A	0.30	a A	64.3	c A	12.5	a A	5.9	a A	1.2	b A	0.8	a A	15.3	a A
Sep 15	Rain-fed	24.0	d B	0.13	d B	76.1	a A	6.0	e B	2.9	e B	0.8	cde B	1.1	ab A	13.0	cd B
Oct 4		24.4	bc A	0.22	bc A	67.6	bcd A	9.4	cd A	5.0	cd A	1.0	bc A	0.9	bc A	16.1	abc A
Oct 17		23.7	e A	0.22	c A	64.9	cd A	9.3	cd A	4.3	de A	0.9	bcd A	1.3	a A	19.3	a A
Oct 31		24.4	bc A	0.34	a A	61.7	d A	12.0	b A	7.5	a A	1.0	abc A	0.9	bcd A	16.9	ab A
Nov 14		24.3	c A	0.21	c A	70.8	abc A	8.6	d B	5.9	bc A	0.7	de A	0.9	bcd A	13.0	cd B
Nov 29		24.3	c A	0.21	c A	73.4	ab A	8.1	de A	6.6	ab A	0.6	e A	0.7	d B	10.6	d A
Dec 12		24.8	a A	0.38	a A	62.5	d A	15.4	a A	7.4	a A	1.2	a A	0.8	cd A	12.7	cd A
Jan 16		24.5	b A	0.31	ab A	64.3	cd A	11.5	bc A	7.2	ab A	1.1	ab A	1.0	bc A	14.9	bc A

Cuticular membranes were isolated from skin samples (around 95 cm²) obtained from 50 to 75 olives, contingent upon ‘Arbequina’ fruit size. Values represent means of three technical replicates. Different capital letters denote significant differences among irrigated and rain-fed samples for a given sampling date, and different lower-case letters stand for significant differences among sampling date and irrigation regime at $P \leq 0.05$ (LSD test).

*Abbreviations: ACL, Average chain length of acyclic wax compounds.

Supplementary Table S4. Composition of cutin monomers (relative % over total cutin) in cuticle isolated from ‘Arbequina’ olives picked at Mas Bové (PDO ‘Siurana’) in 2017-2018 season.

Sampling date	Irrigation regime	C ₁₆ /C ₁₈ *	FA	α,ω -diFA (%)	α,ω -diFA, mcOH (%)	ω -OH FA (%)	ω -OH FA, mcOH (%)	α -OH FA (%)	Alcohols (%)	Unidentified (%)								
Sep 15	Irrigated	0.64	29.88	a A	4.16	f A	0.96	d A	24.47	d A	11.79	de A	2.87	a A	1.74	d A	24.13	d A
Oct 4		0.69	16.58	cd A	7.01	e A	1.68	bc A	27.97	bc A	14.90	bc A	0.78	c A	1.94	d A	29.13	a A
Oct 17		0.59	19.83	bc A	7.79	de B	1.30	cd A	29.56	b A	13.24	cde A	0.93	bc A	2.07	cd A	25.29	cd A
Oct 31		0.52	22.44	b A	9.67	bc A	1.46	cd A	27.79	bc A	11.76	de A	0.92	bc A	1.99	d A	23.96	d B
Nov 14		0.57	17.51	bcd A	9.13	bcd A	1.60	bc A	27.41	bc A	14.39	bcd A	1.21	bc A	2.42	ab A	26.31	bc A
Nov 29		0.69	12.00	d B	8.34	cde B	2.46	a A	27.02	c A	18.26	a A	1.49	bc A	2.75	a A	27.68	ab A
Dec 12		0.42	14.35	cd A	12.40	a A	1.35	cd A	32.42	a A	10.45	e A	1.28	b A	2.64	ab A	25.10	cd A
Jan 16		0.59	17.03	bcd A	10.11	b A	1.99	ab A	25.89	cd B	16.74	ab A	1.39	bc	2.38	bc B	24.48	cd A
Sep 15	Rain-fed	0.59	29.96	a A	4.84	e A	1.53	a A	23.33	c A	12.54	bc A	3.29	a A	1.75	d A	22.76	d A
Oct 4		0.61	13.81	c A	6.58	d A	1.86	a A	29.97	a A	15.30	a A	1.11	bc A	1.95	cd A	29.40	a A
Oct 17		0.57	20.68	b A	9.81	c A	1.77	a A	28.51	ab A	12.71	abc A	1.02	bc A	1.89	cd A	23.62	d B
Oct 31		0.47	21.08	b A	10.49	bc A	1.54	a A	27.44	ab A	10.66	c A	0.74	c A	2.14	bc A	25.91	b A
Nov 14		0.53	17.04	bc A	10.49	bc A	1.84	a A	26.83	abc A	13.43	ab B	1.05	bc A	2.36	a A	26.96	b A
Nov 29		0.55	17.00	bc A	10.23	c A	2.14	a A	26.18	bc A	14.67	ab B	1.08	bc A	2.10	bc B	26.61	b A
Dec 12		0.48	13.06	c A	12.04	a A	1.83	a A	29.77	ab A	14.16	ab A	1.54	bc A	2.29	b A	25.31	bc A
Jan 16		0.49	14.92	bc A	11.28	ab A	1.82	a A	28.30	ab A	14.88	ab A	1.78	b A	2.88	a A	24.13	cd A

Cuticular membranes were isolated from skin samples (around 95 cm²) obtained from 50 to 75 olives, contingent upon ‘Arbequina’ fruit size. Values represent means of three technical replicates. Different capital letters denote significant differences among the cultivars for a given maturity stage, and different lower-case letters stand for significant differences among maturation stages for a given cultivar, at $P \leq 0.05$ (LSD test).

*Abbreviations: C₁₆/C₁₈, Ratio of C₁₆/C₁₈ cutin monomers; FA, Monocarboxylic fatty acids; α,ω -diFA, α,ω -Dicarboxylic fatty acids; α,ω -diFA, mcOH, α,ω -Dicarboxylic fatty acids with midchain hydroxy group; ω -OH FA, ω -Hydroxy fatty acids; ω -OH FA, mcOH, ω -Hydroxy fatty acids with midchain hydroxy group; α -OH FA, α -Hydroxy fatty acids; Other OH FA, other hydroxy fatty acids.

Supplementary Table S5. Cuticular wax constituents (relative %) in cuticles isolated from ‘Arbequina’ olive cultivar:

A) Olives picked at **El Soleràs** (PDO ‘Les Garrigues’) in irrigated regime in 2017-2018 season.

Irrigation regime	Irrigated							
Sampling date	Sept 18	Oct 2	Oct 16	Oct 30	Nov 13	Nov 28	Dec 11	Jan 15
Fatty acids								
C20:0	1.25 ± 0.20	2.11 ± 0.27	2.75 ± 0.43	2.04 ± 0.30	2.09 ± 0.10	1.43 ± 0.06	1.40 ± 0.32	1.75 ± 0.25
C20:1 (c13)	1.83 ± 0.22	1.83 ± 0.23	2.30 ± 0.33	1.87 ± 0.24	2.25 ± 0.06	1.48 ± 0.06	1.50 ± 0.32	1.80 ± 0.24
C22:0	0.57 ± 0.08	0.91 ± 0.09	1.05 ± 0.18	1.19 ± 0.21	1.20 ± 0.06	1.12 ± 0.08	1.38 ± 0.35	1.19 ± 0.18
C24:0	0.73 ± 0.02	1.19 ± 0.11	1.10 ± 0.17	1.70 ± 0.44	1.47 ± 0.09	1.25 ± 0.17	1.93 ± 0.50	1.85 ± 0.34
C26:0	2.03 ± 0.13	2.49 ± 0.37	2.14 ± 0.36	3.31 ± 0.44	2.90 ± 0.10	2.29 ± 0.29	2.90 ± 0.65	2.88 ± 0.39
C28:0	1.03 ± 0.06	1.03 ± 0.18	0.91 ± 0.09	1.37 ± 0.08	1.33 ± 0.04	1.13 ± 0.18	1.13 ± 0.22	1.15 ± 0.09
n-Alkanes								
C25	0.65 ± 0.06	0.64 ± 0.07	0.68 ± 0.17	0.53 ± 0.11	0.38 ± 0.01	0.43 ± 0.06	0.52 ± 0.05	0.26 ± 0.02
C27	0.37 ± 0.02	0.31 ± 0.05	0.37 ± 0.07	0.59 ± 0.11	0.66 ± 0.02	0.62 ± 0.05	0.61 ± 0.07	0.36 ± 0.04
C34	nd	nd	0.74 ± 0.15	nd	nd	nd	0.26 ± 0.13	0.23 ± 0.04
Fatty alcohols								
C22	0.36 ± 0.06	0.29 ± 0.04	0.35 ± 0.07	0.36 ± 0.05	0.37 ± 0.03	0.85 ± 0.06	0.65 ± 0.14	0.63 ± 0.11
C24	0.56 ± 0.07	0.79 ± 0.10	1.15 ± 0.23	1.64 ± 0.29	1.67 ± 0.06	2.58 ± 0.29	2.06 ± 0.42	1.38 ± 0.22
C26	1.78 ± 0.29	1.69 ± 0.28	1.68 ± 0.29	2.96 ± 0.56	2.39 ± 0.02	2.81 ± 0.51	2.24 ± 0.40	1.82 ± 0.26
C28	1.00 ± 0.13	0.82 ± 0.19	0.77 ± 0.13	1.17 ± 0.11	0.98 ± 0.02	1.13 ± 0.22	0.82 ± 0.18	0.69 ± 0.08
Sterols								
Squalene	0.26 ± 0.03	0.14 ± 0.01	0.15 ± 0.02	0.13 ± 0.01	0.18 ± 0.04	0.15 ± 0.02	0.11 ± 0.01	0.08 ± 0.02
β-sitosterol	0.63 ± 0.15	0.63 ± 0.16	1.00 ± 0.33	0.71 ± 0.09	0.58 ± 0.15	0.48 ± 0.13	0.54 ± 0.22	0.68 ± 0.02
Triterpenes								
Oleanolic acid	21.01 ± 1.73	20.04 ± 0.74	20.17 ± 2.94	19.58 ± 0.66	18.06 ± 1.30	20.78 ± 1.47	23.25 ± 3.83	21.14 ± 0.50
Ursolic acid	nd	0.70 ± 0.30	nd	nd	nd	nd	nd	0.38 ± 0.07
Maslinic acid	50.66 ± 4.63	48.26 ± 3.10	45.01 ± 8.76	46.21 ± 3.81	48.54 ± 0.42	49.63 ± 5.00	44.15 ± 8.15	48.91 ± 3.54
Unidentified	15.28 ± 1.51	16.13 ± 1.06	17.70 ± 3.11	14.62 ± 1.03	14.96 ± 0.74	11.83 ± 2.22	14.14 ± 1.62	12.82 ± 0.93

Values represent means of three replicates ± standard deviation (nd, non-detectable).

Supplementary Table S5 – Continued

B) Olives picked at **El Soleràs** (PDO ‘Les Garrigues’) in rain-fed regime in 2017-2018 season.

Irrigation regime	Rain-fed							
Sampling date	Sept 18	Oct 2	Oct 16	Oct 30	Nov 13	Nov 28	Dec 11	Jan 15
Fatty acids								
C20:0	1.35 ± 0.14	1.73 ± 0.14	1.54 ± 0.28	1.84 ± 0.22	2.31 ± 0.18	1.06 ± 0.13	1.19 ± 0.16	1.32 ± 0.13
C20:1 (c13)	1.27 ± 0.10	1.39 ± 0.12	1.23 ± 0.21	1.54 ± 0.17	2.20 ± 0.28	1.10 ± 0.15	1.73 ± 0.82	1.64 ± 0.12
C22:0	0.69 ± 0.05	1.03 ± 0.07	0.92 ± 0.15	1.36 ± 0.18	1.23 ± 0.18	0.93 ± 0.11	1.05 ± 0.17	1.17 ± 0.12
C24:0	0.95 ± 0.08	1.59 ± 0.10	1.39 ± 0.26	1.93 ± 0.20	1.36 ± 0.24	1.19 ± 0.27	1.37 ± 0.27	1.88 ± 0.09
C26:0	2.02 ± 0.15	3.20 ± 0.37	2.25 ± 0.31	2.21 ± 0.16	1.93 ± 0.38	1.59 ± 0.36	1.84 ± 0.29	2.81 ± 0.08
C28:0	0.82 ± 0.02	1.14 ± 0.16	0.78 ± 0.11	0.78 ± 0.06	0.76 ± 0.12	0.70 ± 0.13	0.77 ± 0.12	1.15 ± 0.07
n-Alkanes								
C25	0.90 ± 0.33	0.66 ± 0.04	0.40 ± 0.06	0.41 ± 0.05	0.47 ± 0.13	0.32 ± 0.03	0.43 ± 0.10	0.35 ± 0.13
C27	0.46 ± 0.36	0.41 ± 0.04	nd	nd	nd	nd	nd	nd
C34	nd	1.32 ± 0.12	nd	nd	nd	nd	0.25 ± 0.02	nd
Fatty alcohols								
C22	0.34 ± 0.03	0.43 ± 0.06	0.23 ± 0.01	0.48 ± 0.14	0.38 ± 0.11	0.61 ± 0.14	0.37 ± 0.22	0.84 ± 0.11
C24	0.56 ± 0.01	0.89 ± 0.10	0.90 ± 0.18	1.48 ± 0.09	0.86 ± 0.18	1.73 ± 0.38	1.70 ± 0.18	1.98 ± 0.13
C26	2.03 ± 0.10	3.78 ± 0.62	2.16 ± 0.21	2.33 ± 0.12	1.78 ± 0.66	2.00 ± 0.53	1.61 ± 0.26	2.45 ± 0.18
C28	0.88 ± 0.01	1.52 ± 0.23	0.85 ± 0.03	0.75 ± 0.07	0.64 ± 0.20	0.73 ± 0.17	0.56 ± 0.10	0.87 ± 0.06
Sterols								
Squalene	0.31 ± 0.10	0.15 ± 0.01	0.13 ± 0.01	0.19 ± 0.01	0.19 ± 0.05	0.17 ± 0.03	0.10 ± 0.02	0.10 ± 0.02
β-sitosterol	0.61 ± 0.11	0.59 ± 0.22	0.51 ± 0.25	0.74 ± 0.07	0.57 ± 0.18	0.69 ± 0.09	0.66 ± 0.10	0.53 ± 0.08
Triterpenes								
Oleanolic acid	22.84 ± 1.13	23.60 ± 0.76	22.53 ± 0.70	22.77 ± 2.04	21.08 ± 1.70	24.08 ± 1.39	22.77 ± 1.55	22.24 ± 0.81
Ursolic acid	nd	nd	nd	nd	1.52 ± 0.61	nd	nd	0.37 ± 0.04
Maslinic acid	47.00 ± 4.00	38.81 ± 4.31	49.49 ± 1.39	47.25 ± 3.95	48.05 ± 6.31	52.85 ± 4.58	49.49 ± 3.25	46.48 ± 4.01
Unidentified	16.97 ± 2.40	18.83 ± 1.71	14.69 ± 0.60	13.94 ± 0.62	14.69 ± 2.77	10.25 ± 1.07	13.72 ± 0.82	13.57 ± 3.17

Values represent means of three replicates ± standard deviation (nd, non-detectable).

Supplementary Table S5 – Continued

C) Olive picked at **Mas Bové** (PDO ‘Siurana’) in irrigated regime in 2017-2018 season.

Irrigation regime	Irrigated							
Sampling date	Sept 15	Oct 4	Oct 17	Oct 31	Nov 14	Nov 29	Dec 12	Jan 16
Fatty acids								
C20:0	1.11 ± 0.05	1.29 ± 0.09	2.36 ± 0.37	1.82 ± 0.11	1.88 ± 0.12	0.85 ± 0.08	1.18 ± 0.03	1.66 ± 0.18
C20:1 (c13)	1.53 ± 0.08	1.21 ± 0.02	1.95 ± 0.38	1.57 ± 0.12	2.15 ± 0.09	0.74 ± 0.06	1.42 ± 0.01	1.59 ± 0.18
C22:0	0.60 ± 0.02	0.75 ± 0.02	1.11 ± 0.22	0.94 ± 0.05	1.30 ± 0.04	0.85 ± 0.09	1.44 ± 0.15	1.44 ± 0.04
C24:0	0.94 ± 0.06	1.20 ± 0.12	1.41 ± 0.20	1.49 ± 0.10	1.94 ± 0.17	1.23 ± 0.09	2.73 ± 0.33	2.28 ± 0.12
C26:0	2.30 ± 0.23	2.53 ± 0.12	2.47 ± 0.27	2.52 ± 0.26	2.98 ± 0.26	1.92 ± 0.13	4.35 ± 0.92	3.79 ± 0.50
C28:0	1.07 ± 0.12	0.99 ± 0.06	1.03 ± 0.12	1.13 ± 0.10	1.18 ± 0.07	0.92 ± 0.10	2.12 ± 1.04	1.69 ± 0.39
<i>n</i>-Alkanes								
C25	0.57 ± 0.05	0.63 ± 0.04	0.56 ± 0.14	0.38 ± 0.05	0.38 ± 0.05	0.30 ± 0.07	0.40 ± 0.04	0.47 ± 0.06
C27	0.32 ± 0.07	0.29 ± 0.01	0.39 ± 0.11	0.31 ± 0.03	0.47 ± 0.03	0.31 ± 0.04	0.70 ± 0.07	0.50 ± 0.08
C34	0.30 ± 0.03	nd	nd	nd	nd	nd	0.85 ± 0.97	0.23 ± 0.02
Fatty alcohols								
C22	0.42 ± 0.02	0.35 ± 0.02	0.36 ± 0.04	0.27 ± 0.02	0.37 ± 0.10	0.40 ± 0.10	0.56 ± 0.08	0.67 ± 0.17
C24	0.72 ± 0.05	0.92 ± 0.05	1.34 ± 0.17	1.19 ± 0.10	1.29 ± 0.09	1.90 ± 0.22	2.03 ± 0.11	1.91 ± 0.21
C26	2.04 ± 0.24	2.19 ± 0.18	1.76 ± 0.17	1.83 ± 0.22	2.44 ± 0.10	2.24 ± 0.17	2.44 ± 0.31	2.43 ± 0.05
C28	1.01 ± 0.06	0.94 ± 0.07	0.77 ± 0.06	0.80 ± 0.09	0.94 ± 0.06	0.84 ± 0.07	1.08 ± 0.37	0.93 ± 0.10
Sterols								
Squalene	0.30 ± 0.08	0.27 ± 0.03	0.16 ± 0.01	0.12 ± 0.02	0.14 ± 0.03	0.15 ± 0.03	0.12 ± 0.02	0.11 ± 0.02
β-sitosterol	0.67 ± 0.09	0.68 ± 0.11	0.82 ± 0.28	0.82 ± 0.22	0.51 ± 0.16	0.92 ± 0.20	1.07 ± 0.97	0.65 ± 0.14
Triterpenes								
Oleanolic acid	23.16 ± 0.69	23.26 ± 0.68	19.425 ± 0.89	19.75 ± 1.03	19.44 ± 0.55	20.84 ± 0.91	23.57 ± 0.81	22.01 ± 0.87
Ursolic acid	nd	1.81 ± 0.55	nd	nd	nd	nd	0.57 ± 0.34	0.33 ± 0.06
Maslinic acid	47.13 ± 2.56	44.64 ± 1.31	47.25 ± 5.27	52.88 ± 3.50	46.61 ± 1.91	52.48 ± 3.13	42.47 ± 7.33	42.00 ± 3.25
Unidentified	15.82 ± 1.12	16.05 ± 1.45	16.84 ± 2.95	12.17 ± 1.35	15.98 ± 1.53	12.16 ± 2.04	10.91 ± 1.03	15.30 ± 1.20

Values represent means of three replicates ± standard deviation (nd, non-detectable).

Supplementary Table S5 – Continued

D) Olive picked at **Mas Bové** (PDO ‘Siurana’) in rain-fed regime in 2017-2018 season.

Irrigation regime	Rain-fed							
Sampling date	Sept 15	Oct 4	Oct 17	Oct 31	Nov 14	Nov 29	Dec 12	Jan 16
Fatty acids								
C20:0	1.16 ± 0.17	1.57 ± 0.22	2.39 ± 0.22	1.89 ± 0.23	1.50 ± 0.06	1.11 ± 0.12	1.37 ± 0.12	1.35 ± 0.13
C20:1 (c13)	1.51 ± 0.25	1.42 ± 0.16	2.05 ± 0.19	1.71 ± 0.31	1.51 ± 0.07	1.68 ± 1.10	1.34 ± 0.13	1.56 ± 0.22
C22:0	0.58 ± 0.10	0.89 ± 0.03	0.94 ± 0.06	1.39 ± 0.35	0.97 ± 0.06	0.96 ± 0.14	1.61 ± 0.08	1.24 ± 0.13
C24:0	0.63 ± 0.12	1.41 ± 0.09	0.90 ± 0.13	2.11 ± 0.43	1.34 ± 0.15	1.41 ± 0.37	3.71 ± 0.08	2.21 ± 0.23
C26:0	1.47 ± 0.18	2.97 ± 0.26	2.03 ± 0.10	3.46 ± 0.61	2.37 ± 0.10	2.16 ± 0.48	5.46 ± 0.05	3.69 ± 0.66
C28:0	0.68 ± 0.07	1.15 ± 0.12	0.96 ± 0.12	1.43 ± 0.14	0.94 ± 0.02	0.82 ± 0.18	1.95 ± 0.04	1.49 ± 0.28
n-Alkanes								
C25	0.48 ± 0.10	0.65 ± 0.05	0.55 ± 0.09	0.52 ± 0.12	0.39 ± 0.07	0.31 ± 0.13	0.37 ± 0.02	0.39 ± 0.05
C27	0.31 ± 0.03	0.31 ± 0.01	0.36 ± 0.02	0.48 ± 0.11	0.34 ± 0.02	0.30 ± 0.04	0.54 ± 0.03	0.47 ± 0.08
C34	nd	nd	nd	nd	nd	nd	0.28 ± 0.02	0.22 ± 0.02
Fatty alcohols								
C22	0.33 ± 0.04	0.46 ± 0.20	0.31 ± 0.01	0.49 ± 0.04	0.41 ± 0.06	0.74 ± 0.18	0.62 ± 0.05	1.01 ± 0.10
C24	0.68 ± 0.08	1.14 ± 0.17	1.50 ± 0.14	2.06 ± 0.59	1.51 ± 0.02	2.00 ± 0.24	2.21 ± 0.15	2.36 ± 0.28
C26	1.33 ± 0.22	2.38 ± 0.21	1.77 ± 0.10	3.58 ± 0.94	2.92 ± 0.20	2.84 ± 0.43	3.34 ± 0.14	2.86 ± 0.44
C28	0.61 ± 0.09	1.01 ± 0.09	0.76 ± 0.05	1.37 ± 0.22	1.11 ± 0.06	1.00 ± 0.21	1.20 ± 0.05	1.01 ± 0.15
Sterols								
Squalene	0.31 ± 0.04	0.17 ± 0.00	0.17 ± 0.01	0.14 ± 0.02	0.16 ± 0.02	0.16 ± 0.02	0.12 ± 0.01	0.10 ± 0.02
β-sitosterol	0.77 ± 0.05	0.78 ± 0.13	1.10 ± 0.07	0.75 ± 0.28	0.72 ± 0.15	0.52 ± 0.04	0.71 ± 0.07	0.87 ± 0.14
Triterpenes								
Oleanolic acid	21.67 ± 0.63	21.18 ± 1.47	17.32 ± 0.78	20.22 ± 1.23	20.22 ± 0.85	22.77 ± 1.77	27.82 ± 0.47	22.75 ± 0.58
Ursolic acid	nd	1.30 ± 0.24	nd	nd	nd	nd	0.45 ± 0.07	0.33 ± 0.04
Maslinic acid	54.45 ± 1.75	45.14 ± 4.31	47.60 ± 2.30	41.49 ± 7.74	50.62 ± 1.71	50.64 ± 7.53	34.21 ± 1.72	41.26 ± 4.69
Unidentified	13.02 ± 0.65	16.07 ± 2.52	19.30 ± 2.04	16.90 ± 3.76	12.98 ± 0.68	10.56 ± 2.83	12.70 ± 0.58	14.86 ± 1.29

Values represent means of three replicates ± standard deviation (nd, non-detectable).

Fatty alcohols

C24	0.77 ± 0.27	0.53 ± 0.13	0.64 ± 0.14	0.66 ± 0.00	0.79 ± 0.09	1.07 ± 0.27	0.93 ± 0.15	0.98 ± 0.16
C26	0.73 ± 0.08	0.81 ± 0.04	0.80 ± 0.06	0.94 ± 0.08	0.83 ± 0.11	0.87 ± 0.09	0.97 ± 0.09	1.09 ± 0.05
C28	0.32 ± 0.05	0.29 ± 0.01	0.25 ± 0.02	0.31 ± 0.01	0.43 ± 0.30	0.29 ± 0.04	0.28 ± 0.00	0.32 ± 0.03
Unidentified	26.34 ± 0.53	25.14 ± 1.14	21.86 ± 1.53	23.18 ± 0.70	26.17 ± 1.40	23.36 ± 0.70	24.98 ± 0.67	23.48 ± 0.60

Values represent means of three replicates ± standard deviation (nd, non-detectable).

Fatty alcohols

C24	1.05 ± 0.05	0.60 ± 0.06	0.71 ± 0.04	0.90 ± 0.19	0.99 ± 0.13	1.03 ± 0.00	1.01 ± 0.15	1.11 ± 0.22
C26	0.80 ± 0.11	0.86 ± 0.05	0.88 ± 0.14	0.99 ± 0.08	0.93 ± 0.11	0.87 ± 0.04	0.89 ± 0.15	0.91 ± 0.09
C28	0.23 ± 0.01	0.27 ± 0.03	0.25 ± 0.03	0.27 ± 0.01	0.28 ± 0.04	0.26 ± 0.02	0.26 ± 0.03	0.27 ± 0.05
Unidentified	29.58 ± 2.12	26.52 ± 0.79	26.76 ± 1.80	27.97 ± 0.62	25.41 ± 0.86	27.03 ± 1.34	26.08 ± 0.47	26.62 ± 1.28

Values represent means of three replicates ± standard deviation (nd, non-detectable).

Fatty alcohols

C24	0.61 ± 0.08	0.71 ± 0.12	0.80 ± 0.10	0.83 ± 0.05	1.13 ± 0.23	1.26 ± 0.07	1.14 ± 0.11	1.12 ± 0.17
C26	0.81 ± 0.07	0.91 ± 0.08	0.93 ± 0.13	0.86 ± 0.04	1.00 ± 0.12	1.14 ± 0.04	1.14 ± 0.13	0.95 ± 0.06
C28	0.32 ± 0.04	0.31 ± 0.03	0.33 ± 0.02	0.31 ± 0.03	0.30 ± 0.03	0.35 ± 0.00	0.36 ± 0.02	0.31 ± 0.03
Unidentified	24.13 ± 1.75	29.13 ± 0.65	25.29 ± 0.91	23.96 ± 0.46	26.31 ± 0.38	27.68 ± 0.55	25.10 ± 0.32	24.48 ± 2.56

Values represent means of three replicates ± standard deviation (nd, non-detectable).

Fatty alcohols

C24	0.67 ± 0.18	0.76 ± 0.01	0.62 ± 0.04	0.84 ± 0.04	0.88 ± 0.02	0.95 ± 0.07	1.20 ± 0.13	1.40 ± 0.08
C26	0.81 ± 0.10	0.90 ± 0.03	0.91 ± 0.13	1.00 ± 0.03	1.14 ± 0.04	0.89 ± 0.02	0.85 ± 0.12	1.13 ± 0.04
C28	0.27 ± 0.02	0.29 ± 0.02	0.35 ± 0.03	0.31 ± 0.03	0.35 ± 0.01	0.26 ± 0.02	0.24 ± 0.04	0.34 ± 0.04
Unidentified	22.76 ± 1.75	29.40 ± 0.22	23.62 ± 0.18	25.91 ± 0.94	26.96 ± 1.12	26.61 ± 0.84	25.31 ± 1.16	24.13 ± 0.51

Values represent means of three replicates ± standard deviation (nd, non-detectable).

Chapter V: Firmness and cell wall changes during maturation of ‘Arbequina’ olive fruit grown at two Catalan Protected Designations of Origin: the impact of irrigation

(Manuscript)

Clara Diarte, Anna Iglesias, Agustí Romero, Jordi Graell, and Isabel Lara

Abstract

The olive tree (*Olea europaea* L.) has been cultivated around the Mediterranean basin since ancient times, ‘Arbequina’ being one of the most widely grown varieties. During ripening, modifications in cell wall composition and structure lead to changes in textural properties. To improve the knowledge on the ripening process of olive fruit, cell wall metabolism was studied in irrigated and rain-fed ‘Arbequina’ olives collected at ‘Les Garrigues’ and ‘Siurana’, two different Protected Designations of Origin (PDOs) in Catalonia (NE Spain). Fruit samples were picked periodically at both locations from September to January. Total phenolics and antioxidant capacity were higher in rain-fed than in irrigated samples. Time-course dynamics of firmness loss during maturation was characterized by two phases, namely a first phase of rapid firmness loss followed by a second phase of moderate change. Compositional changes in cell walls of fruit samples and related enzyme activities were studied in each case, and significant differences were observed in some cases between irrigated and rain-fed trees from PDO ‘Les Garrigues’. In contrast, very limited differences between irrigated and rain-fed fruits were found for PDO ‘Siurana’, where the climate is milder, and hence lower impact of irrigation on fruit attributes can be expected.

Keywords: ‘Arbequina’, cell wall; firmness; fruit ripening; irrigation; olive

Oleam (...) ab annis populi Romani CLXXIII, quae nunc pervenit trans Alpibus quoque et in Gallias Hispaniasque medias.

Pliny the Elder (Gaius Plinius Secundus)

Naturalis historia (Book 15)

5.1. Introduction

The olive (*Olea europaea* L.) tree has been farmed at the Mediterranean and Asia Minor areas for thousands of years (Waterman and Lockwood, 2007). Nowadays, olive trees are cultivated as well in other areas of the world, such as southern Africa, Australia, California, Japan, China or Argentina, even though Mediterranean countries remain the strongest olive producers. The largest part of olive production (90 % approximately) is intended for the oil industry and the rest is devoted to the manufacture of table olives. ‘Arbequina’ is one of the most important varieties in Spain, and its fruits are used for both purposes. The tree has low vigour, which makes it suitable for super-high density orchards (Connor et al., 2014) and for the implementation of mechanical harvesting procedures, with the consequent reduction in production costs.

The mechanical properties of fruits have an impact on textural attributes, eating quality and consumers’ perceptions, as well as on the susceptibility to rots, infestations and bruises, and on the efficiency of oil extraction. Fruits typically undergo noticeable softening along the ripening process, leading to textural modifications. Fruit softening results largely from changes in cells walls and middle lamellae, driven by a plethora of pectolytic and non-pectolytic proteins (Goulao and Oliveira, 2008) and resulting in the solubilisation of cell wall polysaccharides. In many fruit species including olive, polysaccharide depolymerisation also occurs (Marsilio et al., 2000; González-Cabrera et al., 2018). Non-enzymatic factors, such as ascorbic acid (AA) and its derivatives, may also contribute to the oxidative disassembly of cell wall polymers in some fruit species, (Dumville and Fry, 2003; Cheng et al., 2008; Duan et al., 2011; Belge et al., 2015).

Cell wall composition changes during olive fruit ripening have received limited attention. Cell wall materials solubilised extensively along ripening of ‘Koroneiki’ olives (Vierhuis et al., 2000), and ripening-related fruit softening was reportedly associated with noticeable arabinose losses in ‘Hojiblanca’ (Jiménez et al., 2001) and ‘Negrinha do Douro’ (Mafra et al., 2001). Cell wall-related enzyme activities and cell wall gene expression levels increased progressively during maturation in ‘Hojiblanca’ (Fernández-Bolaños et al., 1997) and ‘Picual’ (Parra et al., 2013) olives. In agreement with those previous reports, the removal of neutral sugars from pectins during maturation of ‘Arbequina’ fruits was related to increased α -L-arabinofuranosidase (AFase) activity (Lara et al., 2018). This observation was confirmed in a recent study (Diarte et al., 2021) on ‘Arbequina’ and eight additional olive cultivars (‘Argudell’, ‘Empeltre’, ‘Farga’, ‘Manzanilla’, ‘Marfil’, ‘Morrut’, ‘Picual’ and ‘Sevillenca’). Insoluble cell wall materials decreased during fruit ripening, and the concomitant decline in fruit firmness was associated to higher ascorbate content and AFase and β -galactosidase (β -Gal) activities, leading to important losses of neutral sugars.

Olive trees are often cultivated in harsh environmental conditions such as low water availability in combination with high temperatures and UV irradiation. Irrigation helps alleviating these stress factors, but it may also impact fruit metabolism and quality attributes. The influence of water availability on olive crops has been studied in regard to oil yield and quality (Motilva et al., 2000; Dabbou et al., 2010; García et al., 2013) and phenolic content (Petridis et al., 2012; Mechri et al., 2020), but we are not aware of any published study on the impact of irrigation on changes in cell wall metabolism along olive ripening, in spite of their relevance for the mechanical properties of fruit. In this work, therefore, cell wall modifications were assessed during ripening of ‘Arbequina’ olives grown under irrigated and rain-fed conditions at two different geographical areas.

5.2. Material and methods

5.2.1. Plant material and assessment of fruit firmness

‘Arbequina’ olives were hand-collected in Catalonia (NE Spain) at two orchards placed at El Soleràs (41° 24’N; 0° 40’E; altitude 450 m) and Constantí (41° 09’N; 1° 12’E; altitude 100 m), located respectively within the geographical areas covered by the Protected Designations of Origin (PDOs) ‘Les Garrigues’ and ‘Siurana’. Cultural and fertilisation procedures were the usual at each producing area. Total annual rainfall in 2017 was 318 and 340 mm for El Soleràs and Constantí, correspondingly. Precipitations at Constantí concentrated mostly in March (73 mm) and October (47 mm), while those at El Soleràs took place mainly at March (78 mm), June (47 mm) and September (48 mm) with extremely dry July and August (**Supplementary Figure S1**). At both PDOs, fruits were harvested from either rain-fed trees or trees supplied with drip irrigation (207 and 325 L week⁻¹ tree⁻¹ in El Soleràs and Mas Bové, correspondingly; irrigation period was April to October). Olives were picked periodically from September 2017 to January 2018. Samples were coded P1-P8, corresponding to successive picking dates.

Fruit firmness was determined as the maximum strength (N) required to achieve surface breakage in a penetration test using a 1-mm diameter cylindrical probe descending at 1 mm s⁻¹. Firmness assessments were carried out individually on ten olives per sampling date and irrigation regime with a texture analyser (INSTRON 3344, Instron, Bucks, UK, and TA-TX2, Stable Micro Systems, Goldaming, UK, for ‘Siurana’ and ‘Les Garrigues’ samples, respectively).

5.2.2. Extraction, fractionation and analysis of cell wall material

Cell wall materials were extracted as the alcohol-insoluble residue (AIR) from 50 g destoned fruits per sampling date and irrigation regime according to Voragen et al., 1983. Samples were blended in ethanol (80%, v/v) to obtain a 10% (w/v) suspension, heated (20 minutes at 80 °C), cooled down to room temperature, and filtered through Miracloth[®] (Merck Life Science S.L.U., Madrid, Spain). The solid residue was re-extracted twice more in 80% (v/v) ethanol, once in 96% (v/v) ethanol and once in acetone, and the slurry filtered through Miracloth[®] each time. After drying at 50 °C, the AIR was stored at -20 °C until fractionation. AIR yields were expressed as g 100 g⁻¹ fresh weight (FW).

For the fractionation of AIR samples (0.5 g), a modification of a previous procedure (Lefever et al., 2004) was used as described in Diarte et al. (2021). Samples were extracted sequentially in distilled water, 0.1 % (w/v) sodium oxalate (pH 5.6), 0.05 mol L⁻¹ sodium carbonate and 4 mol L⁻¹ potassium hydroxide to recover the water-, sodium oxalate-, sodium carbonate- and potassium hydroxide-soluble fractions (W_{sf}, NaOx_{sf}, Na₂CO_{3sf} and KOH_{sf}, respectively). The supernatants of each fractionation step were concentrated in a rotary evaporator and precipitated with ethanol (96 %, v/v), and then the sediment was washed in water three times, dried completely at 50 °C, and weighed. All the extractions were performed in triplicate, and yields expressed as g 100 g⁻¹ AIR.

Total sugar and uronic acid contents in each recovered fraction were determined by the phenol-sulfuric acid assay (Dubois et al., 1956) and the m-hydroxyphenyl method (Blumenkrantz and Asboe-Hansen, 1973), respectively. For the estimation of neutral sugar amounts, uronic acid content was subtracted from that of total sugars. Analyses were done in triplicate, and data were expressed as g 100 g⁻¹.

The procedure for the analysis of the degree of methyl esterification (d.e.) of pectins was based on the Klavons and Bennet, 1986 method. Briefly, AIR samples (15 mg) were shacked in 1 mol L⁻¹ KOH

(2 h at room temperature) to remove the methyl groups. Released methanol was then oxidised enzymatically in the presence of alcohol oxidase and, after incubating the samples with 0.02 mol L⁻¹ pentane-2,4-dione (2 h at 60 °C), the absorbance at 412 nm was read. Analyses were carried out in triplicate, and results given as the molar ratio (%) of methanol to uronic acid content.

5.2.3. Cell wall-related enzyme activities

The assays of cell wall-related enzyme activities were undertaken on crude extracts obtained from samples (100 mg) of acetone powder (AP) prepared from fruit pericarp (Fernández-Bolaños et al., 1997, with slight modifications). In short, destoned fresh olives (60-80 g) were homogenised in cold acetone (10% (w/v) suspension). After filtration, the solid was washed three more times in acetone, dried at room temperature and kept at -20 °C until the activity assays. The extraction buffers and activity assays for pectin methylesterase (PME; EC 3.1.1.11), polygalacturonase (exo-PG; EC 3.2.1.67 and endo-PG; EC 3.1.2.15), pectate lyase (PL; EC 4.2.2.2), α -L-arabinofuranosidase (AFase; EC 3.2.1.55), β -galactosidase (β -Gal; EC 3.2.1.23), endo-1,4- β -D-glucanase (EGase; EC 3.2.1.4) and β -xylosidase (β -Xyl; EC 3.2.1.37) were as described in Ortiz et al. (2011) and references therein. The Bradford, 1976 method was used to estimate total protein content in the extracts, with bovine serum albumin (BSA) as the standard. Results were given as specific activity (U mg protein⁻¹).

5.2.4. Antioxidant properties

Fisty olives per sampling date and irrigation regime were disinfected in 1% (v/v) Triton X-100, rinsed with deionised water and pitted. Samples were then lyophilised, milled and stored at -80 °C until analysis. For the determination of radical scavenging activity (RSA), the 2,2-diphenyl-1-picrylhydrazyl (DPPH) assay was used, which expresses the antioxidant capacity as the percentage of DPPH reduction in sample extracts in comparison with a control (DPPH without sample). Total phenolics were extracted in methanol solution (80 %, v/v) and determined as mg gallic acid equivalents g⁻¹ DW by the colorimetric Folin-Ciocalteu assay. Anthocyanins were extracted in methanol-HCL-water (50:1:49, v/v/v) and estimated spectrophotometrically as mg cyanidin equivalents g⁻¹ DW. All procedures were carried out as in Lara et al. (2015).

Total (TAA) and reduced (AA) ascorbic acid were estimated colorimetrically (Gillespie and Ainsworth, 2007). Dehydroascorbic acid (DHA) content was calculated as the difference between TAA and AA. Results were expressed as nmol g⁻¹ DW.

5.2.5. Statistical analysis

Multifactorial analysis of variance (ANOVA) and the LSD test ($p \leq 0.05$) were used to separate the means, with sampling date and irrigation regime as the factors, using the JMP[®] Pro 13 software. With the purpose of aiding in the interpretation of results, Principal Component Analysis (PCA) was used. Data were weighed previously by the inverse of the standard deviation of each variable to prevent dependence on the measuring units, and full cross-validation was run as a validation procedure. PCA models were developed with the Unscrambler software (version 9.1.2, CAMO ASA, Oslo, Norway).

5.3. Results and discussion

Morphological and physical characteristics of olive fruits are shown. In PDO ‘Les Garrigues’, fruit weight, size and F:S ratios were higher for irrigated than for rain-fed olives (Table 1), whereas smaller differences were observed for samples from PDO ‘Siurana’ (Supplementary Table 1). Substantial firmness loss was found during fruit maturation for both PDOs (Figure 1), although with some location-related differences. For olives grown at PDO ‘Les Garrigues’, fruit firmness levels were significantly higher in rain-fed than in irrigated olives for most of the sampling period (Figure 1A), picking dates spanning mid-to-late October being the only exception. For rain-fed samples, firmness decreased sharply over the first four sampling points and showed limited variation thereafter (November to January).

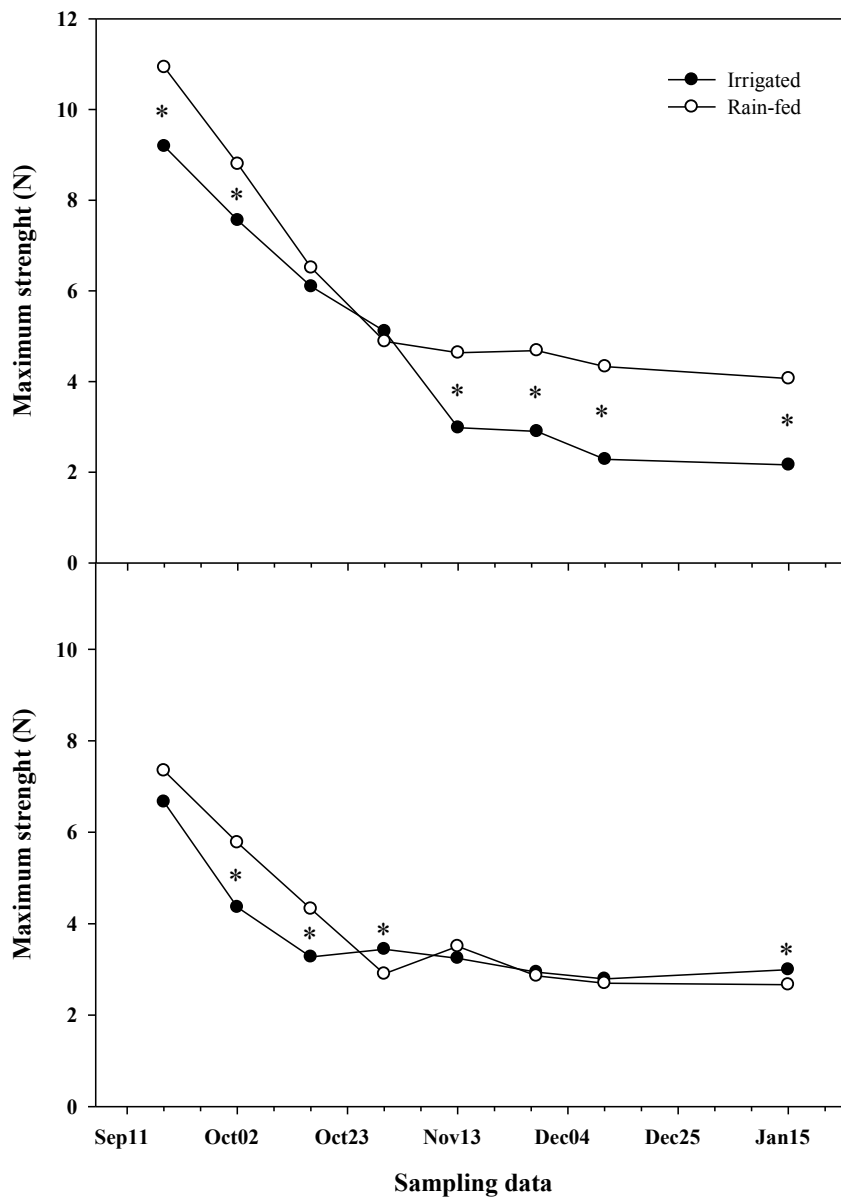


Figure 1. Fruit firmness of ‘Arbequina’ olives during maturation under irrigated and rain-fed conditions at PDOs Les Garrigues (A) and Siurana (B). Values represent means of ten individual fruits. Asterisks stand significant differences between irrigated and rain-fed trees at $P \leq 0.05$ (LSD test).

The same trend was found for irrigated fruits, but the accentuated phase of firmness loss lasted longer, up to mid-November. Higher firmness in fruits from rain-fed plants, particularly during the latter part of the experimental period, may be related to lower humidity in these fruits (**Figure 2**): water content in fruits decreased steadily after October, in parallel to weight loss (**Table 1**), and was significantly lower in fruits from rain-fed plants until January, when no significant differences were found. Overall firmness loss along the experimental period at this PDO amounted respectively to 76.5 and 63.0% for irrigated and rain-fed fruits.

Olives produced at PDO 'Siurana' showed a similar two-phase softening process during fruit maturation, firmness levels decreasing noticeably at earlier picking dates and then remaining approximately steady (**Figure 1B**). During the first phase of rapid firmness loss, rain-fed fruits were significantly firmer than those produced under irrigated conditions, but small differences were observed thereafter. Decrease in firmness was accompanied by an increase in deformation required to achieve surface breakage, indicative of increasing skin elasticity (**Supplementary Table 1**). Contrarily to fruits from PDO 'Les Garrigues', overall firmness loss was higher for rain-fed (63.8%) than for irrigated samples (58.2%), which agrees with a previous study on 'Arbequina' (García et al., 2013) showing higher firmness loss over the harvest period under deficit than under full irrigation. For olives from rain-fed trees, firmness loss was similar to that in PDO 'Les Garrigues', whereas for those from irrigated plants it was much more dramatic. Climatic characteristics at each PDO may underlie these discrepancies: the geographical area covered by PDO 'Les Garrigues' displays harsher conditions than that within PDO 'Siurana', and hence irrigation may have induced more noticeable differences. Annual rainfall was low at both growing sites during the experimental year 2017, amounting to 340 and 318 mm at Constantí (PDO 'Siurana') and El Soleràs (PDO 'Les Garrigues'), respectively (**Supplementary Figure S1**). There were however some differences in maximal temperatures during summer: average maximum temperatures in June, July and August reached respectively 31.2, 32.4 and 32.1 °C in El Soleràs, while they were 28.5, 29.3 and 29.6 °C in Constantí, in the same order. If absolute rather than average maximum temperature was considered, these differences were even more noticeable (**Supplementary Figure S1**). In accordance, water loss along the experimental time was higher for fruits produced at PDO 'Les Garrigues' (27 and 23 % respectively for samples from irrigated and rain-fed trees) (**Figure 2**) than for those grown at PDO 'Siurana' (12 and 16 %, in the same order) (**Supplementary Table 1**). On the basis of these data, we chose to focus preferentially on olives grown at El Soleràs (PDO 'Les Garrigues'), while data corresponding to PDO 'Siurana' are shown as supplementary material (**Supplementary Tables 1 to 6**).

Some antioxidant properties were also analysed throughout fruit maturation (**Table 1**; **Supplementary Table 2**). Anthocyanin content increased reflecting the ripening-related shift in skin colour. For fruit grown at PDO 'Les Garrigues', the amount of total phenolics was significantly higher in rain-fed than in irrigated olives. This observation might relate to environmental stress possibly imposed by lower water availability on rain-fed trees, as suggested in previous studies (Petridis et al., 2012; Mechri et al., 2020) on phenolic compounds in olive tree leaves under drought stress conditions. In agreement, higher anthocyanin levels were found in rain-fed than in irrigated fruits at P3-P5, concomitantly with decreased rainfall and the occurrence of high temperatures at the producing area (**Supplementary Figure S1**), and colour change in rain-fed fruits took place earlier (**Figure 2**). Contrarily, limited differences in total phenolics between rain-fed and irrigated olives were found for PDO 'Siurana', with the exception of very late sampling dates (P7 and P8, respectively mid-December and mid-January).

Table 1. Physical and chemical characteristics during fruit ripening of irrigated and rain-fed ‘Arbequina’ olives produced at El Soleràs (PDO ‘Les Garrigues’).

Picking #	Date	Irrigation regime	Weight (g)		Length (mm)		Diameter (mm)		F:S ratio*		Anthocyanin (mg g ⁻¹ DW)		Phenols (mg g ⁻¹ DW)		RSA* (%)		AA* (nmol g ⁻¹ DW)		DHA* (nmol g ⁻¹ DW)	
1	Sep 18	Irrigated	1.23	e A	14.18	d A	12.66	f A	3.80	c A	0.4	e A	19.8	a B	95.0	a A	0.10	bc B	0.15	a B
2	Oct 2		1.62	cd A	15.41	bc A	14.00	cde A	4.57	b A	0.4	de A	11.1	d B	83.7	b A	0.10	bc A	0.13	ab A
3	Oct 16		1.81	bc A	16.01	a A	14.77	a A	5.55	a A	0.3	e B	16.0	b B	95.5	a A	0.07	d B	0.06	d B
4	Oct 30		1.86	ab A	15.60	abc A	14.08	cd A	5.58	a A	0.6	cd B	13.0	c B	80.7	bc B	0.11	b A	0.08	c B
5	Nov 13		2.03	a A	15.90	ab A	14.52	ab A	4.69	b A	0.7	c B	11.3	d B	72.6	c B	0.11	b A	0.05	de B
6	Nov 28		1.84	ab A	15.48	bc A	14.21	bc A	4.46	b A	0.8	bc A	9.4	e B	38.0	e B	0.09	c A	0.04	e B
7	Dec 11		1.58	d A	15.20	c A	13.68	de A	4.55	b A	1.0	b A	14.4	bc B	53.7	d A	0.10	bc A	0.06	d B
8	Jan 15		1.59	d A	15.40	c A	13.61	e A	3.61	c A	3.1	a A	14.5	bc A	74.1	c A	0.16	a B	0.12	b A
1	Sep 18	Rain-fed	1.08	d B	12.90	c B	11.63	e B	3.19	e B	0.2	f B	25.3	a A	97.0	a A	0.13	b A	0.21	a A
2	Oct 2		1.38	b A	13.54	b B	12.12	cd B	3.66	cd B	0.2	ef B	17.0	bc A	94.0	a A	0.07	de B	0.10	d A
3	Oct 16		1.23	c B	13.32	bc B	11.86	de B	3.63	cd B	0.4	de A	24.5	a A	88.9	ab A	0.08	d A	0.09	d A
4	Oct 30		1.42	b B	13.73	b B	12.53	bc B	4.48	a B	1.0	b A	24.2	a A	96.3	a A	0.13	b A	0.15	b A
5	Nov 13		1.52	a B	14.59	a B	12.96	ab B	3.86	bc A	1.0	b A	19.2	b A	82.1	bc A	0.11	c A	0.10	d A
6	Nov 28		1.28	c B	14.49	a B	12.69	ab B	3.41	de B	0.4	d B	16.4	bc A	58.7	e A	0.06	e B	0.07	e A
7	Dec 11		1.56	a A	14.40	a B	12.59	abc B	4.02	b B	0.8	c A	18.2	b A	66.4	de A	0.10	c A	0.10	d A
8	Jan 15		1.54	a A	14.30	a B	13.04	a A	3.46	de A	2.9	a A	14.1	c A	73.7	cd A	0.19	a A	0.12	c A

Length and diameter data represent means of 10 individual fruits. Weight and F:S ratio correspond to means of two 10-fruit replicates. For chemical properties, values represent means of three replicate analyses undertaken on lyophilized pericarp tissue. Different capital letters denote significant differences between irrigated and rain-fed samples for a given picking date, and different lower-case letters stand for significant differences among sampling dates for a given irrigation regime, at $P \leq 0.05$ (LSD test).

*Abbreviations: F:S ratio, flesh to stone ratio; RSA, radical-scavenging capacity; AA, reduced acid ascorbic; DHA, dehydroascorbic acid.

Phenolic contents generally declined over maturation, as observed in a previous work (Diarte et al., 2021), even though a later increase was observed at P7 regardless of irrigation or producing area. For olives picked from PDO ‘Les Garrigues’, time-course changes in RSA paralleled those in the content of total phenolics and of ascorbic acid (AA), consistent with the antioxidant properties of these compounds. Significantly higher RSA values were found in rain-fed than in irrigated fruits at P4-P6 (November), coincident with a noticeable drop in rainfall in comparison with the preceding months (**Supplementary Figure S1**). No clear differences in AA content were observed between irrigated and rain-fed samples, but significantly higher DHA levels were found in rain-fed than in irrigated fruits (Table 1). In contrast with the observations for ‘Arbequina’ described herein, both the content of phenolics and the antioxidant capacity increased along fruit ripening of ‘Dhokar’ and ‘Chemlali’ olives (Jemai et al., 2009). These discrepancies, however, agree with substantial cultivar-related differences in the evolution of total phenols, RSA and AA content which were found in a previous study spanning nine olive genotypes (Diarte et al., 2021).

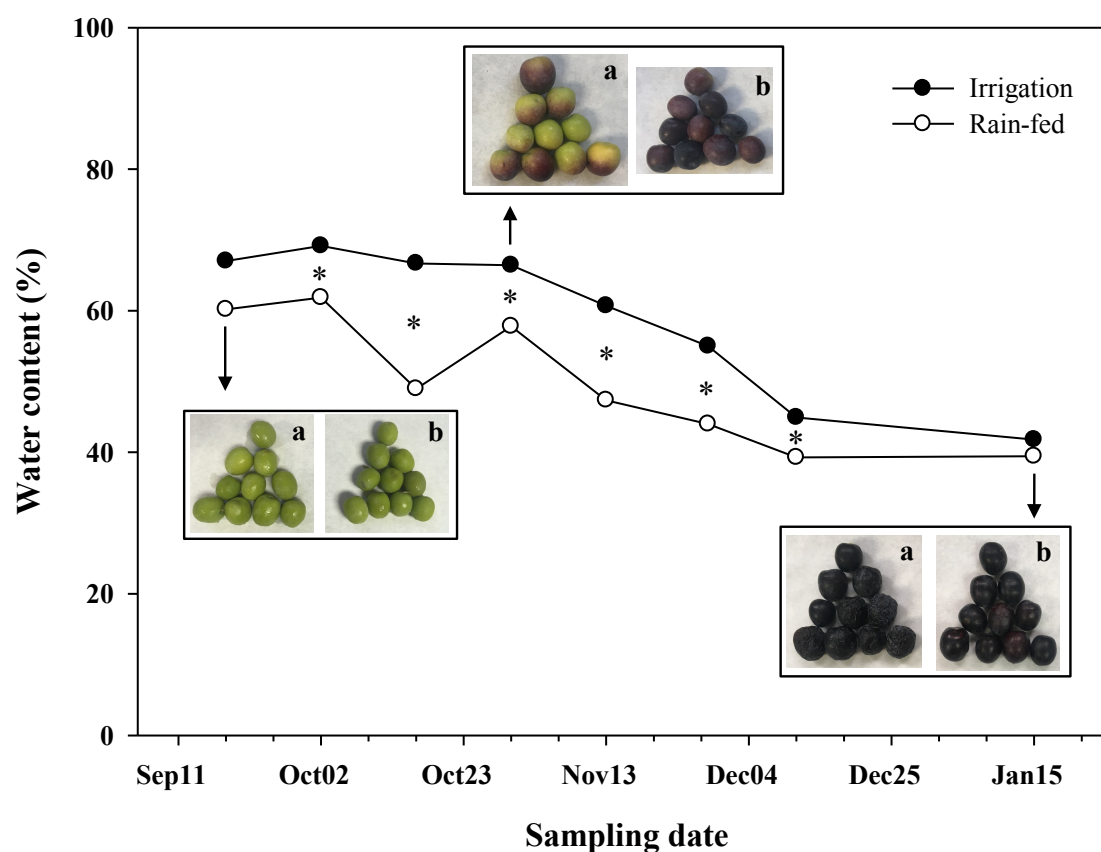


Figure 2. Water (%) and appearance of ‘Arbequina’ olives during maturation under irrigated and rain-fed conditions at PDO ‘Les Garrigues’. Letters (a) and (b) on the images identify fruits from irrigated and rain-fed trees, respectively. Water content values represent the average of 3 replicates (10 fruits/replicate). Asterisks stand for significant differences between irrigated and rain-fed trees at $P \leq 0.05$ (LSD test).

5.3.1. Cell-wall composition and ripening-related changes

In order to investigate the mechanisms underlying differences in firmness levels and in firmness loss along fruit ripening between irrigated and rain-fed olives (**Figure 1**), ripening-related changes in cell walls were examined. It has been reported that firmness loss along fruit maturation of ‘Arbequina’ olives is accompanied by the progressive solubilisation of cell wall polysaccharides (Diarte et al., 2021). In that work, though, the sampling period was shorter, as the last picking of ‘Arbequina’ olives took place in late November. In contrast, a wider sampling period was considered in the present study, fruit samples being taken and analysed up to January (**Table 1**). Time-course changes in AIR amounts over the experimental time were similar for irrigated and rain-fed samples, even though yields were generally higher in the latter. AIR yields declined along maturation until late October (**Table 2**), in parallel with the phase of steady firmness loss observed during the first sampling points (**Figure 1A**). Contrarily, AIR yields increased thereafter, due to substantial decrease in water content (**Figure 2**) leading to higher AIR percentages over fresh weight.

Limited differences in AIR fraction yields were found between irrigated and rain-fed samples. Decreased AIR amounts over the first sampling dates (P1-P4) were accompanied by higher yields of the water-soluble fraction (W_{sf}) of cell wall materials and lower recoveries of the final insoluble residue (**Table 2**), indicative of gradual solubilisation of cell wall polysaccharides which contributed to substantial loss of fruit firmness (**Figure 1**). For later sampling dates (P5 to P8), W_{sf} yields were even higher, particularly for irrigated fruit, which showed significantly higher values as compared to rain-fed olives. Contrarily, a decreasing trend was observed for the rest of AIR fractions isolated, particularly for the Na_2CO_3 - and the KOH-soluble fractions, consistent with the idea of sustained solubilisation of cell wall materials along fruit ripening.

The different cell wall fractions isolated were then analysed for the content of uronic acids and neutral sugars. A steady decline in neutral sugar contents in the alcohol-insoluble materials was observed during ripening of rain-fed olives (**Table 3**), while in contrast limited changes were found for irrigated samples, with the exception of a transient peak at the P4 sampling (end of October). Results suggest that rapid fruit softening over the first sampling dates was linked to loss of neutral sugars (**Table 3**): increasing neutral sugar contents were observed in the W_{sf} in parallel to lowered levels in both the Na_2CO_3 - and the KOH-soluble fractions isolated from AIR. Furthermore rain-fed samples, which incidentally showed higher firmness levels (**Figure 1**), retained higher neutral sugar contents in AIR during that period.

In contrast, data on uronic acid content suggest that uronic acid loss took place mainly at later maturity stages. Progressively reduced contents of uronic acids were found in AIR along fruit ripening (**Table 3**), in agreement with previous reports for ‘Arbequina’ as well as other olive cultivars (Vierhuis et al., 2000; Lara et al., 2018; Diarte et al., 2021). Whereas uronic acid loss was steady but moderate for rain-fed samples, a sharp decrease was observable for irrigated fruits from P5 sampling. At later picking dates (P5 to P8), rain-fed fruits retained significantly higher uronic acid levels in the $NaOx$ -soluble fraction, enriched in pectins linked non-covalently to the cell walls, which might relate to the observation of higher firmness levels in comparison to irrigated olives (**Figure 1**).

Table 2. Yield of alcohol-insoluble residue (AIR) (g 100 g⁻¹ FW), AIR fractions (g 100 g⁻¹ AIR) and final residue (g 100 g⁻¹ FW) recovered during fruit ripening of irrigated and rain-fed ‘Arbequina’ olives produced at El Soleràs (PDO ‘Les Garrigues’).

Sampling date	Irrigation regime	AIR	d.e.	AIR fractions								Final insoluble residue		
				W _{sf} *		NaOx _{sf} *		Na ₂ CO _{3sf} *		KOH _{sf} *				
Sep 18	Irrigated	9.79	75.26	b A	1.52	ef A	7.89	c B	1.33	d B	1.53	bc B	8.59	d B
Oct 2		5.78	61.41	c A	0.86	f B	7.91	c A	3.52	b A	1.20	bc A	5.00	f B
Oct 16		6.05	56.09	cd A	5.31	ab A	8.76	a A	3.98	a A	3.58	a A	4.74	g B
Oct 30		4.85	50.57	d A	3.85	c A	8.64	ab A	2.59	c A	2.99	a A	3.98	h B
Nov 13		9.25	88.43	a A	2.06	de B	8.64	ab A	1.13	d B	1.66	b A	8.01	e A
Nov 28		13.19	84.73	ab A	2.46	d A	8.31	bc A	1.00	d B	0.93	c A	11.52	c A
Dec 11		13.87	49.54	de A	5.45	a A	8.11	c A	1.26	d A	0.93	c A	11.68	b B
Jan 15		14.50	39.88	e A	4.59	bc A	8.11	c A	1.40	d A	1.40	bc A	12.25	a B
Sep 18	Rain-fed	12.00	58.85	bc A	1.59	d A	8.37	ab A	1.99	c A	2.92	a A	10.22	b A
Oct 2		8.82	57.88	bc A	1.33	d A	7.85	bc A	3.32	a A	1.33	bc A	7.60	e A
Oct 16		8.21	69.49	b A	3.86	a A	8.18	abc A	2.79	b B	3.26	a A	6.72	g A
Oct 30		8.57	42.67	d A	2.79	b B	8.63	a A	1.79	c B	1.53	b B	7.31	f A
Nov 13		9.42	92.43	a A	3.79	a A	8.26	abc A	1.73	c A	0.93	cd B	8.04	d A
Nov 28		11.81	90.08	a A	3.13	b A	8.59	a A	2.00	c A	1.07	bcd A	10.07	c B
Dec 11		16.15	53.42	cd A	1.33	d B	8.42	ab A	0.93	d A	0.80	cd A	14.30	a A
Jan 15		16.06	21.12	e B	2.12	c B	7.70	c B	1.20	d A	0.66	d B	14.18	a A

Alcohol-insoluble residue (AIR) was extracted from approximately 50 g olive fruit pericarp. Fraction yield values represent means of three extraction replicates. Different capital letters denote significant differences between irrigated and rain-fed samples for a given picking date, and different lower-case letters stand for significant differences among sampling dates for a given irrigation regime, at $P \leq 0.05$ (LSD test).

* Abbreviations: AIR, alcohol-insoluble residue; d.e., degree of methyl esterification of pectins; W_{sf}, water-soluble fraction; NaOx_{sf}, sodium oxalate-soluble fraction; Na₂CO_{3sf}, sodium carbonate-soluble fraction; KOH_{sf}, potassium hydroxide-soluble fraction.

Table 3. Uronic acid and neutral sugar contents ($\text{g } 100^{-1} \text{ g}$) in AIR and in AIR fractions recovered during fruit ripening of irrigated and rain-fed ‘Arbequina’ olives produced at El Soleràs (PDO ‘Les Garrigues’).

Sampling date	Irrigation regime	Uronic acids ($\text{g } 100^{-1} \text{ g}$)									Neutral sugars ($\text{g } 100^{-1} \text{ g}$)								
		AIR		W_{sf}		NaOx_{sf}		$\text{Na}_2\text{CO}_{3\text{sf}}$		KOH_{sf}		AIR		W_{sf}		Na_2CO_3		KOH_{sf}	
Sep 18	Irrigated	6.40	c A	11.45	b A	4.15	c A	20.77	c A	3.80	c A	3.53	b B	19.87	b A	3.82	de B	27.67	c B
Oct 2		11.16	b A	18.98	a A	4.20	c A	8.56	g B	5.62	a A	3.51	b B	14.24	d B	15.69	a A	35.62	a B
Oct 16		12.38	a A	8.61	c A	6.72	a A	11.88	f A	3.04	d A	3.32	b B	17.61	c A	9.52	b B	36.70	a A
Oct 30		10.61	b A	7.01	e B	6.22	b A	8.69	g B	4.06	c B	8.91	a A	18.62	bc B	15.20	a A	32.70	b B
Nov 13		4.60	d A	7.75	d A	3.44	d B	19.48	d A	4.93	b A	4.25	ab A	20.18	b A	4.58	d A	24.81	e B
Nov 28		4.61	d A	7.78	d A	2.52	e A	27.94	a A	4.00	c A	2.19	b A	13.65	d B	nd		20.26	f B
Dec 11		4.14	de A	11.45	b B	1.80	f B	21.76	b A	4.07	c B	2.91	b A	10.03	e A	1.93	e A	25.54	de A
Jan 15		3.24	e A	11.48	b A	2.01	f B	16.74	e A	4.70	b A	3.54	b A	54.12	a A	6.62	c B	26.87	cd A
Sep 18	Rain-fed	6.73	b A	11.13	b A	2.91	c B	12.43	cd B	2.52	g B	6.50	b A	16.79	c B	12.78	ab A	35.14	b A
Oct 2		7.62	a B	8.04	c B	4.05	b A	10.72	e A	3.08	e B	10.76	a A	18.88	bc A	4.86	de B	40.64	a A
Oct 16		7.58	a B	7.98	c B	4.58	a B	11.67	de A	2.80	f B	10.63	a A	17.58	bc A	10.77	b A	29.88	c B
Oct 30		6.63	b B	7.50	cd A	4.20	b B	13.38	c A	6.21	b A	4.18	c A	20.97	a A	8.02	c B	34.65	b A
Nov 13		5.43	c A	7.58	cd A	4.06	b A	16.37	b B	5.29	c A	5.97	bc A	17.21	bc B	7.04	cd A	41.96	a A
Nov 28		5.01	c A	7.26	d A	2.34	d A	11.22	e B	3.31	d B	2.19	d A	18.10	bc A	14.16	a A	25.66	d A
Dec 11		3.47	d B	18.95	a A	2.87	c A	22.30	a A	8.65	a A	1.14	d B	11.70	e A	3.63	e A	25.25	d A
Jan 15		2.98	d A	11.46	b A	2.34	d A	16.97	b A	3.27	de B	1.05	d B	14.05	d B	11.58	ab A	19.82	e B

Values represent means of three replicates. Different capital letters denote significant differences between irrigated and rain-fed samples for a given picking date, and different lower-case letters stand for significant differences among sampling dates for a given irrigation regime, at $P \leq 0.05$ (LSD test).

* Abbreviations: AIR, alcohol-insoluble residue; W_{sf} , water-soluble fraction, NaOx_{sf} , oxalate-soluble fraction; $\text{Na}_2\text{CO}_{3\text{sf}}$, sodium carbonate-soluble fraction; KOH_{sf} , potassium hydroxide-soluble fraction; nd, non-detectable.

5.3.2. Cell wall-modifying enzyme activities

Data gathered herein suggest that loss of neutral sugars be an early event during ripening-related cell wall disassembly of ‘Arbequina’ olive fruits, which agrees with the observation that AFase activity was detectable at very early picking dates (**Table 4**). AFase cleaves arabinosyl residues from pectin side-chains, arabinose being the main neutral sugar component of olive fruit cell walls in quantitative terms (Mafra et al., 2001). AFase activity increased steadily along fruit maturation, and was generally higher in rain-fed than in irrigated samples, with the exception of the P6 sampling when no significant differences between both irrigation regimes were detected. Even though galactose is reportedly less abundant than arabinose in cell walls of olive fruit, β -Gal-catalysed cleavage of galactosyl residues may also contribute to ripening-related loss of neutral sugars and their mobilisation to the water-soluble fraction. β -Gal activity levels around 0.120 U mg^{-1} protein were detected already at P1 fruits irrespective of irrigation regime, which then declined to rise again from mid October (**Table 4**). Interestingly, β -Gal activity levels were significantly higher in irrigated than in rain-fed fruits at more advanced maturity stages, which coincided with higher sugar loss as shown by superior yields (**Table 2**) and neutral sugar content (**Table 3**) of the water-soluble fraction isolated from those samples.

Enzyme activities acting on pectin side-chains are considered to favour the action of pectin backbone-acting enzymes by increasing cell wall porosity and hence facilitating access to their substrates. Yet for PG- and PL-catalysed cleavage of galacturonic acid residues from cell wall pectins, previous demethylation of these residues is required, which is catalysed by pectin methyl esterases. The high PME activity levels (over 1000 U mg^{-1} protein) at the initial (P1-P2) picking dates (**Table 4**) agree with the idea of an early role in cell wall modifications leading to ripening-related firmness changes. This caused a decline in the degree of methyl esterification (d. e.) of pectins (**Table 2**), which may underlie the steady yields (**Table 2**) and the retention of uronic acids in the NaOx_{sf} over the first sampling dates (P1 to P4) (**Table 3**): in the presence of calcium, PME action allows the establishment of calcium bridges between demethylated, negatively charged galacturonic acid residues thus helping their retention in pectic polymers (Goulao and Oliveira, 2008), in contrast to the fate of neutral sugars. Even though no calcium content analyses were undertaken in this work, a recent study (Diarte et al., 2021) reported around 1200 mg kg^{-1} DW in the pericarp of green ‘Arbequina’ fruit, which declined substantially in later maturity stages.

PME activity decreased noticeably at picking dates later than P2, with the exception of a transient increase during early December (P6-P7) which was preceded by a substantial upsurge in the degree of pectin esterification at P5-P6 (**Table 2**). Pectins are secreted into the cell wall in highly methyl-esterified forms (Micheli, 2001), and are subsequently de-esterified. Therefore, the d. e. peak observed at P5-P6 samples suggests that new cell wall materials were being deposited at this stage, which agrees with data on fruit weight and size showing that fruit were still growing (**Table 1**). PME activity during the P6-P7 upsurge was significantly higher for rain-fed olives, while during the rest of the experimental period it was generally the opposite. These transient increases in PME activity and d. e. of pectins were also observed for olives produced at PDO ‘Siurana’, albeit in that area they occurred around two weeks later (**Supplementary Tables 3 and 5**).

Table 4. Changes in cell wall-related enzyme activities (U mg⁻¹ protein) during fruit ripening of irrigated and rain-fed ‘Arbequina’ olives produced at El Soleràs (PDO ‘Les Garrigues’).

Sampling date	Irrigation regime	Non-pectolytic				Pectolytic									
		β-Xyl		EGase		Backbone-acting PG		Side chain-acting PL							
Sep 18	Irrigated	0.041	a A	0.787	a A	1246.23	a A	5.802	a A	3.949	b A	0.013	e B	0.129	c A
Oct 2		0.015	d A	0.276	d A	1100.28	b A	0.544	d B	2.329	d A	0.023	d B	0.051	d A
Oct 16		0.016	d B	0.328	c A	327.54	c A	0.892	c A	2.139	d A	0.020	d B	0.005	e B
Oct 30		0.011	e B	0.432	b A	299.33	c A	1.922	b A	1.022	e B	0.033	c B	0.164	bc A
Nov 13		0.030	b B	0.401	b A	151.31	d A	0.779	c A	4.661	a A	0.057	b B	0.235	b A
Nov 28		0.017	d B	0.422	b B	310.32	c B	0.842	c B	3.081	c B	0.071	a A	0.331	a A
Dec 11		0.014	de B	0.192	e B	186.01	d B	0.303	e B	4.132	b A	0.073	a B	0.105	cd B
Jan 15		0.026	c B	0.394	b A	205.76	d A	0.770	c B	2.223	d A	0.077	a B	0.091	cd A
Sep 18	Rain-fed	0.031	c B	0.448	bc B	249.57	d B	2.265	ab B	2.909	c B	0.032	d A	0.121	c A
Oct 2		0.012	e B	0.447	c A	1093.25	a A	1.106	d A	2.476	d A	0.035	d A	0.027	e A
Oct 16		0.033	bc A	0.407	cd A	259.03	d B	0.716	d B	0.930	e B	0.061	c A	0.043	e A
Oct 30		0.020	d A	0.255	e B	130.16	e B	0.764	d B	2.528	d A	0.057	c A	0.114	c A
Nov 13		0.038	a A	0.341	de B	122.92	e B	0.804	d A	3.933	b A	0.065	c A	0.159	a B
Nov 28		0.029	c A	0.545	ab A	485.76	b A	1.382	cd A	4.998	a A	0.074	b A	0.132	bc B
Dec 11		0.038	a A	0.624	a A	344.62	c A	2.010	bc A	3.652	b B	0.096	a A	0.151	ab A
Jan 15		0.036	ab A	0.352	cde B	99.48	e B	3.028	a A	2.249	d A	0.095	a A	0.084	d A

Values represent means of three replicates. Different capital letters denote significant differences between irrigated and rain-fed samples for a given picking date, and different lower-case letters stand for significant differences among sampling dates for a given irrigation regime, at $P \leq 0.05$ (LSD test).

* Abbreviations: β-Xyl, β-xylosidase (EC 3.2.1.37); EGase, endo-1,4-β-D-glucanase (EC 3.2.1.4); PME, pectin methylesterase (EC 3.1.1.11); PG, polygalacturonase (EC 3.2.1.67 -exo- and EC 3.1.2.15 -endo-), PL, pectate lyase (EC 4.2.2.2); AFase, α-L-arabinofuranosidase (EC 3.2.1.55); β-Gal, β-galactosidase (EC 3.2.1.23).

High PG and PL activity levels were observed at early (P1) picking dates, which declined thereafter to rise again over the last stages of fruit maturation (**Table 4**). No clear irrigation-related differences were observed for PL activity, while PG activity in rain-fed olives augmented markedly after mid-November (P5), leading to significantly higher activity as compared with irrigated fruit over later picking points. High activity levels at P1 were possibly of little significance for the onset of ripening-related cell wall modifications, as the high degree of pectin esterification at that sampling point (**Table 2**) would prevent PG- and PL-catalysed hydrolysis and β -elimination, respectively, of galacturonic acid residues. In contrast, increased PG and PL activity levels at later picking points were associated to the onset of uronic acid loss (**Table 3**), which hints an actual role on subsequent cell wall disassembly events.

The activities of β -Xyl and EGase, as representatives of non-pectolytic enzymes, were also assessed (**Table 4**). These enzymes act on hemicelluloses, which comprise a variety of polysaccharides such as xyloglucans, xylans, arabinoxylans and glucomannans, and are recovered mainly in the KOH-soluble fraction. As for other enzyme activities considered herein, high activity levels were found at early picking dates (P1) which declined subsequently and rose again at later stages of maturity. The observed trends were generally in accordance with recent reports (Lara et al., 2018; Diarte et al., 2021). However, a longer time-span was considered herein, and thus a more comprehensive dataset was obtained. Results moreover showed irrigation-related differences in β -Xyl activity during the experimental time: activity levels were significantly higher in rain-fed than in irrigated samples from P3 sampling onwards. As to EGase, differences in activity levels between irrigated and rain-fed fruit appeared to arise from asynchronous time-course of activity changes rather than to actual significant differences in activity levels. Indeed, irrigated olives showed some delay in ripening as indicated for example by later colour change (**Figure 2**). A recent work (Diarte et al., 2021) on nine olive genotypes suggested an early role for these enzymes in the onset of ripening-related cell wall disassembly, based on the finding that activity levels were lower at the black than at the green stage. The longer experimental period considered herein, however, allowed the observation of increased activity at very late sampling dates, which may relate to declining KOH_{sf} yields (**Table 2**).

On account of the high dimensionality of the dataset, principal component analysis (PCA) was used to help extract useful information. Irrigated and rain-fed samples produced at PDO ‘Les Garrigues’ at advanced maturity stages (P5 to P8), were included in the model. The two first principal components (PC1 and PC2) explained together up to 63 % of total variance among samples. The scores plot (**Figure 3A**) revealed that picking dates separated mainly along PC1, while irrigation regimes separated along PC2 (37% and 26% of total explained variance, respectively). The corresponding correlation loadings plot (**Figure 3B**) confirmed some relationships among variables. Fruit firmness was associated to yield and neutral sugar content of the $\text{Na}_2\text{CO}_{3\text{sf}}$, supporting the view that loss of neutral sugars was a relevant factor for ripening-related firmness loss. In turn, AFase activity levels correlated inversely with $\text{Na}_2\text{CO}_{3\text{sf}}$ yields, showing the relevance of this enzyme activity for neutral sugar loss and firmness changes along fruit maturation. Similarly, PG and β -Xyl activity correlated inversely with NaOx_{sf} and KOH_{sf} yields, respectively, which hints an actual role in ripening-related modifications in polyuronides and hemicelluloses.

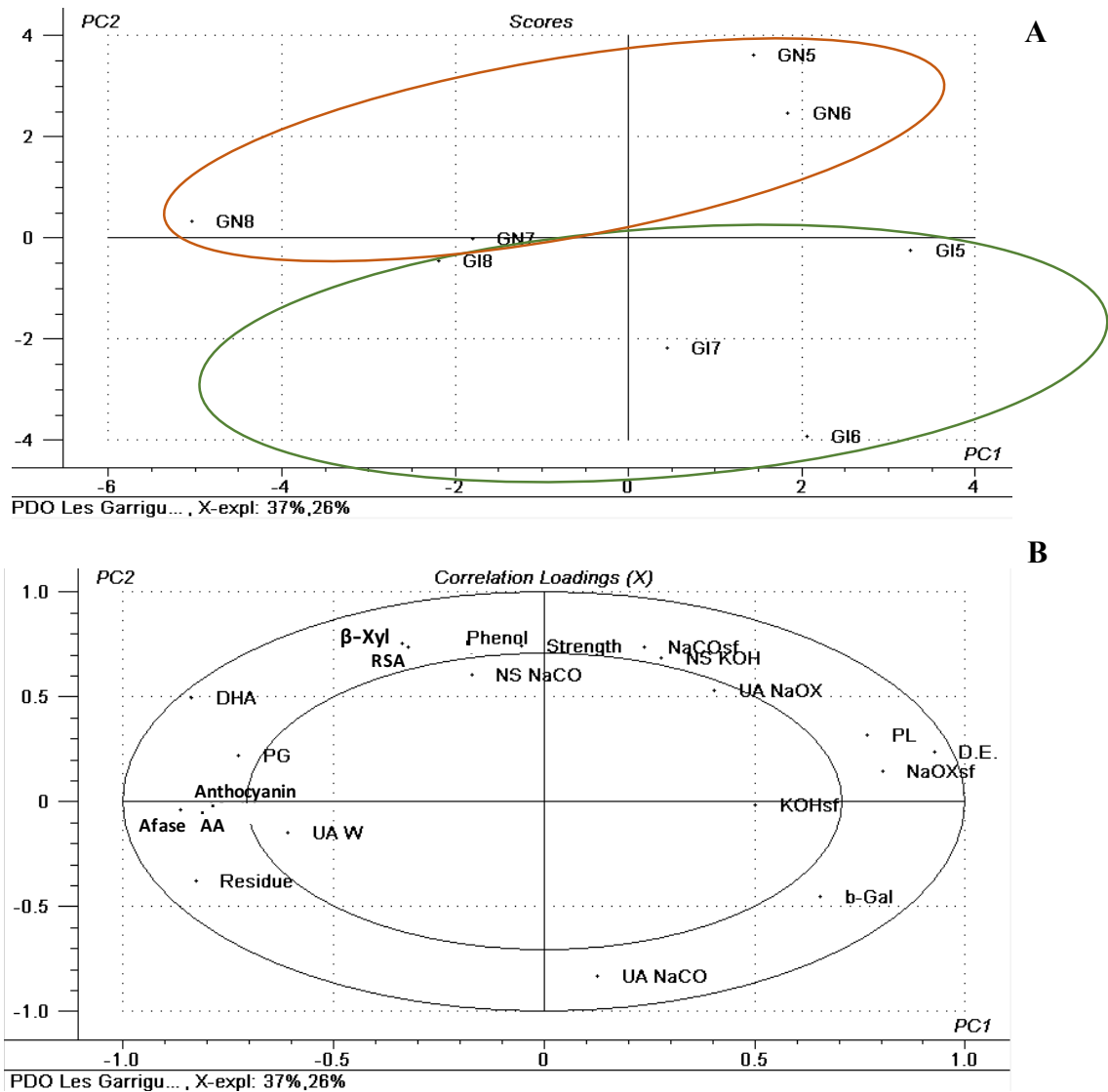


Figure 3. Scores (A) and correlation loading (B) plot of PC1 vs. PC2 corresponding to a PCA model of ‘Arbequina’ olives during the last stages of fruit maturation (P5 to P8) under irrigated (GI) and rain-fed (GN) conditions at PDOs ‘Les Garrigues’. *Abbreviations: NaOx_{sf}, NaCO_{sf} and KOH_{sf}, yields of sodium oxalate-, sodium carbonate- and potassium hydroxide-soluble fractions, respectively; UA W, UA NaOx and UA NaCO, uronic acid contents in W_{sf}, NaOx_{sf} and NaCO_{sf}, respectively; NS (NaCO) and NS (KOH), neutral sugar contents in NaCO_{sf} and KOH_{sf}, respectively; D.E., degree of methyl esterification of pectins; b-Xyl, β -xylosidase; PG, polygalacturonase; PL, pectate lyase; Afase, α -L-arabinofuranosidase; b-Gal, β -galactosidase; AA, reduced ascorbic acid; DHA, dehydroascorbic acid; RSA, radical scavenging activity.

5.4. Conclusions

This study showed significant differences in fruit firmness between irrigated and rain-fed olive fruits produced in PDO ‘Les Garrigues’, while limited differences were observed for olives obtained from PDO ‘Siurana’. Climate- and soil-related factors may underlie this observation, as harsher environmental conditions at PDO ‘Les Garrigues’ may render the effects of irrigation more evident, even though the total water supply was higher at PDO ‘Siurana’. Water availability and water content in the fruit had

an influence on fruit firmness and the yield of insoluble cell wall materials. Neutral sugar loss was an early event in ripening-related cell wall modifications and was a likely contributor to the rapid firmness loss phase at early maturity stages. High PME activity levels in unripe fruit, in contrast, possibly contributed to uronic acid retention at the chelator-soluble fraction during the first stages of fruit maturation.

5.5. References

- Agius F, González-Lamothe R, Caballero JL, Muñoz-Blanco J, Botella M, Valpuesta V. 2003. Engineering increased vitamin C levels in plants by overexpression of a D-galacturonic acid reductase. *Nat. Biotechnol.* 21, 177-181.
- Belge B, Comabella E, Graell J, Lara I. 2015. Post-storage cell wall metabolism in two sweet cherry (*Prunus avium* L.) cultivars displaying different postharvest performance. *Food Sci. Technol. Int.* 21, 416-427.
- Blumenkrantz N, Asboe-Hansen G. 1973. New method for quantitative determination of uronic acids. *Anal. Biochem.* 54, 484-489.
- Bradford MM. 1976. A rapid and sensitive method for the quantitation of microgram quantities of protein utilizing the principle of protein-dye binding. *Anal. Biochem.* 72, 248-254.
- Cheng G, Duan X, Shi J, Lu W, Luo Y, Jiang W, Jiang Y. 2008. Effects of reactive oxygen species on cellular wall disassembly of banana fruit during ripening. *Food Chem.* 109, 319-324.
- Connor DJ, Gómez-del-Campo M, Rousseaux MC, Searles PS. 2014. Structure, management and productivity of hedgerow olive orchards: a review. *Sci. Hortic.* 169, 71-93.
- Dabbou S, Chehab H, Faten B, Dabbou S, Esposto S, Selvaggini R, Taticch, A, Servili M, Montedoro GF, Hammami M. 2010. Effect of three irrigation regimes on Arbequina olive oil produced under Tunisian growing conditions. *Agric. Water Manag.* 97, 763-768.
- Diarte C, Iglesias A, Romero A, Casero T, Ninot A, Gatus F, Graell J, Lara I. 2021. Ripening-related cell wall modifications in olive (*Olea europaea* L.) fruit: A survey of nine genotypes. *Food Chem.* 338, 127754.
- Duan X, Zhang H, Zhang D, Sheng J, Lin H, Jiang Y. 2011. Role of hydroxyl radical in modification of cell wall polysaccharides and aril breakdown during senescence of harvested longan fruit. *Food Chem.* 128, 203-207.
- Dubois M, Gilles KA, Hamilton JK, Rebers PA, Smith F. 1956. Colorimetric method for determination of sugars and related substances. *Anal. Chem.* 28, 350-356.
- Dumville JC, Fry SC. 2003. Solubilisation of tomato fruit pectins by ascorbate: a possible non-enzymic mechanism of fruit softening. *Planta.* 217, 951-961.
- Fernández-Bolaños J, Heredia J, Vioque B, Castellano JM, Guillén R. 1997. Changes in cell-wall-degrading enzyme activities in stored olives in relation to respiration and ethylene production - Influence of exogenous ethylene. *Eur. Food Res. Technol.* 204, 293-299.

Fernández-Hernández A, Mateos R, Garcia-Mesa JA, Beltran G, Fernández-Escobar R. 2010. Determination of mineral elements in fresh olive fruits by flame atomic spectrometry. *Span. J. Agric. Res.* 8, 1183-1190.

García JM, Cuevas MV, Fernández JE. 2013. Production and oil quality in 'Arbequina' olive (*Olea europaea* L.) trees under two deficit irrigation strategies. *Irrig. Sci.* 31, 359-370.

Gillespie KM, Ainsworth EA., 2007. Measurement of reduced, oxidized and total ascorbate content in plants. *Nat. Protoc.* 2, 871-874.

González-Cabrera M, Domingues-Vidal A, Ayora-Cañada MJ. 2018. Hyperspectral FTIR imaging of olive fruit for understanding ripening processes. *Postharvest Biol. Technol.* 145, 74-82.

Goulao LF, Oliveira CM. 2008. Cell wall modifications during fruit ripening: when a fruit is not the fruit. *Trends in Food Sci. Technol.* 19, 4-25.

Jemai H, Bouaziz M, Sayadi S. 2009. Phenolic composition, sugar content and antioxidant activity of Tunisian sweet olive cultivar with regard to fruit ripening. *J. Agric. Food Chem.* 57, 2961-2968.

Jiménez A, Rodríguez R, Fernández-Caro I, Guillén R, Fernández-Bolaños J, Heredia A. 2001. Olive fruit cell wall: degradation of pectic polysaccharides during ripening. *J. Agric. Food Chem.* 49, 409-415.

Klavons JA, Bennet RD. 1986. Determination of methanol using alcohol oxidase and its application to methyl ester content of pectins. *J. Agric. Food Chem.* 34, 597-599.

Lara I, Albrecht R, Comabella E, Riederer M, Graell J. 2018. Cell-wall metabolism of 'Arbequina' olive fruit picked at different maturity stages. *Acta Hortic.* 1199, 133-138.

Lara I, Camats JA, Comabella E, Ortiz A. 2015. Eating quality and health-promoting properties of two sweet cherry (*Prunus avium* L.) cultivars stored in passive modified atmosphere. *Food Sci. Technol. Int.* 21, 133-144.

Lefever G, Vieuille M, Delage N, d'Harlingue A, de Monteclerc J, Bompeix G. 2004. Characterization of cell wall enzyme activities, pectin composition, and technological criteria of strawberry cultivars (*Fragaria x ananassa* Duch). *Food Chem. Toxicol.* 69, 221-226.

Mafra I, Lanza B, Reis A, Marsilio V, Campestre C, De Angelis M, Coimbra MA. 2001. Effect of ripening on texture, microstructure and cell wall polysaccharide composition of olive fruit (*Olea europaea*). *Physiol. Plant.* 111, 439-447.

Marsilio V, Lanza B, Campestre C, De Angelis M. 2000. Oven-dried table olives: textural properties as related to pectic composition. *J. Sci. Food Agric.* 80, 1271-1276.

Mechri B, Tekaya M, Hammami M, Chehab H. 2020. Effects of drought stress on phenolic accumulation in greenhouse-grown olive trees (*Olea europaea*). *Biochem. Syst. Ecol.* 92, 104112.

Micheli F. 2001. Pectin methylesterases: cell wall enzymes with important roles in plant physiology. *Trends Plant Sci.* 6, 414-419.

Motilva MJ, Tovar MJ, Romero MP, Alegre A, Girona J. 2000. Influence of regulated deficit irrigation strategies applied to olive trees (Arbequina cultivar) on oil yield and oil composition during the tree fruit ripening. *J. Sci. Food Agric.* 80, 2037-2043.

Ortiz A, Graell J, Lara I. 2011. Preharvest calcium applications inhibit some cell wall-modifying enzyme activities and delay cell wall disassembly at commercial harvest of 'Fuji Kiku-8' apples. *Post-harvest Biol. Technol.* 62, 161-167.

Parra R, Paredes MA, Sánchez-Calle IM, Gómez-Jiménez MC. 2013. Comparative transcriptional profiling analysis of olive ripe-fruit pericarp and abscission zone tissues shows expression differences and distinct patterns of transcriptional regulation. *BMC Genomics.* 14, 866-886.

Petridis A, Therios I, Samouris G, Koundouras S, Giannakoula A. 2012. Effect of water deficit on leaf phenolic composition, gas exchange, oxidative damage and antioxidant activity of four Greek olives (*Olea europaea* L.) cultivars. *Plant Physiol. Biochem.* 60, 1-11.

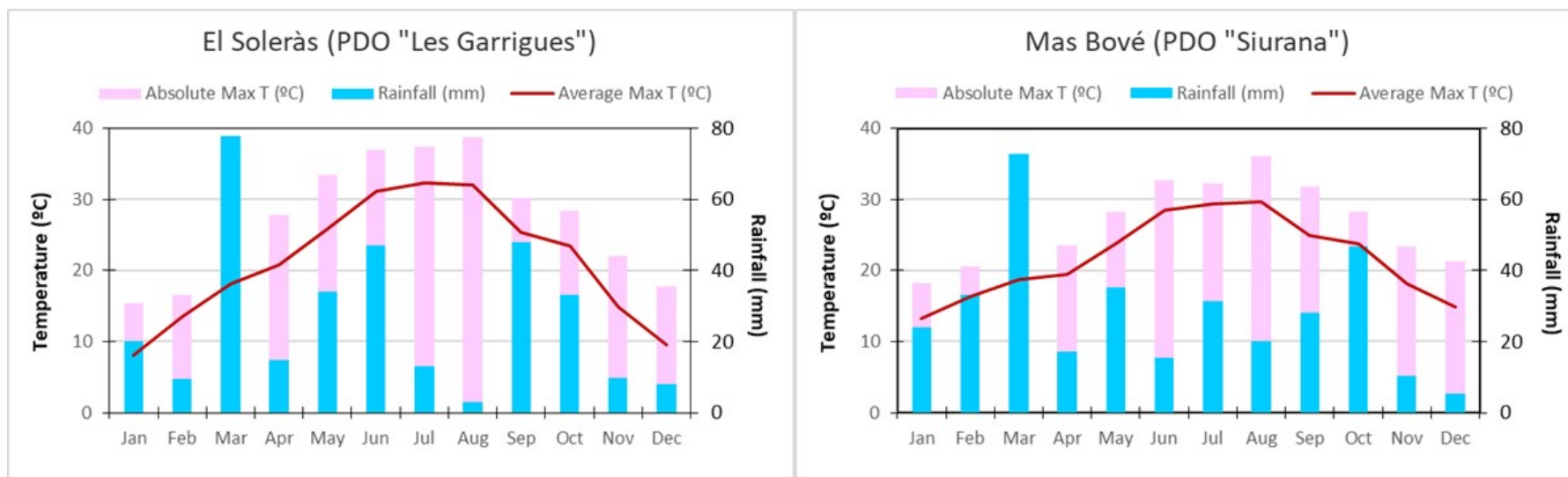
Uceda M, Frías L. 1975. Harvest dates. Evolution of the fruit of content, oil composition and oil quality. In *Proceedings of II Seminario Oleícola Internacional.* p125-130.

Vierhuis E, Schols HA, Beldman G, Voragen AGJ. 2000. Isolation and characterisation of cell wall material from olive fruits (*Olea europaea* cv koroneiki) at different ripening stages. *Carbohydr. Polym.* 43, 11-21.

Voragen FGJ, Timmers JPJ, Linszen JPH, Schols HA, Pilnik W. 1983. Methods of analysis for cell-wall polysaccharides of fruit and vegetables. *Z. Lebensm. Unters. Forch.* 177, 251-256.

Waterman E, Lockwood B. 2007. Active components and clinical applications of olive oil. *Altern. Med. Rev.* 12, 331-342.

Supplementary material



Supplementary Figure S1. Rainfall and maximal temperatures at both olive-producing sites in 2017.

Supplementary Table 1. Physical characteristics during fruit ripening of irrigated and rain-fed ‘Arbequina’ olives produced at Mas Bové (PDO ‘Siurana’).

Sampling date	Irrigation regime	Maturity index	Weight (g)	Water content (%)	F:S ratio	L*	a*	b*	Deformation (mm)	Length (mm)	Diameter (mm)						
Sept 15	Irrigated	0.12	1.14	50.73	2.20	53.96	a A	-13.18	f A	34.24	a A	0.99	d A	13.27	c B	11.56	d B
Oct 4		0.40	1.47	50.79	2.41	53.39	a A	-7.36	e A	32.91	a A	1.30	bc A	13.93	bc B	12.29	c A
Oct 17		3.10	1.35	45.41	2.27	31.52	bcd B	6.43	bc A	9.82	b B	1.34	bc A	13.94	bc B	12.32	c B
Oct 31		2.52	1.45	59.13	2.87	32.15	bcd A	12.67	a A	5.16	bcd A	1.15	cd A	14.55	ab A	13.22	a A
Nov 14		2.42	1.50	54.08	3.24	37.51	b A	8.44	b A	11.71	b A	1.37	b A	14.35	ab A	13.11	ab A
Nov 29		2.86	1.41	48.67	2.58	35.12	bc A	4.82	bcd A	7.33	bc A	1.36	b A	14.34	ab A	12.69	abc A
Dec 12		4.22	1.68	45.85	3.86	25.30	d A	2.71	cd A	0.49	cd A	1.64	a A	14.10	b A	12.50	bc A
Jan 16		4.84	1.79	39.17	3.00	28.61	cd A	1.28	d A	-1.11	d A	1.75	a A	15.01	a A	13.27	a A
Sept 15	Rain-fed	0.16	1.29	55.28	2.73	53.10	a A	-13.65	f A	33.93	a A	0.90	d B	14.59	a A	12.65	bc A
Oct 4		0.22	1.46	54.90	3.03	54.23	a A	-8.05	e A	31.26	a A	0.94	d B	14.94	a A	12.83	abc A
Oct 17		1.48	1.62	53.73	2.77	51.01	a A	-3.42	de B	29.09	a A	1.32	c A	15.20	a A	13.47	a A
Oct 31		3.36	1.54	56.46	4.18	28.39	d A	11.03	a A	4.46	cd A	1.42	bc A	15.00	a A	13.20	ab A
Nov 14		2.10	0.92	48.27	3.64	43.32	b A	5.76	bc A	17.77	b A	1.44	bc A	12.49	b B	10.92	e B
Nov 29		3.00	1.22	47.92	3.16	34.56	c A	8.02	ab A	7.80	c A	1.49	bc A	13.21	b B	11.54	de B
Dec 12		4.74	1.69	43.05	3.63	25.43	d A	1.18	cd A	-0.61	d A	1.80	a A	14.60	a A	12.22	cd A
Jan 16		5.34	1.60	39.75	4.31	27.92	d A	0.64	d A	-1.42	d A	1.58	ab A	15.52	a A	13.31	ab A

Maturity indices represent the weighted average of 50 olives per picking date and irrigation regime (Uceda and Frías, 1975)¹. Weight, F:S ratios and water contents were determined jointly on 50-olive samples, and values divided by 50 to estimate the average value per fruit. Colour parameters (L*, a*, b*)², deformation values, length and diameter correspond to means of 10 individual olives. Different capital letters denote significant differences among both irrigation regime for a given sampling date, and different lower-case letters stand for significant differences among sampling date for a given irrigation regime, at $P \leq 0.05$ (LSD test).

¹ Uceda, M., and Frías, L. (1975). Harvest dates. Evolution of the fruit oil content, oil composition and oil quality, in Proceedings of II Seminario Oleícola Internacional. Córdoba, Spain International Olive Oil Council (IOOC), 125–130.

² Fruit skin colour was assessed on 10 olives with a desktop colorimeter (Chroma Meter CR-300, Minolta Corp., Osaka, Japan) using CIE illuminant D65 with 8-mm aperture diameter and 10° observation angle, and expressed as CIELAB colour space coordinates (L*, a*, b*).

* Abbreviations: F:S ratio, flesh to stone ratio; L*, a*, b*: coordinates of CIELAB colour space.

Supplementary Table 2. Some chemical characteristics during fruit ripening of irrigated and rain-fed ‘Arbequina’ olives produced at Mas Bové (PDO ‘Siurana’).

Sampling date	Irrigation regime	Oil content (g 100 g ⁻¹ DW)	Anthocyanin (mg g ⁻¹ DW)	Phenols (mg g ⁻¹ DW)	RSA (%)	AA* (nmol g ⁻¹ DW)	DHA* (nmol g ⁻¹ DW)
Sep 15	Irrigated	33.77	0.4 e A	21.0 a A	93.3 a A	0.16 a A	0.12 a B
Oct 4		42.64	0.3 e B	20.0 ab A	86.9 a A	0.12 b A	0.14 a A
Oct 17		45.64	0.4 de A	19.1 ab A	97.9 a A	0.09 c A	0.06 de A
Oct 31		42.97	0.3 e B	14.8 c A	87.7 a A	0.08 c A	0.05 de A
Nov 14		44.74	0.6 d B	14.3 c A	88.8 a A	0.10 c A	0.08 bc A
Nov 29		49.13	0.8 c B	14.7 c A	55.1 b A	0.11 b A	0.07 cd A
Dec 12		51.34	3.6 a B	18.7 b B	39.7 bc B	0.17 a B	0.05 e A
Jan 16		51.44	2.2 b B	10.5 d B	36.1 c A	0.17 a B	0.09 b A
Sep 15	Rain-fed	34.91	0.3 e B	22.8 b A	94.0 a A	0.13 c B	0.16 a A
Oct 4		43.18	0.4 ef A	19.1 c A	99.2 a A	0.12 cd A	0.13 b A
Oct 17		47.02	0.5 ef A	14.4 de B	98.5 a A	0.08 ef A	0.06 de A
Oct 31		53.01	0.6 de A	11.0 f B	83.2 b A	0.09 def A	0.05 e A
Nov 14		52.26	0.8 d A	15.3 d A	85.2 b A	0.07 f B	0.09 c A
Nov 29		52.1	1.7 c A	12.9 ef A	62.0 c A	0.12 cde A	0.07 cd A
Dec 12		53.49	9.3 a A	26.6 a A	67.8 c A	0.40 a A	0.06 de A
Jan 16		57.76	4.0 b A	19.6 c A	48.0 d A	0.29 b A	0.08 cd A

Oil content¹ was determined jointly on 50-olive samples, and values divided by 50 to estimate the average content per fruit. For the rest of parameters, values represent means of three replicate analyses undertaken on lyophilized pericarp tissue. Different capital letters denote significant differences between irrigated and rain-fed samples for a given picking date, and different lower-case letters stand for significant differences among sampling dates for a given irrigation regime, at $P \leq 0.05$ (LSD test).

¹ Oil content was determined by nuclear magnetic resonance (NMR) spectroscopy after drying samples in the oven at 105 °C until constant weight.

* Abbreviations: RSA, radical-scavenging capacity; AA, reduced acid ascorbic; DHA, dehydroascorbic acid.

Supplementary Table 3. Yield of alcohol-insoluble residue (AIR) (g 100 g⁻¹ FW), AIR fractions (g 100 g⁻¹ AIR) and final residue (g 100 g⁻¹ FW) recovered during fruit ripening of irrigated and rain-fed ‘Arbequina’ olives produced at Mas Bové (PDO ‘Siurana’).

Sampling date	Irrigation regime	AIR	d.e.	AIR fractions								Final insoluble residue		
				W _{sf}		NaOx _{sf}		Na ₂ CO _{3sf}		KOH _{sf}				
Sep 15	Irrigated	8.54	68.85	b B	1.80	d A	8.24	ab A	2.06	bc B	3.06	a A	7.25	d A
Oct 4		9.37	60.77	b A	2.33	c A	8.17	ab A	2.79	a A	2.19	b B	7.92	d B
Oct 17		9.88	67.14	b A	2.92	b A	7.96	ab A	2.39	ab A	2.92	a A	8.28	c B
Oct 31		6.34	41.72	c A	2.79	b B	8.83	a A	2.12	bc A	2.39	b A	5.31	e A
Nov 14		6.60	59.43	b A	3.52	a A	8.83	a A	1.73	c A	3.19	a A	5.46	e B
Nov 29		14.45	93.26	a A	1.20	e A	8.37	ab A	1.00	d A	0.60	c A	12.84	b B
Dec 12		15.34	94.54	a A	1.07	e B	8.29	ab A	0.67	d B	0.67	c B	14.11	a A
Jan 16		9.36	39.30	c A	2.79	b A	8.32	ab A	2.26	b A	1.93	b A	7.93	c B
Sep 15	Rain-fed	7.06	91.10	a A	2.13	b A	7.30	b B	2.99	a A	2.59	a A	6.00	g B
Oct 4		9.69	75.19	b A	1.06	c B	7.57	b B	1.59	c B	2.66	a A	8.44	e A
Oct 17		10.35	85.16	ab A	2.39	b A	7.57	b A	1.66	c B	1.46	b B	8.99	d A
Oct 31		4.27	46.50	c A	3.99	a A	8.64	a A	2.26	b A	2.79	a A	3.52	h B
Nov 14		8.57	49.16	c B	2.06	b B	8.36	a A	1.53	cd A	2.65	a A	7.32	f A
Nov 29		15.22	97.00	a A	1.20	c A	8.24	a A	1.13	de A	0.60	c A	13.52	b A
Dec 12		12.07	92.22	a A	2.13	b A	8.19	a A	1.80	c A	1.27	b A	10.45	c B
Jan 16		15.52	15.20	d B	1.13	c B	8.33	a A	0.80	e B	0.73	c B	13.82	a A

Alcohol-insoluble residue (AIR) was extracted from approximately 50 g olive fruit pericarp. Fraction yield values represent means of three extraction replicates. Different capital letters denote significant differences between irrigated and rain-fed samples for a given picking date, and different lower-case letters stand for significant differences among sampling dates for a given irrigation regime, at $P \leq 0.05$ (LSD test).

* Abbreviations: AIR, Alcohol-insoluble residue; d.e., degree of methyl esterification of pectins; W_{sf}, water-soluble fraction; NaOx_{sf}, sodium oxalate-soluble fraction; Na₂CO_{3sf}, sodium carbonate-soluble fraction; KOH_{sf}, potassium hydroxide-soluble fraction.

Supplementary Table 4. Uronic acid and neutral sugar contents (g 100 g⁻¹) in AIR and in AIR fractions recovered during fruit ripening of irrigated and rain-fed ‘Arbequina’ olives produced at Mas Bové (PDO ‘Siurana’).

Sampling date	Irrigation regime	Uronic acid in AIR fractions (%)									Neutral sugar in AIR fractions (%)								
		AIR		W _{sf}		NaOx _{sf}		Na ₂ CO _{3sf}		KOH _{sf}		AIR		W _{sf}		Na ₂ CO ₃		KOH _{sf}	
Sep 15	Irrigated	10.10	a A	11.13	c A	4.99	b B	11.02	d A	2.40	e A	6.17	b A	21.15	c A	11.02	d B	28.16	cd B
Oct 4		7.35	c A	8.40	e B	4.58	c A	9.69	e B	3.67	bc A	7.21	a A	25.04	b A	17.84	ab A	33.90	ab B
Oct 17		6.28	d A	9.00	d A	2.82	e B	9.86	e B	3.02	d B	3.30	c B	20.98	c A	13.76	c A	25.98	d B
Oct 31		8.69	b A	6.10	h A	6.15	a B	10.70	d A	3.47	bcd A	3.53	A	23.58	b A	16.08	bc A	31.92	bc A
Nov 14		5.73	d A	6.51	g A	4.67	bc A	14.52	c A	3.28	cd A	6.45	ab A	20.63	c B	7.74	e B	25.34	de A
Nov 29		2.01	e A	26.83	a A	2.29	f A	21.77	b A	5.45	a B	3.43	c A	nd		nd		21.74	e A
Dec 12		2.38	e B	22.58	b A	2.80	e A	30.82	a A	3.83	b B	3.64	c A	13.20	d B	nd		30.60	bc A
Jan 16		5.83	d A	6.90	f B	3.25	d A	9.82	e B	5.84	a A	3.29	c A	29.41	a A	18.86	a A	37.48	a A
Sep 15	Rain-fed	9.83	a A	6.95	e B	5.77	b A	8.18	f B	2.48	d A	5.97	ab A	19.02	c B	15.14	a A	36.00	b A
Oct 4		5.83	c B	17.84	c A	2.62	e B	17.94	b A	3.29	c B	5.27	b B	14.44	d B	4.01	d B	40.65	a A
Oct 17		5.05	d B	8.33	d B	3.83	c A	15.17	c A	5.69	b A	7.30	a A	15.58	d B	5.95	c B	29.55	cd A
Oct 31		8.94	b A	5.96	f A	7.09	a A	9.82	e A	3.36	c A	7.36	a A	20.51	bc B	13.43	a B	30.77	c A
Nov 14		6.17	c A	5.54	f B	3.22	d B	14.95	cd A	3.43	c A	4.25	bc B	26.14	a A	11.00	b A	26.22	ef A
Nov 29		2.35	f A	23.88	b B	2.13	f A	17.53	b B	7.72	a A	4.34	b A	4.76	f A	nd		25.34	f A
Dec 12		3.30	e A	8.19	d B	2.95	de A	14.46	d B	8.06	a A	2.25	c A	22.20	b A	6.98	c A	27.53	de A
Jan 16		2.92	ef B	28.24	a A	2.73	e B	27.60	a A	5.57	b A	4.90	b A	10.55	e B	nd		30.50	c B

Values represent means of three replicates. Different capital letters denote significant differences between irrigated and rain-fed samples for a given picking date, and different lower-case letters stand for significant differences among sampling dates for a given irrigation regime, at $P \leq 0.05$ (LSD test).

* Abbreviations: AIR, alcohol-insoluble residue; W_{sf}, water-soluble fraction; NaOx_{sf}, oxalate-soluble fraction; Na₂CO_{3sf}, sodium carbonate-soluble fraction; KOH_{sf}, potassium hydroxide-soluble fraction; nd, non-detectable.

Supplementary Table 5. Changes in cell wall-related enzyme activities (U mg⁻¹ protein) during fruit ripening of irrigated and rain-fed ‘Arbequina’ olives produced at Mas Bové (PDO ‘Siurana’).

Sampling date	Irrigation regime	Non-pectolytic						Pectolytic							
		β-Xyl		EGase		PME		Backbone-acting PG		PL		Side chain-acting AFase		β-Gal	
Sep 15	Irrigated	0.026	b A	0.563	bc B	370.09	d A	2.809	b B	3.006	b A	0.044	bc A	0.136	cd A
Oct 4		0.018	c A	0.463	a A	1136.42	a A	1.588	c A	2.596	c A	0.042	bc A	0.039	e A
Oct 17		0.034	a A	0.523	bc A	706.22	c A	0.985	d A	4.077	a A	0.044	bc A	0.036	e A
Oct 31		0.022	bc A	0.623	ab A	254.90	e A	3.218	a A	1.153	d A	0.037	c B	0.384	a A
Nov 14		0.027	b B	0.574	b A	57.70	g B	1.515	c A	3.831	a A	0.048	b A	0.156	c A
Nov 29		0.029	ab A	0.555	bc A	146.02	g A	1.358	c A	3.305	b A	0.059	a B	0.111	d A
Dec 12		0.026	b A	0.723	a A	108.88	fg B	3.200	a A	4.110	a A	0.062	a A	0.271	b B
Jan 16		0.034	a A	0.696	a A	791.29	b A	1.563	c A	2.260	c A	0.044	bc B	0.137	cd A
Sep 15	Rain-fed	0.030	b A	0.747	a A	480.79	b B	5.700	a A	2.991	b A	0.033	de A	0.113	c A
Oct 4		0.018	c A	0.316	cd B	657.79	a B	0.655	d B	2.937	b A	0.030	e B	0.036	e A
Oct 17		0.021	c B	0.262	d B	158.72	d B	0.280	e B	2.288	c B	0.037	d A	0.015	e B
Oct 31		0.013	d B	0.363	bc B	102.83	e B	0.996	c B	0.409	f B	0.046	c A	0.116	c B
Nov 14		0.040	a A	0.385	b B	144.10	de A	1.001	c B	3.775	a A	0.048	bc A	0.150	b A
Nov 29		0.019	c B	0.426	b B	166.46	d A	0.658	d B	3.646	a A	0.076	a A	0.095	cd A
Dec 12		0.003	e B	0.074	f B	150.92	d A	0.698	d B	1.977	d B	0.054	b A	0.434	a A
Jan 16		0.014	d B	0.165	e B	215.39	c B	1.926	b A	0.818	e B	0.074	a A	0.070	d B

Values represent means of three replicates. Different capital letters denote significant differences between irrigated and rain-fed samples for a given picking date, and different lower-case letters stand for significant differences among sampling dates for a given irrigation regime, at $P \leq 0.05$ (LSD test).

* Abbreviations: β-Xyl, β-xylosidase (EC 3.2.1.37); EGase, endo-1,4-β-D-glucanase (EC 3.2.1.4); PME, pectin methylesterase (EC 3.1.1.11); PG, polygalacturonase (EC 3.2.1.67 -exo- and EC 3.1.2.15 -endo-), PL, pectate lyase (EC 4.2.2.2); AFase, α-L-arabinofuranosidase (EC 3.2.1.55); β-Gal, β-galactosidase (EC 3.2.1.23).

SECTION III. Inter-specific variation in cuticle features:

***Prunus laurocerasus* L. and *Actinidia spp.* as examples**

Chemical, structural and functional study of leaf and fruit cuticles.

A comparison with *Olea europaea* L.

Chapter VI: Compositional, structural and functional cuticle analysis of *Prunus laurocerasus* L. sheds light on cuticular barrier plasticity

Plant Physiology and Biochemistry 158 (2021) 434–445



Contents lists available at ScienceDirect

Plant Physiology and Biochemistry

journal homepage: www.elsevier.com/locate/plaphy



Research article

Compositional, structural and functional cuticle analysis of *Prunus laurocerasus* L. sheds light on cuticular barrier plasticity

Clara Diarte^a, Aline Xavier de Souza^b, Simona Staiger^{b,1}, Ann-Christin Deininger^{b,2}, Amauri Bueno^b, Markus Burghardt^b, Jordi Graell^a, Markus Riederer^b, Isabel Lara^a, Jana Leide^{b,*}

^a Universitat de Lleida, Postharvest Unit, AGROTÈCNIO, E-25198, Lleida, Spain

^b University of Würzburg, Julius-von-Sachs-Institute for Biosciences, D-97082, Würzburg, Germany



Plant Physiology and Biochemistry (January 2021), 158, 434–445. doi: 10.1016/j.plaphy.2020.11.028

Clara Diarte, Aline Xavier de Souza, Simona Staiger, Ann-Christin Deininger, Amauri Bueno, Markus Burghardt, Jordi Graell, Markus Riederer, Isabel Lara and Jana Leide.

Abstract

Barrier properties of the hydrophobic plant cuticle depend on its physicochemical composition. The cuticular compounds vary considerably among plant species but also among organs and tissues of the same plant and throughout developmental stages. As yet, these intraspecific modifications at the cuticular wax and cutin level are only rarely examined. Attempting to further elucidate cuticle profiles, we analysed the adaxial and abaxial surfaces of the sclerophyllous leaf and three developmental stages of the drupe fruit of *Prunus laurocerasus*, an evergreen model plant native to temperate regions. According to gas chromatographic analyses, the cuticular waxes contained primarily pentacyclic triterpenoids dominated by ursolic acid, whereas the cutin biopolyester mainly consisted of 9/10,ω-dihydroxy hexadecanoic acid. Distinct organ- and side-specific patterns were found for cuticular lipid loads, compositions and carbon chain length distributions. Compositional variations led to different structural and functional barrier properties of the plant cuticle, which were investigated further microscopically, infrared spectroscopically and gravimetrically. The minimum water conductance was highlighted at $1 \times 10^{-5} \text{ m s}^{-1}$ for the perennial, hypostomatous *P. laurocerasus* leaf and at $8 \times 10^{-5} \text{ m s}^{-1}$ for the few-month-living, stomatous fruit suggesting organ-specific cuticular barrier demands.

Keywords: plant cuticle; cuticular waxes; cutin matrix; ATR-FTIR; minimum water conductance; cuticular water permeability; *Prunus laurocerasus*

6.1. Introduction

The plant cuticle is an essential extracellular layer covering the epidermal cells of almost all primary aboveground plant surfaces. It acts as the first barrier against abiotic stresses such as uncontrolled water loss, excessive solar radiation, extreme temperature and mechanical damage, and biotic stresses as susceptibility to microbial infestation or adverse organ fusion (Krauss, Markstädter and Riederer, 1997; Reina-Pinto and Yephremov, 2009; Martin and Rose, 2014). These protective functions of the plant cuticle depend on the physicochemical properties of its components (Bernard and Joubès, 2013). The composition of the hydrophobic plant cuticle varies considerably among plant species, plant organs and tissues of the same plant and throughout developmental stages (Hauke and Schreiber, 1998; Jetter, Kunst and Samuels, 2006; Bourgault et al., 2020). Basically, the plant cuticle consists of a cutin biopolymer mainly composed of esterified ω -hydroxy hexadecanoic acids and octadecanoic acids possessing mid-chain hydroxyl, carbonyl and/or epoxy groups, cuticular waxes which impregnate the cutin matrix, and polysaccharide moieties originating from cell walls (Holloway, 1982; Graça et al., 2002; Fich, Segerson and Rose, 2016; Phillippe et al., 2010). All of these components are responsible for the crucial barrier properties of the plant cuticle, whereas cuticular waxes make a contribution of more than 96% to the barrier against water loss (Burghardt and Riederer, 2006; Leide et al., 2007; Isaacson et al., 2009). Thus, one of the most important features related to the cuticular waxes is the limitation of the non-stomatal water loss, which is the minimum and unavoidable water loss of plants (Kerstiens, 2006; Bueno et al., 2019). In leaves, the water permeability varies from 10^{-7} to 10^{-4} m s⁻¹ (Kerstiens, 1996; Schuster et al., 2017), for example 5×10^{-6} in *Prunus laurocerasus*, 7×10^{-6} in *Prunus avium*, 1×10^{-5} in *Malus domestica* and 2×10^{-5} in *Olea europaea* (Kerstiens, 1995; Schreiber et al., 2006; Huang et al., 2017). The water permeability of fruits was examined only in few cases, and its variability is lower than that of leaves, such as 5×10^{-5} in *M. domestica*, 9×10^{-5} in *O. europaea* and 2×10^{-4} in *P. avium* (Athoo, Winkler and Knoche, 2015; Huang et al., 2017; Leide et al., 2018; Diarte et al., 2019).

P. laurocerasus is a laurophyllous shrub of the Rosaceae family frequently used as a model plant to investigate the physiological significance of cuticular waxes, and how these compounds contribute to the cuticular water permeability (Schreiber and Riederer, 1996; Kirsch et al., 1997; Schreiber, 2001; Zeisler and Schreiber, 2016; Staiger et al., 2019). However, almost all of the prior studies focused exclusively on the astomatous adaxial surface of *P. laurocerasus* leaves. The cuticular lipid composition, the cuticle structure or the functional impact of the abaxial leaf surface of *P. laurocerasus* have not been extensively studied, although previous reports by Jetter, Schäffer and Riederer, 2000 and Yu et al., 2008 indicate that both leaf surfaces differ substantially in their cuticular wax coverage.

For this reason, our study aimed to analyse the interaction of compositional, structural and functional characteristics of both leaf surfaces and, additionally, the fruit of *P. laurocerasus*, whose cuticle profile has never been investigated. To date, the organ specificity of the plant cuticle has been only rarely documented such as for the leaf and fruit cuticle of *O. europaea* (Huang et al., 2017). Using *P. laurocerasus* as a model plant (**Figure 1A**), we aim to improve the understanding of the relationship between the variability of cuticular lipid composition and its respective barrier properties by answering the following main questions:

(I) What are the side-specific differences in cuticular lipid composition and load between the astomatous adaxial and the stomatous abaxial leaf surface (**Figure 1B and 1D**)? What functional effect a discrepancy between both leaf sides may have?

(II) What are the differences at the cuticular level among different plant organs? Does the life span of a perennial leaf and a few-month-living fruit play any role (**Figure 1C**)?

(III) What are the cuticular alterations of the fruit at different developmental stages (**Figure 1E**)? Does the fruit cuticle share common features with fruits of other rosaceous plant species?

6.2. Materials and methods

6.2.1. Plant material

Prunus laurocerasus L. cultivar ‘Herbergii’ plants were cultivated in the Botanical Garden of Würzburg, Germany. Fully expanded leaves and fruits at the mature green (green), the turning red (red) and the fully ripe purple-black (black) developmental stage were investigated.

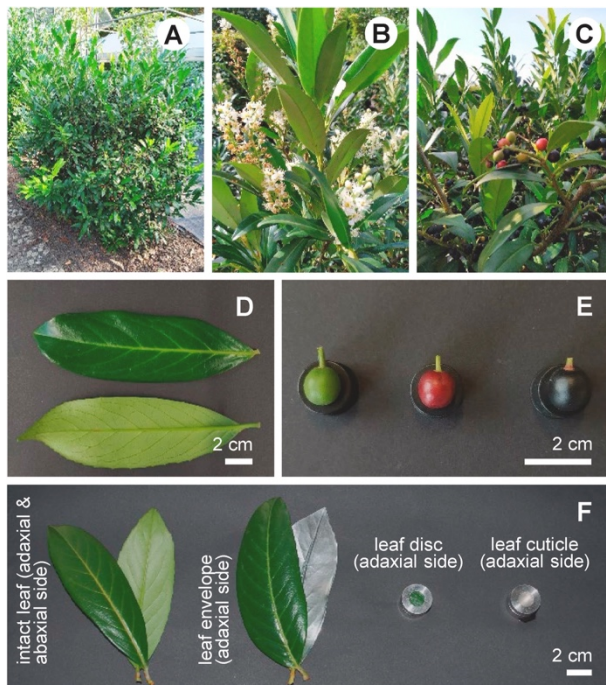


Figure 1. Photographs of rosaceous *Prunus laurocerasus* evergreen woody shrub (A) with perennial, lanceolate leaves. Flowers have five white petals and numerous yellow stamens (B). The fruit is a drupe that ripens within few months until early autumn (C). Fully expanded leaves have a shiny dark-green, adaxial and a dull green, abaxial leaf surface (D). Late stages in fruit development are mature green fruits, turning red fruits and fully ripe purple-black fruits (E). Sample preparation for water permeability measurements of leaves using different experimental techniques (F). Minimum water conductance was determined by means of intact leaves, which petioles were sealed. Cuticular water permeability was examined by leaf envelopes, which abaxial leaf surface and petiole were sealed, as well as leaf discs and isolated leaf cuticles inserted into transpiration chambers.

6.2.2. Functional trait measurements

The surface area of the leaf lamina without the petiole was determined according to the pixel values of the planar surface scanned at high resolution (600 dpi) in comparison to a reference area (Corel PHOTO-PAINT 2018). Fruits were assumed to be perfect spheres to calculate the fruit surface area. Fruit diameter was standardised as the mean between its vertical and horizontal diameter. The fresh weight and the dry weight after five-day dehydration at 60°C (Memmert UF55) were measured (Sartorius MC-1 AC210S). For the relative water content, the fresh weight of leaves and fruits was related to their respective dry weight. The specific surface area was calculated as quotient from the leaf surface area or fruit surface area and the oven-dry weight.

6.2.3. Cuticular membrane isolation

Cuticular membranes were enzymatically isolated by incubating small sections of leaves and fruits at room temperature with 1% (v/v) pectinase (Trenolin Super^{Plus}, Erbslöh), and 1% (v/v) cellulase (Celluclast, Novo Nordisk AIS) in 20 mM citric acid (Roth), pH 3.0, containing 1 mM sodium azide (Sigma-Aldrich). The enzyme solution was exchanged weekly. Isolated cuticular membranes were extensively washed in deionised water and air-dried.

6.2.4. Microscopic examinations

6.2.4.1. Auto-fluorescence microscopy

Small sections of leaves and fruits were cut out and embedded in a tissue-freezing medium (Sakura Tissue-Tek O.C.T.) at -20°C. Afterwards, slices with a thickness of approximately 30 µm were cut with a microtome (Leica CM1900 Cryostat) and examined with a Leica DMR HC microscope (excitation filter BP 355 to 425, suppression filter LP 470) coupled with a Leica DC 50 camera (Leica IM 1000 image software).

6.2.4.2. Scanning electron microscopy

The isolated cuticle of leaves and fruits was mounted on an aluminium holder using a conductive double-sided adhesive tape (Plannet Plano). Surfaces were sputter-coated with 10 nm to 15 nm gold/palladium (80/20, 25 mA, partial argon pressure 0.05 mbar; Balzers Bal-Tec SCD 005) for 150 s and examined with a field emission scanning electron microscope (JEOL JSM-7500F) at 5 kV acceleration voltage and a 10nm working distance. A 200 times magnified scanning electron micrograph was used for the determination of the stomatal density.

6.2.5. Determination of water permeability

6.2.5.1. Minimum water conductance

The minimum water conductance was gravimetrically determined and represented the lowest and unavoidable water loss of stomatous leaves and fruits when their stomata are maximally closed. Stomatal closure was induced by a dehydration process in darkness. The weight loss of leaves and fruits was monitored over time (Sartorius MC-1 AC210S). Petioles and peduncles were sealed with high-melting paraffin (Roth). Silica gel (AppliChem) was used to control the atmospheric humidity. The water vapour flux was calculated from the loss of fresh weight over time and the total surface area defined as: *water vapour flux* = $\Delta \text{fresh weight} / (\Delta \text{time} \times \text{surface area})$.

Dividing the water vapour flux by the driving force for water loss from the outer epidermal cell wall to the surrounding atmosphere, the minimum water conductance was obtained: *minimum water conductance* = *water vapour flux* / $(c_{wv \text{ sat}} \times \alpha_{apo} - c_{wv \text{ sat air}} \times \alpha_{air})$. The driving force for water vapour-based conductance is defined by the difference between the saturation concentration of water vapour in leaves or fruits at the actual temperature ($c_{wv \text{ sat}}$) and the surrounding atmosphere ($c_{wv \text{ sat air}}$) multiplied by the water activity in the epidermal apoplast (α_{apo}) or in the atmosphere (α_{air}). The water activity in the epidermal apoplast (α_{apo}) adjacent to the inner side of cuticle was assumed to be ≈ 1 , and the water activity of the atmosphere (α_{air}) over silica gel was ≈ 0 . The actual temperature of leaves and fruits was measured at intervals of 30 min using an infrared laser thermometer (Harbor Freight Tools), and the corresponding, temperature-depending saturation concentration of water vapour was derived from tabulated values (Nobel, 2009).

6.2.5.2. Cuticular water permeability

The cuticular water permeability of the stomatous adaxial leaf surface was gravimetrically determined using three different experimental techniques (Fig. 1F). At first, the stomatous abaxial leaf surface was masked with adhesive aluminium tape in order to avoid stomatal effects, and the petiole was sealed with high-melting paraffin (Roth). In this technique, the leaf was enveloped (Hoad et al. 1996). Secondly, leaf discs were placed into stainless steel transpiration chambers with the stomatous adaxial surface outwards (Schreiber, 2001). Thirdly, the isolated cuticle of the adaxial leaf surface was mounted into transpiration chambers (Schönherr and Lenzian, 1981). The transpiration chambers were closed with a steel ring, filled with deionised water and the interfaces sealed with Teflon paste (Roth) and adhesive tape (Tesa).

The water vapour flux was calculated from the weight loss (Sartorius MC-1 AC210S) over time per surface area defined as: $water\ vapour\ flux = \Delta fresh\ weight / (\Delta time \times surface\ area)$. The cuticular water permeability was determined from the water vapour flux divided by the driving force for water loss, which was determined by the saturation concentration of water vapour (c_{wv}^* ; Nobel 2009): $cuticular\ water\ permeability = water\ vapour\ flux / c_{wv}^* \times (a - a_{air})$. The water activity (a) in leaves or transpiration chambers was assumed to be ≈ 1 , and the water activity in the surrounding atmosphere (a_{air}) over silica gel (AppliChem) was ≈ 0 .

The water permeability was measured at temperatures ranging from 10°C to 50°C with an interval of 5°C (Memmert IPP110). The atmospheric humidity and temperature were controlled throughout the experiments (Testoterm Thermo-/Hygrometer 6010).

6.2.6. Extraction and gas chromatographic analysis of cuticular waxes

Cuticular waxes were extracted from the isolated cuticle with trichloromethane (Roth) at room temperature for 20 min. For the gas chromatographic analysis, *n*-tetracosane (C₂₄ *n*-alkane; Fluka) was added as internal standard. Afterwards, the extracted cuticular waxes were dried under a continuous flow of nitrogen and derivatised with *N,O*-bis-trimethylsilyl-trifluoroacetamide (Macherey-Nagel) and pyridine (1:1, v/v; Merck) at 70°C for 60 min, in order to obtain trimethylsilyl ether and esters from hydroxyl or carboxyl groups.

For the quantification and identification of the cuticular waxes, extracts were diluted with trichloromethane and injected in a gas chromatograph (Agilent Technologies 6850 Network GC system) coupled to a flame ionisation detector and a gas chromatograph (Agilent Technologies 6890N Network GC system) coupled to a mass spectrometer (Agilent Technologies 5977A MSD) in on-column mode. Capillary columns (Agilent J&W DB-1HT, 30 m length \times 0.32 mm diameter \times 0.10 μ m film) were used and hydrogen or helium as the carrier gas. The gas inlet pressure was programmed at 50 kPa for 5 min, 3 kPa min⁻¹ to 150 kPa, and at 150 kPa for 40 min. Temperature-programmed gas chromatographic conditions consisted of injection at 50°C for 2 min, then raised to 200°C by 40°C min⁻¹, holding for 2 min at 40°C, then raised to 320°C by 3°C min⁻¹, and, finally, held for 30 min at 320°C. Cuticular waxes were identified by the electron ionisation-mass spectra.

The distribution of carbon chain lengths was calculated as the average of carbon chain lengths, defined as: $ACL = \Sigma (C_n \times n) / \Sigma (C_n)$, where C_n was the abundance of aliphatic moieties with n carbon units (Poynter and Eglinton, 1990).

6.2.7. Fourier transform infrared spectroscopy of cuticular waxes

Infrared spectra of cuticular waxes were obtained with a Fourier transform infrared spectrometer (Bruker Tensor 27) in horizontal attenuated total reflection (ATR) mode using the BIO-ATR II unit (Bruker) equipped with a zinc selenide crystal. The extracted cuticular waxes were applied to the crystal as a solution of trichloromethane (Roth). After evaporation of the organic solvent at 90°C, the temperature was adjusted at 20°C by a stainless-steel envelope as part of the BIO-ATR II unit and a custom-made sample holder connected to the water circuit of a thermostat (Thermo Scientific Haake DC30-K20). Infrared spectra were scanned in a wavenumber range from 4000 cm⁻¹ to 670 cm⁻¹. The resolution was set to 2 cm⁻¹ with an acquisition time of 120 scans. The BIO-ATR II unit was continuously purged with dry, carbon dioxide-free air (K-MT-LAB 3, Parker Hannifin). The OPUS 7 (Bruker) software was used to analyse the spectra.

For melting curve analysis of cuticular waxes, infrared spectra were recorded from 20°C to 92°C using the asymmetric stretching vibration of methylene groups between 2916 cm⁻¹ and 2924 cm⁻¹. The initial temperature was set to 20°C and, then, raised at temperature intervals of 4°C to 44°C and in 1°C steps to 92°C.

6.2.8. Transesterification, extraction and gas chromatographic analysis of cutin monomers

The isolated, dewaxed cuticle was transesterified with boron trifluoride in methanol (Sigma-Aldrich) overnight at 70°C to obtain methyl esters of cutin acid monomers. Afterwards, sodium-chloride saturated aqueous solution and trichloromethane (1:1, v/v; Roth) and *n*-dotriacontane (C₃₂ *n*-alkane; Sigma) as internal standard were added. From this two-phase system, the transmethylated cutin monomers were extracted three times with trichloromethane. The combined organic phases were dried over anhydrous sodium sulphate (AppliChem) and filtered. Subsequently, the organic solvent was evaporated under a continuous flow of nitrogen. Derivatisation and gas chromatographic analysis were performed according to the cuticular wax analysis with the same equipment. Separation of cutin monomers was carried out at 50 kPa for 60 min, 10 kPa min⁻¹ to 150 kPa, and at 150 kPa for 30 min. The gas chromatographic conditions consisted of injection at 50°C for 1 min, then raised by 10°C min⁻¹ to 150°C, held for 2 min, and by 3°C min⁻¹ to 300°C, held at this temperature for 30 min.

6.2.9. Statistical analysis

Statistical analysis was performed using Kruskal-Wallis analysis of variance (Dell Statistica 13.1). Values of *p* < 0.05 were considered significantly different.

6.3. Results

6.3.1. Functional attributes of *Prunus laurocerasus* leaves and fruits

In order to characterize both plant organs, different functional leaf and fruit traits of *P. laurocerasus* were measured. Total leaf surface area with 94.3 cm² (**Figure 2A**), specific leaf surface area with 6.1 m² kg⁻¹ (**Figure 2B**), and leaf fresh weight with 2.0 g (**Figure 2C**) were 24 times, six times and two times higher compared to black fruits, respectively. Leaves and black fruits exhibited a relative water content of about 60% but the relative water content of green and red fruits was higher averaging at 73% (**Figure 2D**). A contrasting juxtaposition of fruits at different developmental stages showed that the functional traits were equal in green and red fruits. However, black fruits had a 1.3 times higher total

surface area with 3.9 cm^2 and a two times higher fresh weight with 1.0 g in comparison to green and red fruits, whereas the specific surface area with $1.0 \text{ m}^2 \text{ kg}^{-1}$ was only a half that of the less mature fruits.

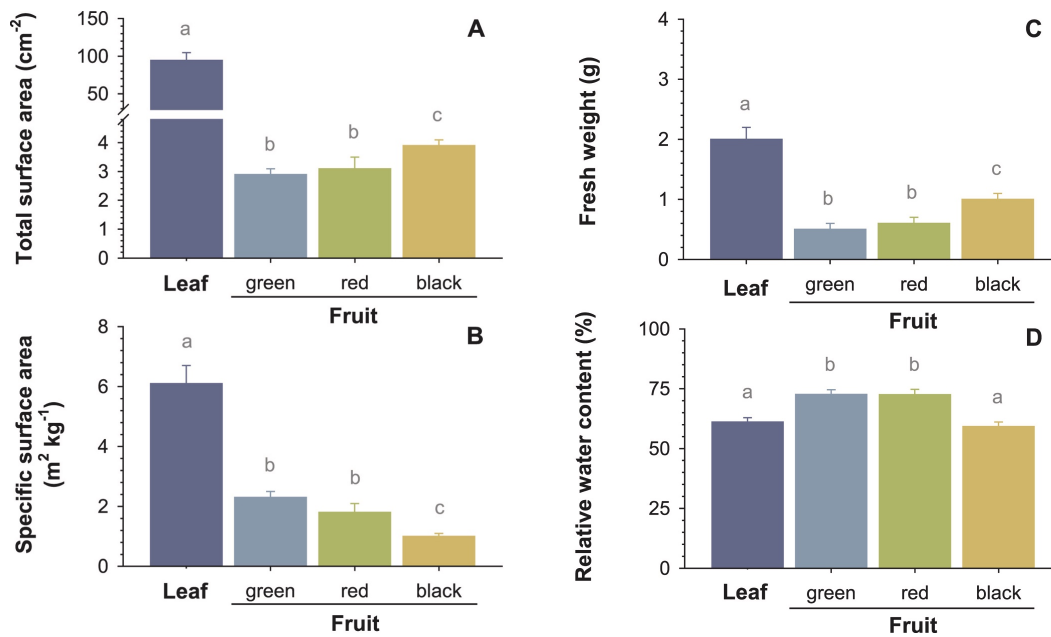


Figure 2. Functional leaf and fruit traits of *Prunus laurocerasus*. Total surface area (A), specific surface area (B), fresh weight (C) and relative water content (D) were determined for fully expanded leaves and mature green fruits, turning red fruits and fully ripe purple-black fruits. Data are shown as mean \pm SD ($n = 20$). Different letters indicate significant differences between both plant organs ($p < 0.05$, Kruskal-Wallis ANOVA).

6.3.2. Cuticular structure of *Prunus laurocerasus* leaves and fruits

Cross sections of *P. laurocerasus* leaves and fruits illustrated the cuticle thickness and revealed differences in cuticle structure between both plant organs. Auto-fluorescence micrographs highlighted the continuous cuticularisation of the outer periclinal, epidermal cell wall in leaves and fruits. Furthermore, these micrographs showed that cuticular pegs indicating to a thickening of the cuticle between anticlinal, epidermal cell walls were only present in fruits (**Figures 3A-3E**).

Electron microscopic studies showed that the adaxial and abaxial leaf surfaces were covered with a smooth epicuticular wax film accompanied by irregular small wax platelets or scales (**Figures 3F-3G**). Moreover, leaves of *P. laurocerasus* were hypostomatous having stomata only on the abaxial leaf surface. The stomatal density averaged at $130.3 \text{ pores mm}^{-2}$. The surface structure of green fruits was comparable to that of *P. laurocerasus* leaves, whereas red and black fruits had a rough epicuticular wax crust with irregular small wax platelets (**Figures 3H-3J**). The stomatal density of fruits with about $32.4 \text{ pores mm}^{-2}$ was four times lower compared to the abaxial leaf surface.

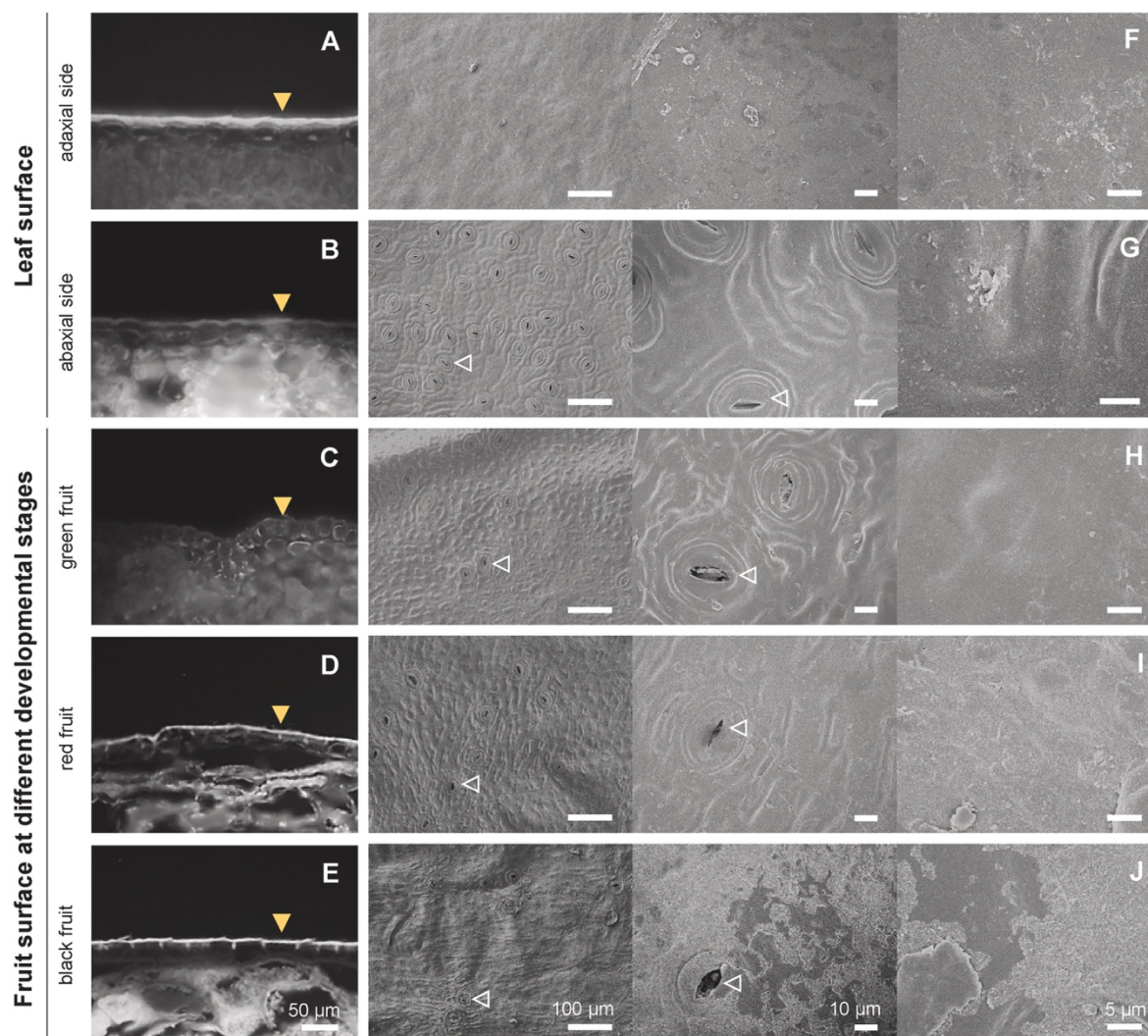


Figure 3. Auto-fluorescence and scanning electron micrograph of *Prunus laurocerasus* leaf and fruit surfaces. Structural characteristics were detected on the adaxial (A, F) and abaxial (B, G) surface of fully expanded leaves and on the surface of mature green fruits (C, H), turning red fruits (D, I) and fully ripe purple-black fruits (E, J) at different magnifications. The outside margin of the cuticle cross sections (A-E) and stomata on plan views (F-J) are marked with arrowheads.

6.3.3. Cuticular lipid composition of *Prunus laurocerasus* leaves and fruits

6.3.3.1. Cutin matrix of *Prunus laurocerasus* leaves and fruits

The total amount of cutin monomers on the adaxial leaf surface of *P. laurocerasus* was twice as high as the cutin deposition on the abaxial leaf surface (**Figure 4A**). Despite these quantitative differences of $136.4 \mu\text{g cm}^{-2}$ and $68.6 \mu\text{g cm}^{-2}$, the cutin matrix composition was similar on both leaf surfaces incorporating ω -hydroxy alkanolic acids, α,ω -dicarboxylic acids, alkanolic acids, primary alkanols and hydroxy cinnamic acids. Predominant aliphatic cutin monomers were 9/10, ω -dihydroxy hexadecanoic acid, 9,10-epoxy ω -hydroxy octadecanoic acid and 9,10, ω -trihydroxy octadecanoic acid (**Figure 5A**). These cutin monomers together represented 75% of the total cutin deposition on the adaxial leaf surface and 71% on the abaxial leaf surface. The main aromatic cutin monomer was *trans* 4-hydroxy cinnamic acid with about 2% of the total cutin deposition.

The cutin matrix on green and red fruit surfaces was significantly reduced compared to both leaf surfaces. The cutin monomeric load was quantified to only $34.1 \mu\text{g cm}^{-2}$ and $30.6 \mu\text{g cm}^{-2}$, respectively. Their cutin composition corresponded to the adaxial leaf surface and was dominated by 9/10, ω -dihydroxy hexadecanoic acid, 9,10-epoxy ω -hydroxy octadecanoic acid and 9,10, ω -trihydroxy octadecanoic acid ($> 70\%$ total cutin monomers; **Figure 5B**). In addition to these three ω -hydroxy alkanolic acid derivatives, black fruits exhibited substantial amounts of hexadecanoic acid and octadecanoic acid, as well as a comparatively high abundance of 3,4-dihydroxy cinnamic acid on their surface. Thus, black fruits accumulated a total of $60.5 \mu\text{g cm}^{-2}$ cutin, which was in the same range as the cutin deposition on the abaxial leaf surface but with a distinctly different cutin matrix composition.

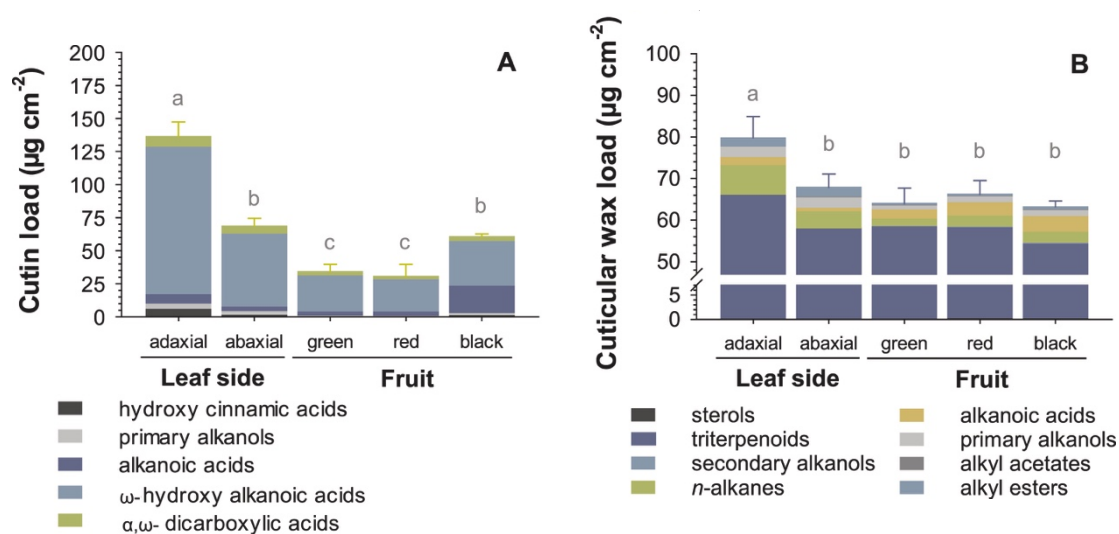


Figure 4. Gas chromatographic analysis of cuticular leaf and fruit lipid composition of *Prunus laurocerasus*. Compound classes of the cutin matrix (A) and cuticular waxes (B) were examined on the adaxial and abaxial surface of fully expanded leaves and on the surface of mature green fruits, turning red fruits and fully ripe purple-black fruits. Data are shown as mean \pm SD ($n = 5$). Different letters indicate significant differences between both plant organs ($p < 0.05$, Kruskal-Wallis ANOVA).

The average carbon chain length of long-chain ω -hydroxy alkanolic acids representing characteristic cutin monomers was proportionally lower on the abaxial leaf surface with 16.8 compared to the adaxial leaf and the green, red and black fruit surfaces with about 17.4. This shift highlighted the reduced proportion of 9,10-epoxy ω -hydroxy octadecanoic acid and 9,10, ω -trihydroxy octadecanoic acid on the abaxial leaf surface. Very-long-chain primary alkanols and alkanolic acids up to a carbon chain length of 34 were identified in the aliphatic cutin fractions of *P. laurocerasus* leaf and fruit surfaces but at a substantially lower level than the long-chain aliphatic cutin monomers. Both compound classes exhibited a carbon chain length distribution similar to that of the cuticular waxes.

6.3.3.2. Cuticular waxes of *Prunus laurocerasus* leaves and fruits

The total amount of cuticular waxes was significantly different between the adaxial and abaxial leaf surfaces of *P. laurocerasus* (**Figure 4B**). The highest cuticular wax load was detected on the adaxial leaf surface with $79.8 \mu\text{g cm}^{-2}$. Distinctly lower was the cuticular wax coverage of the abaxial leaf and the fruit surfaces at the three developmental stages at an average of $65.3 \mu\text{g cm}^{-2}$. Compound classes of

the cuticular waxes were very-long-chain alkanolic acids, *n*-alkanes, secondary alkanols, primary alkanols, alkyl acetates and alkyl esters, as well as tetracyclic sterols and pentacyclic triterpenoids but with organ- and side-specific distributions.

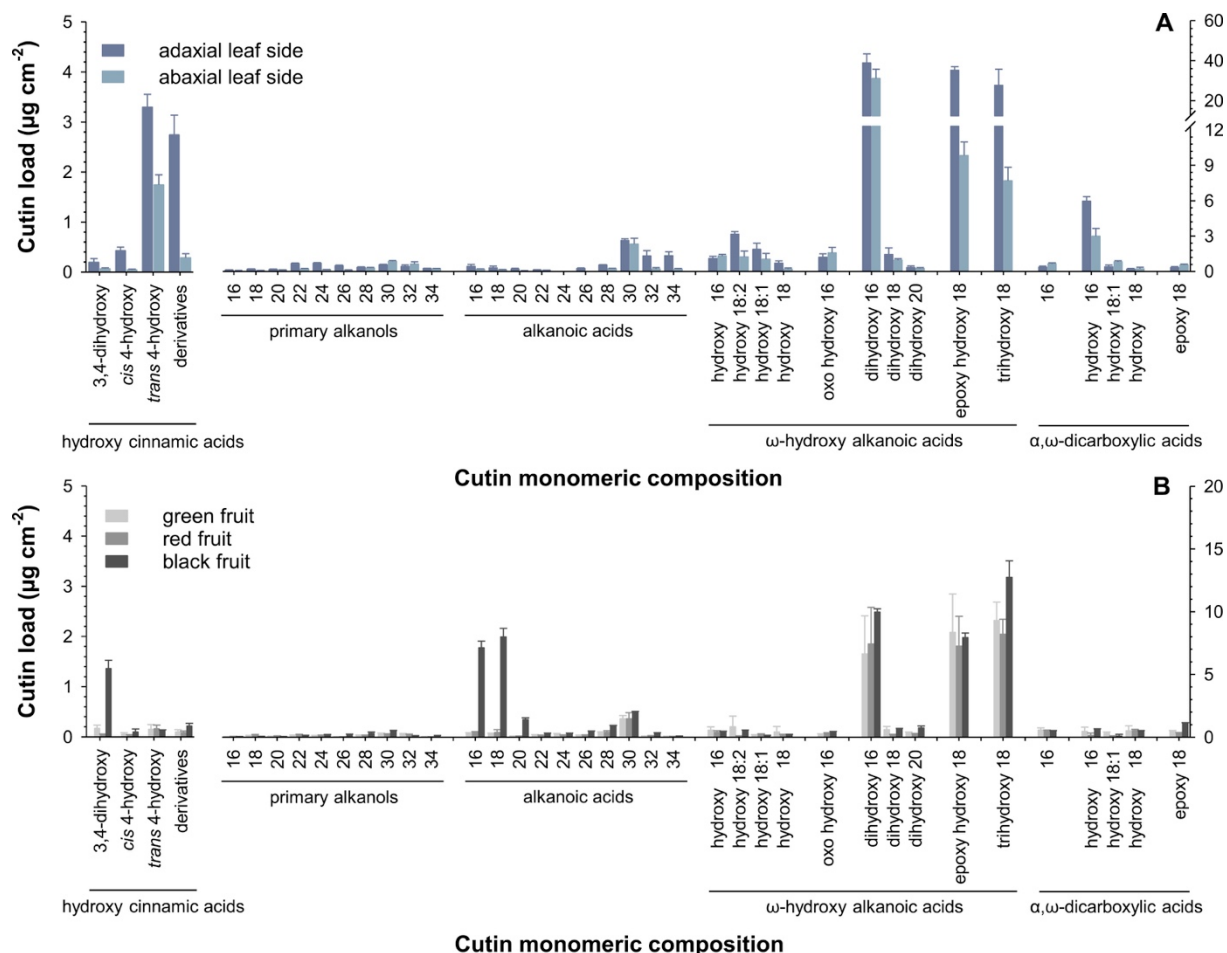


Figure 5. Gas chromatographic analysis of the cutin matrix of *Prunus laurocerasus*. Cutin monomeric composition was investigated on the adaxial and abaxial surface of fully expanded leaves (A) and on the surface of mature green fruits, turning red fruits and fully ripe purple-black fruits (B). Data are shown as mean ± SD (*n* = 5).

The cuticular wax composition of leaves and fruits was dominated by pentacyclic triterpenoids (about 87% of the total cuticular waxes). The alicyclic compounds ursolic acid (about 59%), oleanolic acid (about 11%) and hederagenin (about 7%) were identified in high quantities in the cuticular waxes of both plant organs (Figures 6A-6C). The aliphatic wax fraction of the adaxial and abaxial leaf surfaces mainly consisted of very-long-chain *n*-alkanes, primary alkanols and alkyl esters (about 14% of the total cuticular waxes). The mixture of *n*-alkanes, alkanolic acids and primary alkanols constituted the main proportion of the aliphatic wax fraction of *P. laurocerasus* fruits (about 10%). The principal aliphatic wax compounds in leaves were *n*-nonacosane (C₂₉ *n*-alkane) and *n*-hentriacontane (C₃₁ *n*-alkane) with 8% of the total cuticular waxes on the adaxial and 5% on the abaxial leaf surfaces, but *n*-nonacosane (C₂₉ *n*-alkane) and triacontanoic acid (C₃₀ alkanolic acid) predominated in fruits with 4% for green, 6% for red and 7% for black fruits.

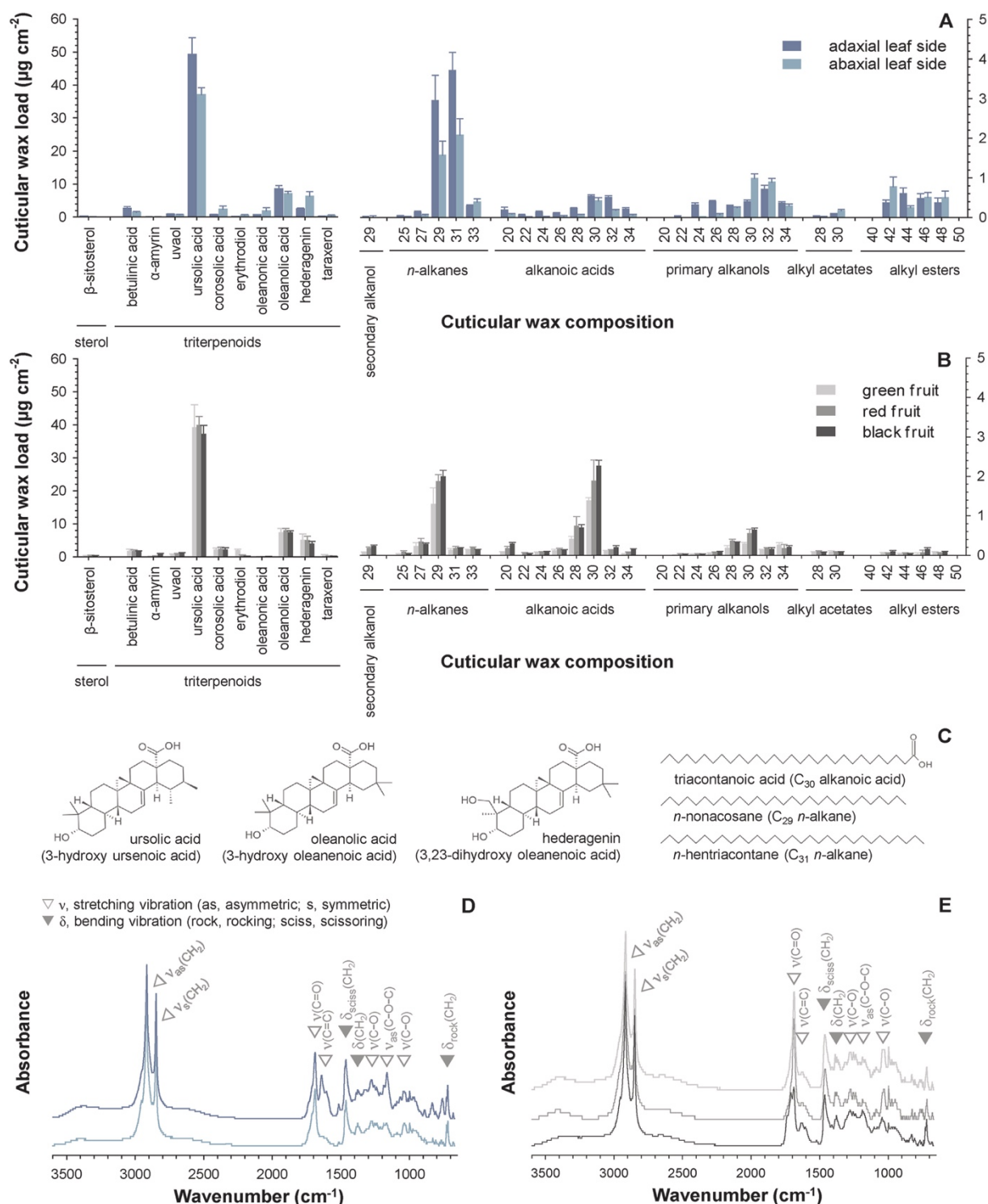


Figure 6. Gas chromatographic analysis of cuticular waxes of *Prunus laurocerasus*. Cuticular wax composition was investigated on the adaxial and abaxial surface of fully expanded leaves (A) and on the surface of mature green fruits, turning red fruits and fully ripe purple-black fruits (B). Data are shown as mean \pm SD ($n = 5$). Chemical structures of pentacyclic triterpenoids and very-long-chain aliphatic compounds mainly present in leaf and fruit cuticular waxes (C). Fourier transform infrared spectra of cuticular waxes of leaves (D) and fruits (E) were scanned. Absorbance maxima of stretching (v) and bending (δ) vibrations of aliphatic and oxygen-bearing moieties are marked.

Hence, the proportionate distribution of the alicyclic and the aliphatic wax fractions was different, with the highest aliphatic proportion found on the adaxial leaf surface and the lowest on the surface of green fruits. An organ- and side-specific carbon chain length distribution resulted from different aliphatic wax compound classes with varying predominate wax compounds. The average of carbon chain length distribution calculated for the aliphatic wax fraction amounted to 31.8 for the adaxial and 33.4 for the abaxial leaf surfaces, and 29.7 for *P. laurocerasus* fruit surfaces.

6.3.4. Spectroscopic features of *Prunus laurocerasus* leaves and fruits cuticular waxes

By means of infrared spectral studies of cuticular waxes, absorbance maxima were obtained by stretching and bending vibrations of hydrocarbons and oxygen-bearing moieties, respectively. The infrared spectra of leaf cuticular waxes were dominated by asymmetric and symmetric hydrocarbon stretching vibration of methylene groups located at 2916 cm^{-1} and 2848 cm^{-1} (**Figure 6D**). Moreover, hydrocarbon bending vibration led to absorbance intensities at 1462 cm^{-1} , 1377 cm^{-1} and 719 cm^{-1} . Strong carbon-oxygen double bond stretching vibration of carbonyl groups centred at 1688 cm^{-1} . Intermediate absorbance at 1255 cm^{-1} and at 1039 cm^{-1} showed carbon-oxygen stretching vibration of hydroxyl groups and at 1166 cm^{-1} asymmetric carbon-oxygen-carbon stretching vibration of esters bonds. High absorbance at 1641 cm^{-1} indicated a stretching vibration of unsaturated hydrocarbons containing a carbon-carbon double bond but predominately for the adaxial leaf surface.

Infrared spectral properties of fruit cuticular waxes were similar to those of the abaxial leaf surface (**Figure 6E**). The main difference was found for the ratio of absorbance intensities of methylene group stretching vibrations versus carbonyl group stretching vibrations, which were distinctly lower for cuticular waxes of green and red fruits in comparison to black fruits and both leaf surfaces.

6.3.5. Cuticular barrier properties of *Prunus laurocerasus* leaves and fruit cuticle

The minimum water conductance was determined for *P. laurocerasus* leaves and fruits with maximally closed stomata (**Figure 7A**). Leaves exhibited a minimum water conductance of $1.2 \times 10^{-5} \text{ m s}^{-1}$ and, thus, a six times lower value compared to fruits with about $8.2 \times 10^{-5} \text{ m s}^{-1}$ regardless of the developmental stage.

The cuticular water permeability was examined for the astomatous adaxial leaf surface of *P. laurocerasus* using three different techniques, leaf envelopes and leaf discs and isolated leaf cuticles placed into transpiration chambers (**Figure 7B**). A contrasting juxtaposition of minimum water conductance of leaves and cuticular water permeability of the adaxial leaf surface resulted in an equivalent water permeability of about $1.4 \times 10^{-5} \text{ m s}^{-1}$. The minimum water conductance of leaves and the cuticular water permeability of the adaxial leaf surface were constant throughout a temperature range of 10°C to 40°C and only slightly increased at temperatures higher than 40°C.

Melting curves of cuticular waxes were analysed within the temperature range of 20°C and 92°C. As indicated by infrared spectroscopy, midpoints of the melting range of cuticular waxes were at 63.7°C for the adaxial and at 63.3°C for the abaxial leaf surfaces (**Figure 7C**). Melting midpoints of cuticular waxes of green, red and black fruits were detected at 67.7°C, 63.7°C and 64.4°C, respectively (**Figure 7D**).

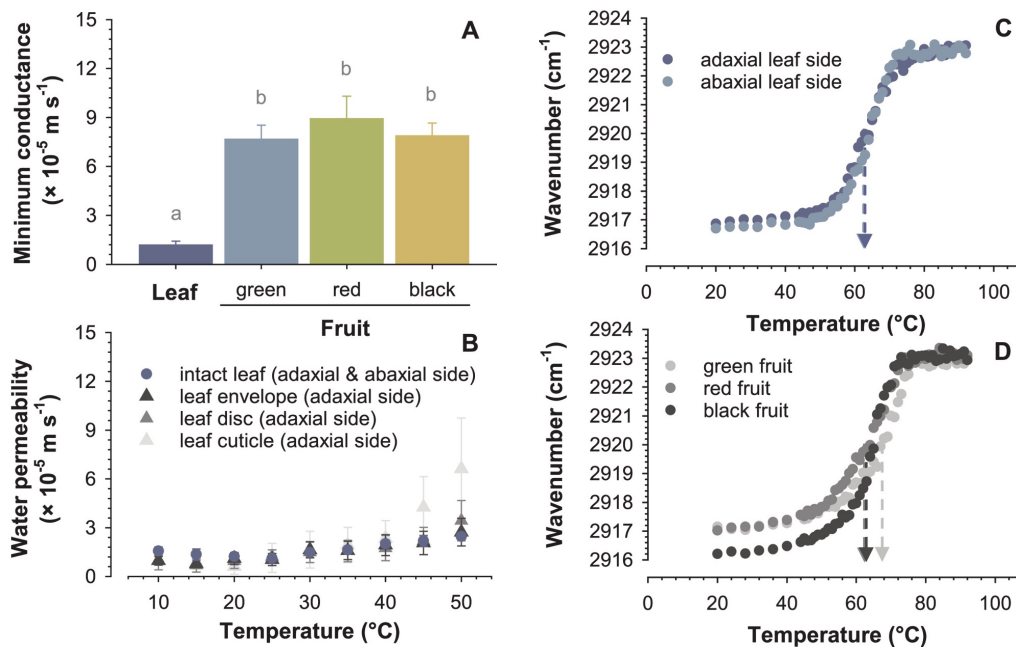


Figure 7. Minimum water conductance was determined for fully expanded leaves and mature green fruits, turning red fruits and fully ripe purple-black fruits (A). Data shown as mean \pm SD ($n = 20$). Different letters indicate significant differences between both plant organs ($p < 0.05$, Kruskal-Wallis ANOVA). Temperature-dependent comparison of minimum water conductance of fully expanded leaves and cuticular water permeability of the adaxial leaf surface measured *via* leaf envelopes, leaf discs and isolated leaf cuticles (B). Melting curve of cuticular waxes of the adaxial and abaxial surface of fully expanded leaves (C) and the surface of mature green fruits, turning red fruits and fully ripe purple-black fruits (D) detected by the temperature-dependent shift of the asymmetric stretching vibration (ν_{as}) of methylene groups. Transition midpoints of the melting curve are marked with arrows.

6.4. Discussion

6.4.1. *Prunus laurocerasus* as a model plant in cuticle research

Evergreen *Prunus* species are woody shrubs or trees that are native to temperate regions with seasonal cold and moderate humid climate. *P. laurocerasus* is an evergreen, broad-leaved woody shrub with drupe fruits consisting of a thin exocarp, a fleshy mesocarp and a lignified endocarp. Studies, which have been focused on its leaf attributes, documented a relative water content of sclerophyllous *P. laurocerasus* leaves between 61% and 65% (Ceccato et al., 2001). The specific surface area of these mesophyll-sized leaves, which possessed a fresh weight of 2 g, was between $6 \text{ m}^2 \text{ kg}^{-1}$ and $7 \text{ m}^2 \text{ kg}^{-1}$ (Leide et al., 2020). Additionally, our analysis showed that *P. laurocerasus* fruits had a smaller surface area and specific surface area, as well as a lower fresh weight compared to leaves. On the other hand, the relative water content of leaves and black fruits was similar but the water gradient within both plant organs differed significantly.

These functional traits have important consequences for both the perennial leaf and the few-month-living fruit of *P. laurocerasus*, for example regarding their growth rate, nutrient conservation and water balance. A longer life span often implicates a crucial investment in plant protection, which also affects most likely the properties of the plant cuticle as a protective barrier.

6.4.2. Implications of side specificities of the plant cuticle: adaxial and abaxial leaf surface analysis of *Prunus laurocerasus*

P. laurocerasus leaves exhibit visually diverse surfaces: a shiny dark-green, adaxial leaf side and a dull green, abaxial leaf side. Microscopically, the leaf surfaces of *P. laurocerasus* are covered by a smooth epicuticular wax film (Jetter et al., 2000). The cuticle profile of the astomatous adaxial leaf surface has been extensively analysed over the past five decades. Previous findings regarding the adaxial leaf surface were verified in our study for the *P. laurocerasus* cultivar ‘Herbergii’ and compared with the corresponding stomatous abaxial leaf surface. In general, the cuticular composition was similar on both leaf surfaces but the cuticular lipid load differed significantly.

The polymeric cutin matrix exhibited ω -hydroxy alkanolic acids, α,ω -dicarboxylic acids, alkanolic acids, primary alkanols and hydroxy cinnamic acids, whereas the long-chain aliphatic 9/10, ω -dihydroxy hexadecanoic acid, 9,10-epoxy ω -hydroxy octadecanoic acid and 9,10, ω -trihydroxy octadecanoic acid significantly dominated the cutin composition (Graça et al., 2002; Leide et al., 2020). Cutin deposition on the adaxial leaf surface was substantiated at $136 \mu\text{g cm}^{-2}$, whereas it was reduced by 50% on the abaxial leaf surface mainly due to a lower amount of 9,10-epoxy ω -hydroxy octadecanoic acid and 9,10, ω -trihydroxy octadecanoic acid. Hydroxy cinnamic acids contributed only to a minor extent to the cutin matrix of *P. laurocerasus* leaves but the abundance of these aromatic cutin acids was three times higher on the adaxial leaf surface compared to the abaxial leaf surface.

These side-specific differences between the adaxial and abaxial cutin matrix of *P. laurocerasus* leaves documented for the total cutin load, the proportion of aromatic cutin acids and the aliphatic cutin acids with differing carbon chain lengths and functional groups might be evidence of a varying polymeric cross-linking, toughness and/or microbial defence on both leaf surfaces (Isaacson et al., 2009; Reina-Pinto and Yephremov, 2009).

The abaxial surface of *P. laurocerasus* leaves also had a 15% lower cuticular wax load compared to the adaxial leaf surface. The latter exhibited a cuticular wax amount of about $80 \mu\text{g cm}^{-2}$ (Schreiber and Riederer, 1996). Cuticular waxes of *P. laurocerasus* leaf surfaces composed of pentacyclic triterpenoids in substantial quantities, tetracyclic sterols and very-long-chain aliphatic compounds most notably *n*-alkanes, alkanolic acids, primary alkanols, secondary alkanols, alkyl acetates and alkyl esters. Previous studies additionally detected *n*-alkanals in small quantities (Jetter et al., 2000; Zeisler and Schreiber, 2016; Leide et al., 2020). The alicyclic wax fraction was dominated by hydroxy pentacyclic triterpene acids. Ursolic acid (3-hydroxy ursenoic acid) was the principal alicyclic wax compound and *n*-nonacosane (C_{29} *n*-alkane) and *n*-hentriacontane (C_{31} *n*-alkane) were the major aliphatic wax compounds on both leaf surfaces. Carbon chain lengths of the aliphatic wax compounds ranged from C_{20} to C_{50} with even-numbered alkanolic acids, primary alkanols, alkyl acetates, alkyl esters and odd-numbered of *n*-alkanes and secondary alkanols. Accordingly, the cuticular wax mixture varied by the amount of aliphatic and alicyclic compound classes, functional groups and carbon chain length distribution. Altogether, differences in cuticular composition and structure between the adaxial and abaxial leaf surfaces of *P. laurocerasus* may arise by reasons of differential physical and physiological demands such as mechanical stress, sun exposure or stomatal gas and water exchange resulting in a different microclimate at both boundary layers and, thus, requiring side-specific cuticular barrier properties.

A comparison of the evergreen shrub *P. laurocerasus* with other rosaceous plant species brings out interspecific characteristics. Lower cuticular wax coverages from $5 \mu\text{g cm}^{-2}$ to $31 \mu\text{g cm}^{-2}$ have been reported for leaves of deciduous shrubs *Rosa rubiginosa*, *Rosa chinensis* and *Rosa canina*, respectively

(Buschhaus, Herz and Jetter, 2007; Wissemann, Riedel and Riederer, 2007; Cheng et al., 2019). Similarly, leaves of the deciduous trees *P. avium* and *Prunus persica* showed lower cuticular wax loads ranging from 20 $\mu\text{g cm}^{-2}$ to 54 $\mu\text{g cm}^{-2}$ depending on cultivar, climate, leaf canopy position, leaf age and leaf side (Baker, Bukovac and Flore, 1979; Hunsche and Noga, 2011).

6.4.3. Impact of developmental changes and organ specificities of the plant cuticle: fruit surface analysis of *Prunus laurocerasus*

Throughout the late developmental stages, stomatous *P. laurocerasus* fruits were subjected to a multitude of alterations reflecting in colour change due to anthocyanin accumulation, fruit surface expansion, fresh weight increase and, simultaneously, reduction in specific surface area and relative water content. However, the epicuticular structure varied only slightly between green, red and black fruits. Fruits at these different developmental stages had a similar cuticular composition and load except for black fruits that also possessed an uncommon, striking accumulation of 3,4-dihydroxy cinnamic acid, hexadecanoic acid and octadecanoic acid in their cutin matrix. This divergence in the cutin deposition resulted finally in a doubling of the cutin load on the surface of black fruits of *P. laurocerasus* compared to green and red fruits. Hence, these findings might indicate an increased stabilising impact of the cutin matrix on the cuticle integrity due to the modified stress-strain properties during fruit ripening, which probably meet specific requirements of fruit softening and changes in turgor pressure (López-Casado et al., 2007).

Thus, cutin and cuticular wax loads of stomatous black fruits were comparable to the stomatous abaxial leaf surface of *P. laurocerasus*. However, the composition of both cuticular components differed considerably. On the black fruit surface, ursolic acid was the principal alicyclic wax compound but *n*-nonacosane (C_{29} *n*-alkane) and triacontanoic acid (C_{30} alkanic acid) were the major aliphatic wax compounds. An organ-specific preference of aliphatic wax compound classes resulted in a modified carbon chain length distribution between *P. laurocerasus* leaves and fruits.

Despite cuticular differences between leaves of the evergreen shrub *P. laurocerasus* and the deciduous tree *P. avium*, the stomatous surfaces of their drupes that are also referred to as cherry fruits have numerous cuticular features in common. The cutin deposition of *P. avium* fruits ranged from 35 $\mu\text{g cm}^{-2}$ to 85 $\mu\text{g cm}^{-2}$ depending on the cultivar (Peschel et al., 2007; Belge et al., 2014a). Furthermore, the cuticular wax coverage of *P. avium* fruits composed of pentacyclic triterpenoids mainly ursolic acid as well as *n*-alkanes, primary alkanols, secondary alkanols, alkanic acids and sterols within a cultivar-specific range of 10 $\mu\text{g cm}^{-2}$ and 48 $\mu\text{g cm}^{-2}$ (Peschel et al., 2007; Hunsche and Noga, 2011; Belge et al., 2014a). Comparing with *P. laurocerasus* and *P. avium* fruits, substantial differences in cuticular composition, load and/or structure have been reported for drupes of *P. persica* and *Prunus domestica* (Ismail et al., 1977; Storey and Price, 1999; Fernández et al., 2011; Belge et al., 2014b; Konarska, 2015).

6.4.4. Functional impact of the plant cuticle and the effect of temperature: organ-specific barrier properties of *Prunus laurocerasus*

It is well established that the cutin matrix and polysaccharides from the underlying cell walls essentially contribute to the physical integrity of fruits and leaves, whereas cuticular waxes provide their main barrier against uncontrolled water loss (Schönherr, 1976; Isaacson et al., 2009; Philippe et al., 2020). In case of maximally closed stomata, the minimum water conductance was $1 \times 10^{-5} \text{ m s}^{-1}$ for the hypostomatous *P. laurocerasus* leaves and $8 \times 10^{-5} \text{ m s}^{-1}$ for the stomatous black fruits. This difference in the minimum water conductance possibly rooted in an unequal efficiency of stomatal closure taking into account a potential residual stomatal conductance even under conditions of darkness and desiccation

(Kerstiens, 2006; Duursma et al., 2019). Our comparison of the minimum water conductance of leaves and the cuticular water permeability of the astomatous adaxial leaf surface showed that an assumed stomatal effect could be excluded, at least for the *P. laurocerasus* leaves. Already in numerous previous studies, the cuticular water permeability of the adaxial leaf surface of *P. laurocerasus* was also detected between 5×10^{-6} and $2 \times 10^{-5} \text{ m s}^{-1}$ (Schreiber and Riederer, 1996; Schreiber, 2001; Schreiber et al., 2001; Schreiber et al., 2006).

Moreover, the congruence of minimum water conductance and cuticular water permeability held for a temperature range between 10°C and 50°C. Temperature-dependent water permeability measurements of *P. laurocerasus* leaves showed a slight increase at temperatures higher than 40°C (Schönherr et al., 1979; Schreiber, 2001). Although, the actual midpoint of the melting range of the leaf cuticular waxes was located at temperatures higher than 60°C, this reduction of cuticular barrier properties indicates changes in the physical arrangement within the plant cuticle. These alterations are attributed to arising micro-cracks caused by volume expansion of the cutin matrix or the incipient melting of cuticular waxes (Eckl and Gruler, 1980; Schreiber and Schönherr, 1990; Merk, Blume and Riederer, 1998). A decline of cuticular barrier properties of the isolated leaf cuticle specifies the volume expansion of the polymeric cutin matrix at elevated temperatures and, consequently, the stabilising impact of the absent, underlying cell wall for the integrity of the cuticular transpiration barrier (Schreiber and Schönherr, 1990).

Nevertheless, it is most likely that differences in the minimum water conductance of *P. laurocerasus* leaves and fruits were based on the cuticle itself. Differing leaf and fruit cuticular waxes point to divergent cuticular barrier properties against the uncontrolled water loss. Tsubaki et al., 2013 and Schuster et al., 2016 proposed that high amounts of pentacyclic triterpenoids physically strengthen the cutin matrix and, thus, donate cuticle fracture toughness, whereas very-long-chain aliphatic wax compounds were shown to be the key factor for determining the cuticular water permeability (Riederer and Schreiber, 1995; Vogg et al., 2004).

Noteworthy, the very-long-chain aliphatic wax fraction amounted to $14 \mu\text{g cm}^{-2}$ on the adaxial and $10 \mu\text{g cm}^{-2}$ on the abaxial leaf surfaces, whereas that in fruits was only between $5 \mu\text{g cm}^{-2}$ and $9 \mu\text{g cm}^{-2}$ depending on the developmental stage. In accordance with the amount of aliphatic wax compounds, the compound class preference and/or the carbon chain length distribution are suggested to be crucial factors in cuticular permeability. *N*-alkanes were the principal aliphatic compound class of *P. laurocerasus* leaves with 53% of the aliphatic wax fraction on the adaxial and 42% on the abaxial leaf surfaces. The aliphatic wax fraction of *P. laurocerasus* fruits composed mainly of alkanolic acids (about 42%). Alkanolic acids have a significantly lower impact on the cuticular barrier properties against the uncontrolled water loss compared to *n*-alkanes (Grncarevic and Radler, 1967), probably, due to the functional group, which affects hydrophilic and/or physical properties of cuticular waxes. A higher carbon chain length of aliphatic wax compounds might have a beneficial impact on the waterproofing properties of cuticular waxes (Bueno et al., 2019). The average carbon chain length was distinctly lower for *P. laurocerasus* fruits with 29 to 30 compared to leaves with 32 on the adaxial and 33 on the abaxial surfaces.

6.5. Conclusions

Based on a common genetic background, *P. laurocerasus* leaves and fruits generate different cuticle profiles indicating the phenotypic plasticity of the cuticular transpiration barrier. Strengthening and water-proofing functions of the plant cuticle can be attributed to different cuticular components. The deposition of cutin and pentacyclic triterpenoids, which are mainly responsible for the physical stability and integrity of the cuticle, were distinctly higher for *P. laurocerasus* leaves but only on the stomatous adaxial surface. Moreover, the adaxial leaf surface exhibited a higher proportion of aliphatic ω -hydroxy octadecanoic acids and aromatic hydroxy cinnamic acids compared to the stomatous abaxial leaf surface suggesting side-specific polymeric characteristics to cope with unequal challenges.

Compared to *P. laurocerasus* fruits, the amount of very-long-chain aliphatic wax compounds was also higher for leaves but in this case on both the adaxial and the abaxial leaf surfaces. This quantitative factor and, additionally, a higher average carbon chain length of aliphatic wax compounds plus an organ-specific clear preference for *n*-alkane accumulation constituted a strikingly higher efficiency of the cuticular transpiration barrier of leaves compared to stomatous fruits of *P. laurocerasus*. This higher investment in the atmosphere-exposed surface of hypostomatous *P. laurocerasus* leaves is essential since perennial leaves have to cope with different abiotic and biotic stresses during the seasonal course and the protective cuticle is the boundary layer of the plant to its abiotic and biotic environment.

6.6. References

- Athoo TO, Winkler A, Knoche M. 2015. Pedicel transpiration in sweet cherry fruit: mechanisms pathways, and factors. *J. Am. Soc. Hortic. Sci.* 140, 136-143.
- Baker EA, Bukovac MJ, Flore JA. 1979. Ontogenetic variations in the composition of peach leaf wax. *Phytochemistry.* 18, 781-784.
- Belge B, Llovera M, Comabella E, Gatus F, Guillén P, Graell J, Lara I. 2014a. Characterization of cuticle composition after cold storage of “Celeste” and “Somerset” sweet cherry fruit. *J. Agric. Food Chem.* 62, 8722-8729.
- Belge B, Llovera M, Comabella E, Graell J, Lara I. 2014b. Fruit cuticle composition of a melting and a nonmelting peach cultivar. *J. Agric. Food Chem.* 62, 3488-3495.
- Bernard J, Joubès J. 2013. *Arabidopsis* cuticular waxes: advances in synthesis, export and regulation. *Prog. Lipid Res.* 52, 110-129.
- Bourgault R, Matschi S, Vasquez M, Qiao P, Sonntag A, Charlebois C, Mohammadi M, Scanlon MJ, Smith LG, Molina I. 2020. Constructing functional cuticles: analysis of relationships between cuticle lipid composition, ultrastructure and water barrier function in developing adult maize leaves. *Ann. Bot.* 125, 79-91.
- Bueno A, Alfarhan A, Arand K, Burghardt M, Deininger A, Hedrich R, Leide J, Seufert P, Staiger S, Riederer M. 2019. Effects of temperature on the cuticular transpiration barrier of two desert plants with water-spender and water-saver strategies. *J. Exp. Bot.* 70, 1613-1625.
- Burghardt M, Riederer M. 2006. Cuticular transpiration. In *Biology of the plant cuticle*. Chapter 9. (ISBN 9781405132688).

Buschhaus C, Herz H, Jetter R. 2007. Chemical composition of the epicuticular and intracuticular wax layers on adaxial sides of *Rosa canina* leaves. *Ann. Bot.* 100, 1557-1564.

Ceccato P, Flasse S, Tarantola S, Jacquemoud S, Grégoire JM. 2001. Detecting vegetation leaf water content using reflectance in the optical domain. *Remote Sens. Environ.* 77, 22-33.

Cheng G, Huang H, Zhou L, He S, Zhang Y, Cheng X. 2019. Chemical composition and water permeability of the cuticular wax barrier in rose leaf and petal: a comparative investigation. *Plant Physiol. Biochem.* 135, 404-410.

Diarte C, Lai PH, Huang H, Romero A, Casero T, Gatiús F, Graell J, Medina V, East A, Riederer M, Lara I. 2019. Insights into olive fruit surface functions: a comparison of cuticular composition, water permeability, and surface topography in nine cultivars during maturation. *Front. Plant Sci.* 19, 1484.

Duursma RA, Blackman CJ, López R, Martin-StPaul NK, Cochard H, Medlyn BE. 2019. On the minimum leaf conductance: its role in models of plant water use, and ecological and environmental controls. *New Phytol.* 221, 693-705.

Eckl K, Gruler H. 1980. Phase transitions in plant cuticles. *Planta* 150, 102-113.

Fernández V, Khayet M, Montero-Prado P, Heredia-Guerrero JA, Liakopoulos G, Karabourniotis G, del Río V, Domínguez E, Tacchini I, Nerín C, Val J, Heredia A. 2011. New insights into the properties of pubescent surfaces: peach fruit as a model. *Plant Physiol.* 156, 2098-2108.

Fich EA, Segerson NA, Rose JKC. 2016. The plant polyester cutin: biosynthesis, structure, and biological roles. *Annu. Rev. Plant Biol.* 67, 207-233.

Graça J, Schreiber L, Rodrigues J, Pereira H. 2002. Glycerol and glyceryl esters of ω -hydroxyacids in cutins. *Phytochemistry* 61, 205-215.

Grncarevic M, Radler F. 1967. The effect of wax components on cuticular transpiration - model experiments. *Planta* 75, 23-27.

Hauke V, Schreiber L. 1998. Ontogenetic and seasonal development of wax composition and cuticular transpiration of ivy (*Hedera helix* L.) sun and shade leaves. *Planta* 207, 67-75.

Hoad SP, Grace J, Jeffrey CE. 1996. A leaf disc method for measuring cuticular conductance. *J. Exp. Bot.* 47, 431-437.

Holloway PJ. 1982. The chemical constitution of plant cutins. In *The plant cuticle*. Pages 45-85.

Huang H, Burghardt M, Schuster AC, Leide J, Lara I, Riederer M. 2017. Chemical composition and water permeability of fruit and leaf cuticles of *Olea europaea* L. *J. Agr. Food Chem.* 65, 8790-8797.

Hunsche M, Noga G. 2011. Cuticular wax load and surface wettability of leaves and fruits collected from sweet cherry (*Prunus avium*) trees grown under field conditions or inside a polytunnel. *Acta Physiol. Plant* 33, 1785-1792.

Isaacson T, Kosma DK, Matas AJ, Buda GJ, He Y, Yu B, Pravitasari A, Batteas JD, Stark RE, Jenks MA, Rose JKC. 2009. Cutin deficiency in the tomato fruit cuticle consistently affects resistance to microbial infection and biomechanical properties, but not transpirational water loss. *Plant J.* 60, 363-377.

Ismail HM, Brown GA, Tucknott OG, Holloway PJ, Williams AA. 1977. Nonanal in epicuticular wax of golden egg plums (*Prunus domestica*). *Phytochemistry* 16, 769-770.

Jetter R, Kunst L, Samuels AL. 2006. Composition of plant cuticular waxes. In *Biology of the plant cuticle*. Chapter 4. (ISBN 978-1-4051-3268-8).

Jetter R, Schäffer S, Riederer M. 2000. Leaf cuticular waxes are arranged in chemically and mechanically distinct layers: evidence from *Prunus laurocerasus* L. *Plant Cell Environ.* 619-628.

Kerstiens G. 1995. Cuticular water permeance of European trees and shrubs grown in polluted and unpolluted atmospheres, and its relation to stomatal response to humidity in beech (*Fagus sylvatica* L.). *New Phytol.* 129, 495-503.

Kerstiens G. 1996. Cuticular water permeability and its physiological significance. *J. Exp. Bot.* 47, 1813-1832.

Kerstiens G. 2006. Water transport in plant cuticles: an update. *J. Exp. Bot.* 57, 2493-2499.

Kirsch T, Kaffarnik F, Riederer M, Schreiber L. 1997. Cuticular permeability of the three tree species *Prunus laurocerasus* L., *Ginkgo biloba* L. and *Juglans regia* L.: comparative investigation of the transport properties of intact leaves, isolated cuticles and reconstituted cuticular waxes. *J. Exp. Bot.* 48, 1035-1045.

Konarska A. 2015. Characteristics of fruit (*Prunus domestica* L.) skin: structure and antioxidant content. *Int. J. Food Prop.* 18, 2487-2499.

Krauss P, Markstädter C, Riederer M. 1997. Attenuation of UV radiation by plant cuticles from woody species. *Plant Cell Environ.* 20, 1079-1085.

Leide J, Hildebrandt U, Reussing K, Riederer M, Vogg G. 2007. The developmental pattern of tomato fruit wax accumulation and its impact on cuticular transpiration barrier properties: effects of a deficiency in a β -ketoacyl-coenzyme A synthase (LeCER6). *Plant Physiol.* 144, 1667-1679.

Leide J, de Souza AX, Papp I, Riederer M. 2018. Specific characteristics of the apple fruit cuticle: investigation of early and late season cultivars 'Prima' and 'Florina' (*Malus domestica* Borkh.). *Sci. Hort.* 229, 137-147.

Leide J, Nierop KGJ, Deininger AC, Staiger S, Riederer M, de Leeuw JW. 2020. Leaf cuticle analyses: implications for the existence of cutan/non-ester cutin and its biosynthetic origin. *Ann. Bot.* 126, 141-162.

López-Casado G, Matas AJ, Domínguez E, Cuartero J, Heredia A. 2007. Biomechanics of isolated tomato (*Solanum lycopersicum* L.) fruit cuticles: the role of the cutin matrix and polysaccharides. *J. Exp. Bot.* 58, 3875-3883.

Martin LBB, Rose JKC. 2014. There's more than one way to skin a fruit: formation and functions of fruit cuticles. *J. Exp. Bot.* 65, 4639-4651.

Merk S, Blume A, Riederer M. 1998. Phase behavior and crystallinity of plant cuticular waxes studied by Fourier transform infrared spectroscopy. *Planta* 204, 44-53.

Nobel PS. 2009. Leaves and fluxes. In *Physicochemical and environmental plant physiology*. Chapter 8. (ISBN 978-0-12-520026-4).

Peschel S, Franke R, Schreiber L, Knoche M. 2007. Composition of the cuticle of developing sweet cherry fruit. *Phytochemistry* 68, 1017-1025.

Philippe G, Geneix N, Petit J, Guillon F, Sandt C, Rothan C, Lahaye M, Marion D, Bakan B. 2020. Assembly of tomato fruit cuticles: a cross-talk between the cutin polyester and cell wall polysaccharides. *New Phytol.* 226, 809-822.

Poynter J, Eglinton G. 1990. Molecular composition of three sediments from Hole 717c: the Bengal fan. *Proc. Ocean Drill. Program Sci. Results* 116, 155-161.

Reina-Pinto JJ, Yephremov A. 2009. Surface lipids and plant defences. *Plant Physiol. Biochem.* 47, 540-549.

Riederer M, Schreiber L. 1995. Waxes: the transport barriers of plant cuticles. In *Waxes: chemistry, molecular biology and functions*. Pages 131-156. (ISBN 9780951417157).

Samuels L, Kunst L, Jetter R. 2008. Sealing plant surfaces: cuticular wax formation by epidermal cell. *Annu. Rev. Plant Biol.* 59, 683-707.

Schönherr J. 1976. Water permeability of isolated cuticular membranes: the effect of cuticular waxes on diffusion of water. *Planta* 131, 159-164.

Schönherr J, Eckl K, Gruler H. 1979. Water permeability of plant cuticles: the effect of temperature on diffusion of water. *Planta* 147, 21-26.

Schönherr J, Lenzian K. 1981. A simple and inexpensive method of measuring water permeability of isolated plant cuticular membranes. *Z. Pflanzenphysiol.* 102, 321-327.

Schreiber L, Schönherr J. 1990. Phase transitions and thermal expansion coefficients of plant cuticles, the effects of temperature on structure and function. *Planta* 182, 186-193.

Schreiber L, Riederer M. 1996. Ecophysiology of cuticular transpiration: comparative investigation of cuticular water permeability of plant species from different habitats. *Oecologia* 107, 426-432.

Schreiber L. 2001. Effect of temperature on cuticular transpiration of isolated cuticular membranes and leaf discs. *J. Exp. Bot.* 52, 1893-1900.

Schreiber L, Skrabs M, Hartmann K, Diamantopoulos P, Simanova E, Šantrůček J. 2001. Effect of humidity on cuticular water permeability of isolated cuticular membranes and leaf disks. *Planta* 214, 274-282.

Schreiber L, Elshatshat S, Koch K, Lin J, Šantrůček J. 2006. AgCl precipitates in isolated cuticular membranes reduce rates of cuticular transpiration. *Planta* 223, 283-290.

Schuster AC, Burghardt M, Alfarhan A, Bueno A, Hedrich R, Leide J, Thomas J, Riederer M. 2016. Effectiveness of cuticular transpiration barriers in a desert plant at controlling water loss at high temperatures. *AoB Plants*, plw027.

Schuster AC, Burghardt M, Riederer M. 2017. The ecophysiology of leaf cuticular transpiration: are cuticular water permeabilities adapted to ecological conditions? *J. Exp. Bot.* 68, 5271–5279.

Staiger S, Seufert P, Arand K, Burghardt M, Popp C, Riederer M. 2019. The permeation barrier of plant cuticles: uptake of active ingredients is limited by very long-chain aliphatic rather than cyclic wax compounds. *Pest Manag. Sci.* 75, 3405-3412.

Storey R, Price WE. 1999. Microstructure of the skin of d'Agen plums. *Sci. Hort.* 81, 279-286.

Tsubaki S, Sugimura K, Teramoto Y, Yonemori K, Azuma JI. 2013. Cuticular membrane of *Fuyu persimmon* fruit is strengthened by triterpenoid nano-fillers. *PLOS ONE* 8, e75275.

Vogg G, Fischer S, Leide J, Emmanuel E, Jetter R, Levy AA, Riederer M. 2004. Tomato fruit cuticular waxes and their effects on transpiration barrier properties: functional characterization of a mutant deficient in a very-long-chain fatty acid β -ketoacyl-CoA synthase. *J. Exp. Bot.* 55, 1401-1410.

Wissemann V, Riedel M, Riederer M. 2007. Matroclinal inheritance of cuticular waxes in reciprocal hybrids of *Rosa* species, sect. *Caninae* (Rosaceae). *Pl. Syst. Evol.* 263, 181-190.

Yeats TH, Rose JKC. 2013. The formation and function of plant cuticles. *Plant Physiol.* 163, 5-20.

Yu MML, Konorov SO, Schulze G, Blades MW, Turner RFB, Jetter R. 2008. *In situ* analysis by microspectroscopy reveals triterpenoid compositional pattern with leaf cuticles of *Prunus laurocerasus*. *Planta* 227, 823-834.

Zeisler V, Schreiber L. 2016. Epicuticular wax on cherry laurel (*Prunus laurocerasus*) leaves does not constitute the cuticular transpiration barrier. *Planta* 243, 65-81.

General discussion

In this Doctoral Thesis, fruit cuticle and cell wall composition of *Olea europaea* L. were studied with the purpose of assessing the effect thereupon of agronomic factors such as cultivar, irrigation regime or cultivation area. To widen the overview of cuticle composition and functions, the composition of cuticular waxes and cutin monomers of fruits and leaves (both adaxial and abaxial sides) of *Prunus laurocerasus* L. was also studied.

SECTION I: A survey of nine olive cultivars

Fruit cuticle and cell wall composition at three maturity stages. Composition of waxes in nine monovarietal olive oils.

In general, a better knowledge of the cuticle and cell wall composition of fruits may help improve postharvest management, since the fruit cuticle plays a paramount role in final fruit quality, shelf life and storage potential. In the case of fruits such as olive, structure and composition of cuticle and cell wall may have an influence over the different stages of the industrial processes required for the manufacture of either table olives or olive oil. This study included nine different Spanish olive fruits cultivars ('Arbequina', 'Argudell', 'Empeltre', 'Farga', 'Manzanilla', 'Marfil', 'Morrut', 'Picual' and 'Sevillanca') at the green, turning and ripe stages. Except for 'Arbequina' (Huang et al., 2017), cutin monomer composition was reported for the first time. All olive fruit samples used were picked from the same orchard, and hence were grown at the same soil type and under the same climactic conditions and cultural practices. Therefore, the chemical and physical differences observed across the nine genotypes considered in the study cannot be ascribed to different environmental conditions, but rather reflect actual cultivar-related differences.

The characterization of olive fruit cuticle composition revealed cultivar- and maturity stage-related differences which are considered in **Chapter I** of this Thesis. Total cuticle yields remained steady throughout fruit maturation of eight out of the nine cultivars studied, with the exception of 'Arbequina' uniquely. Despite similar total cuticle loads along maturation, chemical composition changed during the process as reflected by wax-to-cutin ratios, which declined along fruit ripening due to lowered amounts of cuticular waxes per unit of surface area. This observation is in contrast with a previous report by Huang et al. (2017) that wax-to-cutin ratio of 'Arbequina' fruit cuticles did not change significantly over fruit maturation. This difference could be related to the irrigation conditions and the production area: whereas olives analysed in Huang et al. (2017) were obtained from rain-fed trees grown at El Soleràs (PDO 'Les Garrigues', characterized by low rainfall and extreme temperatures), work described in **Chapter I** (Diarte et al., 2019) was undertaken on olives picked from an irrigated grove at Constantí (PDO 'Siurana'). Indeed, a previous study on grape berries (Dimopoulos et al., 2020) indicated that cuticular wax loads increased under water deficit conditions. Increased amounts of cuticular waxes in water stress conditions were also demonstrated for the model plant *Arabidopsis* (Seo et al., 2011; Lee and Suh, 2015; Patwari et al., 2019).

I.1. Wax and cutin components of olive fruit cuticles during maturation

Triterpenoid acids dominated quantitatively in the cuticular wax fraction, in accordance with observations on other drupe-type fruits such as sweet cherry and peach (Peschel et al., 2007; Belge et al., 2014a, 2014b) and in berry-type fruits such as blueberry (Chu et al., 2016). In contrast, in other fruits including Asian pear as well as many fruit species within the *Solanaceae* family (Lara et al., 2015; Wu

et al., 2017), the cuticular wax fraction is dominated by triterpenoid alcohols. The identity of triterpenoids present is species-dependent: oleanolic acid is the only triterpenoid reported in grapes (Casado and Heredia, 1999), whereas both ursolic and oleanolic acids were found in fruit cuticles from peach and sweet cherry (Pechel et al., 2007; Belge et al., 2014a; Belge et al., 2014b). In olive fruit cuticles, maslinic and oleanolic acids were the most abundant triterpenoid acids detected (**Chapter I**), in agreement with previous observations (Bianchi, 2003; Stiti, Triki and Hartmann, 2007; Guinda et al., 2010). Both compounds display reportedly interesting bioactive properties such as antimicrobial and health-promoting effects (Chouaib et al., 2015; Rodriguez-Rodriguez, 2015; Liou et al., 2019). From a nutritional point of view, this may be relevant for some table olives such as natural black olives, as they will naturally contain important concentrations of triterpenoid acids. Nevertheless, this will be also dependent on the specific treatments applied during the manufacturing process, since triterpenoid acids are soluble in alkaline solutions. For example, a NaOH treatment is used to de-bitter fruits in the course of the production of Spanish-style green olives, which will cause significant losses of maslinic and oleanolic acids from fruits (Romero et al., 2010). At present, maslinic and oleic acid acids are often recovered from by-products of olive oil extraction and of table olive production (olive pomace or wastewaters of NaOH treatments, respectively) for possible applications in the pharmaceutical and food industries (Romero et al., 2010, Blanco-Cabra et al., 2019; Claro-Cala et al., 2020). The evolution of maslinic acid content during fruit ripening showed a declining trend in some cases ('Farga' and 'Picual'), while for other cultivars it increased ('Sevillenca') or remained steady. Contrarily to maslinic acid, the content of oleanolic acid generally declined substantially during the experimental time.

C₂₄ and C₂₆ fatty acids and fatty alcohols were also prominent components of cuticular waxes in olive fruits, but the content of *n*-alkanes was low (0.5 to 4.8 % over total waxes), in contrast to other fruits species where *n*-alkanes represent a major component of cuticular waxes (Lara et al., 2015). Low amounts of *n*-alkanes coincide with previous reports on cuticular waxes of olive fruit (Bianchi, Murelli and Vlahov, 1992; Huang et al., 2017), thus confirming this as a characteristic trait of olive fruit cuticles. The presence of triterpenoids, fatty acids, and *n*-alkanes have been related to antifungal activity in Asian pear (Chen et al., 2014; Li et al., 2014), so the relationship to important fungal diseases of olive fruit such as *Camasporium dalmaticum* or *Verticillium dahliae* would be worth targeting in future investigations. ACL of acyclic wax compounds in all nine olive cultivars studied in this Thesis were lower than those reported for other fruit species, for instance apple or sweet cherry (Leide et al., 2018; Athoo, Winkler and Knoche, 2015). In six out of the nine studied olive cultivars, the ACL of the acyclic compounds decreased along maturation, generally owing to the augment of shorter-chain fatty acids (C_{20:0} and C_{20:1}) and the reduction of long-chain fatty alcohols (C₂₆ and C₂₈). Yet this trend was not common to all nine studied cultivars: no significant changes in ACL along maturation were found for 'Arbequina' or 'Marfil', whereas an increase was observed for 'Morrut' (**Chapter I**).

Additionally, the wax ester profiles were determined in monovarietal olive oils extracted from the same nine cultivars (**Figure 1**). One of the objectives of this additional study (described in **Chapter III**) was to assess whether a part of cuticular waxes may be transferred to the oil upon mechanical extraction. If so, some correspondence between the components of cuticular waxes (**Chapter I**) and oil waxes should be apparent. Results showed that the wax ester fraction recovered from monovarietal oils contained high amounts of diterpene esters, which were not detected within cuticular waxes. In turn, monovarietal oils did not contain detectable amounts of any of the major in quantitative terms cuticular wax compounds, and hence no evidence was obtained of such transference. Even so, data obtained confirmed previous reports that diterpenic esters, formed by a phytol group esterified to a variety of fatty acids,

were the most abundant compound type in olive oil waxes (Mariani, Lucci and Conte, 2018). The metabolic origin of phytyl esters is currently unclear, and future investigations on the biosynthesis of these molecules in plants may thus improve the knowledge on these metabolic pathways and on how the shelf life of olive oils can be altered as a result. On the other hand, analyses showed great disparity in total wax contents among the monovarietal olive oils assessed, ‘Arbequina’ being the cultivar showing the highest concentrations, which were close to the legal limit (150 mg kg^{-1}). This could be related to the fruit size, since smaller fruits have more proportion of cuticle, and wax load per surface area is higher.

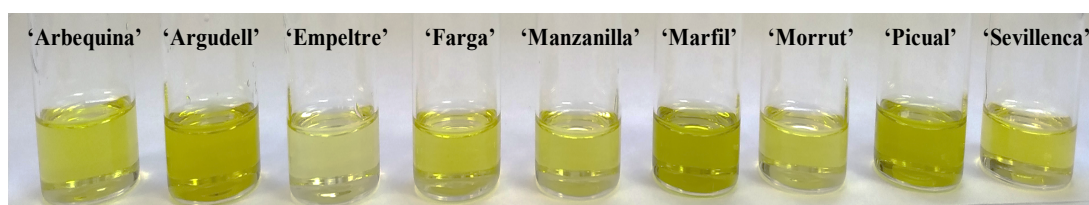


Figure 1. Monovarietal olive oils studied in the present Doctoral Thesis

A full-data PCA model showed this negative correlation (**Figure 2 in Chapter III**), albeit this relationship did not hold for all the studied cultivars, indicating that other factors must be involved in determining total wax content in virgin and extra-virgin olive oils. The PCA model also revealed an association of waxes in oil with ripe and sweetness organoleptic notes. The composition of the wax fraction could help distinguishing between extra-virgin or virgin olive oils and seed oils such as sunflower or canola oil. In contrast, results suggest that the usefulness of wax profiles to discriminate among different monovarietal olive oils be more dubious, since only ‘Picual’ oils showed noticeable differences (both in quantitative and qualitative terms) in comparison with the rest of monovarietal oils studied in this Thesis.

As regards cutin monomers identified in olive fruit cuticles, hydroxy-fatty acids were the predominant compounds detected along fruit ripening, 9/10,16-dihydroxyhexadecanoic acid being the most important of these compounds in ‘Arbequina’, ‘Argudell’, ‘Empeltre’, ‘Farga’, and ‘Sevillena’ fruits. This compound has also been reported as the most abundant ω -hydroxy-acid with mid-chain hydroxyl groups in other fruit species such as mango, pepper, sweet cherry, and tomato (Camacho-Vázquez et al., 2019; Parsons et al., 2012; Peschel et al., 2007; Romero and Rose, 2019, respectively). Some cultivar-associated diversity was however detected, as 9-hydroxyoctadecenoic acid was the most prominent hydroxy-fatty acid in ‘Manzanilla’, ‘Marfil’, ‘Morrut’, and ‘Picual’, which might be regarded as a distinctive trait. Similarly, Leide et al., 2018 investigated fruits of the ‘Florina’ and ‘Prima’ apple cultivars and found that, although the most abundant compound in cutin matrix was also 9/10,16-dihydroxyhexadecanoic acid, C_{18} -type cutin monomers showed a striking accumulation in comparison to C_{16} -type monomers. These differences were even greater in olive fruits considered herein (**Chapter I**).

In addition to hydroxy-fatty acids, α,ω -dicarboxylic and monocarboxylic fatty acids were also prominent quantitatively as major components of the cutin matrix, as reported for peach fruit (Belge et al., 2019). It should be pointed out that a negative relationship between total cutin yields and olive fly (*Bactrocera oleae* Rossi) egg deposition was detected. This might be indicating a possible cultivar-related factor in egg deposition preferences of olive fly females. Furthermore, an association was observed between the percentage of affected olives and the contents of maslinic and oleanolic acids, the most important triterpenoids in quantitative terms in olive fruit cuticles, in agreement with earlier observations that triterpenoid acid amounts were related to olive fly egg deposition (Kombargi, Michelakis and Petrakis, 1998). All these chemical and physical factors, including roughness parameters (**Chapter**

I), and the changes therein along the fruit maturation process, possibly contribute to defining the oviposition preferences of olive fly (Malheiro, 2015). All these findings may lay the foundations for important advances into the development of new strategies to manage this pest.

With the exception of ‘Arbequina’, results showed significant changes in cuticular water permeance along fruit ripening (**Table 3 in Chapter I**), but this parameter was apparently not associated with the different surface characteristics determined in the present Doctoral Thesis, including wax and cutin composition, skin surface topography or cuticle thickness. This may indicate that the permeability of olive fruit cuticles may be affected rather by additional properties such as the physical and biomechanical characteristics of wax and cutin compounds. On the other hand, although cuticle thickness is reportedly not related to cuticle stiffness and deformation (Khanal and Knoche, 2017), it is known that permeability can be directly affected by post-harvest conditions. Unsuitable management, added to pressure increases resulting from cell wall disruption, could decrease the cuticle deformation modulus and lead to an undesirable water movement across this barrier natural barrier (Domínguez et al., 2011; Matas et al., 2005). Besides, previous reports concluded that cuticle thickness could be related to different susceptibility to bruising damage during mechanical harvest among different cultivars (Hammami and Rapoport 2012; Jiménez et al., 2017; Goldental-Cohen et al., 2019). Bruising damage is usually discernible as dark spots on fruit exocarp and mesocarp, and it decreases the commercial value of fruits, especially for table olive consumption. Fruits of ‘Manzanilla’, for instance, which are used preferentially for the manufacture of table olives, display the thinnest cuticles among the nine cultivars studied in this Thesis, and hence the possibility of bruising fruits during harvest implies the unsuitability of mechanical harvest methods such as straddle harvesters used in super high-density orchards. The use of nitrogen atmosphere and commercial coatings has been suggested for the minimisation of bruising damages during harvest of ‘Manzanilla’ olives (Ramírez et al., 2015), which highlights the importance of postharvest management as an aid to keep the commercial quality in some varieties.

I.2. Modifications in cell walls of olive fruit during maturation

Ripening-related cell wall disassembly was studied in all nine olive cultivars through the analysis of changes in cell wall composition and in some pectolytic and non-pectolytic enzyme activities (**Chapter II**). These modifications were accompanied by textural changes in fruits, perceptible as lessened firmness and increased elasticity of fruit skin. Fruits underwent noticeable softening along ripening, driven to a great extent by cell wall-related enzyme activities.

AFase and β -Gal activities, which act respectively on arabinosyl- and galactosyl-rich pectic sidechains, were associated to substantial losses of neutral sugars, and showed different patterns during the maturation process. In blueberries, where in contrast to olive the main neutral sugar is galactose followed by arabinose, no clear trends were observed for β -Gal activity during fruit ripening of different cultivars (‘O’Neal’, ‘Emerald’ and ‘Snowchaser’) (Montecchiarini et al., 2019), showing cultivar-dependent variation. Cultivar-to-cultivar variation for AFase and β -Gal activities was also found in this Thesis among the different olive genotypes considered. For example, AFase activity increased during maturation of ‘Arbequina’, ‘Empeltre’, ‘Farga’, ‘Manzanilla’ and ‘Sevillena’ olives, whereas declining activity levels were found for ‘Argudell’ and ‘Picual’ fruit. Clear augments in β -Gal activity were observed during maturation of ‘Arbequina’, ‘Manzanilla’ and ‘Marfil’ samples uniquely. The action of these two enzymes leads to increased porosity of the cell wall resulting from the removal of a large part of these sidechains, which in turn favours the access of other enzymes (such as PME, PG and PL) to

their pectin backbone substrate. Accordingly, neutral sugar content in the different AIR fractions isolated was variable among the selected cultivars, reflecting these differences. For each specific cultivar, neutral sugar content also varied significantly along fruit maturation, indicating reallocation among AIR fractions along the process.

Altogether, PME, PG, and PL activities showed a decreasing trend during fruit maturation, suggesting an early role in ripening-related cell wall modifications (Mafra et al, 2001; Lara et al., 2018). PME catalyses the demethylation of galacturonic acid residues in the pectin backbone, which has an impact on the degree of methyl esterification of pectins. In the presence of calcium, this demethylating action promotes the establishment of calcium bridges between the negatively-charged free carboxyl groups (egg-box model) (Goulao and Oliveira, 2008), resulting in cell wall reinforcement which prevents extensive firmness loss at early stages of the ripening process. Accordingly, the corresponding PLRS model (**Chapter II, Figure 1**) revealed that fruit firmness was related to PME activity and to calcium content. Yet, calcium content in fruit pericarp declined significantly during maturation, suggesting that calcium loss paved the way for the disassembly of the egg-box structures hence enabling PG and PL to depolymerise polygalacturonans. The apoplastic environment is also modified by PME action, since the scission of methyl groups decreases the pH in the apoplast, which favours pectin hydration and modifies protein diffusion (Grignon and Sentenac, 1991). Additionally, PME action is paramount for PG and PL activities, because these enzymes require previous demethylation of residues to be cleaved. Therefore, and since data show that all three pectin backbone-acting enzyme activities considered herein (PME, PG, PL) were higher in fruits at the green stage, it was concluded that the presence of neutral sugar-containing sidechains in pectins at early maturity stages would prevent the action of those enzymes and extensive firmness loss by precluding access to their substrates, while the presence of significant AFase and β -Gal activity levels would translate in the liberation of neutral sugars at the onset of the maturation process. In accordance, AFase and β -Gal activities were inversely related to fruit firmness. This view agrees with a previous hypothesis (Jiménez et al., 2001) that the degradation of cell wall polysaccharides along ripening of ‘Hojiblanca’ olives be sequential and display preferential loss of particular cell wall polymer constituents at specific maturity stages.

As to non-pectolytic enzymes, β -Xyl and EGase activities were also considered in this Thesis, and their time-course change patterns suggest likewise an early role in cell wall modifications, as they generally decreased along the experimental time. The hemicellulosic fraction of the cell walls contains a range of different types of non-pectic polysaccharides including xyloglucans, xylans, glucomannans and arabinoxylans among others, often decorated with xylose- and galactose-rich sidechains, forms strengthening cross-links with cellulose, and is mostly recovered within the KOH_{sf} . KOH_{sf} yields generally decreased over fruit ripening, in agreement with previous observations of constant xylose losses during ripening of ‘Negrinha do Douro’ olives (Mafra et al., 2001) and with data in **Chapter II** of this Thesis showing that KOH_{sf} yields were related inversely to β -Xyl and EGase activity levels. A previous study on cell wall modifications during ripening of strawberry fruits reported that most cell wall modifications at more mature stages occur in the hemicellulose-cellulose matrix, whereas pectin solubilisation takes place at more green stages (Vicente et al., 2005). In the present Doctoral Thesis, sequential solubilisation of cell wall polysaccharides was reflected in yields and composition of the water-soluble fraction: W_{sf} yields increased along fruit maturation, whereas the uronic acid-to-neutral sugar ratio in this AIR fraction decreased, which indicated preferential loss of neutral sugars from cell wall polymers at early steps of fruit maturation. In accordance with this idea, the uronic acid content in the NaOx_{sf} fraction increased,

suggesting that uronic acids were retained in the chelator-soluble fraction, possibly as a consequence of the establishment of egg-box structures in the presence of high calcium contents.

In connection with the above, a previous study (Agius et al., 2003) indicated that free D-galacturonic acid resulting from cell wall solubilisation be a major precursor for biosynthesis of ascorbic acid in fruits, which agrees with results in **Chapter II** showing augmented ascorbic acid contents in the pericarp of ‘Empeltre’, ‘Farga’, ‘Manzanilla’, ‘Morrut’ and ‘Picual’ olives during fruit ripening. Even so, this trend did not hold for the rest of cultivars studied in this Thesis. Ascorbic acid levels might be involved in fruit ripening-associated cell wall disruption, and hence related to firmness loss (Cheng et al, 2008; Duan et al., 2011; Belge et al., 2017). Ascorbate is believed to impact cell wall disassembly by favouring non-enzymic oxidative scission of cell wall polysaccharides, particularly of xyloglycans. Accordingly, the PLSR model developed showed that ascorbic acid was inversely related to fruit firmness. Moreover, de-esterified pectin is more susceptible to ascorbate-induced scission than methyl-esterified pectin (Agius et al., 2003; Dumville and Fry, 2003), which may represent an additional mechanism for PME impact on cell wall disassembly.

Data indicate that calcium contributed to cell wall reinforcement. This is particularly important for table olives, for which firmness is considered a relevant quality parameter of the final product. In connection with this point, the use of calcium salts (calcium chloride and calcium lactate) has been proved advantageous over sodium chloride for the industrial manufacture of table olives such as black ripe olives (García-Serrano et al., 2020; 2021). Calcium salts reportedly preserved better textural characteristics while avoiding problems with the wastewaters from the olive table factories as well as potential health risks related to high sodium levels in the final product. Some treatments used to produce olive tables such as the black oxidising or the dry-salt processes are also related to olive fruit firmness due to rearrangements and biosynthesis of polysaccharides induced by these procedures (Mafra, Barros and Coimbra, 2006; Cardoso et al., 2008). It has been also shown that it be possible to improve textural attributes of table olives by applying ethylene treatments in dark green olives (Kafkaletou, Fasseas and Tsantili, 2019). This improvement probably arose from the partial reorganization of cell wall polysaccharides caused by stress-induced ethylene in non-climacteric fruits. Therefore, a deeper knowledge of cell wall composition, structure and ripening-related changes in fruit of a wide variety of olive cultivars may help improve textural properties, particularly in those genotypes used preferentially as table olives, for which firmness is an essential quality parameter.

SECTION II: A focus on ‘Arbequina’ olive fruit

Fruit cuticle and cell wall composition of ‘Arbequina’ olives over maturation at two Protected Designations of Origin (PDO) (‘Les Garrigues’ and ‘Siurana’), and the effect of irrigation.

Agronomic factors, such as water stress (Zarrouk et al., 2018), directly affect cuticle properties and, consequently, show be kept in consideration during olive fruit management. Similarly, cell wall composition also undergoes modifications associated for example with fruit ripening, growing conditions and postharvest handling. To improve the knowledge on the impact of environment conditions on the composition of cuticle and cell wall of olive fruits, ‘Arbequina’ fruit samples were studied as a model olive genotype. Olives were produced at two sites in Catalonia covered by two different Protected Designations of Origin (PDO): El Soleràs (PDO ‘Les Garrigues’) and Mas Bové (PDO ‘Siurana’). At both areas, olive trees were either rain-fed or supplied with drip irrigation.

Irrigation regime did not apparently have a significant impact on total cuticle yields (**Chapter IV**). In addition, total cuticle and cutin yields were largely unaffected by maturity stage of fruit, although cutin yields were higher at the latest picking date. In contrast, irrigation-related differences were found for wax yields, albeit an influence of the cultivation site was also observed: higher wax yields were detected for olives produced under rain-fed than under irrigated conditions at El Soleràs (8.9 to 37.1 % and 8.5 to 20.0 % over total cuticle, correspondingly), whereas no clear differences were found for fruits picked from trees grown at Mas Bové (9.2 to 23.9 %). This suggests that cuticular wax deposition increases in response to drought stress, in accordance with reports on leaves of *Arabidopsis thaliana* (Kosma et al., 2009; Seo et al., 2011). Cuticle thickness decreased over maturation of fruit produced at Mas Bové regardless of irrigation regime, while for those grown at El Soleràs cuticle thickness decreased in olives picked from rain-fed trees uniquely, which agrees with previous observations that cuticle thickness of ‘Manzanilla de Sevilla’ olives was similar both at optimal water status and under water stress conditions (Casanova et al., 2019). Toluidine blue (TB) test results revealed the existence of pores on the surface of irrigated fruits grown at El Soleràs, whereas for olives picked from rain-fed trees such surface discontinuities were visible during the first half of October uniquely. These observations suggest a relationship to the water stress resulting from lowered rainfall as compared with September combined with the occurrence of high temperatures in October, when absolute maximum temperatures reached 28 °C. For olives picked from El Soleràs, moreover, significantly increased cutin loads were observed at mid-October in fruits from rain-fed trees, suggesting compositional and structural rearrangements in fruit cuticle in response to climate adversities.

In relation to cuticular waxes, data confirmed results of the previous producing season (**Chapter I**) showing triterpenoids, and mainly maslinic and oleanolic acids, as the predominant components of the wax fraction, together with substantial amounts of fatty acids, fatty alcohols and *n*-alkanes as the major acyclic compound types. The percentage of fatty acids increased along fruit maturation and displayed similar values regardless of production site and irrigation conditions, cerotic acid (C_{26:0}) standing out quantitatively among these compounds. Similar trends were found for fatty alcohols, with hexacosanol (C₂₆), tetracosanol (C₂₄) and octacosanol (C₂₈) as the main representatives. Even so, fruits picked from Mas Bové showed increased fatty alcohol amounts along maturation, especially for C₂₄. Aliphatic wax content in grape cuticles has been shown to increase under water deficiency conditions (Dimopoulos et al., 2020), whereas the opposite, particularly as regards *n*-alkanes, has been observed in the present Thesis for olive fruits (**Chapter IV**). In previous studies on olive fruit cuticle, Huang et al. (2017) reported an increase in *n*-alkanes during the ‘Arbequina’ fruit maturation, while reduced *n*-alkane contents were found during ripening of ‘Meski’ olives (Sakouhi et al., 2011). The content of *n*-alkanes in olive oil also decreased during maturation of fruit from nine different Italian cultivars (Giuffrè 2021). ACL did not display notable differences between El Soleràs and Mas Bové, or between irrigated and rain-fed fruits from whichever site.

Concerning cutin monomers, the main detected types were ω -hydroxy fatty acids followed by monocarboxylic fatty acids and ω -hydroxy fatty acids with midchain hydroxyl groups, hence also confirming data obtained in the preceding season (**Chapter I**). Even so, some differences as regards the predominant cutin monomer types were found in comparison to a previous study on ‘Arbequina’ olive fruits (Huang et al., 2017) reporting that ω -hydroxy fatty acids with midchain hydroxyl groups stood out quantitatively and accounted for 72 to 77 % of total cutin, depending on maturity stage.

The bulk of results obtained in this study show more irrigation-related differences for olive fruits produced at El Soleràs than at Mas Bové. On the basis that El Soleràs is characterized by harsher climate

General discussion

conditions as compared with Mas Bové, it can be concluded that environmental conditions play an important role in determining cuticle properties. Furthermore, the seemingly stronger impact of the environment on cuticular waxes than on cutin loads or cutin monomers suggest a major role for these compounds in the responses to water deficiency.

The same experiment was carried out during the following producing season (2018), and data are displayed within the Annexes section (**Tables A1 – A5**). Fruit samples were obtained from the same producing areas as in **Chapter IV**, and in both cases trees either remained rain-fed or were supplied with drip irrigation. For the sake of clarity, these data are not discussed jointly with those obtained during the previous (2017) season (**Chapter IV** of this Thesis), but some differences were found in the relative amounts (percentage over total cuticle) of the different wax and cutin compounds identified in fruit cuticles during the ripening process. Even so, in order to include and to discuss the producing season as an agronomic factor, more producing seasons need to be considered, which would allow to carefully examine the impact of the meteorological phenomena on the composition and properties of fruit cuticles. For example, monthly temperature and rainfall in 2017 and in 2018 showed some differences. Specifically, total rainfall was higher in 2018 than in 2017 at both locations (443.8 vs. 318.0 mm at el Soleràs, and 848.4 vs. 339.9 mm at Mas Bové, respectively). Therefore, more replications of the experiment would be required before drawing conclusions on the influence of these factors on the definition of cuticle characteristics, which are known to be highly influenced by the environment, and particularly by temperature and humidity.

Time-course changes in cell wall composition during fruit maturation under rain-fed or irrigated conditions was also assessed in ‘Arbequina’ olives picked from both PDOs in 2017 (**Chapter V**). AFase activity levels increased during fruit maturation, and were highest in olives obtained from El Soleràs, in PDO ‘Les Garrigues’. This tendency was related to yields of the water-soluble fraction which augmented significantly over the first samplings, reflecting the gradual solubilisation of cell wall polysaccharides from very early maturity stages. In accordance with AFase activity trends, neutral sugar content in AIR decreased, particularly in samples picked from rain-fed trees, maybe in association with faster softening rates in these fruit at early sampling dates. The early role for PME activity in ripening-related cell wall modifications observed in fruit samples of different cultivars during the previous season (**Chapter II**) was also confirmed in this study. The degree of pectin esterification generally decreased along fruit maturation, with the exception of a transient rise at P5-P6 stages which may indicate the deposition of new cell wall materials as fruit size was still increasing, and which was followed by a similar temporary rise in PME activity at P6-P7 stages.

PG and PL activities displayed similar change trends, data suggesting a direct relationship to the progressive loss of uronic acids at later maturity stages as also observed during the preceding season (**Chapter II**). On the whole, results suggest that uronic acid loss may be relevant in cell wall disassembly chiefly at later phases of fruit ripening. This study likewise reasserted the previous observations for non-pectolytic β -Xyl and EGase activities (**Chapter II**), which declined with fruit maturation hence indicating an early role in fruit firmness changes. Particularly, an inverse correlation between β -Xyl activity and KOH_{sf} yields was observed, suggestive of an actual role in ripening-related changes in this AIR fraction. Interestingly, β -Xyl activity levels were significantly higher in rain-fed than in irrigated samples from early sampling dates.

Total phenolics contents were significantly higher in rain-fed than in irrigated fruit produced at El Soleràs (PDO ‘Les Garrigues’), suggesting that water stress scarcity led to higher biosynthesis of these compounds, as reported for olive leaves (Petridis et al., 2012; Mechri et al., 2020), even though in other

instances the opposite has been observed (García et al., 2020; Valente et al., 2020). Even so, no clear differences were detected between fruits from rain-fed and irrigated trees grown in Mas Bové (PDO ‘Siurana’). These discrepancies may relate to the environmental conditions being harsher and more extreme at PDO ‘Les Garrigues’. Indeed, water loss was more intense in olives produced at El Soleràs than at Mas Bové (around 25 and 14%, correspondingly).

The bulk of results reported in Chapters IV and V suggest that ripening-related changes in fruit cuticle and cell wall composition were dependent to a certain extent on agronomic factors. The impact of irrigation was particularly perceptible in El Soleràs (PDO ‘Les Garrigues’), possibly in connection with more extreme climate conditions therein. Even so, it is important to highlight that such studies need to be undertaken during more producing seasons and on a wider choice of genotypes in order to acquire a clear overview and to draw firm conclusions on the influence of the environment on these changes.

SECTION III: Inter-specific variation in cuticle features: *Prunus laurocerasus* L. and *Actinidia* spp. as examples

Chemical, structural and functional study of leaf and fruit cuticles. A comparison with *Olea europaea* L.

Prunus laurocerasus L. is an evergreen used as a model plant, and its fruit is a drupe like olive fruit. In the course of a research stay at the University of Würzburg (Germany) related to the present Doctoral Thesis, cuticles of *P. laurocerasus* fruits (at the green, red and black maturity stages) and leaves (adaxial and abaxial sides) were studied (**Chapter VI**). In this way, not only species- and maturity- but also organ-related differences were examined. *P. laurocerasus* is native to temperate regions characterized by cold temperatures during winter and a moderately humid climate. Fruits and leaves were harvested from plants grown at the Botanical Garden of Würzburg University. Hence, differences in cuticle composition between *P. laurocerasus* and *O. europaea* fruits may be also related to different climate, rainfall or soil in both producing areas.



Figure 2. ‘Hayward’ (left) and ‘Jintao’ (right) kiwifruit (*Actinidia* spp.) cultivars

Moreover, in a collaborative study with Massey University (Palmerston North, New Zealand), a preliminary study on fruit cuticle composition of kiwifruit (*Actinidia* spp.) was carried out. Cultivars ‘Hayward’ (*Actinidia deliciosa* (A. Chev.) C.F. Liang & A.R. Ferguson) and ‘Jintao’ (*Actinidia chinensis* Planch.) were selected for this study (**Figure 2**). ‘Hayward’ is the most widely grown kiwifruit cultivar around the world, and produces hairy, green-fleshed fruits. In contrast, ‘Jintao’ fruits are hairless and yellow-fleshed, and their commercial production is more recent than that of ‘Hayward’. The cultivar

originated from wild vines in southeast China, but it is cultivated currently in Italy and in other European countries as it adapts well to colder Mediterranean areas.

III.1. Species-related variety in the chemical composition of fruit cuticles

The quantitatively predominant cuticular wax components and cutin monomers in kiwifruit were very different than those in *P. laurocerasus* and olive fruit, particularly as regards waxes (Table 1). It should be stressed that cuticle composition of kiwifruit has not been described in any previous publication, and hence that to the best of our knowledge this information is reported for the first time.

Table 1. Main components of cuticular waxes and cutin monomers in fruits of four species.

Species	Predominant wax components	Predominant cutin monomers
<i>Olea europaea</i> cv. 'Arbequina'	Triterpenoid acids (maslinic and oleanolic acids)	ω -hydroxy fatty acids (9/10,16-dihydroxy C _{16:0} ; and 9-hydroxy C _{18:1}) α,ω - dicarboxylic fatty acids (1,18-dicarboxy C _{18:1})
<i>Prunus laurocerasus</i> cv. 'Herbergii'	Triterpenoid acids (ursolic acid)	ω -hydroxy fatty acids (9/10,16-dihydroxy C _{16:0} ; 9,10-epoxy 18-hydroxy C _{18:X} ; and 9,10,18-trihydroxy C _{18:X}) Monocarboxylic fatty acids at the black stage (C _{16:X} and C _{18:X}) uniquely
<i>Actinidia deliciosa</i> cv. 'Hayward' (hairy)*	Fatty acids (lignoceric acid)	α,ω - dicarboxylic fatty acids (1,18-dicarboxy C _{18:1}) ω -hydroxy fatty acids (18-hydroxy C _{18:1})
<i>Actinidia chinensis</i> cv. 'Jintao' (hairless)*	Sterols (α -tocopherol)	Monocarboxylic fatty acids (C ₁₆ , C _{18:0} , C ₂₂ , C ₂₄ and C ₂₆ acids) α,ω - dicarboxylic fatty acids (1,18-dicarboxy C _{18:1}) ω -hydroxy fatty acids (18-hydroxy C _{18:1})

* Unpublished data

In olive and *P. laurocerasus* fruit, triterpenoid acids and ω -hydroxy fatty acids were the most common wax and cutin monomer types, respectively. Interestingly, while the main components of cuticular waxes and cutin monomer types in olive fruit were the same across all nine cultivars assessed, substantial differences were detected between both kiwifruit species studied. In fruit of *A. deliciosa* cv. 'Hayward', fatty acids were the most important cuticular wax compounds in terms of percentage (46.2% over total waxes), while α,ω -dicarboxylic fatty acids and ω -hydroxy fatty acids were the predominant cutin components (30.7 and 28.3% over total cutin, respectively). In *A. chinensis* cv. 'Jintao' fruit, in contrast, sterols were the main wax compounds in quantitative terms (43.8 %), whereas monocarboxylic fatty acids, α,ω -dicarboxylic fatty acids and ω -hydroxy fatty acids were the most abundant cutin monomer types (29.1, 22.2 and 21.1%, in the same order).

The surface of 'Hayward' kiwifruit presents numerous trichomes and the fruit is characteristically hairy, while 'Jintao' fruit lacks trichomes and is therefore hairless. These epidermal structures are unicellular or multicellular appendages that develop outwards on the surface of several plant organs, and protect the organ in front of abiotic and biotic stress (Werker, 2000). A previous study on a non-melting,

hairy peach cultivar ('Calrico') demonstrated differences in wax and cutin composition in isolated trichomes in comparison with the rest of fruit surface (Fernández et al., 2011). Hence the question arises whether compositional differences detected between both kiwifruit species considered could be linked to the presence of trichomes on the surface of 'Hayward' fruit. Additionally, 'Hayward' fruit used in this study were harvested in New Zealand, whereas 'Jintao' fruit were produced in Italy. Therefore, the agronomic and climatic differences between both producing areas, as well as shipping conditions, may also have had an impact on cuticle features.

Regarding waxes, the main discrepancies among the four fruit species considered herein referred to triterpenoid acids. Maslinic and oleanolic acids were the most common triterpenoid acids detected in olive fruits, whereas ursolic acid predominated in *P. laurocerasus* fruits. In contrast, no triterpenoid acids were found in 'Jintao' kiwifruit, and only very marginally in 'Hayward' samples. This difference is interesting, as high triterpenoid content has been suggested to help physical strengthening of the cuticle (Tsubaki et al., 2013; Schuster et al., 2016). Therefore, other mechanisms and/or compounds must contribute to this trait in kiwifruit. The predominant cuticular wax compounds in 'Jintao' and 'Hayward' kiwifruit were α -tocopherol and lignoceric acid, respectively.

Differences were observed likewise for cutin monomers: 9/10,16-dihydroxyhexadecanoic, 9-hydroxyoctadecenoic, and 1,18-octadecenedioic acid acids predominated quantitatively in olives, 9/10,16-dihydroxyhexadecanoic, 9,10-epoxy 18-hydroxyoctadecanoic and 9,10,18-trihydroxyoctadecanoic acids in *P. laurocerasus* fruits, and 1,18-octadecenedioic acid in kiwifruit. Therefore, as for cuticular waxes, olives and *P. laurocerasus* fruit (both of them drupes) displayed more similarities between them in comparison to kiwifruits (berry-type fruits). A noticeable difference in cutin composition between *P. laurocerasus* and olive fruits was the presence of 3,4-dihydroxycinnamic acid (caffeic acid) in the former, an intermediate in the biosynthesis of lignin (Boerjan et al., 2003). Furthermore, the accumulation of this compound along fruit ripening, together with that of hexadecanoic and octadecanoic acids led to increased cutin yields at the last stage of maturation (**Chapter VI**). Contrarily, changes in cutin yields over maturation of olive fruit displayed different trends among cultivars. Nevertheless, in all nine studied olive cultivars as well as in *P. laurocerasus*, monocarboxylic C₁₆ and C₁₈ fatty acids and ω -hydroxy fatty acids generally increased in the cutin matrix during fruit ripening, in accordance with published studies on sweet cherry and tomato (Peschel et al., 2007; Leide et al., 2007). In contrast, reduced contents of 10,16-dihydroxyhexadecanoic acid, the most abundant cutin monomer in mango fruit, were found during maturation in a range of different cultivars (Camacho-Vázquez et al., 2019). These findings clearly show species-related variations in time-course evolution of cutin constituents during fruit ripening.

III.2. Organ-related variety in the chemical composition of plant cuticles

Leaves and fruits of *P. laurocerasus* were studied in order to assess organ-related specificities in cuticle composition. Interestingly, the abaxial side of leaves and black fruits displayed similar wax and cutin yields, whereas cuticle loads on the adaxial leaf side were greater. This may relate to the presence of stomata on leaves, which is restricted to the adaxial side uniquely. As in fruits, ursolic acid was the main cuticular wax compound in leaves. Besides, *n*-alkanes were quantitatively prominent in leaves, particularly on the adaxial side, being the principal aliphatic wax compound class (53 and 42% on the adaxial and the abaxial sides, respectively). Differences between both leaf sides regarding total cutin yields, concentration of aliphatic compounds and hydroxycinnamic acids might reflect differences in some characteristics or functions, as toughness or antimicrobial protection (Isaacson et al., 2019; Reina-

General discussion

Pinto and Yephremov, 2009). In contrast, *n*-alkane content in fruits was lower than that in leaves, fatty acids being the most abundant aliphatic wax compounds (42% over total waxes). In olive fruit, *n*-alkanes constituted the second wax fraction in percentage over total cuticular waxes, although levels were below those in *P. laurocerasus* fruits. It has been suggested that *n*-alkanes be more effective in the prevention of water loss in comparison to acids (Grncarevic and Radler, 1967), and leaves may display better water exchange mechanisms than other plant organs. This assertion was demonstrated by assessing minimum water conductance values in fruits and leaves (**Chapter VI**). For example, cuticular permeance to water (**Chapters I and VI**) did not change significantly during maturation of either *P. laurocerasus* or olive fruits, and values ranged between 6 and $11 \times 10^{-5} \text{ m s}^{-1}$ in both cases. In contrast, water permeance of *P. laurocerasus* leaf cuticles was lower (around $2 \times 10^{-5} \text{ m s}^{-1}$), in accordance with previous observations on ‘Arbequina’ olive leaves (Huang et al., 2017).

In addition to the important role of *n*-alkanes in preventing unrestricted water loss, water permeability may be regulated by different cuticle characteristics as the presence of stomata or surface discontinuities, the wax-to-cutin ratio and ACL of acyclic wax compounds. For example, cuticular waxes are believed to provide an essential barrier which protects plant organs from uncontrolled water loss, whereas the cutin matrix reportedly plays an important role on the biomechanical integrity of fruits and leaves (Samuels, Kunst and Jetter, 2018; Isaacson et al., 2009). The ACL was lower in olive (24 to 26) than in *P. laurocerasus* fruits (29 to 30). Regarding organ-to-organ differences, ACL values in the fruits of *P. laurocerasus* were below those in the leaves (32 and 33 on the adaxial and abaxial sides, respectively). Even though no analyses of olive leaves were undertaken in this Doctoral Thesis, these data agree with a previous study on ‘Arbequina’ (Huang et al., 2017) reporting similar values (26 to 28 in fruits and 30 in leaves). These values hence reflect the higher content of longer-chain acyclic wax compounds in leaves than in fruits, and suggest that higher ACL be beneficial for waterproofing characteristics of cuticular waxes by reinforcing their barrier properties (Jetter and Rieder, 2016). *P. laurocerasus* are perennial plants bearing hypostomatous and large leaves, and they are therefore more exposed than fruit to different abiotic and biotic factors during the seasonal course. In this context, higher ACL values would be expected to protect the organ. This idea agrees with minimum conductance data, showing statistically lower values for leaves ($1 \times 10^{-5} \text{ m s}^{-1}$) than for fruits (around $8 \times 10^{-5} \text{ m s}^{-1}$). For olive fruits studied in this Doctoral Thesis, cuticular permeability in fruit of ‘Arbequina’, ‘Empeltre’, ‘Farga’, ‘Manzanilla’, ‘Picual’ and ‘Morrut’ were comparable to those in fruit of *P. laurocerasus*, whereas values were higher for ripe fruit of ‘Argudell’, ‘Marfil’ and ‘Morrut’ ($1 \times 10^{-4} \text{ m s}^{-1}$). Yet no apparent relationship was found between ACL and water permeability in olive fruits. Even so, previous studies suggest that very long-chain aliphatic wax compounds are the main determinants of water permeability of cuticles (Riederer and Schreiber 1995; Voggt et al., 2004). Finally, the study of *P. laurocerasus* leaves indicated that temperature is an important environmental aspect having an impact on plant cuticle features, in accordance with reports that temperatures beyond 40 °C cause cuticle changes (Schreiber, 2001), possibly as a consequence of physical rearrangements of cuticular waxes as their melting range is approached.

References

Agius F, González-Lamothe R, Caballero JL, Muñoz-Blanco J, Botella MA, Valpuesta V. 2003. Engineering increased vitamin C levels in plants by overexpression of a D-galacturonic acid reductase. *Nat. Biotechnol.* 21, 177-181.

Athoo TO, Winkler A, Knoche M. 2015. Pedicel transpiration in sweet cherry fruit: mechanisms, pathways, and factors. *J. Am. Hortic. Sci.* 140, 136-143.

Belge B, Llovera M, Comabella E, Graell J, Lara I. 2014a. Fruit cuticle composition of a melting and nonmelting peach cultivar. *J. Agric. Food Chem.* 62, 3488-3495.

Belge B, Llovera M, Comabella E, Gatus F, Guillén P, Graell J. 2014b. Characterization of cuticle composition after cold storage of ‘Celeste’ and ‘Somerset’ sweet cherry fruit. *J. Agric. Food. Chem.* 62, 8722-8729.

Belge B, Goulao LF, Comabella E, Graell J, Lara I. 2017. Refrigerated storage and calcium dips of ripe ‘Celeste’ sweet cherry fruit: combined effects on cell wall metabolism. *Sci. Hortic.* 219, 182-190.

Belge B, Goulao LF, Comabella E, Graell J, Lara I. 2019. Postharvest heat and CO₂ shocks induce changes in cuticle composition and cuticle-related gene expression in ‘October Sun’ peach fruit. *Post-harvest Biol. Technol.* 148, 200-207.

Bianchi G, Murelli C, Vlahov G. 1992. Surface waxes from olive fruits. *Phytochemistry.* 31, 3503-3506.

Bianchi G. 2003. Lipids and phenol in table olives. *Eur. J. Lipid Sci. Technol.* 105, 229-242.

Blanco-Cabra N, Vega-Granados K, Moya-Andérico L, Vukomanovic M, Parra A, Álvarez de Cienfuegos L, Torrents E. 2019. Novel oleanolic and maslinic acid derivatives as a promising treatment against bacterial biofilm in nosocomial infections: an in vitro and in vivo study. *ACS Infect. Dis.* 5, 1581-1589.

Boerjan W, Ralph J, Baucher M. 2003. Lignin biosynthesis. *Annu. Rev. Plant Biol.* 54, 519-546.

Camacho-Vázquez C, Ruiz-May E, Guerrero-Analco JA, Elizalde-Contreras JM, Enciso-Ortiz EJ, Rosas-Saito G. 2019. Filling gaps in our knowledge on the cuticle of mangoes (*Mangifera indica*) by analyzing six fruit cultivars: architecture/structure, postharvest physiology and possible resistance to fruit fly (Tephritidae) attack. *Postharvest Biol. Technol.* 148, 83-96.

Cardoso SM, Mafra I, Reis A, Georget DMR, Smith AC, Waldron KW, Coimbra MA. 2008. Effect of dry-salt processing on the textural properties and cell wall polysaccharides of cv. *Thasos* black olives. *J. Sci. Food Agric.* 88, 2079-2086.

Casado CG, Heredia A. 1999. Structure and dynamic of reconstituted cuticular waxes of grape berry cuticle (*Vitis vinifera* L.) *J. Exp. Bot.* 50 175-182.

Casanova L, Corell M, Suárez MP, Rallo P, Martín-Palomo MJ, Morales-Sillero A, Moriana A, Jiménez MR. 2019. Bruising response in ‘Manzanilla de Sevilla’ olives to RDI strategies based on water potential. *Agric. Water Manag.* 222, 265-273.

Chen S, Li Y, Bi Y, Yin Y, Ge Y, Wang Y. 2014. Solvent effects on the ultrastructure and chemical composition of cuticular and its potential bioactive role against *Alternaria alternata* in Pingguoli pear. *J. Integr. Agric.* 13, 1137-1145.

Cheng G, Duan X, Shi J, Lu W, Luo Y, Jiang W, Jiang Y. 2008. Effects of reactive oxygen species on cellular wall disassembly of banana fruit during ripening. *Food Chem.* 109, 319-324.

Chouaib K, Hichri F, Nguir A, Daami-Remadi M, Elie N, Touboul D, Jannet HB, Hamza MA. 2015.

General discussion

Semi-synthesis of new antimicrobial esters from the natural oleanolic and maslinic acids. *Food Chem.* 183, 8-17.

Chu W, Gao H, Cao S, Fang X, Chen H, Xiao S. 2016. Composition and morphology of cuticular wax in blueberry (*Vaccinium spp.*) fruits. *Food Chem.* 219, 436-442.

Claro-Cala C, Quintela JC, Pérez-Montero M, Miñano J, de Sotomayor MA, Herrera MD, Rodríguez-Rodríguez R. 2020. Pomace olive oil concentrated in triterpenic acids restores vascular function, glucose tolerance and obesity progression in mice. *Nutrients.* 12, 323.

Dimopoulos N, Tindjau R, Wong DCJ, Matzat T, Haslam T, Song C, Gambetta GA, Castellarin SM. 2020. Drought stress modulates cuticular waxes composition of the grape berry (*Vitis vinifera* L.). *J. Exp. Bot.* 71, 3126-3141.

Domínguez E, López-Casado G, Cuartero J, Heredia A. 2008. Development of fruit cuticle in cherry tomato (*Solanum lycopersicum*). *Funct. Plant Biol.* 35, 403-411.

Duan X, Zhang H, Zhang D, Sheng J, Lin H, Jiang Y. 2011. Role of hydroxyl radical in modification of cell wall polysaccharides and aril breakdown during senescence of harvested longan fruit. *Food Chem.* 128, 203-207.

Dumville JC, Fry SC. 2003. Solubilisation of tomato fruit pectins by ascorbate: A possible non-enzymic mechanism of fruit softening. *Planta.* 217, 951-961.

Fernández V, Khayet M, Montero-Prado P, Heredia-Guerrero A, Liakopoulos G, Karabourniotis G, del Río V, Domínguez E, Tacchini I, Nerín C, Val J, Heredia A. 2011. New insights into the properties of pubescent surfaces: peach fruit as a model. *Plant physiol.* 156, 2098-2108.

García JM, Hueso A, Gómez-del-Campo M. Deficit irrigation during the oil synthesis period affects olive oil quality in high-density orchards (cv. Arbequina). *Agric. Water Manag.* 230, 105858.

García-Serrano P, Romero C, García-García P, Brenes M. 2021. Influence of the type of calcium salt on the cation absorption and firmness of black ripe olives. *Int. J. Food Sci. Technol.* 56, 919-926.

García-Serrano P, Romero C, Medina E, García-García P, de Castro A, Brenes M. 2020. Effect of calcium on the preservation of green olives intended for black ripe olive processing under free-sodium chloride condition. *LWT.* 118, 108870.

Goldental-Cohen S, Biton I, Many Y, Ben-Sason S, Zemach H, Avidan B, Ben-Ari G. 2019. Green olive browning differ between cultivars. *Front. Plant Sci.* 10, 1260.

Goulao LF, Oliveira CM. 2008. Cell wall modification during fruit ripening: when a fruit is not the fruit. *Trens Food Sci. Technol.* 19, 4-25.

Grignon C, Sentenac H. 1991. pH and ionic conditions in the apoplast. *Annu. Rev. Plant Physiol. Plant Mol. Biol.* 42, 103-128.

Grncarevic M, Radler F. 1967. The effect of wax components on cuticular transpiration model experiments. *Planta.* 75, 23-27.

Guinda A, Rada M, Delgado T, Gutiérrez-Adán P, Castellano JM. 2010. Pentacyclic triterpenoids from olive fruit and leaf. *J. Agric. Food Chem.* 58, 9685-9691.

Hammami SBM, Rapoport HF. 2012. Quantitative analysis of cell organization in the external region of the olive fruit. *Int. J. Plant Sci.* 173, 993-1004.

Huang H, Burghardt M, Schuster A, Leide J, Lara I, Riederer M. 2017. Chemical Composition and Water Permeability of Fruit and Leaf Cuticles of *Olea europaea* L. *J. Agric. Food Chem.* 65, 8790-8797.

Isaacson T, Kosma DK, Matas AJ, Buda GJ, He Y, Yu B, Pravitasari A, Batteas JD, Stark RE, Jenks MA, Rose JKC. 2009. Cutin deficiency in the tomato fruit cuticle consistently affects resistance to microbial infection and biomechanical properties, but not transpirational water loss. *Plant J.* 60, 363-377.

Jetter R, Riederer M. 2016. Localization of the transpiration barrier in the epi- and intracuticular waxes of eight plant species: water transport resistances are associated with fatty acyl rather than alicyclic components. *Plant Physiol.* 170, 921-934.

Jiménez A, Rodríguez R, Fernández-Caro I, Guillén R, Fernández-Bolaños J, Heredia A. 2001. Olive fruit cell wall: Degradation of pectic polysaccharides during ripening. *J. Agric. Food Chem.* 49, 409-415.

Jiménez MR, Casanova L, Suárez MP, Rallo P, Morales-Sillero A. 2017. Internal fruit damage in table olive cultivars under superhigh-density hedgerows. *Postharvest Biol. Technol.* 132, 130-137.

Kafkaletou M, Fasseas C, Tsantili E. 2019. Increased firmness and modified cell wall composition by ethylene were reversed by the ethylene inhibitor 1-methylcyclopropene (1-MCP) in the non-climacteric olives harvested at dark green stage - Possible implementation of ethylene for olive quality. *J. Plant Physiol.* 238, 63-71.

Khanal BP, Knoche M. 2017. Mechanical properties of cuticles and their primary determinants. *J. Exp. Bot.* 68, 5351-5367.

Kombargi WS, Michelakis SE, Petrakis CA. 1998. Effect of olive surface waxes on oviposition by *Bactrocera oleae* (Diptera: Tephritidae). *J. Econ. Entomol.* 91, 993-998.

Kosma DK, Bourdenx B, Bernard A, Parsons EP, Lü S, Joubès J, Jenks MA. 2009. The impact of water deficiency on leaf cuticle lipids of *Arabidopsis*. *Plant Physiol.* 151, 1918.

Lara I, Albrecht R, Comabella E, Riederer M, Graell J. 2018. Cell-wall metabolism of 'Arbequina' olive fruit picked at different maturity stages. *Acta Hortic.* 1199, 133-138.

Lee SB, Suh MC. 2015. Advances in the understanding of cuticular waxes in *Arabidopsis thaliana* and crops species. *Plant Cell Rep.* 34, 557-572.

Leide J, Hildebrandt U, Reussing K, Riederer M, Vogg G. 2007. The developmental pattern of tomato fruit wax accumulation and its impact on cuticular transpiration barrier properties: effects of a deficiency in a β -Ketoacyl-coenzyme A synthase (LeCER6). *Plant Physiol.* 144, 1667-1679.

Leide J, de Souza AX, Papp I, Riederer M. 2018. Specific characteristics of the apple fruit cuticle: investigation of early and late season cultivars 'Prima' and 'Florina' (*Malus domestica* Borkh). *Sci. Hortic.* 229, 137-147.

Li Y, Yin Y, Chen S, Bi Y, Ge Y. 2014. Chemical composition of cuticular waxes during fruit development of Pinguoli pear and their potential role on early events of *Alternaria alternata* infection. *Funct. Plant. Biol.* 41, 313-320.

General discussion

Liou CJ, Dai YM, Wang CL, Fang LW, Huang WC. 2019. Maslinic acid protect against obesity-induced non-alcoholic fatty liver disease in mice through regulation of the Sirt1/AMPK signaling pathway. *FASEB J.* 33, 11791-11803.

Mafra I, Lanza B, Reis A, Marsilio V, Campestre C, De Angelis M, Coimbra MA. 2001. Effect of ripening on texture, microstructure and cell wall polysaccharide composition of olive fruit (*Olea europaea*). *Physiol. Plant.* 111, 439-477.

Mafra I, Barros AS, Coimbra MA. 2006. Effect of black oxidising table olive process on the cell wall polysaccharides of olive pulp (*Olea europaea* L. var. Negrinha do Douro). *Carbohydr. Polym.* 65, 1-8.

Malheiro R. 2015. Olive fruit fly (*Bactrocera oleae* Rossi) – olive tree interactions: Study of physical and chemical aspects. PhD dissertation. Universidade do Porto, Portugal.

Mariani C, Lucci P, Conte L. 2018. Identification of phytyl vaccinate as a major component of wax ester fraction of extra virgin olive oil. *Eur. J. Lipid Sci.* 120, 1800154.

Matas AJ, López-Casado G, Cuartero J, Heredia A. 2005. Relative humidity and temperature modify the mechanical properties of isolated tomato fruit cuticles. *Am. J. Bot.* 92, 462-468.

Mechri B, Tekaya M, Hammami M, Chehab H. 2020. Effect of drought stress on phenolic accumulation in greenhouse-grown olive trees (*Olea europaea*). *Biochem. Syst. Ecol.* 92, 104112.

Montecchiarini ML, Bello F, Rivadeneira MF, Vázquez D, Podestá FE, Tripodi KEJ. 2018. Metabolic and physiologic profile during the fruit ripening of three blueberries highbush (*Vaccinium corymbosum*) cultivars. *J. Berry Res.* 8, 177-192.

Parsons EP, Popovsky S, Lohrey GT, Lü S, Alkalai-Tuvia S, Perzelan Y. 2012. Fruit cuticle lipid composition and fruit post-harvest water loss in an advanced backcross generation of pepper (*Capsicum* sp.). *Physiol. Plant.* 146, 15-25.

Patwari P, Salewski V, Gutbrod K, Kreszies T, Dresen-Scholz B, Peisker H, Steiner U, Meyer AJ, Schreiber L, Dörmann P. 2019. Surface wax esters contribute to drought tolerance in Arabidopsis. *Plant J.* 98,727-744

Peschel S, Franke R, Schreiber L, Knoche M. 2007. Composition of the cuticle of developing sweet cherry fruit. *Phytochemistry.* 68, 1017-1025.

Petridis A, Therios I, Samouris G, Koundouras S, Giannakoula A. 2012. Effect of water deficit on leaf phenolic composition, gas exchange, oxidative damage and antioxidant activity of four Greek olive (*Olea europaea* L.) cultivars. *Plant Physiol. Biochem.* 60, 1-11.

Ramírez E, Sánchez AH, Romero C, Brenes M. 2015. Combined use of nitrogen and coatings to improve the quality mechanically harvested Manzanilla olives. *Food Chem.* 171, 50-55.

Reina-Pinto JJ, Yephremov A. 2009. Surface lipids and plant defences. *Plant Physiol. Biochem.* 47, 540-549.

Riederer M, Schreiber L. 1995. Waxes: the transport barriers of plant cuticles, in: Hamilton RJ (Ed), *Waxes: chemistry, molecular biology and functions*. The Oily Press, Dundee, pp. 131-156.

Rodríguez-Rodríguez R. 2015. Oleanolic acid and related triterpenoids from olives on vascular

function: Molecular mechanism and therapeutic perspectives. *Curr. Med. Chem.* 22, 1414-1425.

Romero C, García A, Medina E, Ruíz-Méndez MV, de Castro A, Brenes M. 2010. Triterpenic acids in table olives. *Food Chem.* 118, 670-674.

Romero P, Rose JKC. 2019. A relationship between tomato fruit softening, cuticle properties and water availability. *Food Chem.* 295, 300-310.

Sakouhi F, Herchi W, Sbei K, Absalon C, Boukhchina. Characterisation and accumulation of squalene and *n*-alkanes in developing Tunisian *Olea europaea* L. fruits. *Int. J. Food Sci. Technol.* 46, 2281-2286.

Samuels L, Kunst L, Jetter R. 2008. Sealing plant surfaces: cuticular wax formation by epidermal cells. *Annu. Rev. Plant Biol.* 59, 683-707.

Schreiber L, Sckrabs M, Hartmann K, Diamantopoulos P, Simanova E, Šantrůček J. 2001. Effect of humidity on cuticular water permeability of isolated cuticular membranes and leaf disks. *Planta.* 214, 274-282.

Schuster AC, Burghardt M, Alfarhan A, Bueno A, Hedrich R, Leide J, Thomas J, Riderer, M. 2016. Effectiveness of cuticular transpiration barriers in a desert plant at controlling water loss at high temperatures. *AoB Plants.* plw027.

Seo PJ, Lee SB, Suh MC, Park MJ, Go YS, Park CM. 2011. The MYB96 transcription factor regulates cuticular wax biosynthesis under drought conditions in *Arabidopsis*. *Plant Cell Rep.* 23, 1138-1152.

Stiti N, Triki S, Hartmann MA. 2007. Formation of triterpenoids throughout *Olea europaea* fruit ontogeny. *Lipids.* 42, 55-67.

Tsubaki S, Sugimura K, Teramoto Y, Yonemori K, Azuma JI. 2013. Cuticular membrane of *Fuyu persimmon* fruit is strengthened by triterpenoids nano-fillers. *PLOS ONE.* 8, e75275.

Valente S, Machado B, Pinto DCGA, Santos C, Silva AMS, Dias MC. 2020. Modulation of phenolic and lipophilic compounds of olive fruits in response to combined drought and heat. *Food Chem.* 329, 127191.

Vicente AR, Costa ML, Martínez GA, Chaves AR, Civello PM. 2005. Effect of heat treatments on cell wall degradation and softening in strawberry fruit. *Postharvest Biol. Technol.* 38, 213-222.

Vogg G., Fischer S, Leide J, Emmanuel E, Jetter R, Levy AA, Riederer M. 2004. Tomato fruit cuticular waxes and their effects on transpiration barrier properties: functional characterization of a mutant deficient in a very-long chain fatty acid β -ketoacyl-CoA synthase. *J. Exp. Bot.* 55, 1401-1410.

Werker E. 2000. Trichome diversity and development. *Adv. Bot. Res.* 31, 1-35.

Wu X, Yin H, Chen Y, Li L, Wang Y, Hao P. 2017. Chemical composition, crystal morphology and key gene of cuticular waxes of Asian pears at harvest and after storage. *Postharvest Biol. Technol.* 32, 71-80.

General discussion

Zarrouk O, Pinheiro C, Misra CS, Fernández V, Chaves MM. 2018. Fleshy fruit epidermis is a protective barrier under water stress. In *Water scarcity and sustainable agriculture in semiarid environment*. Chapter 20. (ISBN 978-0-12-813164-0).

Conclusions

The main goal of this Doctoral Thesis was to widen current knowledge of changes in fruit cuticle and cell wall composition during fruit ripening of *Olea europaea* L., and of the modifications therein, if any, in response to different agronomic factors. Complementary studies on the cuticular composition of fruits and leaves of *Prunus laurocerasus* L. and of fruits of *Actidinia spp.* were also carried out. Based on the results obtained from the different experiments described in this document, the following can be concluded:

SECTION I: A survey of nine olive cultivars

- Total yields and composition of fruit cuticle, wax and cutin varied widely along fruit ripening, and time-course changes showed different patterns depending on the cultivar. Triterpenoids were the most abundant components of the cuticular wax fraction, maslinic and oleanolic acids being the predominant compounds. Hydroxy-fatty acids dominated the cutin fraction, 18-hydroxyoctadecenoic and 16-hydroxyhexadecanoic acids being the most common cutin monomer types identified.
- Fruit surface microtopography was significantly different across the nine olive genotypes considered herein, and it is suggested that, in addition to the composition of cuticular waxes and cutin, this may be one of the factors underlying or modulating cuticle response to abiotic and biotic stresses, including proneness to olive fly infestation.
- Progressive solubilisation of cell wall polysaccharides was observed throughout fruit maturation, with increasing yields of the water-soluble fraction isolated from cell wall material. Preferential loss of neutral sugars was detected at early stages of fruit maturation, and a relevant role therein for Afase activity was shown. High PME activity levels and calcium contents in green fruit suggest that formation of egg-box structures between pectic polysaccharides prevented massive uronic acid loss at early maturity stages.
- Wax profile in fruit cuticle and in oil were very different, and hence no cuticular waxes were apparently transferred to oil during mechanical extraction. Phytol esters were the most abundant compounds of the wax ester fraction in extra-virgin and virgin olive oils, vaccenic acid being the main fatty acid constituent.

SECTION II: A focus on ‘Arbequina’ olive fruits

- Harsher environmental conditions at El Soleràs as compared with Mas Bové resulted in larger differences in physical and chemical properties, cuticle composition and cell wall metabolism between fruit samples from irrigated and rain-fed trees. Therefore, environmental conditions were shown to impact these traits, even though more producing seasons are required in order to draw conclusions on the implications for the management of olive groves.
- The composition of cuticular waxes was found to influence barrier properties of the cuticle, whereas cuticle thickness or total yields were apparently unrelated to water-proofing functions.
- Neutral sugar loss (mainly arabinose as the most abundant neutral sugar component of cell walls in olive fruit) at early maturity stages was associated to a sharp phase of fruit firmness decrease.

Conclusions

SECTION III: Inter-specific variation in cuticles features: *Prunus laurocerasus* L. and *Acinidia spp.* as examples

- Cuticle composition is dependent upon species, cultivar and plant organ. Quantitative and qualitative differences in fruit cuticle features were found among all four species studied. The percentage of *n*-alkanes in leaves of *Prunus laurocerasus* was higher than that in the fruits, in agreement with the idea of higher efficiency against water loss.
- Adaxial and abaxial sides of *P. laurocerasus* leaves display different yields of cutin and pentacyclic triterpenoids. The content of both cuticular compound types was higher in the adaxial (astomatous) than in the abaxial (stomatous) surface, suggesting a relationship to the presence or lack of stomata and to water-proofing efficiency.

Future research

Results obtained in this Doctoral Thesis show that cell walls and cuticle composition of olive fruit change along ripening, and are influenced by different agronomic factors. Nonetheless, further information is required in order to understand the impact of these factors according to genotype and cultivation area. More research would be also necessary to widen knowledge of specificities for different plant species or plant organs. Therefore, the following research lines are proposed for future investigations:

- To study the modifications in cuticle and cell walls along fruit maturation for a wider choice of cultivars and during several producing seasons at the same orchard, in order to exclude the influence of site-to-site variation (soil, climate) and thus to enhance the robustness of conclusions from such investigations.
- To analyse the metabolic origin of waxes present in olive oil.
- To evaluate the potenciality of cuticle properties of secondary or local olive cultivars as adaptive traits to each particular environment, and hence to take advantage of this knowledge for improving the pre- and postharvest management of produce while in turn protecting phyto-genetic resources.
- To go in-depth in the relation between the cuticle compounds of olive fruits, the changes therein during the corresponding industrial process, and the final characteristics of the product (table olives or olive oil).

Annexes

Table A1. Rainfall and temperatures at El Soleràs (PDO ‘Les Garrigues’) and Mas Bové (PDO ‘Siurana’) in 2018.

		Jan	Feb	Mar	Apr	May	Jun	Jul	Aug	Sep	Oct	Nov	Dec	Total rainfall (mm)
El Soleràs (PDO ‘Les Garrigues’)	Rainfall (mm)	32.6	40.8	41.8	61.8	NA	13	20.4	29.2	2.2	124.6	66.4	11	443.8
	Absolute Max T (°C)	19.5	17.4	22.4	27.9	27.7	34.3	36.5	38.2	32.8	27.3	19.5	15.7	
	Average Max T (°C)	12.2	10.2	15.1	19.4	23.1	28.5	33.5	32.5	29.3	20.5	13.9	10.4	
	Average T (°C)	8	5.4	9.8	13.8	17	22.1	26	25.7	22.8	15.3	10.1	6.9	
	Average Min T (°C)	3.8	0.6	4.5	8.1	10.9	15.7	18.5	19	16.4	10.1	6.3	3.4	
	Absolute Min T (°C)	-1.7	-4.4	-1.1	3.4	3.8	10	15	14	10.8	2.8	1.5	-1.7	
Mas Bové (PDO ‘Siurana’)	Rainfall (mm)	13.5	94.2	28.3	67.3	40.1	6.9	4.7	94.6	87.3	336.5	67.1	7.9	848.4
	Absolute Max T (°C)	22.6	18.6	24.6	25.6	26	30.7	33.2	37.8	30.4	26.4	22.9	20	
	Average Max T (°C)	NA	NA	NA	NA	NA	NA	NA	NA	NA	NA	NA	NA	
	Average T (°C)	10.8	7.2	11.4	14.5	17.4	21.6	24.9	25.1	22.4	16.7	12.2	9.8	
	Average Min T (°C)	NA	NA	NA	NA	NA	NA	NA	NA	NA	NA	NA	NA	
	Absolute Min T (°C)	-2	-3.9	-0.6	3.8	3.5	11.8	16.9	14.1	12.2	4.4	3.2	-0.4	

Abbreviations: Max T and Min T, maximum and minimum temperature, respectively; NA, Not available.

Table A2. Physical characteristics and toluidine blue test of ‘Arbequina’ olives picket at:

A) El Soleràs (PDO ‘Les Garrigues’) in 2018-2019 season.

Sampling date	Irrigation regime	Weight (g)		Length (mm)		Diameter (mm)		F:S ratio*		Water content (%)		TB test
Sept 13	Irrigated	1.13	e A	13.86	e A	12.28	d A	3.20	d A	65.62	cd A	+
Sept 25		1.21	e A	14.09	de A	12.40	d A	3.33	d A	68.54	ab A	+
Oct 10		1.37	d A	14.56	cd A	13.24	bc A	4.16	b A	67.43	bc A	+
Oct 23		1.57	c A	15.12	bc A	13.53	ab A	4.63	a A	69.81	a A	+
Nov 07		1.69	a A	15.35	ab A	13.87	a A	4.52	a A	65.52	cd A	+
Nov 23		1.68	ab A	14.87	bc A	13.94	a A	4.71	a A	65.12	d A	+
Dec 05		1.60	bc A	15.73	a A	13.38	bc A	4.18	b A	55.46	e A	+
Dec 18		1.53	c A	15.79	a A	13.62	ab A	4.05	bc A	51.60	f A	ne
Jan 15		1.33	d A	15.39	ab A	13.00	c A	3.91	c A	56.89	e A	ne
Sept 13	Rain-fed	0.95	de A	13.37	e A	11.36	d B	2.65	e B	48.35	c B	-
Sept 25		0.88	e B	13.45	de B	11.51	d B	2.47	f B	44.03	d B	-
Oct 10		0.96	d B	13.28	e B	11.40	d B	2.90	d B	44.21	d B	-
Oct 23		1.39	b B	13.93	cd B	12.72	ab B	3.73	a B	56.37	a B	+
Nov 07		1.09	c B	13.71	cde B	11.64	d B	3.40	b B	58.31	a B	+
Nov 23		1.36	b B	14.12	bc A	12.22	c B	3.31	c B	52.02	b B	+
Dec 05		1.34	b B	14.57	ab B	12.35	bc B	3.39	bc B	48.11	c B	-
Dec 18		1.33	b B	14.59	ab B	12.72	ab B	3.42	b B	43.11	d B	ne
Jan 15		1.48	a A	15.03	a A	12.81	a A	3.67	a B	38.11	e B	ne

Values represent means of 10 fruits. Different capital letters denote significant differences among the irrigated and rain-fed olive for a given date of sampling, and different lower-case letters stand for significant differences among the sampling date for a given irrigation regime, at $P \leq 0.05$ (LSD test).

*Abbreviations: F:S ratio, flesh to stone ratio; TB test, toluidine blue test (Tanaka et al., 2004): stained and non-stained ‘Arbequina’ fruits are denote respectively as + and -; ne, not evaluated.

Table A2 – Continued

B) Mas Bové (PDO ‘Siurana’) in 2018-2019 season.

Sampling date	Irrigation regime	Weight (g)	Length (mm)	Diameter (mm)	F:S ratio*	Water content (%)	TB test
Sept 12	Irrigated	1.27	13.68	12.09	2.48	59.92	+
Sept 26		2.06	17.56	14.46	2.93	62.31	+
Oct 11		2.35	17.43	15.30	4.55	63.77	+
Oct 24		2.45	17.29	15.77	4.94	65.93	+
Nov 08		2.53	17.01	15.22	4.84	65.02	+
Nov 22						66.03	+
Dec 04		2.67	18.13	16.08	5.68	65.12	+
Dec 19		2.61	16.48	14.84	5.36	61.56	ne
Jan 16		1.87	15.14	13.36	5.04	53.07	ne
Sept 12		Rain-fed	1.08	13.62	11.3	2.64	57.61
Sept 26	1.39		15.04	13.11	2.64	58.15	-
Oct 11	1.25		14.56	12.47	3.13	58.80	-
Oct 24	1.57		15.11	13.32	3.88	61.41	+
Nov 08	1.42		14.73	13.19	3.83	60.49	+
Nov 22	ne		ne	ne	ne	58.63	+
Dec 04	1.59		14.57	13.09	3.97	55.41	+
Dec 19	1.45		14.94	13.41	3.68	55.01	+
Jan 16	1.15		13.11	11.58	3.54	49.38	+

Values represent means of 50 fruits for weight, F:S ratio and water content, and of 10 fruits for length, diameter and TB test. Different capital letters denote significant differences among irrigated and rain-fed samples for a given sampling date, and different lower-case letters stand for significant differences among sampling date and irrigation regime at $P \leq 0.05$ (LSD test).

*Abbreviations: F:S ratio, flesh to stone ratio; TB test, toluidine blue test (Tanaka et al., 2004): stained and non-stained ‘Arbequina’ fruits are denote respectively as + and -; ne, not evaluated.

Table A3. Cuticle, cuticular wax and cutin yields, wax to cutin ratio and cuticle thickness of ‘Arbequina’ olives picked at:

A) El Soleràs (PDO ‘Les Garrigues’) in 2018-2019 season.

Sampling date	Irrigation regime	Cuticle yield (mg cm ⁻²)		Wax yield (µg cm ⁻²)		Wax (%)		Cutin yield (µg cm ⁻²)		Cutin (%)		C ₁₆ /C ₁₈	Wax/ cutin ratio		Thickness (µm)	
Sept 13	Irrigated	3.6	a B	663.9	abcd B	18.3	b B	592.4	ab A	16.3	d A	0.89	1.12	bcd B	3.6	a B
Sept 25		3.5	a B	777.5	a B	22.3	ab A	597.7	ab B	17.1	cd B	0.66	1.30	bcd A	3.5	a B
Oct 10		3.0	b B	768.3	ab A	25.9	ab A	672.9	a A	22.7	a A	0.61	1.14	bcd A	3.0	b B
Oct 23		2.1	e B	459.8	d B	22.1	ab A	444.5	d B	21.4	ab A	0.88	1.03	cd B	2.1	e B
Nov 07		2.6	cd A	739.2	abc B	28.8	a A	493.0	cd A	19.2	bc A	0.53	1.50	bc A	2.6	cd A
Nov 23		2.0	e B	536.4	bcd A	26.9	ab A	344.0	e B	17.2	cd A	0.57	1.56	b A	2.0	e B
Dec 05		2.4	de A	632.6	abcd A	26.5	ab A	233.2	f B	9.8	e B	0.47	2.71	a A	2.4	de A
Dec 18		2.8	bc A	752.9	abc A	26.9	ab A	490.6	cd B	17.5	cd B	0.59	1.53	b A	2.8	bc A
Jan 15		2.6	cd B	518.1	cd B	20.2	ab A	572.1	bc B	22.3	a A	0.49	0.91	d A	2.6	cd B
Sept 13	Rain-fed	4.9	a A	1379.5	a A	28.3	b A	844.6	b B	17.3	cd A	0.46	1.63	b A	4.9	a A
Sept 25		4.6	a A	1099.3	b A	23.6	cd A	1232.5	a A	26.5	a A	0.63	0.89	ef A	4.6	a A
Oct 10		4.1	b A	990.3	b A	24.1	c A	810.1	b A	19.7	bc A	0.59	1.22	cd A	4.1	b A
Oct 23		3.3	d A	851.2	c A	25.9	bc A	590.2	de A	18.0	cd B	0.46	1.44	bc A	3.3	d A
Nov 07		2.7	e A	1027.1	b A	38.6	a A	466.0	f A	17.5	cd A	0.40	2.20	a A	2.7	e A
Nov 23		3.2	d A	661.6	d A	20.5	de A	570.8	de A	17.7	cd A	0.51	1.16	de A	3.2	d A
Dec 05		3.1	d A	615.1	d A	20.0	e B	495.1	ef A	16.1	d A	0.46	1.24	cd B	3.1	d A
Dec 18		3.2	d A	467.6	e B	14.4	f B	701.8	c A	21.7	b A	0.46	0.67	f B	3.2	d A
Jan 15		3.7	c A	602.0	d A	16.2	f B	641.2	cd A	17.2	cd B	0.47	0.94	ef A	3.7	c A

Cuticular membranes were isolated from skin samples (around 95 cm²) obtained from 50 to 75 olives, contingent upon ‘Arbequina’ fruit size. Wax and cutin data represent means of three technical replicates of this starting material. For cuticle thickness values represent means of four biological replicates. Different capital letters denote significant differences among irrigated and rain-fed samples for a given sampling date, and different lower-case letters stand for significant differences among sampling date and irrigation regime at $P \leq 0.05$ (LSD test).

*Ratio of C₁₆/C₁₈cutin monomers.

Table A3 – Continued

B) Mas Bové (PDO ‘Siurana’) in 2018-2019 season.

Sampling date	Irrigation regime	Cuticle yield (mg cm ⁻²)		Wax yield (µg cm ⁻²)		Wax (%)		Cutin yield (µg cm ⁻²)		Cutin (%)		C ₁₆ /C ₁₈	Wax/ cutin ratio		Thickness (µm)	
Sept 12	Irrigated	3.1	a B	718.5	a B	22.9	cd A	567.1	a B	18.0	c A	1.10	1.27	b A	3.1	a B
Sept 26		2.6	b B	645.3	b A	24.9	c A	500.8	abc A	19.3	c A	0.60	1.29	b A	2.6	b B
Oct 11		2.3	cd B	446.4	de B	19.6	ef A	539.0	ab A	23.6	a A	0.49	0.83	cd B	2.3	cd B
Oct 24		1.9	e A	561.2	c A	29.8	b A	371.1	e B	19.7	bcB	0.54	1.51	b A	1.9	e A
Nov 08		1.9	e B	645.4	b A	33.1	a A	199.4	f B	10.2	d B	0.57	3.24	a A	1.9	e B
Nov 22		2.0	e B	360.0	f A	18.4	f A	458.5	bcd A	23.4	ab A	0.39	0.79	d A	2.0	e B
Dec 04		2.4	bc A	589.8	bc A	24.1	cd A	440.0	cde A	18.0	c A	0.50	1.34	b A	2.4	bc A
Dec 19		2.2	d B	485.2	d B	21.8	de A	405.5	de A	18.2	c A	0.47	1.20	bc A	2.2	d B
Jan 16		2.6	b A	393.8	ef A	15.2	g A	467.0	bcd B	18.1	c A	0.43	0.84	cd A	2.6	b A
Sept 12	Rain-fed	3.5	a A	894.1	a A	25.5	a A	653.6	a A	18.6	cd A	1.14	1.37	a A	3.5	a A
Sept 26		3.0	a A	511.9	d B	16.9	cd B	569.0	bc A	18.8	cd A	0.63	0.90	de B	3.0	a A
Oct 11		3.0	a A	670.8	bc A	22.2	b A	573.4	bc A	19.0	cd A	0.51	1.17	bc A	3.0	a A
Oct 24		2.2	d A	371.5	e B	16.9	cd B	609.1	ab A	27.8	a A	0.80	0.61	f B	2.2	d A
Nov 08		2.6	c A	712.1	b A	27.0	a B	525.0	cd A	19.9	c A	0.65	1.36	a B	2.6	c A
Nov 22		2.4	d A	419.3	e A	17.8	cd A	548.9	bcd A	23.3	b A	0.52	0.76	ef A	2.4	d A
Dec 04		2.8	c A	531.0	d A	19.3	c B	495.4	de A	18.0	cd A	0.49	1.07	cd B	2.8	c A
Dec 19		2.7	c A	605.7	c A	22.3	b A	456.5	e A	16.8	d A	0.56	1.33	ab A	2.7	c A
Jan 16		2.7	c A	423.3	e A	15.4	d A	522.3	cde A	19.0	cd A	0.54	0.81	e A	2.7	c A

Cuticular membranes were isolated from skin samples (around 95 cm⁻²) obtained from 50 to 75 olives, contingent upon ‘Arbequina’ fruit size. Wax and cutin data represent means of three technical replicates of this starting material. For cuticle thickness values represent means of four biological replicates. Different capital letters denote significant differences among irrigated and rain-fed samples for a given sampling date, and different lower-case letters stand for significant differences among sampling date and irrigation regime at $P \leq 0.05$ (LSD test).

*Ratio of C₁₆/C₁₈cutin monomers.

Table A4. Composition of wax constituents (relative % over total waxes) in cuticles isolated from ‘Arbequina’ olives picked at:
A) El Soleràs (PDO ‘Les Garrigues’) in 2018-2019 season.

Sampling date	Irrigation regime	ACL*		Acyclic/cyclic ratio		Triterpenoids (%)		Fatty acids (%)		Fatty alcohols (%)		<i>n</i> -Alkanes (%)		Sterols (%)		Unidentified (%)	
Sept 13	Irrigated	25.4	cd B	0.15	e A	78.7	a A	6.3	e A	4.7	f A	1.0	e A	0.5	a A	8.9	cd A
Sept 25		26.1	b A	0.20	de A	76.5	a A	7.6	de A	7.0	de A	1.1	de A	0.5	a A	7.3	d A
Oct 10		26.3	a A	0.23	cde A	76.3	a B	8.3	cd A	7.2	de A	1.8	a A	nd		6.3	d A
Oct 23		25.2	de B	0.30	bc A	66.4	b B	10.7	b A	7.9	de A	1.2	cde A	0.5	a A	13.2	ab A
Nov 07		25.5	c A	0.33	b A	66.3	b A	10.0	bc A	10.3	bc A	1.0	e A	0.5	a B	11.8	bc A
Nov 23		25.3	cde A	0.46	a A	58.8	c B	12.9	a A	12.4	ab A	1.6	ab A	0.5	a A	13.6	ab A
Dec 05		25.1	e B	0.46	a A	57.5	c A	12.8	a A	12.6	a A	1.4	bcd A	0.6	aA	15.0	a A
Dec 18		25.1	e A	0.26	bcd A	69.2	b A	8.4	cd B	8.6	cd A	1.0	e B	0.5	a A	12.2	ab A
Jan 15		24.5	f B	0.30	bc A	65.1	b A	11.5	ab A	6.3	ef A	1.5	abc A	0.5	a A	15.0	a A
Sept 13		Rain-fed	26.1	a A	0.15	f A	81.2	a A	5.2	f A	6.1	de A	0.8	cd A	0.5	cd A	6.3
Sept 25	26.0		a A	0.17	ef A	79.4	a A	6.1	ef A	6.1	de A	1.1	b A	0.6	ab A	6.7	d A
Oct 10	25.7		b B	0.15	ef B	80.2	a A	6.5	ef B	4.8	e B	1.0	bc B	0.5	cd A	7.1	d A
Oct 23	25.6		b A	0.21	de B	73.6	b A	7.5	de B	6.1	de B	1.5	a A	0.4	de A	10.8	c A
Nov 07	25.4		c A	0.37	a A	63.9	cd A	10.5	ab A	12.3	a A	1.2	b A	0.6	a A	11.6	c A
Nov 23	25.2		cd A	0.29	c B	68.1	c A	9.3	bc B	9.4	b B	1.0	b B	0.5	cd A	11.8	c A
Dec 05	25.2		d A	0.36	ab B	61.9	d A	9.9	ab B	11.7	a A	1.0	bc B	0.5	bc A	15.1	b A
Dec 18	24.9		e B	0.31	bc A	66.4	c A	10.9	a A	8.0	bc A	1.5	a A	0.5	bc A	12.6	c A
Jan 15	24.7		e A	0.23	d B	67.3	c A	8.1	cd B	6.6	cd A	0.5	d B	0.3	e A	17.1	a A

Cuticular membranes were isolated from skin samples (around 95 cm⁻²) obtained from 50 to 75 olives, contingent upon ‘Arbequina’ fruit size. Values represent means of three technical replicates. Different capital letters denote significant differences among irrigated and rain-fed samples for a given sampling date, and different lower-case letters stand for significant differences among sampling date and irrigation regime at $P \leq 0.05$ (LSD test).

*Abbreviations: ACL, Average chain length of acyclic wax compounds.

Table A4 – Continued

B) Mas Bové (PDO ‘Siurana’) in 2018-2019 season.

Sampling date	Irrigation regime	ACL*		Acyclic/cyclic ratio		Triterpenoids (%)		Fatty acids (%)		Fatty alcohols (%)		<i>n</i> -Alkanes (%)		Sterols (%)		Unidentified (%)	
Sept 12	Irrigated	25.7	ab B	0.17	d A	77.9	a A	6.6	d A	5.6	c A	0.7	c B	0.5	bc A	8.7	de A
Sept 26		25.8	a A	0.22	d A	76.0	a A	9.2	c A	7.0	c A	0.7	c A	0.4	bc B	6.8	e A
Oct 11		25.7	ab A	0.26	cd A	72.5	a A	10.4	c A	7.3	c A	1.4	b A	0.5	b A	7.9	e A
Oct 24		25.3	cd A	0.40	b A	61.3	bc A	13.0	a A	10.5	b A	1.3	b A	0.5	ab A	13.4	ab A
Nov 08		25.6	b A	0.23	d B	74.5	a A	9.2	c A	7.5	c B	0.6	c B	0.6	a A	7.5	e B
Nov 22		25.4	c A	0.53	a A	56.3	c A	14.1	a A	13.5	a A	2.2	a A	0.5	b A	13.4	ab A
Dec 04		25.4	cd A	0.40	b A	62.4	b A	10.8	bcA	12.3	ab A	1.6	b A	0.5	bc A	12.5	bc A
Dec 19		25.2	de A	0.50	a A	56.5	c B	12.3	ab A	13.5	a A	2.4	a A	0.4	cd A	14.9	a A
Jan 16		25.1	e A	0.35	bc A	65.9	b A	10.6	bc A	11.2	b A	1.5	b A	0.3	d A	10.4	cd A
Sept 12	Rain-fed	26.0	a A	0.19	c A	75.1	a A	6.5	c A	6.9	f A	1.0	cd A	0.5	b A	9.9	c A
Sept 26		25.6	b B	0.23	c A	74.5	a A	9.2	b A	7.5	ef A	0.6	e A	0.6	a A	7.5	d A
Oct 11		25.7	b A	0.24	c A	75.6	a A	9.5	b A	7.7	ef A	0.9	de B	0.5	ab A	5.8	d B
Oct 24		25.1	fg B	0.35	b A	63.7	b A	12.8	a A	8.5	eB	1.3	bc A	0.5	ab A	13.2	ab A
Nov 08		25.5	c A	0.32	b A	66.4	b B	9.3	b A	10.5	d A	1.3	ab A	0.4	bc B	12.1	b A
Nov 22		25.3	d A	0.46	a A	57.8	c A	12.5	a B	12.7	ab A	1.6	a B	0.5	ab A	14.9	a A
Dec 04		25.2	de A	0.34	b A	65.4	b A	10.1	b A	10.9	cd A	1.3	bc A	0.5	b A	11.7	bc A
Dec 19		25.1	ef A	0.38	b A	63.6	b A	10.6	b A	12.1	bc A	1.2	bc B	0.4	c A	12.1	b B
Jan 16		25.0	g B	0.48	a A	59.1	c A	12.9	a A	13.8	a A	1.6	a A	0.4	c A	12.2	b A

Cuticular membranes were isolated from skin samples (around 95 cm⁻²) obtained from 50 to 75 olives, contingent upon ‘Arbequina’ fruit size. Values represent means of three technical replicates. Different capital letters denote significant differences among irrigated and rain-fed samples for a given sampling date, and different lower-case letters stand for significant differences among sampling date and irrigation regime at $P \leq 0.05$ (LSD test).

*Abbreviations: ACL, Average chain length of acyclic wax compounds.

Table A5. Composition of cutin monomers (relative % over total cutin) in cuticles isolated from ‘Arbequina’ olives picked at:

A) El Soleràs (PDO ‘Les Garrigues’) in 2018-2019 season.

Sampling date	Irrigation regime	FA*	α,ω -diFA (%)	α,ω -diFA, mcOH (%)	ω -OH FA (%)	ω -OH FA, mcOH (%)	α -OH FA (%)	Other OH FA (%)	Alcohols (%)	Unidentified (%)
Sept 13	Irrigated	14.2 a A	5.5 c B	1.2 b A	27.2 c B	17.5 b A	2.2 a B	nd	1.9 a A	30.1 a A
Sept 25		8.2 bc A	11.0 ab A	1.3 b A	32.7 b A	17.2 b A	2.3 a A	nd	1.7 abc A	25.7 cd A
Oct 10		9.4 b A	11.5 a A	1.2 b A	33.5 b A	15.9 bc A	2.1 a B	nd	1.6 bcd A	24.9 cde A
Oct 23		9.1 bc A	8.4 b B	1.7 a A	27.9 c B	24.3 a A	2.3 a A	nd	1.8 abc A	24.5 cde A
Nov 07		12.6 a A	11.8 a A	0.7 c A	36.2 a A	10.0 d A	1.6 b A	nd	1.5 cd A	25.6 cd A
Nov 23		7.6 bc A	11.1 ab A	0.8 c B	37.9 a A	12.7 cd A	1.7 b A	nd	1.9 ab A	26.3 bc A
Dec 05		12.6 a A	11.1 a A	0.7 c A	38.0 a A	10.0 d A	1.6 b A	nd	1.7 abc A	24.2 de B
Dec 18		6.4 c B	9.9 ab A	1.3 b A	33.3 b B	17.1 b A	2.4 a A	nd	1.8 ab A	27.7 b A
Jan 15		12.3 a A	9.8 ab A	1.1 b A	36.4 a A	13.3 c A	2.1 a A	nd	1.3 d A	23.6 e A
Sept 13		Rain-fed	7.3 cd B	12.1 ab A	1.3 a A	34.0 de A	13.7 bc B	2.7 a A	0.2 b	1.6 b A
Sept 25	7.1 cd A		10.3 cA	1.5 a A	32.4 e A	18.2 a A	2.6 ab A	0.2 b	1.7 b A	26.0 abc A
Oct 10	8.3 cd B		11.0 bc A	1.3 a A	32.7 e A	17.1 ab A	2.3 bc A	0.2 ab	1.7 b A	25.4 bc A
Oct 23	15.0 a A		11.7 abc A	0.6 c B	35.5 bcd A	9.2 d B	1.5 e B	0.2 b	1.6 b A	24.7 cd A
Nov 07	9.7 bcd A		13.0 a A	0.7 c A	38.4 a A	8.4 d A	1.6 de A	0.2 ab	1.8 ab A	26.1 abc A
Nov 23	6.5 d A		11.8 abc A	1.4 a A	34.6 cde A	16.2 ab A	2.4 ab A	0.1 b	1.7 b A	25.3 bc A
Dec 05	8.0 cd B		11.9 abc A	1.0 b A	36.5 abc A	11.7 cd A	2.0 cd A	0.2 a	1.8 ab A	26.8 ab A
Dec 18	11.4 b A		10.6 bc A	0.9 bc A	38.8 a A	11.2 cd B	1.9 d A	nd	1.8 ab A	23.4 d B
Jan 15	9.5 bc B		11.0 bc A	0.8 bc B	37.7 ab A	11.5 cd A	1.9 d A	nd	1.8 ab A	25.8 abc A

Cuticular membranes were isolated from skin samples (around 95 cm²) obtained from 50 to 75 olives, contingent upon ‘Arbequina’ fruit size. Values represent means of three technical replicates). Different capital letters denote significant differences among the cultivars for a given maturity stage, and different lower-case letters stand for significant differences among maturation stages for a given cultivar, at $P \leq 0.05$ (LSD test).

*Abbreviations: FA, Monocarboxylic fatty acids; α,ω -diFA, α,ω -Dicarboxylic fatty acids; α,ω -diFA, mcOH, α,ω -Dicarboxylic fatty acids with midchain hydroxy group; ω -OH FA, ω -Hydroxy fatty acids; ω -OH FA, mcOH, ω -Hydroxy fatty acids with midchain hydroxy group; α -OH FA, α -Hydroxy fatty acids; Other OH FA, other hydroxy fatty acids.

Table A5 – Continued

B) Mas Bové (PDO ‘Siurana’) in 2018-2019 season.

Sampling date	Irrigation regime	FA*	α,ω -diFA (%)	α,ω -diFA, mcOH (%)	ω -OH FA (%)	ω -OH FA, mcOH (%)	α -OH FA (%)	Other OH FA (%)	Alcohols (%)	Unidentified (%)
Sept 12	Irrigated	8.9 d A	4.6 c A	1.4 ab A	26.9 d A	19.6 a A	2.7 ab A	nd	1.9 bc A	33.9 a A
Sept 26		9.3 cd A	10.6 b A	1.5 ab A	33.0 c A	15.6 b A	2.9 a A	nd	1.4 de A	25.6 b A
Oct 11		13.5 a A	11.5 b B	1.2 bc A	33.6 bc A	12.0 c A	2.5 bc A	nd	1.2 e B	24.4 b A
Oct 24		9.3 cd A	11.6 b A	1.5 a B	32.9 c A	15.7 b B	2.9 ab A	nd	1.5 de B	24.7 b A
Nov 08		7.6 d A	10.8 b A	1.7 a A	32.8 c A	17.0 ab A	3.0 a A	nd	1.5 de A	25.6 b A
Nov 22		11.2 bc A	13.8 a A	0.7 d A	38.5 a A	7.4 e A	1.7 e B	nd	1.6 cd A	25.0 b A
Dec 04		8.0 d A	11.5 b A	1.4 ab A	35.6 bc A	14.2 bc A	2.6 ab A	nd	1.5 de B	25.1 b A
Dec 19		11.5 b A	10.1 b A	1.0 cd A	36.2 ab A	11.6 cd A	2.3 cd A	nd	2.3 a A	25.1 b A
Jan 16		10.9 bc A	11.4 b A	0.8 d B	38.6 a A	9.0 de B	2.0 de B	nd	2.2 ab A	25.2 b A
Sept 12		Rain-fed	12.9 a A	3.3 e B	1.3 bc A	24.7 f A	18.1 b A	2.7 ab A	nd	2.2 a A
Sept 26	8.1 b B		10.3 bc A	1.6 ab A	31.4 d A	17.6 bc A	2.8 a A	nd	1.6 bcd A	26.4 b A
Oct 11	10.8 ab A		12.7 a A	1.2 bcd A	34.5 bc A	12.7 de A	2.4 abc A	nd	1.5 d A	24.1 cd A
Oct 24	8.8 b A		8.5 d B	2.0 a A	28.9 e B	23.6 a A	2.7 ab A	nd	1.7 b A	23.7 d A
Nov 08	8.1 b A		9.7 cd A	1.6 ab A	32.4 cd A	17.9 b A	2.7 a A	nd	1.7 bcd A	25.8 bcd A
Nov 22	8.6 b A		10.6 bc B	1.2 bcd A	36.4 ab A	14.0 bcde A	2.5 abc A	nd	1.6 cd A	25.1 bcd A
Dec 04	8.6 b A		11.1 b A	0.9 d A	38.4 a A	10.6 e A	2.1 c A	nd	1.8 b A	26.3 b A
Dec 19	9.0 b A		9.9 bc A	1.1 cd A	36.5 ab A	13.4 cde A	2.3 bc A	nd	1.8 b A	26.0 bc A
Jan 16	7.8 b B		10.8 bc A	1.3 bc A	36.1 b B	15.2 bcd A	2.6 ab A	nd	1.5 d B	24.6 bcd A

Cuticular membranes were isolated from skin samples (around 95 cm²) obtained from 50 to 75 olives, contingent upon ‘Arbequina’ fruit size. Values represent means of three technical replicates). Different capital letters denote significant differences among the cultivars for a given maturity stage, and different lower-case letters stand for significant differences among maturation stages for a given cultivar, at $P \leq 0.05$ (LSD test).

*Abbreviations: FA, Monocarboxylic fatty acids; α,ω -diFA, α,ω -Dicarboxylic fatty acids; α,ω -diFA, mcOH, α,ω -Dicarboxylic fatty acids with midchain hydroxy group; ω -OH FA, ω -Hydroxy fatty acids; ω -OH FA, mcOH, ω -Hydroxy fatty acids with midchain hydroxy group; α -OH FA, α -Hydroxy fatty acids; Other OH FA, other hydroxy fatty acids.